CHAPTER 8

Variable-Reluctance Machines and Stepping Motors

Variable-reluctance machines[1] (often abbreviated as *VRMs*) are perhaps the simplest of electrical machines. They consist of a stator with excitation windings and a magnetic rotor with saliency. Rotor conductors are not required because torque is produced by the tendency of the rotor to align with the stator-produced flux wave in such a fashion as to maximize the stator flux linkages that result from a given applied stator current. Torque production in these machines can be evaluated by using the techniques of Chapter 3 and the fact that the stator winding inductances are functions of the angular position of the rotor.

Although the concept of the VRM has been around for a long time, only in the past few decades have these machines begun to see widespread use in engineering applications. This is due in large part to the fact that although they are simple in construction, they are somewhat complicated to control. For example, the position of the rotor must be known in order to properly energize the phase windings to produce torque. It is the widespread availability and low cost of micro and power electronics that has made the VRM competitive with other motor technologies in a wide range of applications.

By sequentially exciting the phases of a VRM, the rotor will rotate in a stepwise fashion, rotating through a specific angle per step. *Stepper motors* are designed to take advantage of this characteristic. Such motors often combine the use of a variable-reluctance geometry with permanent magnets to produce increased torque and precision position accuracy.

[1] Variable-reluctance machines are often referred to as *switched-reluctance machines* (*SRMs*) to indicate the combination of a VRM and the switching inverter required to drive it. This term is popular in the technical literature.

8.1 BASICS OF VRM ANALYSIS

Common variable-reluctance machines can be categorized into two types: singly-salient and doubly-salient. In both cases, their most noticeable features are that there are no windings or permanent magnets on their rotors and that their only source of excitation consists of stator windings. This can be a significant feature because it means that all the resistive winding losses in the VRM occur on the stator. Because the stator can typically be cooled much more effectively and easily than the rotor, the result is often a smaller motor for a given rating and frame size.

As is discussed in Chapter 3, to produce torque, VRMs must be designed such that the stator-winding inductances vary with the position of the rotor. Figure 8.1a shows a cross-sectional view of a *singly-salient VRM,* which can be seen to consist of a nonsalient stator and a two-pole salient rotor, both constructed of high-permeability magnetic material. In the figure, a two-phase stator winding is shown although any number of phases are possible.

Figure 8.2a shows the form of the variation of the stator inductances as a function of rotor angle θ_m for a singly-salient VRM of the form of Fig. 8.1a. Notice that the inductance of each stator phase winding varies with rotor position such that the inductance is maximum when the rotor axis is aligned with the magnetic axis of that phase and minimum when the two axes are perpendicular. The figure also shows that the mutual inductance between the phase windings is zero when the rotor is aligned with the magnetic axis of either phase but otherwise varies periodically with rotor position.

Figure 8.1b shows the cross-sectional view of a two-phase *doubly-salient VRM* in which both the rotor and stator have salient poles. In this machine, the stator has four poles, each with a winding. However, the windings on opposite poles are of the same phase; they may be connected either in series or in parallel. Thus this machine is quite similar to that of Fig. 8.1a in that there is a two-phase stator winding and a two-pole salient rotor. Similarly, the phase inductance of this configuration varies from a maximum value when the rotor axis is aligned with the axis of that phase to a minimum when they are perpendicular.

Unlike the singly-salient machine of Fig. 8.1a, under the assumption of negligible iron reluctance the mutual inductances between the phases of the doubly-salient VRM of Fig. 8.1b will be zero, with the exception of a small, essentially-constant component associated with leakage flux. In addition, the saliency of the stator enhances the difference between the maximum and minimum inductances, which in turn enhances the torque-producing characteristics of the doubly-salient machine. Figure 8.2b shows the form of the variation of the phase inductances for the doubly-salient VRM of Fig. 8.1b.

The relationship between flux linkage and current for the singly-salient VRM is of the form

$$\begin{bmatrix} \lambda_1 \\ \lambda_2 \end{bmatrix} = \begin{bmatrix} L_{11}(\theta_m) & L_{12}(\theta_m) \\ L_{12}(\theta_m) & L_{22}(\theta_m) \end{bmatrix} \begin{bmatrix} i_1 \\ i_2 \end{bmatrix} \tag{8.1}$$

Here $L_{11}(\theta_m)$ and $L_{22}(\theta_m)$ are the self-inductances of phases 1 and 2, respectively, and $L_{12}(\theta_m)$ is the mutual inductances. Note that, by symmetry

$$L_{22}(\theta_m) = L_{11}(\theta_m - 90^\circ) \tag{8.2}$$

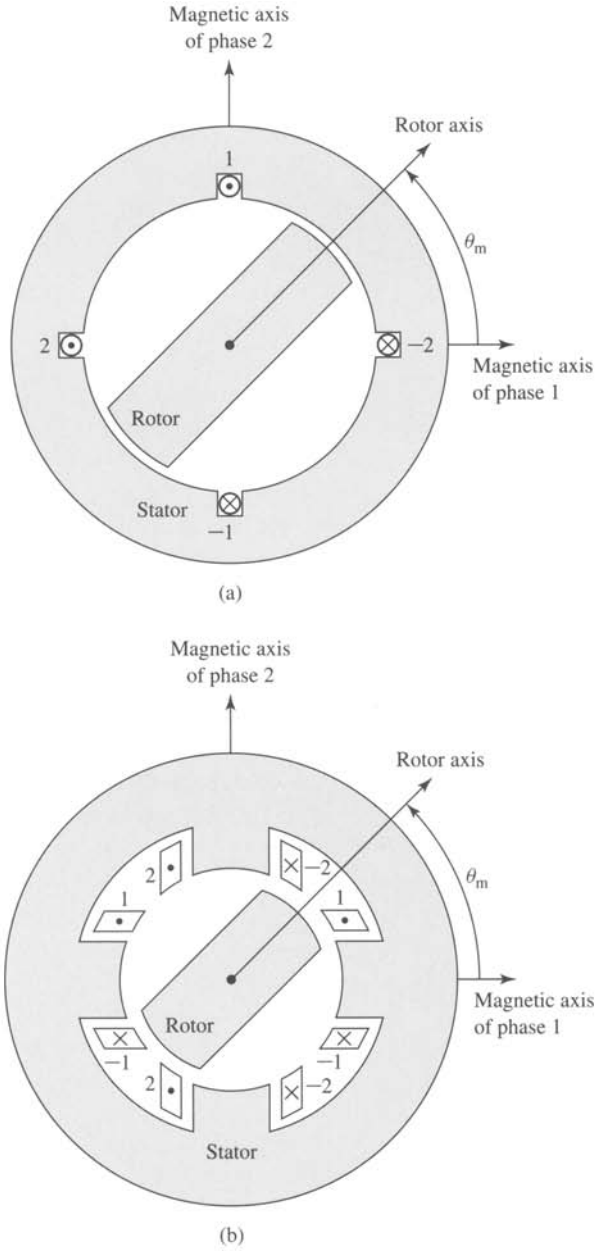

Figure 8.1 Basic two-phase VRMs: (a) singly-salient and (b) doubly-salient.

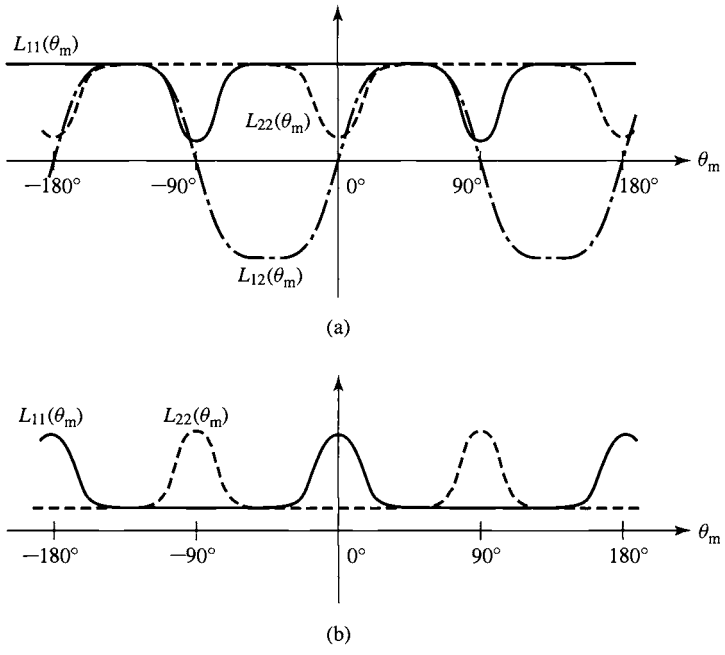

Figure 8.2 Plots of inductance versus θ_m for (a) the singly-salient VRM of Fig. 8.1a and (b) the doubly-salient VRM of Fig. 8.1b.

Note also that all of these inductances are periodic with a period of 180° because rotation of the rotor through 180° from any given angular position results in no change in the magnetic circuit of the machine.

From Eq. 3.68 the electromagnetic torque of this system can be determined from the coenergy as

$$T_{\text{mech}} = \frac{\partial W'_{\text{fld}}(i_1, i_2, \theta_m)}{\partial \theta_m} \tag{8.3}$$

where the partial derivative is taken while holding currents i_1 and i_2 constant. Here, the coenergy can be found from Eq. 3.70,

$$W'_{\text{fld}} = \frac{1}{2}L_{11}(\theta_m)i_1^2 + L_{12}(\theta_m)i_1 i_2 + \frac{1}{2}L_{22}(\theta_m)i_2^2 \tag{8.4}$$

Thus, combining Eqs. 8.3 and 8.4 gives the torque as

$$T_{\text{mech}} = \frac{1}{2}i_1^2\frac{dL_{11}(\theta_m)}{d\theta_m} + i_1 i_2\frac{dL_{12}(\theta_m)}{d\theta_m} + \frac{1}{2}i_2^2\frac{dL_{22}(\theta_m)}{d\theta_m} \tag{8.5}$$

For the double-salient VRM of Fig. 8.1b, the mutual-inductance term $dL_{12}(\theta_m)/d\theta_m$ is zero and the torque expression of Eq. 8.5 simplifies to

$$T_{\text{mech}} = \frac{1}{2}i_1^2\frac{dL_{11}(\theta_m)}{d\theta_m} + \frac{1}{2}i_2^2\frac{dL_{22}(\theta_m)}{d\theta_m} \tag{8.6}$$

Substitution of Eq. 8.2 then gives

$$T_{\text{mech}} = \frac{1}{2} i_1^2 \frac{dL_{11}(\theta_{\text{m}})}{d\theta_{\text{m}}} + \frac{1}{2} i_2^2 \frac{dL_{11}(\theta_{\text{m}} - 90°)}{d\theta_{\text{m}}} \tag{8.7}$$

Equations 8.6 and 8.7 illustrate an important characteristic of VRMs in which mutual-inductance effects are negligible. In such machines the torque expression consists of a sum of terms, each of which is proportional to the square of an individual phase current. As a result, the torque depends only on the magnitude of the phase currents and not on their polarity. Thus the electronics which supply the phase currents to these machines can be unidirectional; i.e., bidirectional currents are not required.

Since the phase currents are typically switched on and off by solid-state switches such as transistors or thyristors and since each switch need only handle currents in a single direction, this means that the motor drive requires only half the number of switches (as well as half the corresponding control electronics) that would be required in a corresponding bidirectional drive. The result is a drive system which is less complex and may be less expensive. Typical VRM motor drives are discussed in Section 11.4.

The assumption of negligible mutual inductance is valid for the doubly-salient VRM of Fig. 8.1b both due to symmetry of the machine geometry and due to the assumption of negligible iron reluctance. In practice, even in situations where symmetry might suggest that the mutual inductances are zero or can be ignored because they are independent of rotor position (e.g., the phases are coupled through leakage fluxes), significant nonlinear and mutual-inductance effects can arise due to saturation of the machine iron. In such cases, although the techniques of Chapter 3, and indeed torque expressions of the form of Eq. 8.3, remain valid, analytical expressions are often difficult to obtain (see Section 8.4).

At the design and analysis stage, the winding flux-current relationships and the motor torque can be determined by using numerical-analysis packages which can account for the nonlinearity of the machine magnetic material. Once a machine has been constructed, measurements can be made, both to validate the various assumptions and approximations which were made as well as to obtain an accurate measure of actual machine performance.

From this point on, we shall use the symbol p_{s} to indicate the number of stator poles and p_{r} to indicate the number of rotor poles, and the corresponding machine is called a $p_{\text{s}}/p_{\text{r}}$ machine. Example 8.1 examines a 4/2 VRM.

EXAMPLE 8.1

A 4/2 VRM is shown in Fig. 8.3. Its dimensions are

$$R = 3.8 \text{ cm} \qquad \alpha = \beta = 60° = \pi/3 \text{ rad}$$

$$g = 2.54 \times 10^{-2} \text{ cm} \qquad D = 13.0 \text{ cm}$$

and the poles of each phase winding are connected in series such that there are a total of $N = 100$ turns (50 turns per pole) in each phase winding. Assume the rotor and stator to be of infinite magnetic permeability.

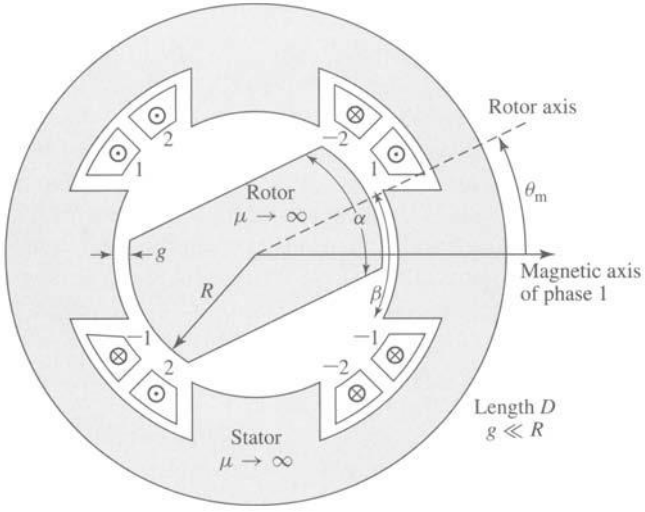

Figure 8.3 4/2 VRM for Example 8.1.

a. Neglecting leakage and fringing fluxes, plot the phase-1 inductance $L(\theta_m)$ as a function of θ_m.
b. Plot the torque, assuming (*i*) $i_1 = I_1$ and $i_2 = 0$ and (*ii*) $i_1 = 0$ and $i_2 = I_2$.
c. Calculate the net torque (in N · m) acting on the rotor when both windings are excited such that $i_1 = i_2 = 5$ A and at angles (*i*) $\theta_m = 0°$, (*ii*) $\theta_m = 45°$, (*iii*) $\theta_m = 75°$.

■ Solution

a. Using the magnetic circuit techniques of Chapter 1, we see that the maximum inductance L_{max} for phase 1 occurs when the rotor axis is aligned with the phase-1 magnetic axis. From Eq. 1.31, we see that L_{max} is equal to

$$L_{max} = \frac{N^2 \mu_0 \alpha R D}{2g}$$

where αRD is the cross-sectional area of the air gap and $2g$ is the total gap length in the magnetic circuit. For the values given,

$$\begin{aligned} L_{max} &= \frac{N^2 \mu_0 \alpha R D}{2g} \\ &= \frac{(100)^2 (4\pi \times 10^{-7})(\pi/3)(3.8 \times 10^{-2})(0.13)}{2 \times (2.54 \times 10^{-4})} \\ &= 0.128 \text{ H} \end{aligned}$$

Neglecting fringing, the inductance $L(\theta_m)$ will vary linearly with the air-gap cross-sectional area as shown in Fig. 8.4a. Note that this idealization predicts that the inductance is zero when there is no overlap when in fact there will be some small value of inductance, as shown in Fig. 8.2.

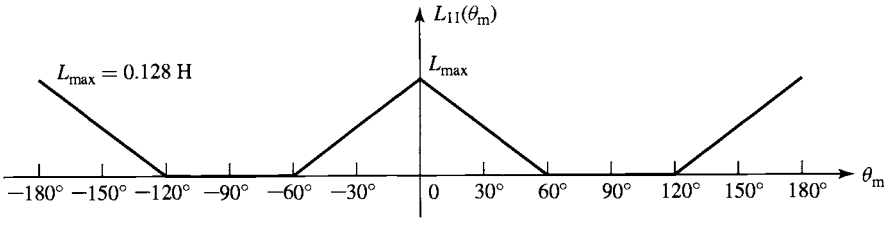

(a)

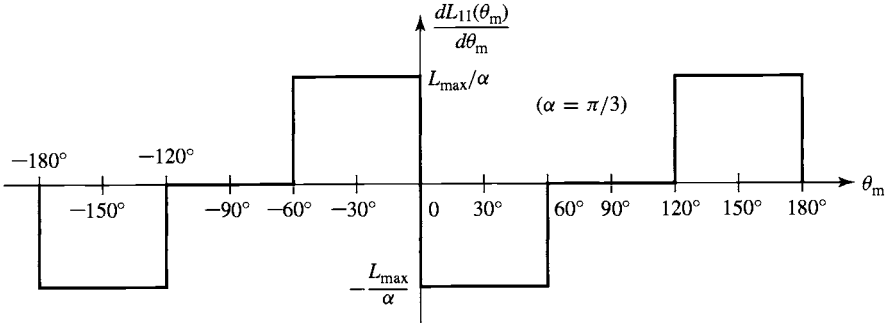

(b)

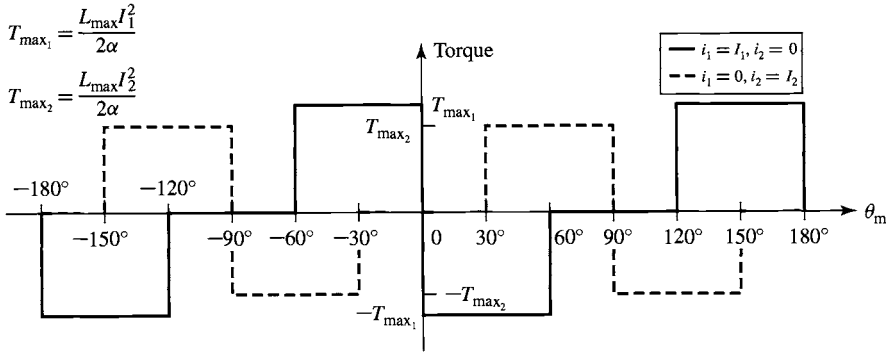

(c)

Figure 8.4 (a) $L_{11}(\theta_m)$ versus θ_m, (b) $dL_{11}(\theta_m)/d\theta_m$ versus θ_m, and (c) torque versus θ_m.

b. From Eq. 8.7, the torque consists of two terms

$$T_{mech} = \frac{1}{2} i_1^2 \frac{dL_{11}(\theta_m)}{d\theta_m} + \frac{1}{2} i_2^2 \frac{dL_{11}(\theta_m - 90°)}{d\theta_m}$$

and $dL_{11}/d\theta_m$ can be seen to be the stepped waveform of Fig. 8.4b whose maximum values are given by $\pm L_{max}/\alpha$ (with α expressed in radians!). Thus the torque is as shown in Fig. 8.4c.

c. The peak torque due to each of the windings is given by

$$T_{max} = \left(\frac{L_{max}}{2\alpha}\right) i^2 = \left(\frac{0.128}{2(\pi/3)}\right) 5^2 = 1.53 \text{ N} \cdot \text{m}$$

(*i*) From the plot in Fig. 8.4c, at $\theta_m = 0°$, the torque contribution from phase 2 is clearly zero. Although the phase-1 contribution appears to be indeterminate, in an actual machine the torque change from T_{max_1} to $-T_{max_1}$ at $\theta_m = 0°$ would have a finite slope and the torque would be zero at $\theta = 0°$. Thus the net torque from phases 1 and 2 at this position is zero.

Notice that the torque at $\theta_m = 0$ is zero independent of the current levels in phases 1 and 2. This is a problem with the 4/2 configuration of Fig. 8.3 since the rotor can get "stuck" at this position (as well as at $\theta_m = \pm 90°, \pm 180°$), and there is no way that electrical torque can be produced to move it.

(*ii*) At $\theta_m = 45°$ both phases are providing torque. That of phase 1 is negative while that of phase 2 is positive. Because the phase currents are equal, the torques are thus equal and opposite and the net torque is zero. However, unlike the case of $\theta_m = 0°$, the torque at this point can be made either positive or negative simply by appropriate selection of the phase currents.

(*iii*) At $\theta_m = 75°$ phase 1 produces no torque while phase 2 produces a positive torque of magnitude T_{max_2}. Thus the net torque at this position is positive and of magnitude 1.53 N · m. Notice that there is no combination of phase currents that will produce a negative torque at this position since the phase-1 torque is always zero while that of phase 2 can be only positive (or zero).

Practice Problem 8.1

Repeat the calculation of Example 8.1, part (c), for the case in which $\alpha = \beta = 70°$.

Solution

(i) $T = 0 \text{ N} \cdot \text{m}$
(ii) $T = 0 \text{ N} \cdot \text{m}$
(iii) $T = 1.59 \text{ N} \cdot \text{m}$

Example 8.1 illustrates a number of important considerations for the design of VRMs. Clearly these machines must be designed to avoid the occurrence of rotor positions for which none of the phases can produce torque. This is of concern in the design of 4/2 machines which will always have such positions if they are constructed with uniform, symmetric air gaps.

It is also clear that to operate VRMs with specified torque characteristics, the phase currents must be applied in a fashion consistent with the rotor position. For example, positive torque production from each phase winding in Example 8.1 can be seen from Fig. 8.4c to occur only for specific values of θ_m. Thus operation of VRMs must include some sort of rotor-position sensing as well as a controller which

determines both the sequence and the waveform of the phase currents to achieve the desired operation. This is typically implemented by using electronic switching devices (transistors, thyristors, gate-turn-off devices, etc.) under the supervision of a microprocessor-based controller.

Although a 4/2 VRM such as in Example 8.1 can be made to work, as a practical matter it is not particularly useful because of undesirable characteristics such as its zero-torque positions and the fact that there are angular locations at which it is not possible to achieve a positive torque. For example, because of these limitations, this machine cannot be made to generate a constant torque independent of rotor angle; certainly no combination of phase currents can result in torque at the zero-torque positions or positive torque in the range of angular locations where only negative torque can be produced. As discussed in Section 8.2, these difficulties can be eliminated by 4/2 designs with asymmetric geometries, and so practical 4/2 machines can be constructed.

As has been seen in this section, the analysis of VRMs is conceptually straightforward. In the case of linear machine iron (no magnetic saturation), finding the torque is simply a matter of finding the stator-phase inductances (self and mutual) as a function of rotor position, expressing the coenergy in terms of these inductances, and then calculating the derivative of the coenergy with respect to angular position (holding the phase currents constant when taking the derivative). Similarly, as discussed in Section 3.8, the electric terminal voltage for each of the phases can be found from the sum of the time derivative of the phase flux linkage and the iR drop across the phase resistance.

In the case of nonlinear machine iron (where saturation effects are important) as is discussed in Section 8.4, the coenergy can be found by appropriate integration of the phase flux linkages, and the torque can again be found from the derivative of the coenergy with respect to the angular position of the rotor. In either case, there are no rotor windings and typically no other rotor currents in a well-designed variable-reluctance motor; hence, unlike other ac machine types (synchronous and induction), there are no electrical dynamics associated with the machine rotor. This greatly simplifies their analysis.

Although VRMs are simple in concept and construction, their operation is somewhat complicated and requires sophisticated control and motor-drive electronics to achieve useful operating characteristics. These issues and others are discussed in Sections 8.2 to 8.5.

8.2 PRACTICAL VRM CONFIGURATIONS

Practical VRM drive systems (the motor and its inverter) are designed to meet operating criteria such as

- Low cost.
- Constant torque independent of rotor angular position.
- A desired operating speed range.
- High efficiency.
- A large torque-to-mass ratio.

As in any engineering situation, the final design for a specific application will involve a compromise between the variety of options available to the designer. Because VRMs require some sort of electronics and control to operate, often the designer is concerned with optimizing a characteristic of the complete drive system, and this will impose additional constraints on the motor design.

VRMs can be built in a wide variety of configurations. In Fig. 8.1, two forms of a 4/2 machine are shown: a singly-salient machine in Fig. 8.1a and a doubly-salient machine in Fig. 8.1b. Although both types of design can be made to work, a doubly-salient design is often the superior choice because it can generally produce a larger torque for a given frame size.

This can be seen qualitatively (under the assumption of a high-permeability, nonsaturating magnetic structure) by reference to Eq. 8.7, which shows that the torque is a function of $dL_{11}(\theta_m)/d\theta_m$, the derivative of the phase inductance with respect to angular position of the rotor. Clearly, all else being equal, the machine with the largest derivative will produce the largest torque.

This derivative can be thought of as being determined by the ratio of the maximum to minimum phase inductances L_{max}/L_{min}. In other words, we can write,

$$\frac{dL_{11}(\theta_m)}{d\theta_m} \cong \frac{L_{max} - L_{min}}{\Delta\theta_m} = \frac{L_{max}}{\Delta\theta_m}\left(1 - \frac{L_{min}}{L_{max}}\right) \tag{8.8}$$

where $\Delta\theta_m$ is the angular displacement of the rotor between the positions of maximum and minimum phase inductance. From Eq. 8.8, we see that, for a given L_{max} and $\Delta\theta_m$, the largest value of L_{max}/L_{min} will give the largest torque. Because of its geometry, a doubly-salient structure will typically have a lower minimum inductance and thus a larger value of L_{max}/L_{min}; hence it will produce a larger torque for the same rotor structure.

For this reason doubly-salient machines are the predominant type of VRM, and hence for the remainder of this chapter we consider only doubly-salient VRMs. In general, doubly-salient machines can be constructed with two or more poles on each of the stator and rotor. It should be pointed out that once the basic structure of a VRM is determined, L_{max} is fairly well determined by such quantities as the number of turns, air-gap length, and basic pole dimensions. The challenge to the VRM designer is to achieve a small value of L_{min}. This is a difficult task because L_{min} is dominated by leakage fluxes and other quantities which are difficult to calculate and analyze.

As shown in Example 8.1, the geometry of a symmetric 4/2 VRM with a uniform air gap gives rise to rotor positions for which no torque can be developed for any combination of excitation of the phase windings. These torque zeros can be seen to occur at rotor positions where all the stator phases are simultaneously at a position of either maximum or minimum inductance. Since the torque depends on the derivative of inductance with respect to angular position, this simultaneous alignment of maximum and minimum inductance points necessarily results in zero net torque.

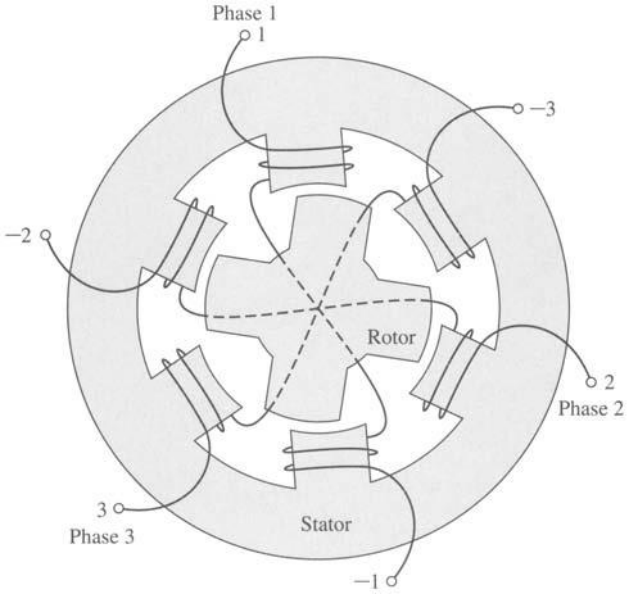

Figure 8.5 Cross-sectional view of a 6/4 three-phase VRM.

Figure 8.5 shows a 6/4 VRM from which we see that a fundamental feature of the 6/4 machine is that no such simultaneous alignment of phase inductances is possible. As a result, this machine does not have any zero-torque positions. This is a significant point because it eliminates the possibility that the rotor might get stuck in one of these positions at standstill, requiring that it be mechanically moved to a new position before it can be started. In addition to the fact that there are not positions of simultaneous alignment for the 6/4 VRM, it can be seen that there also are no rotor positions at which only a torque of a single sign (either positive or negative) can be produced. Hence by proper control of the phase currents, it should be possible to achieve constant-torque, independent of rotor position.

In the case of a symmetric VRM with p_s stator poles and p_r rotor poles, a simple test can be used to determine if zero-torque positions exist. If the ratio p_s/p_r (or alternatively p_r/p_s if p_r is larger than p_s) is an integer, there will be zero-torque positions. For example, for a 6/4 machine the ratio is 1.5, and there will be no zero-torque positions. However, the ratio is 2.0 for a 6/3 machine, and there will be zero-torque positions.

In some instances, design constraints may dictate that a machine with an integral pole ratio is desirable. In these cases, it is possible to eliminate the zero-torque positions by constructing a machine with an asymmetric rotor. For example, the rotor radius can be made to vary with angle as shown in grossly exaggerated fashion in Fig. 8.6a. This design, which also requires that the width of the rotor pole be wider than that of the stator, will not produce zero torque at positions of alignment because $dL(\theta_m)/d\theta_m$ is not zero at these points, as can be seen with reference to Fig. 8.6b.

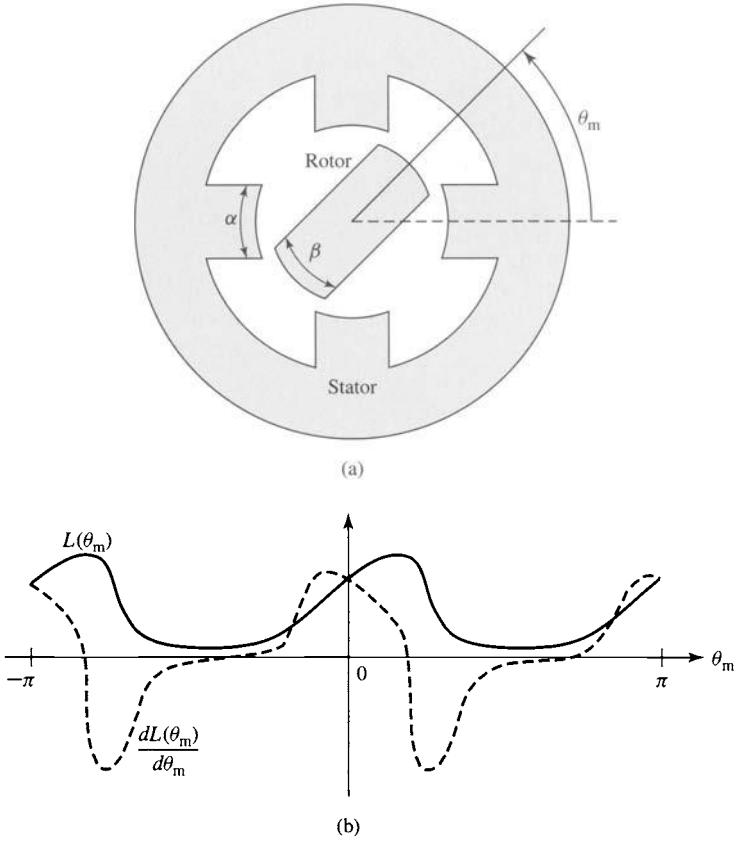

Figure 8.6 A 4/2 VRM with nonuniform air gap: (a) exaggerated schematic view and (b) plots of $L(\theta_m)$ and $dL(\theta_m)/d\theta_m$ versus θ_m.

An alternative procedure for constructing an integral-pole-ratio VRM without zero-torque positions is to construct a stack of two or more VRMs in series, aligned such that each of the VRMs is displaced in angle from the others and with all rotors sharing a common shaft. In this fashion, the zero-torque positions of the individual machines will not align, and thus the complete machine will not have any torque zeros. For example, a series stack of two two-phase, 4/2 VRMs such as that of Example 8.1 (Fig. 8.3) with a 45° angular displacement between the individual VRMs will result in a four-phase VRM without zero-torque positions.

Generally VRMs are wound with a single coil on each pole. Although it is possible to control each of these windings separately as individual phases, it is common practice to combine them into groups of poles which are excited simultaneously. For example, the 4/2 VRM of Fig. 8.3 is shown connected as a two-phase machine. As shown in Fig. 8.5, a 6/4 VRM is commonly connected as a three-phase machine with opposite poles connected to the same phase and in such a fashion that the windings drive flux in the same direction through the rotor.

In some cases, VRMs are wound with a parallel set of windings on each phase. This configuration, known as a *bifilar winding,* in some cases can result in a simple inverter configuration and thus a simple, inexpensive motor drive. The use of a bifilar winding in VRM drives is discussed in Section 11.4.

In general, when a given phase is excited, the torque is such that the rotor is pulled to the nearest position of maximum flux linkage. As excitation is removed from that phase and the next phase is excited, the rotor "follows" as it is then pulled to a new maximum flux-linkage position. Thus, the rotor speed is determined by the frequency of the phase currents. However, unlike the case of a synchronous machine, the relationship between the rotor speed and the frequency and sequence of the phase-winding excitation can be quite complex, depending on the number of rotor poles and the number of stator poles and phases. This is illustrated in Example 8.2.

EXAMPLE 8.2

Consider a four-phase, 8/6 VRM. If the stator phases are excited sequentially, with a total time of T_0 sec required to excite the four phases (i.e., each phase is excited for a time of $T_0/4$ sec), find the angular velocity of the stator flux wave and the corresponding angular velocity of the rotor. Neglect any system dynamics and assume that the rotor will instantaneously track the stator excitation.

■ Solution

Figure 8.7 shows in schematic form an 8/6 VRM. The details of the pole shapes are not of importance for this example and thus the rotor and stator poles are shown simply as arrows indicating their locations. The figure shows the rotor aligned with the stator phase-1 poles. This position corresponds to that which would occur if there were no load on the rotor and the stator phase-1 windings were excited, since it corresponds to a position of maximum phase-1 flux linkage.

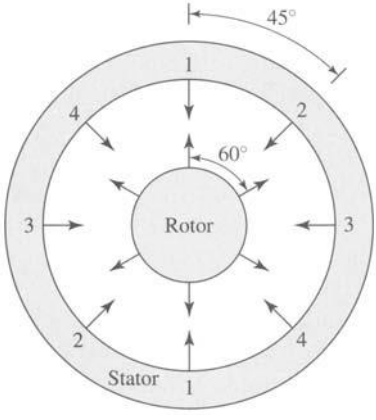

Figure 8.7 Schematic view of a four-phase 8/6 VRM. Pole locations are indicated by arrows.

Consider next that the excitation on phase 1 is removed and phase 2 is excited. At this point, the stator flux wave has rotated 45° in the clockwise direction. Similarly, as the excitation on phase 2 is removed and phase 3 is excited, the stator flux wave will move an additional 45° clockwise. Thus the angular velocity ω_s of the stator flux wave can be calculated quite simply as $\pi/4$ rad (45°) divided by $T_0/4$ sec, or $\omega_s = \pi/T_0$ rad/sec.

Note, however, that this is not the angular velocity of the rotor itself. As the phase-1 excitation is removed and phase 2 is excited, the rotor will move in such a fashion as to maximize the phase-2 flux linkages. In this case, Fig. 8.7 shows that the rotor will move 15° counterclockwise since the nearest rotor poles to phase 2 are actually 15° ahead of the phase-2 poles. Thus the angular velocity of the rotor can be calculated as $-\pi/12$ rad (15°, with the minus sign indicating counterclockwise rotation) divided by $T_0/4$ sec, or $\omega_m = -\pi/(3T_0)$ rad/sec.

In this case, the rotor travels at one-third the angular velocity of the stator excitation and in the opposite direction!

Practice Problem 8.2

Repeat the calculation of Example 8.2 for the case of a four-phase, 8/10 VRM.

Solution

$$\omega_m = \pi/(5T_0) \text{ rad/sec}$$

Example 8.2 illustrates the complex relationship that can exist between the excitation frequency of a VRM and the "synchronous" rotor frequency. This relationship is directly analogous to that between two mechanical gears for which the choice of different gear shapes and configurations gives rise to a wide range of speed ratios. It is difficult to derive a single rule which will describe this relationship for the immense variety of VRM configurations which can be envisioned. It is, however, a fairly simple matter to follow a procedure similar to that shown in Example 8.2 to investigate any particular configuration of interest.

Further variations on VRM configurations are possible if the main stator and rotor poles are subdivided by the addition of individual teeth (which can be thought of as a set of small poles excited simultaneously by a single winding). The basic concept is illustrated in Fig. 8.8, which shows a schematic view of three poles of a three-phase VRM with a total of six main stator poles. Such a machine, with the stator and rotor poles subdivided into teeth, is known as a *castleated* VRM, the name resulting from the fact that the stator teeth appear much like the towers of a medieval castle.

In Fig. 8.8 each stator pole has been divided into four subpoles by the addition of four teeth of width $6\frac{3}{7}^\circ$ (indicated by the angle β in the figure), with a slot of the same width between each tooth. The same tooth/slot spacing is chosen for the rotor, resulting in a total of 28 teeth on the rotor. Notice that this number of rotor teeth and the corresponding value of β were chosen so that when the rotor teeth are aligned with those of the phase-1 stator pole, they are not aligned with those of phases 2 and 3. In this fashion, successive excitation of the stator phases will result in a rotation of the rotor.

Castleation further complicates the relationship between the rotor speed and the frequency and sequence of the stator-winding excitation. For example, from Fig. 8.8

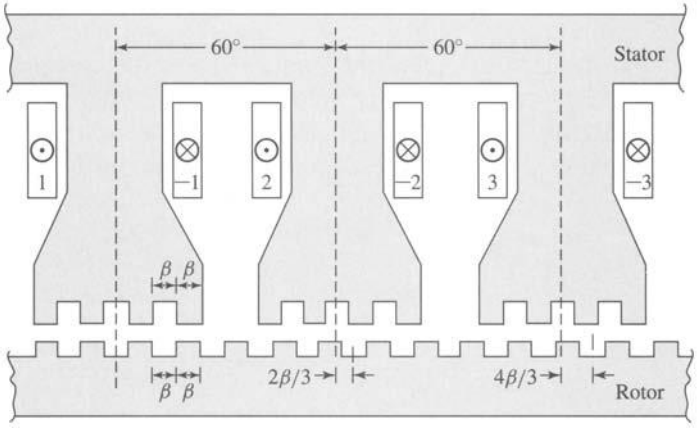

Figure 8.8 Schematic view of a three-phase castleated VRM with six stator poles and four teeth per pole and 28 rotor poles.

it can be seen that for this configuration, when the excitation of phase 1 is removed and phase 2 is excited (corresponding to a rotation of the stator flux wave by 60° in the clockwise direction), the rotor will rotate by an angle of $(2\beta/3) = 4\frac{2}{7}^\circ$ in the counterclockwise direction.

From the preceding analysis, we see that the technique of castleation can be used to create VRMs capable of operating at low speeds (and hence producing high torque for a given stator power input) and with very precise rotor position accuracy. For example, the machine of Fig. 8.8 can be rotated precisely by angular increments of $(2\beta/3)$. The use of more teeth can further increase the position resolution of these machines. Such machines can be found in applications where low speed, high torque, and precise angular resolution are required. This castleated configuration is one example of a class of VRMs commonly referred to as *stepping motors* because of their capability to produce small steps in angular resolution.

8.3 CURRENT WAVEFORMS FOR TORQUE PRODUCTION

As is seen in Section 8.1, the torque produced by a VRM in which saturation and mutual-inductance effects can be neglected is determined by the summation of terms consisting of the derivatives of the phase inductances with respect to the rotor angular position, each multiplied by the square of the corresponding phase current. For example, we see from Eqs. 8.6 and 8.7 that the torque of the two-phase, 4/2 VRM of Fig. 8.1b is given by

$$T_{\text{mech}} = \frac{1}{2}i_1^2\frac{dL_{11}(\theta_{\text{m}})}{d\theta_{\text{m}}} + \frac{1}{2}i_2^2\frac{dL_{22}(\theta_{\text{m}})}{d\theta_{\text{m}}}$$

$$= \frac{1}{2}i_1^2\frac{dL_{11}(\theta_{\text{m}})}{d\theta_{\text{m}}} + \frac{1}{2}i_2^2\frac{dL_{11}(\theta_{\text{m}} - 90^\circ)}{d\theta_{\text{m}}} \tag{8.9}$$

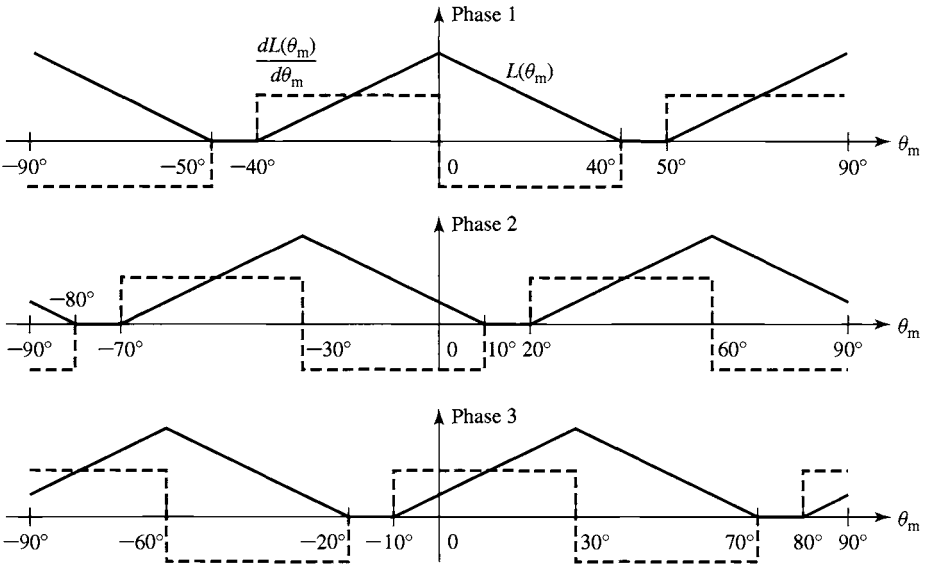

Figure 8.9 Idealized inductance and $dL/d\theta_m$ curves for a three-phase 6/4 VRM with 40° rotor and stator poles.

For each phase of a VRM, the phase inductance is periodic in rotor angular position, and thus the area under the curve of $dL/d\theta_m$ calculated over a complete period of $L(\theta_m)$ is zero, i.e.,

$$\int_0^{2\pi/p_r} \frac{dL(\theta_m)}{d\theta_m}\, d\theta_m = L(2\pi/p_r) - L(0) = 0 \tag{8.10}$$

where p_r is the number of rotor poles.

The average torque produced by a VRM can be found by integrating the torque equation (Eq. 8.9) over a complete period of rotation. Clearly, if the stator currents are held constant, Eq. 8.10 shows that the average torque will be zero. Thus, to produce a time-averaged torque, the stator currents must vary with rotor position. The desired average output torque for a VRM depends on the nature of the application. For example, motor operation requires a positive time-averaged shaft torque. Similarly, braking or generator action requires negative time-averaged torque.

Positive torque is produced when a phase is excited at angular positions with positive $dL/d\theta_m$ for that phase, and negative torque is produced by excitation at positions at which $dL/d\theta_m$ is negative. Consider a three-phase, 6/4 VRM (similar to that shown in Fig. 8.5) with 40° rotor and stator poles. The inductance versus rotor position for this machine will be similar to the idealized representation shown in Fig. 8.9.

Operation of this machine as a motor requires a net positive torque. Alternatively, it can be operated as a generator under conditions of net negative torque. Noting that

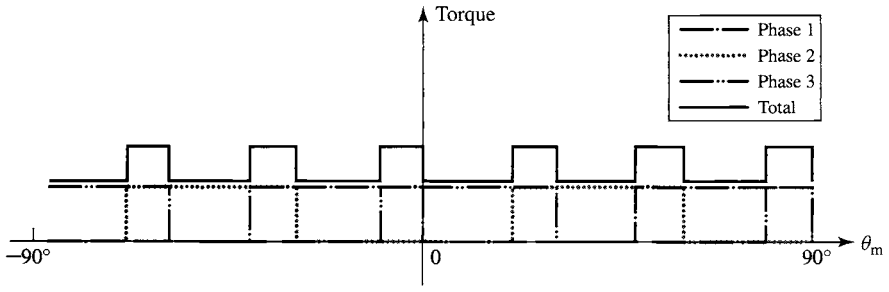

Figure 8.10 Individual phase torques and total torque for the motor of Fig. 8.9. Each phase is excited with a constant current I_0 only at positions where $dL/d\theta_m > 0$.

positive torque is generated when excitation is applied at rotor positions at which $dL/d\theta_m$ is positive, we see that a control system is required that determines rotor position and applies the phase-winding excitations at the appropriate time. It is, in fact, the need for this sort of control that makes VRM drive systems more complex than might perhaps be thought, considering only the simplicity of the VRM itself.

One of the reasons that VRMs have found application in a wide variety of situations is because the widespread availability and low cost of microprocessors and power electronics have brought the cost of the sensing and control required to successfully operate VRM drive systems down to a level where these systems can be competitive with competing technologies. Although the control of VRM drives is more complex than that required for dc, induction, and permanent-magnet ac motor systems, in many applications the overall VRM drive system turns out to be less expensive and more flexible than the competition.

Assuming that the appropriate rotor-position sensor and control system is available, the question still remains as to how to excite the armature phases. From Fig. 8.9, one possible excitation scheme would be to apply a constant current to each phase at those angular positions at which $dL/d\theta_m$ is positive and zero current otherwise.

If this is done, the resultant torque waveform will be that of Fig. 8.10. Note that because the torque waveforms of the individual phases overlap, the resultant torque will not be constant but rather will have a pulsating component on top of its average value. In general, such pulsating torques are to be avoided both because they may produce damaging stresses in the VRM and because they may result in the generation of excessive vibration and noise.

Consideration of Fig. 8.9 shows that there are alternative excitation strategies which can reduce the torque pulsations of Fig. 8.10. Perhaps the simplest strategy is to excite each phase for only 30° of angular position instead of the 40° which resulted in Fig. 8.9. Thus, each phase would simply be turned off as the next phase is turned on, and there would be no torque overlap between phases.

Although this strategy would be an ideal solution to the problem, as a practical matter it is not possible to implement. The problem is that because each phase winding has a self-inductance, it is not possible to instantaneously switch on or off the phase

currents. Specifically, for a VRM with independent (uncoupled) phases,[2] the voltage-current relationship of the jth phase is given by

$$v_j = R_j i_j + \frac{d\lambda_j}{dt} \tag{8.11}$$

where

$$\lambda_j = L_{jj}(\theta_m) i_j \tag{8.12}$$

Thus,

$$v_j = R_j i_j + \frac{d}{dt}[L_{jj}(\theta_m) i_j] \tag{8.13}$$

Equation 8.13 can be rewritten as

$$v_j = \left\{ R_j + \frac{d}{dt}[L_{jj}(\theta_m)] \right\} i_j + L_{jj}(\theta_m) \frac{di_j}{dt} \tag{8.14}$$

or

$$v_j = \left[R_j + \frac{dL_{jj}(\theta_m)}{d(\theta_m)} \frac{d\theta_m}{dt} \right] i_j + L_{jj}(\theta_m) \frac{di_j}{dt} \tag{8.15}$$

Although Eqs. 8.13 through 8.15 are mathematically complex and often require numerical solution, they clearly indicate that some time is required to build up currents in the phase windings following application of voltage to that phase. A similar analysis can be done for conditions associated with removal of the phase currents. The delay time associated with current build up can limit the maximum achievable torque while the current decay time can result in negative torque if current is still flowing when $dL(\theta_m)/d\theta_m$ reverses sign. These effects are illustrated in Example 8.3 which also shows that in cases where winding resistance can be neglected, an approximate solution to these equations can be found.

EXAMPLE 8.3

Consider the idealized 4/2 VRM of Example 8.1. Assume that it has a winding resistance of $R = 1.5\ \Omega$/phase and a leakage inductance $L_l = 5$ mH in each phase. For a constant rotor speed of 4000 r/min, calculate (a) the phase-1 current as a function of time during the interval $-60° \le \theta_m \le 0°$, assuming that a constant voltage of $V_0 = 100$ V is applied to phase 1 just as $dL_{11}(\theta_m)/d\theta_m$ becomes positive (i.e., at $\theta_m = -60° = -\pi/3$ rad), and (b) the decay of phase-1 current if a negative voltage of -200 V is applied at $\theta_m = 0°$ and maintained until the current reaches zero. (c) Using MATLAB†, plot these currents as well as the corresponding torque. Also calculate the integral under the torque-versus-time plot and compare it to the integral under the torque-versus-time curve for the time period during which the torque is positive.

[2] The reader is reminded that in some cases the assumption of independent phases is not justified, and then a more complex analysis of the VRM is required (see the discussion following the derivation of Eq. 8.5).

† MATLAB is a registered trademark of The MathWorks, Inc.

■ Solution

a. From Eq. 8.15, the differential equation governing the current buildup in phase 1 is given by

$$v_1 = \left[R + \frac{dL_{11}(\theta_m)}{d\theta_m}\frac{d\theta_m}{dt}\right] i_1 + L_{11}(\theta_m)\frac{di_1}{dt}$$

At 4000 r/min,

$$\omega_m = \frac{d\theta_m}{dt} = 4000 \text{ r/min} \times \frac{\pi}{30}\left[\frac{\text{rad/sec}}{\text{r/min}}\right] = \frac{400\pi}{3} \text{ rad/sec}$$

From Fig. 8.4 (for $-60° \leq \theta_m \leq 0°$)

$$\begin{aligned} L_{11}(\theta_m) &= L_l + \frac{L_{max}}{\pi/3}\left(\theta_m + \frac{\pi}{3}\right) \\ &= 0.005 + 0.122(\theta_m + \pi/3) \end{aligned}$$

Thus

$$\frac{dL_{11}(\theta_m)}{d\theta_m} = 0.122 \text{ H/rad}$$

and

$$\frac{dL_{11}(\theta_m)}{d\theta_m}\frac{d\theta_m}{dt} = 51.1\ \Omega$$

which is much greater than the resistance $R = 1.5\ \Omega$

This will enable us to obtain an approximate solution for the current by neglecting the Ri term in Eq. 8.13. We must then solve

$$\frac{d(L_{11}i_1)}{dt} = v_1$$

for which the solution is

$$i_1(t) = \frac{\int_0^t v_1 dt}{L_{11}(t)} = \frac{V_0 t}{L_{11}(t)}$$

Substituting

$$\theta_m = -\frac{\pi}{3} + \omega_m t$$

into the expression for $L_{11}(\theta_m)$ then gives

$$i_1(t) = \frac{100t}{0.005 + 51.1t} \text{ A}$$

which is valid until $\theta_m = 0°$ at $t = 2.5$ msec, at which point $i_1(t) = 1.88$ A.

b. During the period of current decay the solution proceeds as in part (a). From Fig. 8.4, for $0° \leq \theta_m \leq 60°$, $dL_{11}(\theta_m)/dt = -51.1\ \Omega$ and the Ri term can again be ignored in Eq. 8.13.

Thus, since the applied voltage is -200 V for this time period ($t \geq 2.5$ msec until $i_1(t) = 0$) in an effort to bring the current rapidly to zero, since the current must be

continuous at time $t_0 = 2.5$ msec, and since, from Fig. 8.4 (for $0° \leq \theta_m \leq 60°$)

$$L_{11}(\theta_m) = L_l + \frac{L_{max}}{\pi/3}\left(\frac{\pi}{3} - \theta_m\right)$$
$$= 0.005 + 0.122(\pi/3 - \theta_m)$$

we see that the solution becomes

$$i_1(t) = \frac{L_{11}(t_0)i_1(t_0) + \int_{t_0}^{t} v_1\, dt}{L_{11}(t)}$$
$$= \frac{0.25 - 200(t - 2.5 \times 10^{-3})}{0.005 + 51.1(5 \times 10^{-3} - t)}$$

From this equation, we see that the current reaches zero at $t = 3.75$ msec.

c. The torque can be found from Eq. 8.9 by setting $i_2 = 0$. Thus

$$T_{mech} = \frac{1}{2} i_1^2 \frac{dL_{11}}{d\theta_m}$$

Using MATLAB and the results of parts (a) and (b), the current waveform is plotted in Fig. 8.11a and the torque in Fig. 8.11b. The integral under the torque curve is 3.35×10^{-4} N · m · sec while that under the positive portion of the torque curve corresponding to positive torque is 4.56×10^{-4} N · m · sec. Thus we see that the negative torque produces a 27 percent reduction in average torque from that which would otherwise be available if the current could be reduced instantaneously to zero.

Notice first from the results of part (b) and from Fig. 8.11a that, in spite of applying a negative voltage of twice the magnitude of the voltage used to build up the current, current continues to flow in the winding for 1.25 ms after reversal of the applied voltage. From Fig. 8.11b, we see that the result is a significant period of negative torque production. In practice, this may, for example, dictate a control scheme which reverses the phase current in advance of the time that the sign of $dL(\theta_m)/d\theta_m$ reverses, achieving a larger average torque by trading off some reduction in average positive torque against a larger decrease in average negative torque.

This example also illustrates another important aspect of VRM operation. For a system of resistance of 1.5 Ω and constant inductance, one would expect a steady-state current of $100/1.5 = 66.7$ A. Yet in this system the steady-state current is less than 2 A. The reason for this is evident from Eqs. 8.14 and 8.15 where we see that $dL_{11}(\theta_m)/dt = 51.1$ Ω appears as an apparent resistance in series with the winding resistance which is much larger than the winding resistance itself. The corresponding voltage drop (the speed voltage) is of sufficient magnitude to limit the steady-state current to a value of $100/51.1 = 1.96$ A.

Here is the MATLAB script:

```
clc
clear

% Here are the inductances
Lmax = 0.128;
Lleak = 0.005;

Posintegral = 0;
integral = 0;
```

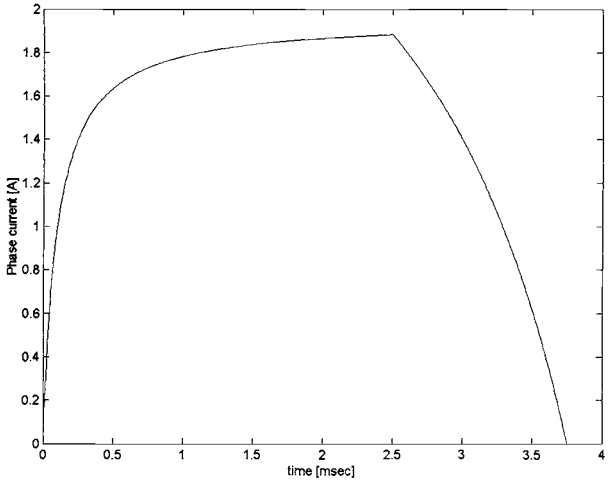

(a)

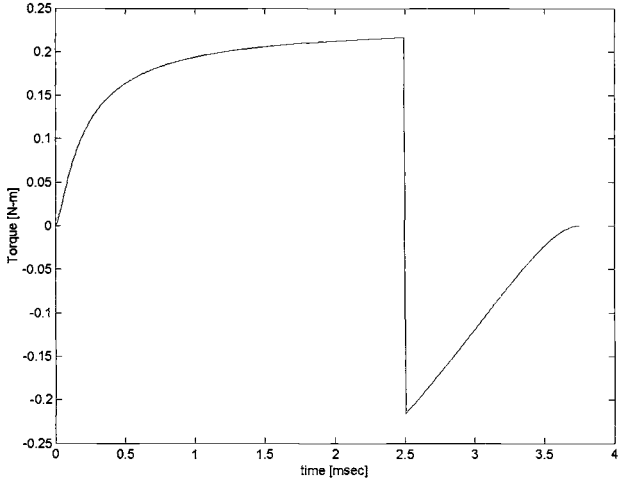

(b)

Figure 8.11 Example 8.3: (a) phase-1 current and (b) torque profile.

```
N = 500;
tmax = 3.75e-3;
deltat = tmax/N;

% Now do the calculations
for n = 1:(N+1)

   t(n) = tmax*(n-1)/N;
   thetam(n) = -(pi/3) + (400*pi/3) * t(n);
```

```
    if (thetam(n) <= 0)
      i(n) = 100*t(n)/(0.005 + 51.1 *t(n));
      dld11dtheta = 0.122;
      Torque(n) = 0.5*i(n)^2*dld11dtheta;
      Posintegral = Posintegral + Torque(n)*deltat;
      integral = Posintegral;
    else
      i(n) = (0.25 - 200*(t(n) - 2.5e-3))/(0.005+51.1*(5e-3 - t(n)));
      dld11dtheta = -0.122;
      Torque(n) = 0.5*i(n)^2*dld11dtheta;
      integral = integral + Torque(n)*deltat;
    end
end

fprintf('\nPositive torque integral = %g [N-m-sec]',Posintegral)
fprintf('\nTorque integral = %g [N-m-sec]\n',integral)

plot(t*1000,i)
xlabel('time [msec]')
ylabel('Phase current [A]')

pause

plot(t*1000,Torque)
xlabel('time [msec]')
ylabel('Torque [N-m]')
```

Practice Problem 8.3

Reconsider Example 8.3 under the condition that a voltage of -250 V is applied to turn off the phase current. Use MATLAB to calculate the integral under the torque-versus-time plot and compare it to the integral under the torque-versus-time curve for the time period during which the torque is positive.

Solution

The current returns to zero at $t = 3.5$ msec. The integral under the torque curve is 3.67×10^{-4} N · m · s while that under the positive portion of the torque curve corresponding to positive torque remains equal to 4.56×10^{-4} N · m · s. In this case, the negative torque produces a 20 percent reduction in torque from that which would otherwise be available if the current could be reduced instantaneously to zero.

Example 8.3 illustrates important aspects of VRM performance which do not appear in an idealized analysis such as that of Example 8.1 but which play an extremely important role in practical applications. It is clear that it is not possible to readily apply phase currents of arbitrary waveshapes. Winding inductances (and their time

derivatives) significantly affect the current waveforms that can be achieved for a given applied voltage.

In general, the problem becomes more severe as the rotor speed is increased. Consideration of Example 8.3 shows, for a given applied voltage, (1) that as the speed is increased, the current will take a larger fraction of the available time during which $dL(\theta_m)/d\theta_m$ is positive to achieve a given level and (2) that the steady-state current which can be achieved is progressively lowered. One common method for maximizing the available torque is to apply the phase voltage somewhat in advance of the time when $dL(\theta_m)/d\theta_m$ begins to increase. This gives the current time to build up to a significant level before torque production begins.

Yet a more significant difficulty (also illustrated in Example 8.3) is that just as the currents require a significant amount of time to increase at the beginning of a turn-on cycle, they also require time to decrease at the end. As a result, if the phase excitation is removed at or near the end of the positive $dL(\theta_m)/d\theta_m$ period, it is highly likely that there will be phase current remaining as $dL(\theta_m)/d\theta_m$ becomes negative, so there will be a period of negative torque production, reducing the effective torque-producing capability of the VRM.

One way to avoid such negative torque production would be to turn off the phase excitation sufficiently early in the cycle that the current will have decayed essentially to zero by the time that $dL(\theta_m)/d\theta_m$ becomes negative. However, there is clearly a point of diminishing returns, because turning off the phase current while $dL(\theta_m)/d\theta_m$ is positive also reduces positive torque production. As a result, it is often necessary to accept a certain amount of negative torque (to get the required positive torque) and to compensate for it by the production of additional positive torque from another phase.

Another possibility is illustrated in Fig. 8.12. Figure 8.12a shows the cross-sectional view of a 4/2 VRM similar to that of Fig. 8.3 with the exception that the rotor pole angle has been increased from 60° to 75°, with the result that the rotor pole overhangs that of the stator by 15°. As can be seen from Fig. 8.12b, this results in a region of constant inductance separating the positive and negative $dL(\theta_m)/d\theta_m$ regions, which in turn provides additional time for the phase current to be turned off before the region of negative torque production is reached.

Although Fig. 8.12 shows an example with 15° of rotor overhang, in any particular design the amount of overhang would be determined as part of the overall design process and would depend on such issues as the amount of time required for the phase current to decay and the operating speed of the VRM. Also included in this design process must be recognition that the use of wider rotor poles will result in a larger value of L_{min}, which itself tends to reduce torque production (see the discussion of Eq. 8.8) and to increase the time for current buildup.

Under conditions of constant-speed operation, it is often desirable to achieve constant torque independent of rotor position. Such operation will minimize pulsating torques which may cause excessive noise and vibration and perhaps ultimately lead to component failure due to material fatigue. This means that as the torque production of one phase begins to decrease, that of another phase must increase to compensate. As can be seen from torque waveforms such as those found in Fig. 8.11, this represents a

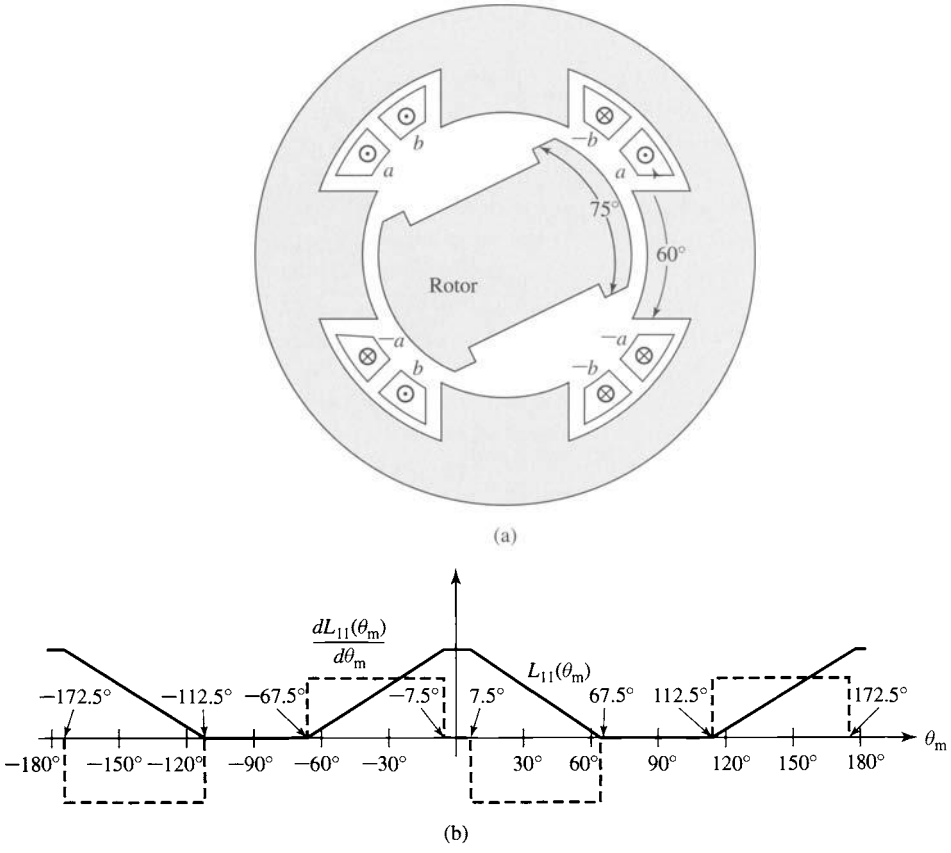

Figure 8.12 A 4/2 VRM with 15° rotor overhang: (a) cross-sectional view and (b) plots of $L_{11}(\theta_m)$ and $dL_{11}(\theta_m)/d\theta_m$ versus θ_m.

complex control problem for the phase excitation, and totally ripple-free torque will be difficult to achieve in many cases.

8.4 NONLINEAR ANALYSIS

Like most electric machines, VRMs employ magnetic materials both to direct and shape the magnetic fields in the machine and to increase the magnetic flux density that can be achieved from a given amplitude of current. To obtain the maximum benefit from the magnetic material, practical VRMs are operated with the magnetic flux density high enough so that the magnetic material is in saturation under normal operating conditions.

As with the synchronous, induction, and dc machines discussed in Chapters 5–7, the actual operating flux density is determined by trading off such quantities as cost, efficiency, and torque-to-mass ratio. However, because the VRM and its drive electronics are quite closely interrelated, VRMs design typically involves additional trade-offs that in turn affect the choice of operating flux density.

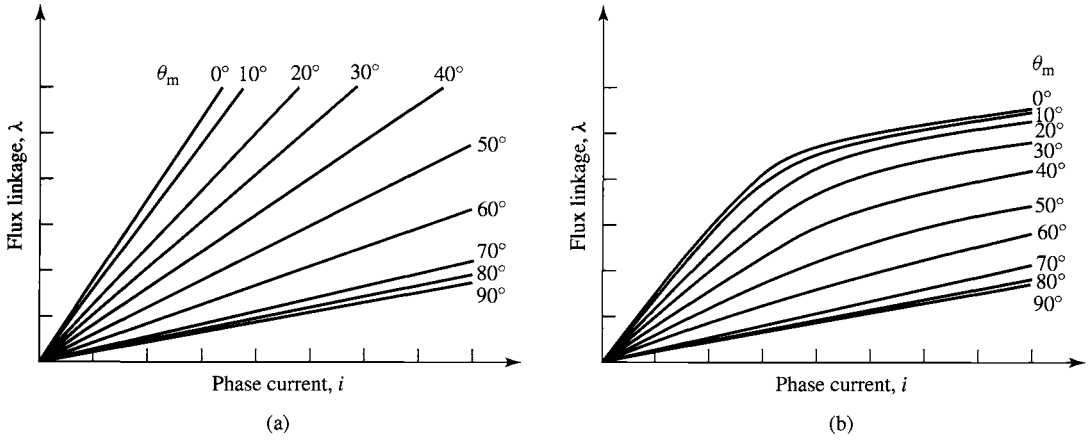

Figure 8.13 Plots of λ versus i for a VRM with (a) linear and (b) nonlinear magnetics.

Figure 8.2 shows typical inductance-versus-angle curves for the VRMs of Fig. 8.1. Such curves are characteristic of all VRMs. It must be recognized that the use of the concept of inductance is strictly valid only under the condition that the magnetic circuit in the machine is linear so that the flux density (and hence the winding flux linkage) is proportional to the winding current. This linear analysis is based on the assumption that the magnetic material in the motor has constant magnetic permeability. This assumption was used for all the analyses earlier in this chapter.

An alternate representation of the flux-linkage versus current characteristic of a VRM is shown in Fig. 8.13. This representation consists of a series of plots of the flux linkage versus current at various rotor angles. In this figure, the curves correspond to a machine with a two-pole rotor such as in Fig. 8.1, and hence a plot of curves from 0° to 90° is sufficient to completely characterize the machine.

Figure 8.13a shows the set of λ-i characteristics which would be measured in a machine with linear magnetics, i.e., constant magnetic permeability and no magnetic saturation. For each rotor angle, the curve is a straight line whose slope corresponds to the inductance $L(\theta_m)$ at that angular position. In fact, a plot of $L(\theta_m)$ versus θ_m such as in Fig. 8.2 is an equivalent representation to that of Fig. 8.13a.

In practice, VRMs do operate with their magnetic material in saturation and their λ-i characteristics take on the form of Fig. 8.13b. Notice that for low current levels, the curves are linear, corresponding to the assumption of linear magnetics of Fig. 8.13a. However, for higher current levels, saturation begins to occur and the curves bend over steeply, with the result that there is significantly less flux linkage for a given current level. Finally, note that saturation effects are maximum at $\theta_m = 0°$ (for which the rotor and stator poles are aligned) and minimal for higher angles as the rotor approaches the nonaligned position.

Saturation has two important, somewhat contradictory effects on VRM performance. On the one hand, saturation limits flux densities for a given current level and thus tends to limit the amount of torque available from the VRM. On the other hand, it can be shown that saturation tends to lower the required inverter volt-ampere rating

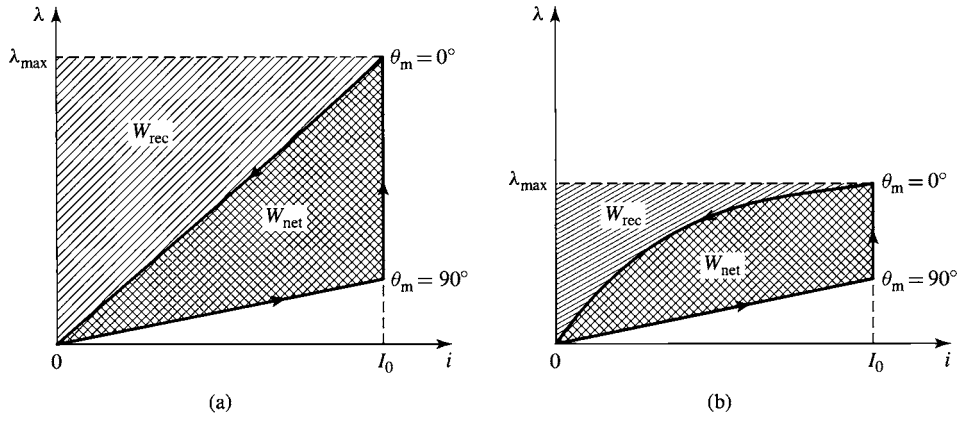

Figure 8.14 (a) Flux-linkage-current trajectory for the (a) linear and (b) nonlinear machines of Fig. 8.13.

for a given VRM output power and thus tends to make the inverter smaller and less costly. A well-designed VRM system will be based on a trade-off between the two effects.[3]

These effects of saturation can be investigated by considering the two machines of Figs. 8.13a and b operating at the same rotational speed and under the same operating condition. For the sake of simplicity, we assume a somewhat idealized condition in which the phase-1 current is instantaneously switched on to a value I_0 at $\theta_m = -90°$ (the unaligned position for phase 1) and is instantaneously switched off at $\theta_m = 0°$ (the aligned position). This operation is similar to that discussed in Example 8.1 in that we will neglect the complicating effects of the current buildup and decay transients which are illustrated in Example 8.3.

Because of rotor symmetry, the flux linkages for negative rotor angles are identical to those for positive angles. Thus, the flux linkage-current trajectories for one current cycle can be determined from Figs. 8.13a and b and are shown for the two machines in Figs. 8.14a and b.

As each trajectory is traversed, the power input to the winding is given by its volt-ampere product

$$p_{in} = iv = i\frac{d\lambda}{dt} \tag{8.16}$$

The net electric energy input to the machine (the energy that is converted to mechanical work) in a cycle can be determined by integrating Eq. 8.16 around the

[3] For a discussion of saturation effects in VRM drive systems, see T. J. E. Miller, "Converter Volt-Ampere Requirements of the Switched Reluctance Motor," *IEEE Trans. Ind. Appl.*, IA-21:1136–1144 (1985).

trajectory

$$\text{Net work} = \int p_{\text{in}}\, dt = \oint i\, d\lambda \tag{8.17}$$

This can be seen graphically as the area enclosed by the trajectory, labeled W_{net} in Figs. 8.14a and b. Note that the saturated machine converts less useful work per cycle than the unsaturated machine. As a result, to get a machine of the same power output, the saturated machine will have to be larger than a corresponding (hypothetical) unsaturated machine. This analysis demonstrates the effects of saturation in lowering torque and power output.

The peak energy input to the winding from the inverter can also be calculated. It is equal to the integral of the input power from the start of the trajectory to the point $(I_0, \lambda_{\max})$:

$$\text{Peak energy} = \int_0^{\lambda_{\max}} i\, d\lambda \tag{8.18}$$

This is the total area under the λ-i curve, shown in Fig. 8.14a and b as the sum of the areas labeled W_{rec} and W_{net}.

Since we have seen that the energy represented by the area W_{net} corresponds to useful output energy, it is clear that the energy represented by the area W_{rec} corresponds to energy input that is required to make the VRM operate (i.e., it goes into creating the magnetic fields in the VRM). This energy produced no useful work; rather it must be recycled back into the inverter at the end of the trajectory.

The inverter volt-ampere rating is determined by the average power per phase processed by the inverter as the motor operates, equal to the peak energy input to the VRM divided by the time T between cycles. Similarly, the average output power per phase of the VRM is given by the net energy input per cycle divided by T. Thus the ratio of the inverter volt-ampere rating to power output is

$$\frac{\text{Inverter volt-ampere rating}}{\text{Net output area}} = \frac{\text{area}(W_{\text{rec}} + W_{\text{net}})}{\text{area}(W_{\text{net}})} \tag{8.19}$$

In general, the inverter volt-ampere rating determines its cost and size. Thus, for a given power output from a VRM, a smaller ratio of inverter volt-ampere rating to output power means that the inverter will be both smaller and cheaper. Comparison of Figs. 8.14a and b shows that this ratio is smaller in the machine which saturates; the effect of saturation is to lower the amount of energy which must be recycled each cycle and hence the volt-ampere rating of the inverter required to supply the VRM.

EXAMPLE 8.4

Consider a symmetrical two-phase 4/2 VRM whose λ-i characteristic can be represented by the following λ-i expression (for phase 1) as a function of θ_{m} over the range $0 \le \theta_{\text{m}} \le 90°$

$$\lambda_1 = \left(0.005 + 0.09\left(\frac{90° - \theta_{\text{m}}}{90°}\right)\left(\frac{8.0}{8.0 + i_1}\right)\right) i_1$$

Phase 2 of this motor is identical to that of phase 1, and there is no significant mutual inductance between the phases. Assume that the winding resistance is negligible.

a. Using MATLAB, plot a family of λ_1-i_1 curves for this motor as θ_m varies from 0 to 90° in 10° increments and as i_1 is varied from 0 to 30 A.
b. Again using MATLAB, use Eq. 8.19 and Fig. 8.14 to calculate the ratio of the inverter volt-ampere rating to the VRM net power output for the following idealized operating cycle:

   (*i*) The current is instantaneously raised to 25 A when $\theta_m = -90°$.
   (*ii*) The current is then held constant as the rotor rotates to $\theta_m = 0°$.
   (*iii*) At $\theta_m = 0°$, the current is reduced to zero.

c. Assuming the VRM to be operating as a motor using the cycle described in part (b) and rotating at a constant speed of 2500 r/min, calculate the net electromechanical power supplied to the rotor.

■ Solution

a. The λ_1-i_1 curves are shown in Fig. 8.15a.
b. Figure 8.15b shows the areas W_{net} and W_{rec}. Note that, as pointed out in the text, the λ-i curves are symmetrical around $\theta_m = 0°$ and thus the curves for negative values of θ_m are identical to those for the corresponding positive values. The area W_{net} is bounded by the λ_1-i_1 curves corresponding to $\theta_m = 0°$ and $\theta_m = 90°$ and the line $i_1 = 25$ A. The area W_{rec} is bounded by the line $\lambda_1 = \lambda_{max}$ and the λ_1-i_1 curve corresponding to $\theta_m = 0°$, where $\lambda_{max} = \lambda_1(25\text{ A}, 0°)$.

   Using MATLAB to integrate the areas, the desired ratio can be calculated from Eq. 8.19 as

$$\frac{\text{Inverter volt-ampere rating}}{\text{Net output power}} = \frac{\text{area}(W_{rec} + W_{net})}{\text{area}(W_{net})} = 1.55$$

c. Energy equal to area(W_{net}) is supplied by each phase to the rotor twice during each revolution of the rotor. If area(W_{net}) is measured in joules, the power in watts supplied per phase is thus equal to

$$P_{phase} = 2\left(\frac{\text{area}(W_{net})}{T}\right) \text{ W}$$

   where T is the time for one revolution (in seconds).

   From MATLAB, area(W_{net}) = 9.91 joules and for 2500 r/min, $T = 60/2500 = 0.024$ sec,

$$P_{phase} = 2\left(\frac{9.91}{0.024}\right) = 825 \text{ W}$$

   and thus

$$P_{mech} = 2P_{phase} = 1650 \text{ W}$$

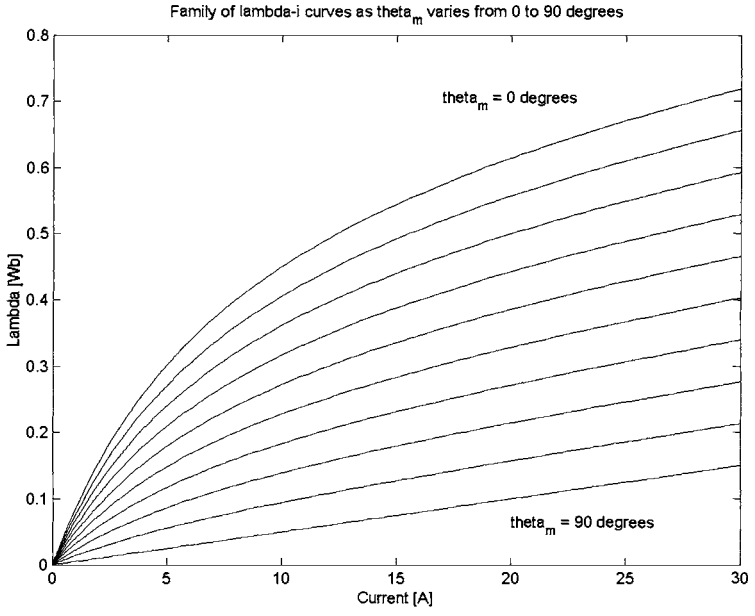

(a)

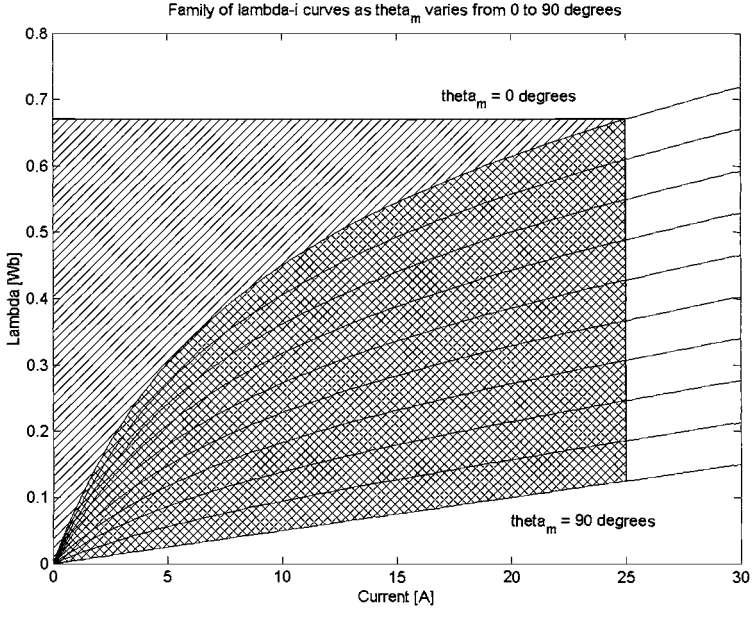

(b)

Figure 8.15 (a) λ_1-i_1 curves for Example 8.4. (b) Areas used in the calculation of part (b).

Here is the MATLAB script:

```
clc
clear
%(a) First plot the lambda i characteristics

for m = 1:10
theta(m) = 10*(m-1);
   for n=1:101
i(n) = 30*(n-1)/100;
Lambda(n) = i(n)*(0.005 + 0.09*((90-theta(m))/90)*(8/(i(n)+8)));
   end

   plot(i,Lambda)
   if m==1
hold
   end
end

hold
xlabel('Current [A]')
ylabel('Lambda [Wb]')
title('Family of lambda-i curves as theta_m varies from 0 to 90 degrees')
text(17,.7,'theta_m = 0 degrees')
text(20,.06,'theta_m = 90 degrees')
%(b) Now integrate to find the areas.

%Peak lambda at 0 degrees, 25 Amps
lambdamax = 25*(0.005+0.09*(8/(25+8)));

AreaWnet = 0;
AreaWrec = 0;

% 100 integration step
deli = 25/100;

for n=1:101
  i(n) = 25*(n-1)/100;
  AreaWnet = AreaWnet + deli*i(n)*(0.09)*(8/(i(n)+8));
  AreaWrec = AreaWrec + deli*(lambdamax - i(n)*(0.005+0.09*(8/(i(n)+8))));
end

Ratio = (AreaWrec + AreaWnet)/AreaWnet;

fprintf('\nPart(b) Ratio = %g',Ratio)

%(c) Calculate the power

rpm = 2500;
rps = 2500/60;
T = 1/rps;
Pphase = 2*AreaWnet/T;
Ptot = 2*Pphase;
```

```
fprintf('\n\nPart(c) AreaWnet = %g [Joules]',AreaWnet)
fprintf('\n          Pphase = %g [W] and Ptot = %g [W]\n',Pphase,Ptot)
```

Practice Problem 8.4

Consider a two-phase VRM which is identical to that of Example 8.4 with the exception of an additional 5 mH of leakage inductance in each phase. (*a*) Calculate the ratio of the inverter volt-ampere rating to the VRM net power output for the following idealized operating cycle:

(*i*) The current is instantaneously raised to 25 A when $\theta_m = -90°$.
(*ii*) The current is then held constant as the rotor rotates to $\theta_m = 10°$.
(*iii*) At $\theta_m = 10°$, the current is reduced to zero.

(*b*) Assuming the VRM to be operating as a motor using the cycle described in part (a) and rotating at a constant speed of 2500 r/min, calculate the net electromechanical power supplied to the rotor.

Solution

a.

$$\frac{\text{Inverter volt-ampere rating}}{\text{Net output power}} = 1.75$$

b. $P_{mech} = 1467$ W

Saturation effects clearly play a significant role in the performance of most VRMs and must be taken into account. In addition, the idealized operating cycle illustrated in Example 8.4 cannot, of course, be achieved in practice since some rotor motion is likely to take place over the time scale over which current changes occur. As a result, it is often necessary to resort to numerical-analysis packages such as finite-element programs as part of the design process for practical VRM systems. Many of these programs incorporate the ability to model the nonlinear effects of magnetic saturation as well as mechanical (e.g., rotor motion) and electrical (e.g., current buildup) dynamic effects.

As we have seen, the design of a VRM drive system typically requires that a trade-off be made. On the one hand, saturation tends to increase the size of the VRM for a given power output. On the other hand, on comparing two VRM systems with the same power output, the system with the higher level of saturation will typically require an inverter with a lower volt-ampere rating. Thus the ultimate design will be determined by a trade-off between the size, cost, and efficiency of the VRM and of the inverter.

8.5 STEPPING MOTORS

As we have seen, when the phases of a VRM are energized sequentially in an appropriate step-wise fashion, the VRM will rotate a specific angle for each step. Motors designed specifically to take advantage of this characteristic are referred to as *stepping*

motors or *stepper motors*. Frequently stepping motors are designed to produce a large number of steps per revolution, for example 50, 100, or 200 steps per revolution (corresponding to a rotation of 7.2°, 3.6° and 1.8° per step).

An important characteristic of the stepping motor is its compatibility with digital-electronic systems. These systems are common in a wide variety of applications and continue to become more powerful and less expensive. For example, the stepping motor is often used in digital control systems where the motor receives open-loop commands in the form of a train of pulses to turn a shaft or move an object a specific distance. Typical applications include paper-feed and print-head-positioning motors in printers and plotters, drive and head-positioning motors in disk drives and CD players, and worktable and tool positioning in numerically controlled machining equipment. In many applications, position information can be obtained simply by keeping count of the pulses sent to the motor, in which case position sensors and feedback control are not required.

The angular resolution of a VRM is determined by the number of rotor and stator teeth and can be greatly enhanced by techniques such as *castleation,* as is discussed in Section 8.2. Stepping motors come in a wide variety of designs and configurations. In addition to variable-reluctance configurations, these include permanent-magnet and hybrid configurations. The use of permanent magnets in combination with a variable-reluctance geometry can significantly enhance the torque and positional accuracy of a stepper motor.

The VRM configurations discussed in Sections 8.1 through 8.3 consist of a single rotor and stator with multiple phases. A stepping motor of this configuration is called a *single-stack, variable-reluctance stepping motor.* An alternate form of variable-reluctance stepping motor is known as a *multistack variable-reluctance stepping motor.* In this configuration, the motor can be considered to be made up of a set of axially displaced, single-phase VRMs mounted on a single shaft.

Figure 8.16 shows a multistack variable-reluctance stepping motor. This type of motor consists of a series of stacks, each axially displaced, of identical geometry and each excited by a single phase winding, as shown in Fig. 8.17. The motor of Fig. 8.16 has three stacks and three phases, although motors with additional phases and stacks are common. For an n_s-stack motor, the rotor or stator (but not both) on each stack is displaced by $1/n_s$ times the pole-pitch angle. In Fig. 8.16, the rotor poles are aligned, but the stators are offset in angular displacement by one-third of the pole pitch. By successively exciting the individual phases, the rotor can be turned in increments of this displacement angle.

A schematic diagram of a two-phase stepping motor with a permanent-magnet, two-pole rotor is shown in Fig. 8.18. Note that this machine is in fact a two-phase synchronous machine, similar for example to the three-phase permanent-magnet ac machine of Fig. 5.29. The distinction between such a stepping motor and a synchronous motor arises not from the construction of the motor but rather from how the motor is operated. The synchronous motor is typically intended to drive a load at a specified speed, and the stepping motor is typically intended to control the position of a load.

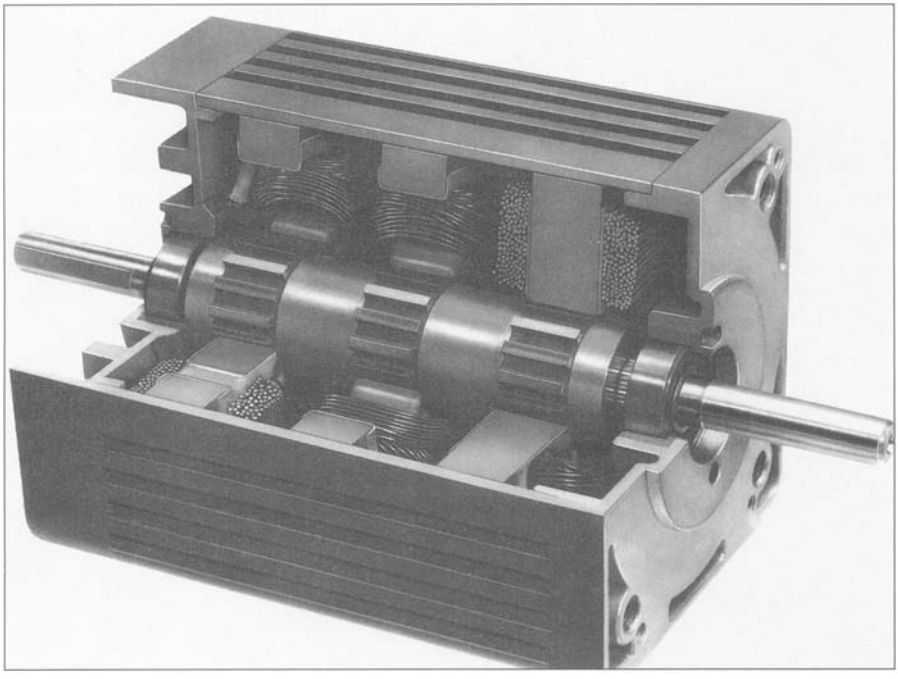

Figure 8.16 Cutaway view of a three-phase, three-stack variable-reluctance stepping motor. (*Warner Electric.*)

The rotor of the stepping motor of Fig. 8.18 assumes the angles $\theta_m = 0, 45°, 90°, \ldots$ as the windings are excited in the sequence:

1. Positive current in phase 1 alone.
2. Equal-magnitude positive currents in phase 1 and phase 2.
3. Positive current in phase 2 alone.
4. Equal-magnitude negative current in phase 1 and positive current in phase 2.
5. Negative current in phase 1 alone.
6. And so on.

Note that if a ferromagnetic rotor were substituted for the permanent-magnet rotor, the rotor would move in a similar fashion.

The stepping motor of Fig. 8.18 can also be used for 90° steps by exciting the coils singly. In the latter case, only a permanent-magnet rotor can be used. This can be seen from the torque-angle curves for the two types of rotors shown in Fig. 8.19. Whereas the permanent-magnet rotor produces peak torque when the excitation is shifted 90°, the ferromagnetic rotor produces zero torque and may move in either direction.

The rotor position in the permanent-magnet stepping motor of Fig. 8.18 is defined by the winding currents with no ambiguity and depends on the direction of the phase

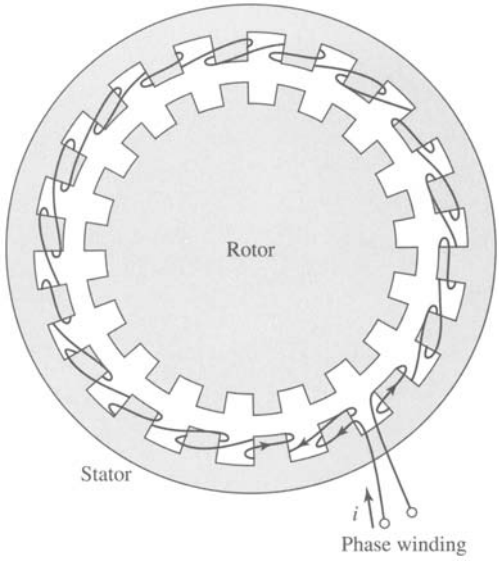

Figure 8.17 Diagram of one stack and phase of a multiphase, multistack variable-reluctance stepping motor, such as that in Fig. 8.16. For an n_s-stack motor, the rotor or stator (but not both) on each stack is displaced by $1/n_s$ times the pole pitch.

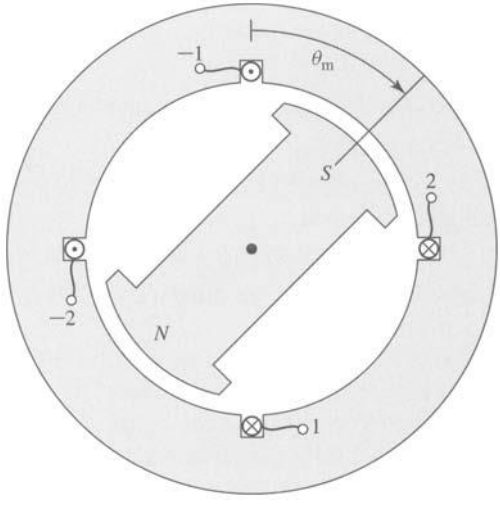

Figure 8.18 Schematic diagram of a two-phase permanent-magnet stepping motor.

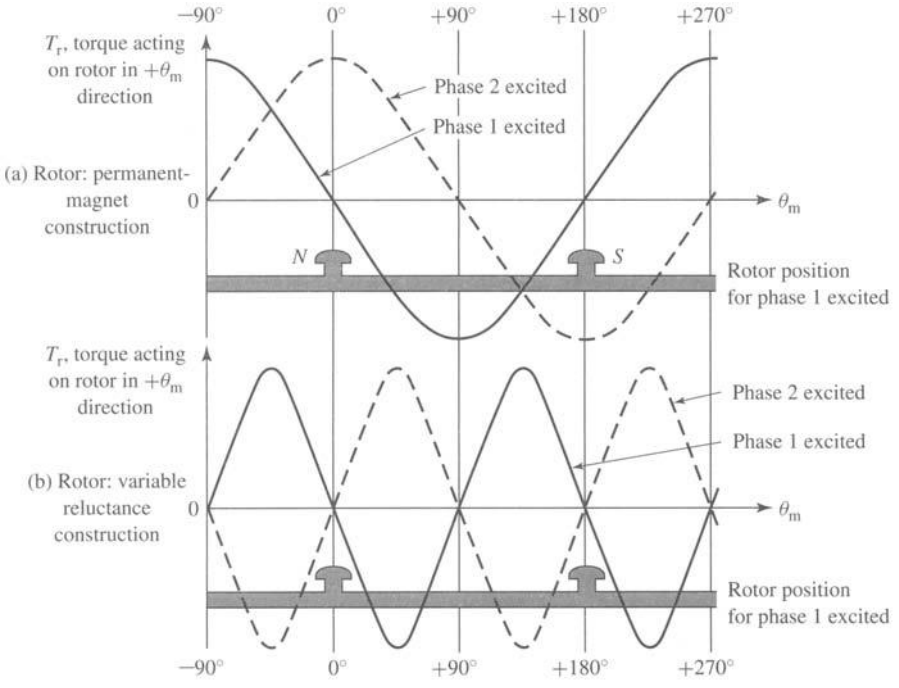

Figure 8.19 Torque-angle curves for the stepping motor of Fig. 8.18: (a) permanent-magnet rotor and (b) variable-reluctance rotor.

currents. Reversing the phase currents will cause the rotor to reverse its orientation. This is in contrast to VRM configuration with a ferromagnetic rotor, in which two rotor positions are equally stable for any particular set of phase currents, and hence the rotor position cannot be determined uniquely. Permanent-magnet stepping motors are also unlike their VRM counterparts in that torque tending to align the rotor with the stator poles will be generated even when there is no excitation applied to the phase windings. Thus the rotor will have preferred unexcited rest positions, a fact which can be used to advantage in some applications.

EXAMPLE 8.5

Using the techniques of Chapter 3 and neglecting saturation effects, the torque of a two-phase, permanent-magnet stepping motor of the form of Fig. 8.18 can be expressed as

$$T_{\text{mech}} = T_0 \, (i_1 \cos \theta_m + i_2 \sin \theta_m)$$

where T_0 is a positive constant that depends upon the motor geometry and the properties of the permanent magnet.

Calculate the rest (zero-torque) positions which will result if the motor is driven by a drive such that each phase current can be set equal to three values $-I_0$, 0, and I_0. Using such a drive, what is the motor step size?

■ Solution

In general, the zero-torque positions of the motor can be found by setting the torque expression to zero and solving for the resultant rotor position. Thus setting

$$T_{\text{mech}} = T_0 (i_1 \sin\theta_m - i_2 \cos\theta_m) = 0$$

gives

$$i_1 \sin\theta_m - i_2 \cos\theta_m = 0$$

or

$$\theta_m = \tan^{-1}\left(\frac{i_2}{i_1}\right)$$

Note that not all of these zero-torque positions correspond to stable equilibrium positions. For example, operation with $i_1 = I_0$ and $i_2 = 0$ gives two zero-torque positions: $\theta_m = 0°$ and $\theta_m = 180°$. Yet only the position $\theta_m = 0°$ is stable. This is directly analogous to the case of a hanging pendulum which sees zero torque both when it is hanging downward ($\theta = 0°$) and when it is sitting inverted ($\theta = 180°$). Yet, it is clear that the slightest perturbation of the position of the inverted pendulum will cause it to rotate downwards and that it will eventually come to rest in the stable hanging position.

Stable rest positions of the rotor are determined by the requirement that a restoring torque is produced as the rotor moves from that position. Thus, a negative torque should result if the rotor moves in the $+\theta_m$ direction, and a positive torque should result for motion in the $-\theta_m$ direction. Mathematically, this can be expressed as an additional constraint on the torque at the rest position

$$\left.\frac{\partial T_{\text{mech}}}{\partial \theta_m}\right|_{i_1, i_2} < 0$$

where the partial derivative is evaluated at the zero-torque position and is taken with the phase currents held constant. Thus, in this case, the rest position must satisfy the additional constraint that

$$\left.\frac{\partial T_{\text{mech}}}{\partial \theta_m}\right|_{i_1, i_2} = -T_0 (i_1 \cos\theta_m + i_2 \sin\theta_m) < 0$$

From this equation, we see for example that with $i_1 = I_0$ and $i_2 = 0$, at $\theta_m = 0°$, $\partial T_{\text{mech}}/\partial\theta_m < 0$ and thus $\theta_m = 0°$ is a stable rest position. Similarly, at $\theta_m = 180°$, $\partial T_{\text{mech}}/\partial\theta_m > 0$ and thus $\theta_m = 180°$ is not a stable rest position.

Using these relationships, Table 8.1 lists the stable rest positions of the rotor for the various combinations of phase currents.

From this table we see that this drive results in a step size of 45°.

Table 8.1 Rotor rest positions for Example 8.5.

i_1	i_2	θ_m
0	0	-
0	$-I_0$	270°
0	I_0	90°
$-I_0$	0	180°
$-I_0$	$-I_0$	225°
$-I_0$	I_0	135°
I_0	0	0°
I_0	$-I_0$	315°
I_0	I_0	45°

Practice Problem 8.5

In order to achieve a step size of 22.5°, the motor drive of Example 8.5 is modified so that each phase can be driven by currents of magnitude 0, $\pm kI_0$, and $\pm I_0$. Find the required value of the constant k.

Solution

$$k = \tan^{-1}(22.5°) = 0.4142$$

In Example 8.5 we see that stable equilibrium positions of an unloaded stepping motor satisfy the conditions that there is zero torque, i.e.,

$$T_{mech} = 0 \tag{8.20}$$

and that there is positive restoring torque, i.e.,

$$\left.\frac{\partial T_{mech}}{\partial \theta_m}\right|_{i_1,i_2} < 0 \tag{8.21}$$

In practice, there will of course be a finite load torque tending to perturb the stepping motor from these idealized positions. For open-loop control systems (i.e., control systems in which there is no mechanism for position feedback), a high-degree of position control can be achieved by designing the stepping motor to produce large restoring torque (i.e., a large magnitude of $\partial T_{mech}/\partial \theta_m$). In such a stepping motor, load torques will result in only a small movement of the rotor from the idealized positions which satisfies Eqs. 8.20 and 8.21.

Example 8.5 also shows how carefully controlled combinations of phase currents can enhance the resolution of a stepper motor. This technique, referred to as *microstepping,* can be used to achieve increased step resolution of a wide variety of stepper motors. As the following example shows, microstepping can be used to produce extremely fine position resolution. The increased resolution comes, however, at the expense of an increase in complexity of the stepping-motor drive electronics and control algorithms, which must accurately control the distribution of current to multiple phases simultaneously.

EXAMPLE 8.6

Consider again the two-phase, permanent-magnet stepping motor of Example 8.5. Calculate the rotor position which will result if the phase currents are controlled to be sinusoidal functions of a reference angle θ_{ref} in the form

$$i_1 = I_0 \cos\theta_{ref}$$

$$i_2 = I_0 \sin\theta_{ref}$$

■ Solution

Substitution of the current expressions into the torque expression of Example 8.5 gives

$$T_{mech} = T_0 (i_1 \cos\theta_m + i_2 \sin\theta_m) = T_0 I_0 (\cos\theta_{ref} \cos\theta_m + \sin\theta_{ref} \sin\theta_m)$$

Use of the trigonometric identity $\cos(\alpha - \beta) = \cos\alpha \cos\beta + \sin\alpha \sin\beta$ gives

$$T_{mech} = T_0 I_0 \cos(\theta_{ref} - \theta_m)$$

From this expression and using the analysis of Example 8.5, we see that the rotor equilibrium position will be equal to the reference angle, i.e., $\theta_m = \theta_{ref}$. In a practical implementation, a digital controller is likely to be used to increment θ_{ref} in finite steps, which will result in finite steps in the position of the stepping-motor.

The *hybrid stepping motor* combines characteristics of the variable-reluctance and permanent-magnet stepping motors. A photo of a hybrid stepping motor is shown in Fig. 8.20, and a schematic view of a hybrid stepping motor is shown in Fig. 8.21. The hybrid-stepping-motor rotor configuration appears much like that of a multistack variable-reluctance stepping motor. In the rotor of Fig. 8.21a, two identical rotor stacks are displaced axially along the rotor and displaced in angle by one-half the rotor pole pitch, while the stator pole structure is continuous along the length of the rotor. Unlike the multistack variable-reluctance stepping motor, in the hybrid stepping motor, the rotor stacks are separated by an axially-directed permanent magnet. As a result, in Fig. 8.21a one end of the rotor can be considered to have a north magnetic pole and

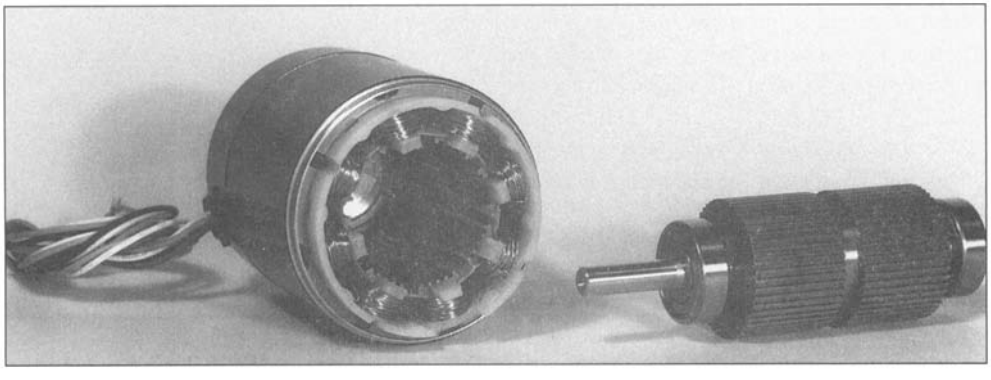

Figure 8.20 Disassembled 1.8°/step hybrid stepping motor. (*Oriental Motor.*)

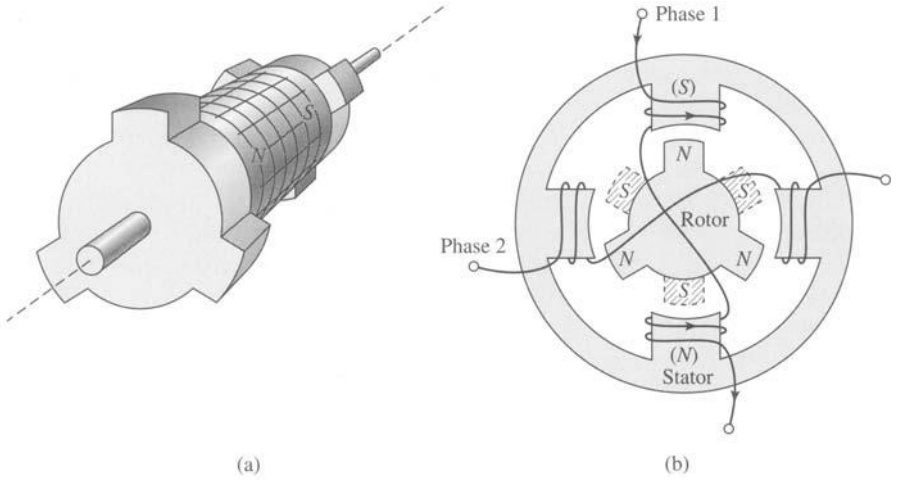

Figure 8.21 Schematic view of a hybrid stepping motor. (a) Two-stack rotor showing the axially-directed permanent magnet and the pole pieces displaced by one-half the pole pitch. (b) End view from the rotor north poles and showing the rotor south poles at the far end (shown crosshatched). Phase 1 of the stator is energized to align the rotor as shown.

the other end a south magnetic pole. Figure 8.21b shows a schematic end view of a hybrid stepping motor. The stator has four poles with the phase-1 winding wound on the vertical poles and the phase-2 winding wound on the horizontal poles. The rotor is shown with its north-pole end at the near end of the motor and the south-pole end (shown crosshatched) at the far end.

In Fig. 8.21b, phase 1 is shown excited such that the top stator pole is a south pole while the bottom pole is a north pole. This stator excitation interacts with the permanent-magnet flux of the rotor to align the rotor with a pole on its north-pole end vertically upward and a pole on its south-pole end vertically downward, as shown in the figure. Note that if the stator excitation is removed, there will still be a permanent-magnet torque tending to maintain the rotor in the position shown.

To turn the rotor, excitation is removed from phase 1, and phase 2 is excited. If phase 2 is excited such that the right-hand stator pole is a south pole and the left-hand one is a north pole, the rotor will rotate 30° counterclockwise. Similarly, if the opposite excitation is applied to the phase-2 winding, a 30° rotation in the clockwise direction will occur. Thus, by alternately applying phase-1 and phase-2 excitation of the appropriate polarity, the rotor can be made to rotate in either direction by a specified angular increment.

Practical hybrid stepping motors are generally built with more rotor poles than are indicated in the schematic motor of Fig. 8.21, in order to give much better angular resolution. Correspondingly, the stator poles are often castleated (see Fig. 8.8) to further increase the angular resolution. In addition, they may be built with more than two stacks per rotor.

The hybrid stepping motor design offers advantages over the permanent-magnet design discussed earlier. It can achieve small step sizes easily and with a simple

magnet structure while a purely permanent-magnet motor would require a multipole permanent magnet. In comparison with the variable-reluctance stepping motor, the hybrid design may require less excitation to achieve a given torque because some of the excitation is supplied by the permanent magnet. In addition, the hybrid stepping motor will tend to maintain its position when the stator excitation is removed, as does the permanent-magnet design.

The actual choice of a stepping-motor design for a particular application is determined based on the desired operating characteristics, availability, size, and cost. In addition to the three classifications of stepping motors discussed in this chapter, a number of other different and often quite clever designs have been developed. Although these encompass a wide range of configurations and construction techniques, the operating principles remain the same.

Stepping motors may be driven by electronic drive components similar to those discussed in Section 11.4 in the context of VRM drives. Note that the issue of controlling a stepping motor to obtain the desired response under dynamic, transient conditions is quite complex and remains the subject of considerable investigation.[4]

8.6 SUMMARY

Variable-reluctance machines are perhaps the simplest of electrical machines. They consist of a stator with excitation windings and a magnetic rotor with saliency. Torque is produced by the tendency of the salient-pole rotor to align with excited magnetic poles on the stator.

VRMs are synchronous machines in that they produce net torque only when the rotor motion is in some sense synchronous with the applied stator mmf. This synchronous relationship may be complex, with the rotor speed being some specific fraction of the applied electrical frequency as determined not only by the number of stator and rotor poles but also by the number of stator and rotor teeth on these poles. In fact, in some cases, the rotor will be found to rotate in the direction opposite to the rotation direction of the applied stator mmf.

Successful operation of a VRM depends on exciting the stator phase windings in a specific fashion correlated to the instantaneous position of the rotor. Thus, rotor position must be measured, and a controller must be employed to determine the appropriate excitation waveforms and to control the output of the inverter. Typically chopping is required to obtain these waveforms. The net result is that although the VRM is itself a simple device, somewhat complex electronics are typically required to make a complete drive system.

The significance of VRMs in engineering applications stems from their low cost, reliability, and controllability. Because their torque depends only on the square of the applied stator currents and not on their direction, these machines can be operated from

---

[4] For further information on stepping motors, see P. Acarnley, *Stepping Motors: A Guide to Modern Theory and Practice*, 2nd ed., Peter Peregrinus Ltd., London, 1982; Takashi Kenjo, *Stepping Motors and Their Microprocessor Controls*, Clarendon Press, Oxford, 1984; and Benjamin C. Kuo, *Theory and Applications of Step Motors*, West Publishing Co., St. Paul, Minnesota, 1974.

unidirectional drive systems, reducing the cost of the power electronics. However, it is only recently, with the advent of low-cost, flexible power electronic circuitry and microprocessor-based control systems, that VRMs have begun to see widespread application in systems ranging from traction drives to high-torque, precision position control systems for robotics applications.

Practical experience with VRMs has shown that they have the potential for high reliability. This is due in part to the simplicity of their construction and to the fact that there are no windings on their rotors. In addition, VRM drives can be operated successfully (at a somewhat reduced rating) following the failure of one or more phases, either in the machine or in the inverter. VRMs typically have a large number of stator phases (four or more), and significant output can be achieved even if some of these phases are out of service. Because there is no rotor excitation, there will be no voltage generated in a phase winding which fails open-circuited or current generated in a phase winding which fails short-circuited, and thus the machine can continue to be operated without risk of further damage or additional losses and heating.

Because VRMs can be readily manufactured with a large number of rotor and stator teeth (resulting in large inductance changes for small changes in rotor angle), they can be constructed to produce very large torque per unit volume. There is, however, a trade-off between torque and velocity, and such machines will have a low rotational velocity (consistent with the fact that only so much power can be produced by a given machine frame size). On the opposite extreme, the simple configuration of a VRM rotor and the fact that it contains no windings suggest that it is possible to build extremely rugged VRM rotors. These rotors can withstand high speeds, and motors which operate in excess of 200,000 r/min have been built.

Finally, we have seen that saturation plays a large role in VRM performance. As recent advances in power electronic and microelectronic circuitry have brought VRM drive systems into the realm of practicality, so have advances in computer-based analytical techniques for magnetic-field analysis. Use of these techniques now makes it practical to perform optimized designs of VRM drive systems which are competitive with alternative technologies in many applications.

Stepping motors are closely related to VRMs in that excitation of each successive phase of the stator results in a specific angular rotation of the rotor. Stepping motors come in a wide variety of designs and configurations. These include variable-reluctance, permanent-magnet, and hybrid configurations. The rotor position of a variable-reluctance stepper motor is not uniquely determined by the phase currents since the phase inductances are not unique functions of the rotor angle. The addition of a permanent magnet changes this situation and the rotor position of a permanent-magnet stepper motor is a unique function of the phase currents.

Stepping motors are the electromechanical companions to digital electronics. By proper application of phase currents to the stator windings, these motors can be made to rotate in well-defined steps ranging down to a fraction of a degree per pulse. They are thus essential components of digitally controlled electromechanical systems where a high degree of precision is required. They are found in a wide range of applications including numerically controlled machine tools, in printers and plotters, and in disk drives.

8.7 PROBLEMS

8.1 Repeat Example 8.1 for a machine identical to that considered in the example except that the stator pole-face angle is $\beta = 45°$.

8.2 In the paragraph preceeding Eq. 8.1, the text states that "under the assumption of negligible iron reluctance the mutual inductances between the phases of the doubly-salient VRM of Fig. 8.1b will be zero, with the exception of a small, essentially constant component associated with leakage flux." Neglect any leakage flux effects and use magnetic circuit techniques to show that this statement is true.

8.3 Use magnetic-circuit techniques to show that the phase-to-phase mutual inductance in the 6/4 VRM of Fig. 8.5 is zero under the assumption of infinite rotor- and stator-iron permeability. Neglect any contributions of leakage flux.

8.4 A 6/4 VRM of the form of Fig. 8.5 has the following properties:

Stator pole angle $\beta = 30°$
Rotor pole angle $\alpha = 30°$
Air-gap length $g = 0.35$ mm
Rotor outer radius $R = 5.1$ cm
Active length $D = 7$ cm

This machine is connected as a three-phase motor with opposite poles connected in series to form each phase winding. There are 40 turns per pole (80 turns per phase). The rotor and stator iron can be considered to be of infinite permeability and hence mutual-inductance effects can be neglected.

a. Defining the zero of rotor angle θ_m at the position when the phase-1 inductance is maximum, plot and label the inductance of phase 1 as a function of rotor angle.

b. On the plot of part (a), plot the inductances of phases 2 and 3.

c. Find the phase-1 current I_0 which results in a magnetic flux density of 1.0 T in the air gap under the phase-1 pole face when the rotor is in a position of maximum phase-1 inductance.

d. Assuming that the phase-1 current is held constant at the value found in part (c) and that there is no current in phases 2 and 3, plot the torque as a function of rotor position.

The motor is to be driven from a three-phase current-source inverter which can be switched on or off to supply either zero current or a constant current of magnitude I_0 in phases 2 and 3; plot the torque as a function of rotor position.

e. Under the idealized assumption that the currents can be instantaneously switched, determine the sequence of phase currents (as a function of rotor position) that will result in constant positive motor torque, independent of rotor position.

f. If the frequency of the stator excitation is such that a time $T_0 = 35$ msec is required to sequence through all three phases under the excitation

conditions of part (e), find the rotor angular velocity and its direction of rotation.

8.5 In Section 8.2, when discussing Fig. 8.5, the text states: "In addition to the fact that there are not positions of simultaneous alignment for the 6/4 VRM, it can be seen that there also are no rotor positions at which only a torque of a single sign (either positive or negative) can be produced." Show that this statement is true.

8.6 Consider a three-phase 6/8 VRM. The stator phases are excited sequentially, requiring a total time of 15 msec. Find the angular velocity of the rotor in r/min.

8.7 The phase windings of the castleated machine of Fig. 8.8 are to be excited by turning the phases on and off individually (i.e., only one phase can be on at any given time).

a. Describe the sequence of phase excitations required to move the rotor to the right (clockwise) by an angle of approximately 21.4°.

b. The stator phases are to be excited as a regular sequence of pulses. Calculate the phase order and the time between pulses required to produce a steady-state rotor rotation of 125 r/min in the counterclockwise direction.

8.8 Replace the 28-tooth rotor of Problem 8.7 with a rotor with 26 teeth.

a. Phase 1 is excited, and the rotor is allowed to come to rest. If the excitation on phase 1 is removed and excitation is applied to phase 2, calculate the resultant direction and magnitude (in degrees) of rotor rotation.

b. The stator phases are to be excited as a regular sequence of pulses. Calculate the phase order and the time between pulses required to produce a steady-state rotor rotation of 80 r/min in the counterclockwise direction.

8.9 Repeat Example 8.3 for a rotor speed of 4500 r/min.

8.10 Repeat Example 8.3 under the condition that the rotor speed is 4500 r/min and that a negative voltage of −250 V is used to turn off the phase current.

8.11 The three-phase 6/4 VRM of Problem 8.4 has a winding resistance of 0.15 Ω/phase and a leakage inductance of 4.5 mH in each phase. Assume that the rotor is rotating at a constant angular velocity of 1750 r/min.

a. Plot the phase-1 inductance as a function of the rotor angle θ_m.

b. A voltage of 75 V is applied to phase 1 as the rotor reaches the position $\theta_m = -30°$ and is maintained constant until $\theta_m = 0°$. Calculate and plot the phase-1 current as a function of time during this period.

c. When the rotor reaches $\theta = 0°$, the applied voltage is reversed so that a voltage of −75 V is applied to the winding. This voltage is maintained until the winding current reaches zero, at which point the winding is open-circuited. Calculate and plot the current decay during the time until the current decays to zero.

d. Calculate and plot the torque during the time periods investigated in parts (b) and (c).

8.12 Assume that the VRM of Examples 8.1 and 8.3 is modified by replacing its rotor with a rotor with 75° pole-face angles as shown in Fig. 8.12a. All other dimensions and parameters of the VRM are unchanged.

a. Calculate and plot $L(\theta_m)$ for this machine.

b. Repeat Example 8.3 except that the constant voltage 100 V is first applied at $\theta_m = -67.5°$ when $dL(\theta_m)/d\theta_m$ becomes positive and the constant voltage of -100 V is then applied at $\theta_m = -7.5°$ (i.e., when $dL(\theta_m)/d\theta_m$ becomes zero) and is maintained until the winding current reaches zero.

c. Plot the corresponding torque.

8.13 Repeat Example 8.4 for a symmetrical two-phase 4/2 VRM whose λ-i characteristic can be represented by the following expression (for phase 1) as a function of θ_m over the range $0 \le \theta_m \le 90°$:

$$\lambda_1 = \left(0.01 + 0.15\left(\frac{90° - \theta_m}{90°}\right)\left(\frac{12.0}{12.0 + i_1}\right)^{1.2}\right) i_1$$

8.14 Consider a two-phase stepper motor with a permanent-magnet rotor such as shown in Fig. 8.18 and whose torque-angle curve is as shown in Fig. 8.19a. This machine is to be excited by a four-bit digital sequence corresponding to the following winding excitation:

bit			bit		
1	2	i_1	3	4	i_2
0	0	0	0	0	0
0	1	$-I_0$	0	1	$-I_0$
1	0	I_0	1	0	I_0
1	1	0	1	1	0

a. Make a table of 4-bit patterns which will produce rotor angular positions of $0, 45°, \ldots, 315°$.

b. By sequencing through the bit pattern found in part (a) the motor can be made to rotate. What time interval (in milliseconds) between bit-pattern changes will result in a rotor speed of 1200 r/min?

8.15 Figure 8.22 shows a two-phase hybrid stepping motor with castleated poles on the stator. The rotor is shown in the position it occupies when current is flowing into the positive lead of phase 1.

a. If phase one is turned off and phase 2 is excited with current flowing into its positive lead, calculate the corresponding angular rotation of the rotor. Is it in the clockwise or counterclockwise direction?

b. Describe an excitation sequence for the phase windings which will result in a steady rotation of the rotor in the clockwise direction.

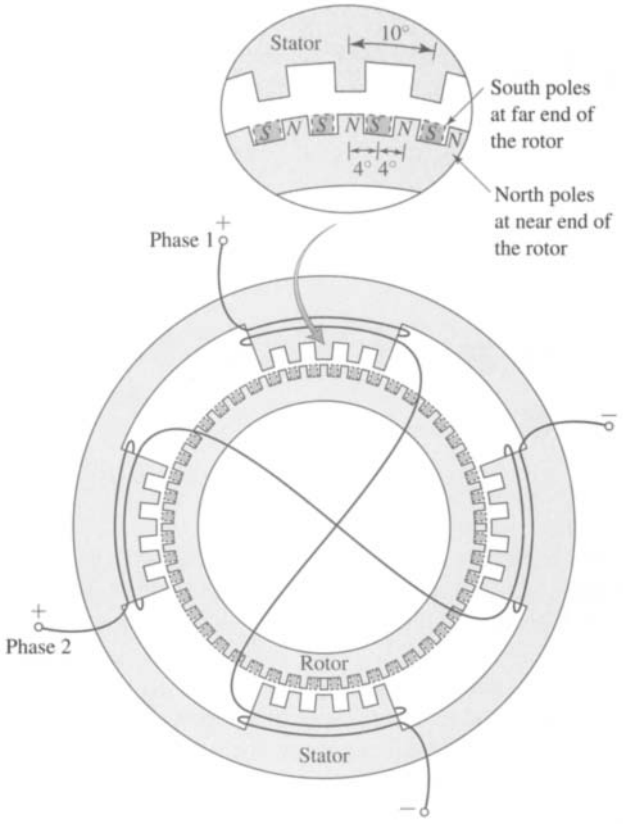

Figure 8.22 Castleated hybrid stepping motor for Problem 8.15.

c. Determine the frequency of the phase currents required to achieve a rotor speed of 8 r/min.

8.16 Consider a multistack, multiphase variable-reluctance stepping motor, such as that shown schematically in Fig. 8.17, with 14 poles on each of the rotor and stator stacks and three stacks with one phase winding per stack. The motor is built such that the stator poles of each stack are aligned.

a. Calculate the angular displacement between the rotor stacks.

b. Determine the frequency of phase currents required to achieve a rotor speed of 900 r/min.

9 CHAPTER

Single- and Two-Phase Motors

This chapter discusses single-phase motors. While focusing on induction motors, synchronous-reluctance, hysteresis, and shaded-pole induction motors are also discussed. Note that another common single-phase motor, the series universal motor, is discussed in Section 7.10. Most induction motors of fractional-kilowatt (fractional horsepower) rating are single-phase motors. In residential and commercial applications, they are found in a wide range of equipment including refrigerators, air conditioners and heat pumps, fans, pumps, washers, and dryers.

In this chapter, we will describe these motors qualitatively in terms of rotating-field theory and will begin with a rigorous analysis of a single-phase motor operating off of a single winding. However, most single-phase induction motors are actually two-phase motors with unsymmetrical windings; the two windings are typically quite different, with different numbers of turns and/or winding distributions. Thus this chapter also discusses two-phase motors and includes a development of a quantitative theory for the analysis of single-phase induction motors when operating off both their main and auxiliary windings.

9.1 SINGLE-PHASE INDUCTION MOTORS: QUALITATIVE EXAMINATION

Structurally, the most common types of single-phase induction motors resemble polyphase squirrel-cage motors except for the arrangement of the stator windings. An induction motor with a squirrel-cage rotor and a single-phase stator winding is represented schematically in Fig. 9.1. Instead of being a concentrated coil, the actual stator winding is distributed in slots to produce an approximately sinusoidal space distribution of mmf. As we saw in Section 4.5.1, a single-phase winding produces equal forward- and backward-rotating mmf waves. By symmetry, it is clear that such a motor inherently will produce no starting torque since at standstill, it will produce equal torque in both directions. However, we will show that if it is started by auxiliary

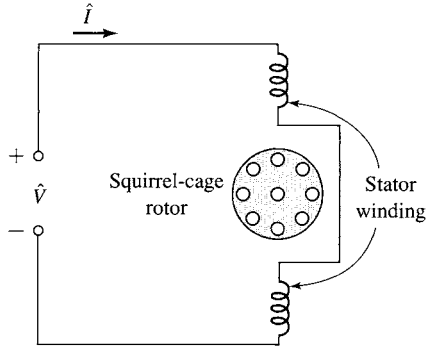

Figure 9.1 Schematic view of a single-phase induction motor.

means, the result will be a net torque in the direction in which it is started, and hence the motor will continue to run.

Before we consider auxiliary starting methods, we will discuss the basic properties of the schematic motor of Fig. 9.1. If the stator current is a cosinusoidal function of time, the resultant air-gap mmf is given by Eq. 4.18

$$\mathcal{F}_{ag1} = F_{max} \cos(\theta_{ae}) \cos \omega_e t \tag{9.1}$$

which, as shown in Section 4.5.1, can be written as the sum of positive- and negative-traveling mmf waves of equal magnitude. The positive-traveling wave is given by

$$\mathcal{F}^{+}_{ag1} = \frac{1}{2} F_{max} \cos(\theta_{ae} - \omega_e t) \tag{9.2}$$

and the negative-traveling wave is given by

$$\mathcal{F}^{-}_{ag1} = \frac{1}{2} F_{max} \cos(\theta_{ae} + \omega_e t) \tag{9.3}$$

Each of these component mmf waves produces induction-motor action, but the corresponding torques are in opposite directions. With the rotor at rest, the forward and backward air-gap flux waves created by the combined mmf's of the stator and rotor currents are equal, the component torques are equal, and no starting torque is produced. If the forward and backward air-gap flux waves were to remain equal when the rotor revolves, each of the component fields would produce a torque-speed characteristic similar to that of a polyphase motor with negligible stator leakage impedance, as illustrated by the dashed curves f and b in Fig. 9.2a. The resultant torque-speed characteristic, which is the algebraic sum of the two component curves, shows that if the motor were started by auxiliary means, it would produce torque in whatever direction it was started.

The assumption that the air-gap flux waves remain equal when the rotor is in motion is a rather drastic simplification of the actual state of affairs. First, the effects of stator leakage impedance are ignored. Second, the effects of induced rotor currents are not properly accounted for. Both these effects will ultimately be included in the

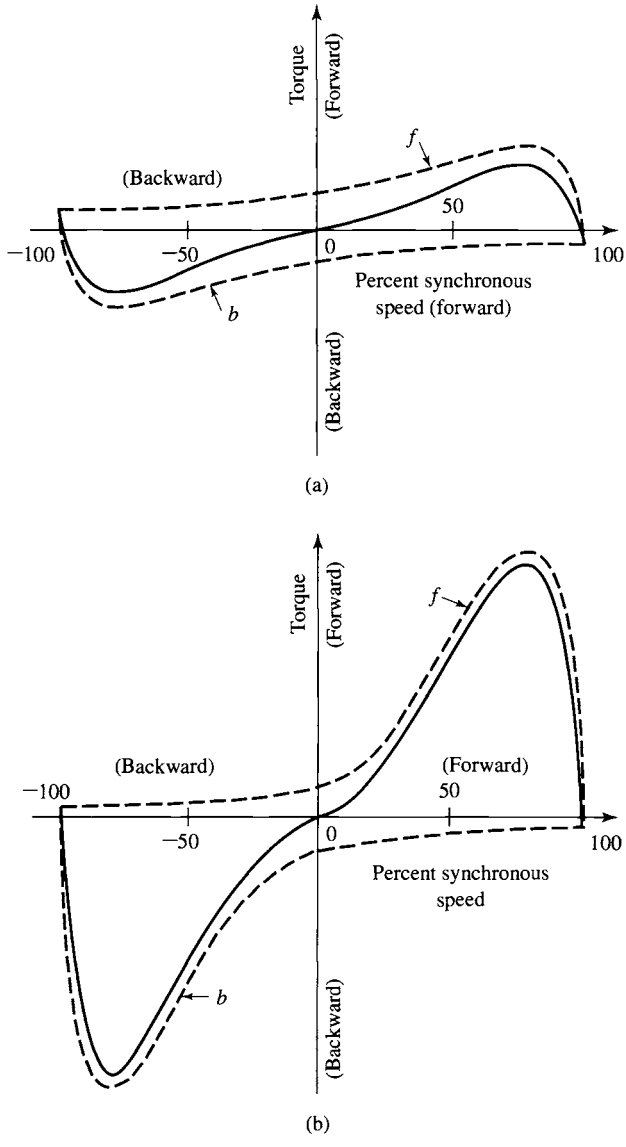

Figure 9.2 Torque-speed characteristic of a single-phase induction motor (a) on the basis of constant forward and backward flux waves, (b) taking into account changes in the flux waves.

detailed quantitative theory of Section 9.3. The following qualitative explanation shows that the performance of a single-phase induction motor is considerably better than would be predicted on the basis of equal forward and backward flux waves.

When the rotor is in motion, the component rotor currents induced by the backward field are greater than at standstill, and their power factor is lower. Their mmf,

which opposes that of the stator current, results in a reduction of the backward flux wave. Conversely, the magnetic effect of the component currents induced by the forward field is less than at standstill because the rotor currents are less and their power factor is higher. As speed increases, therefore, the forward flux wave increases while the backward flux wave decreases. The sum of these flux waves must remain roughly constant since it must induce the stator counter emf, which is approximately constant if the stator leakage-impedance voltage drop is small.

Hence, with the rotor in motion, the torque of the forward field is greater and that of the backward field less than in Fig. 9.2a, the true situation being about that shown in Fig. 9.2b. In the normal running region at a few percent slip, the forward field is several times greater than the backward field, and the flux wave does not differ greatly from the constant-amplitude revolving field in the air gap of a balanced polyphase motor. In the normal running region, therefore, the torque-speed characteristic of a single-phase motor is not too greatly inferior to that of a polyphase motor having the same rotor and operating with the same maximum air-gap flux density.

In addition to the torques shown in Fig. 9.2, double-stator-frequency torque pulsations are produced by the interactions of the oppositely rotating flux and mmf waves which rotate past each other at twice synchronous speed. These interactions produce no average torque, but they tend to make the motor noisier than a polyphase motor. Such torque pulsations are unavoidable in a single-phase motor because of the pulsations in instantaneous power input inherent in a single-phase circuit. The effects of the pulsating torque can be minimized by using an elastic mounting for the motor. The torque referred to on the torque-speed curves of a single-phase motor is the time average of the instantaneous torque.

9.2 STARTING AND RUNNING PERFORMANCE OF SINGLE-PHASE INDUCTION AND SYNCHRONOUS MOTORS

Single-phase induction motors are classified in accordance with their starting methods and are usually referred to by names descriptive of these methods. Selection of the appropriate motor is based on the starting- and running-torque requirements of the load, the duty cycle of the load, and the limitations on starting and running current from the supply line for the motor. The cost of single-phase motors increases with their rating and with their performance characteristics such as starting-torque-to-current ratio. Typically, in order to minimize cost, an application engineer will select the motor with the lowest rating and performance that can meet the specifications of the application. Where a large number of motors are to be used for a specific purpose, a special motor may be designed in order to ensure the least cost. In the fractional-kilowatt motor business, small differences in cost are important.

Starting methods and the resulting torque-speed characteristics are considered qualitatively in this section. A quantitative theory for analyzing these motors is developed in Section 9.4.2.

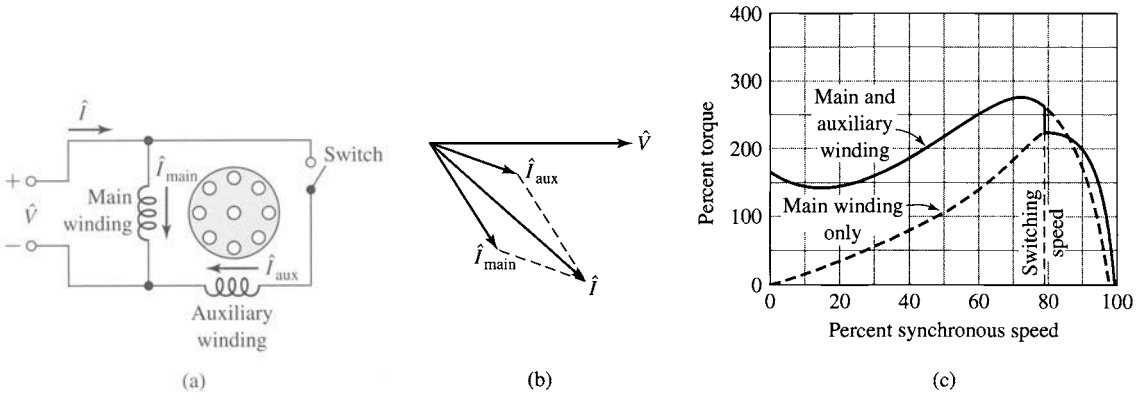

Figure 9.3 Split-phase motor: (a) connections, (b) phasor diagram at starting, and (c) typical torque-speed characteristic.

9.2.1 Split-Phase Motors

Split-phase motors have two stator windings, a *main winding* (also referred to as the *run winding*) which we will refer to with the subscript 'main' and an *auxiliary winding* (also referred to as the *start winding*) which we will refer to with the subscript 'aux'. As in a two-phase motor, the axes of these windings are displaced 90 electrical degrees in space, and they are connected as shown in Fig. 9.3a. The auxiliary winding has a higher resistance-to-reactance ratio than the main winding, with the result that the two currents will be out of phase, as indicated in the phasor diagram of Fig. 9.3b, which is representative of conditions at starting. Since the auxiliary-winding current $\hat{I}_{aux}$ leads the main-winding current $\hat{I}_{main}$, the stator field first reaches a maximum along the axis of the auxiliary winding and then somewhat later in time reaches a maximum along the axis of the main winding.

The winding currents are equivalent to unbalanced two-phase currents, and the motor is equivalent to an unbalanced two-phase motor. The result is a rotating stator field which causes the motor to start. After the motor starts, the auxiliary winding is disconnected, usually by means of a centrifugal switch that operates at about 75 percent of synchronous speed. The simple way to obtain the high resistance-to-reactance ratio for the auxiliary winding is to wind it with smaller wire than the main winding, a permissible procedure because this winding operates only during starting. Its reactance can be reduced somewhat by placing it in the tops of the slots. A typical torque-speed characteristic for such a motor is shown in Fig. 9.3c.

Split-phase motors have moderate starting torque with low starting current. Typical applications include fans, blowers, centrifugal pumps, and office equipment. Typical ratings are 50 to 500 watts; in this range they are the lowest-cost motors available.

9.2.2 Capacitor-Type Motors

Capacitors can be used to improve motor starting performance, running performance, or both, depending on the size and connection of the capacitor. The *capacitor-start*

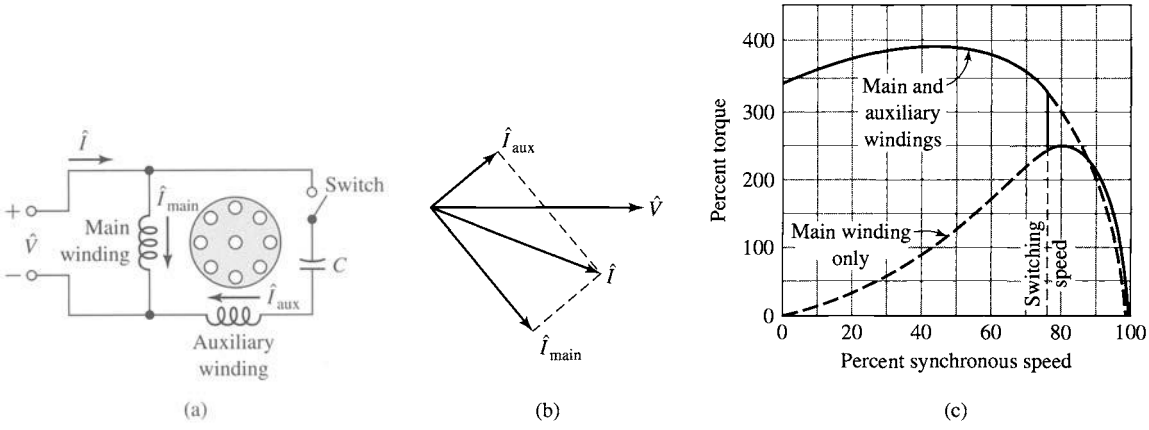

Figure 9.4 Capacitor-start motor: (a) connections, (b) phasor diagram at starting, and (c) typical torque-speed characteristic.

motor is also a split-phase motor, but the time-phase displacement between the two currents is obtained by means of a capacitor in series with the auxiliary winding, as shown in Fig. 9.4a. Again the auxiliary winding is disconnected after the motor has started, and consequently the auxiliary winding and capacitor can be designed at minimum cost for intermittent service.

By using a *starting capacitor* of appropriate value, the auxiliary-winding current $\hat{I}_{aux}$ at standstill can be made to lead the main-winding current $\hat{I}_{main}$ by 90 electrical degrees, as it would in a balanced two-phase motor (see Fig. 9.4b). In practice, the best compromise between starting torque, starting current, and cost typically results with a phase angle somewhat less than 90°. A typical torque-speed characteristic is shown in Fig. 9.4c, high starting torque being an outstanding feature. These motors are used for compressors, pumps, refrigeration and air-conditioning equipment, and other hard-to-start loads. A cutaway view of a capacitor-start motor is shown in Fig. 9.5.

In the *permanent-split-capacitor motor,* the capacitor and auxiliary winding are not cut out after starting; the construction can be simplified by omission of the switch, and the power factor, efficiency, and torque pulsations improved. For example, the capacitor and auxiliary winding could be designed for perfect two-phase operation (i.e., no backwards flux wave) at any one desired load. The losses due to the backward field at this operating point would then be eliminated, with resulting improvement in efficiency. The double-stator-frequency torque pulsations would also be eliminated, with the capacitor serving as an energy storage reservoir for smoothing out the pulsations in power input from the single-phase line, resulting in quieter operation. Starting torque must be sacrificed because the choice of capacitance is necessarily a compromise between the best starting and running values. The resulting torque-speed characteristic and a schematic diagram are given in Fig. 9.6.

If two capacitors are used, one for starting and one for running, theoretically optimum starting and running performance can both be obtained. One way of accomplishing this result is shown in Fig. 9.7a. The small value of capacitance required for

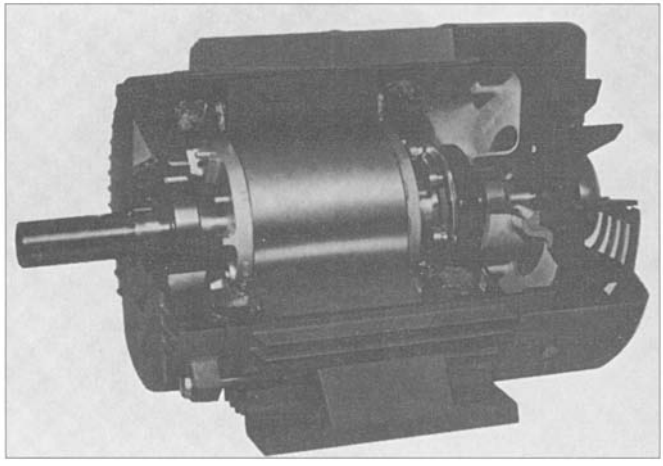

Figure 9.5 Cutaway view of a capacitor-start induction motor. The starting switch is at the right of the rotor. The motor is of drip-proof construction. (*General Electric Company.*)

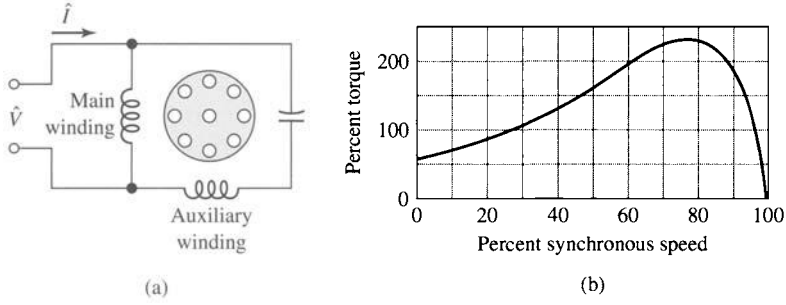

Figure 9.6 Permanent-split-capacitor motor and typical torque-speed characteristic.

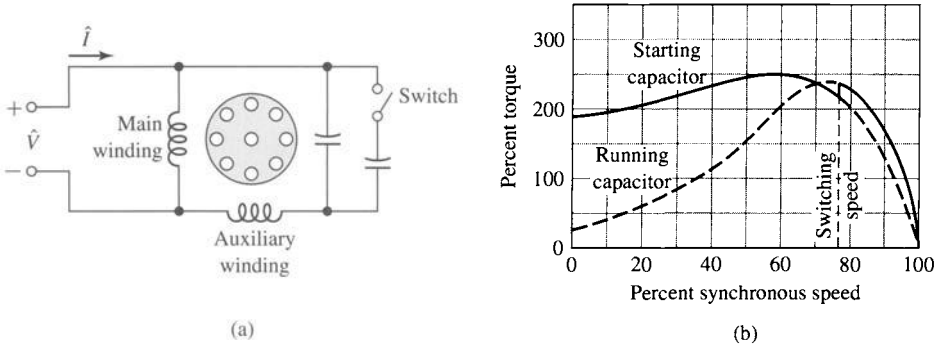

Figure 9.7 Capacitor-start, capacitor-run motor and typical torque-speed characteristic.

optimum running conditions is permanently connected in series with the auxiliary winding, and the much larger value required for starting is obtained by a capacitor connected in parallel with the running capacitor via a switch with opens as the motor comes up to speed. Such a motor is known as a *capacitor-start, capacitor-run motor.*

The capacitor for a capacitor-start motor has a typical value of 300 μF for a 500-W motor. Since it must carry current for just the starting time, the capacitor is a special compact ac electrolytic type made for motor-starting duty. The capacitor for the same motor permanently connected has a typical rating of 40 μF, and since it operates continuously, the capacitor is an ac paper, foil, and oil type. The cost of the various motor types is related to performance: the capacitor-start motor has the lowest cost, the permanent-split-capacitor motor next, and the capacitor-start, capacitor-run motor the highest cost.

EXAMPLE 9.1

A 2.5-kW 120-V 60-Hz capacitor-start motor has the following impedances for the main and auxiliary windings (at starting):

$$Z_{\text{main}} = 4.5 + j3.7\ \Omega \qquad \text{main winding}$$

$$Z_{\text{aux}} = 9.5 + j3.5\ \Omega \qquad \text{auxiliary winding}$$

Find the value of starting capacitance that will place the main and auxiliary winding currents in quadrature at starting.

■ Solution

The currents $\hat{I}_{\text{main}}$ and $\hat{I}_{\text{aux}}$ are shown in Fig. 9.4a and b. The impedance angle of the main winding is

$$\phi_{\text{main}} = \tan^{-1}\left(\frac{3.7}{4.5}\right) = 39.6^\circ$$

To produce currents in time quadrature with the main winding, the impedance angle of the auxiliary winding circuit (including the starting capacitor) must be

$$\phi = 39.6^\circ - 90.0^\circ = -50.4^\circ$$

The combined impedance of the auxiliary winding and starting capacitor is equal to

$$Z_{\text{total}} = Z_{\text{aux}} + jX_c = 9.5 + j(3.5 + X_c)\ \Omega$$

where $X_c = -\frac{1}{\omega C}$ is the reactance of the capacitor and $\omega = 2\pi 60 \approx 377$ rad/sec. Thus

$$\tan^{-1}\left(\frac{3.5 + X_c}{9.5}\right) = -50.4^\circ$$

$$\frac{3.5 + X_c}{9.5} = \tan(-50.4^\circ) = -1.21$$

and hence

$$X_c = -1.21 \times 9.5 - 3.5 = -15.0\ \Omega$$

The capacitance C is then

$$C = \frac{-1}{\omega X_c} = \frac{-1}{377 \times (-15.0)} = 177\ \mu\text{F}$$

Practice Problem 9.1

Consider the motor of Example 9.1. Find the phase angle between the main- and auxiliary-winding currents if the 177-μF capacitor is replaced by a 200-μF capacitor.

Solution

85.2°

9.2.3 Shaded-Pole Induction Motors

As illustrated schematically in Fig. 9.8a, the *shaded-pole induction motor* usually has salient poles with one portion of each pole surrounded by a short-circuited turn of copper called a *shading coil*. Induced currents in the shading coil cause the flux in the shaded portion of the pole to lag the flux in the other portion. The result is similar to a rotating field moving in the direction from the unshaded to the shaded portion of the pole; currents are induced in the squirrel-cage rotor and a low starting torque is produced. A typical torque-speed characteristic is shown in Fig. 9.8b. Their efficiency is low, but shaded-pole motors are the least expensive type of subfractional-kilowatt motor. They are found in ratings up to about 50 watts.

9.2.4 Self-Starting Synchronous-Reluctance Motors

Any one of the induction-motor types described above can be made into a *self-starting synchronous-reluctance motor*. Anything which makes the reluctance of the air gap a function of the angular position of the rotor with respect to the stator coil axis will produce reluctance torque when the rotor is revolving at synchronous speed. For

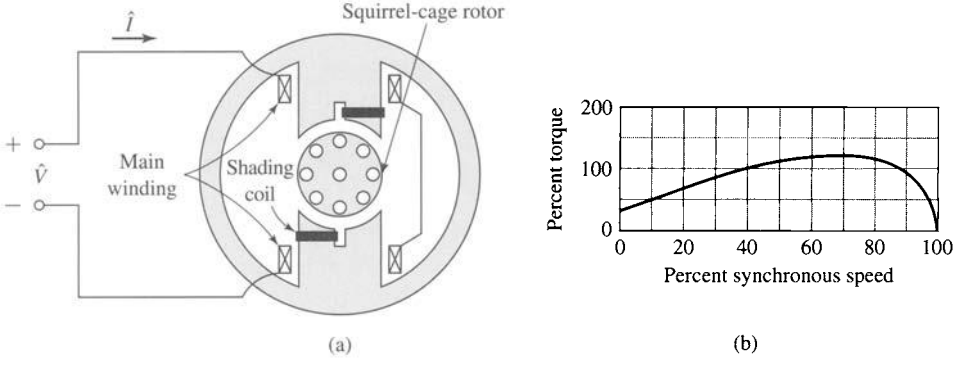

Figure 9.8 Shaded-pole induction motor and typical torque-speed characteristic.

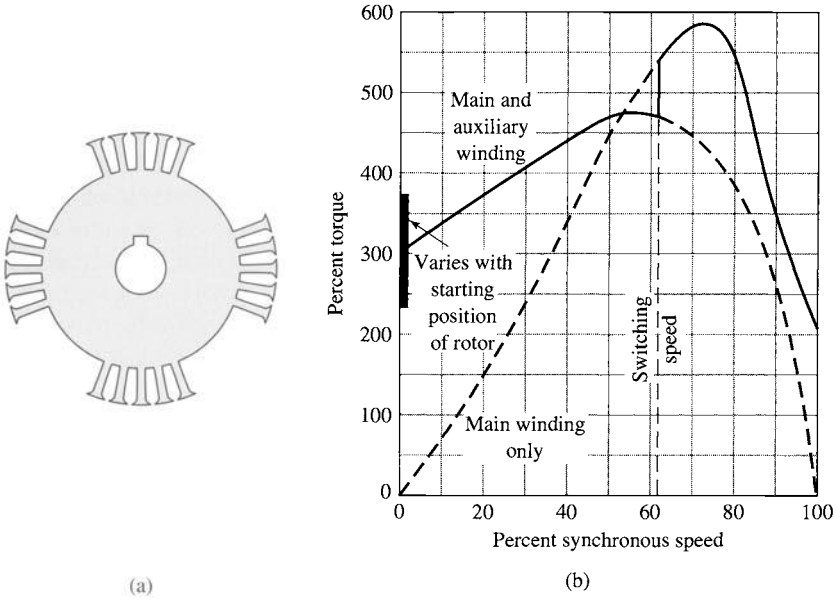

Figure 9.9 Rotor punching for four-pole synchronous-reluctance motor and typical torque-speed characteristic.

example, suppose some of the teeth are removed from a squirrel-cage rotor, leaving the bars and end rings intact, as in an ordinary squirrel-cage induction motor. Figure 9.9a shows a lamination for such a rotor designed for use with a four-pole stator. The stator may be polyphase or any one of the single-phase types described above.

The motor will start as an induction motor and at light loads will speed up to a small value of slip. The reluctance torque arises from the tendency of the rotor to try to align itself in the minimum-reluctance position with respect to the synchronously revolving forward air-gap flux wave, in accordance with the principles discussed in Chapter 3. At a small slip, this torque alternates slowly in direction; the rotor is accelerated during a positive half cycle of the torque variation and decelerated during the succeeding negative half cycle. If the moment of inertia of the rotor and its mechanical load are sufficiently small, the rotor will be accelerated from slip speed up to synchronous speed during an accelerating half cycle of the reluctance torque. The rotor will then pull into synchronism and continue to run at synchronous speed. The presence of any backward-revolving stator flux wave will produce torque ripple and additional losses, but synchronous operation will be maintained provided the load torque is not excessive.

A typical torque-speed characteristic for a split-phase-start synchronous-reluctance motor is shown in Fig. 9.9b. Notice the high values of induction-motor torque. The reason for this is that in order to obtain satisfactory synchronous-motor characteristics, it has been found necessary to build synchronous-reluctance motors in frames which would be suitable for induction motors of two or three times their synchronous-motor rating. Also notice that the principal effect of the salient-pole rotor

on the induction-motor characteristic is at standstill, where considerable "cogging" is evident; i.e., the torque varies considerably with rotor position.

9.2.5 Hysteresis Motors

The phenomenon of hysteresis can be used to produce mechanical torque. In its simplest form, the rotor of a *hysteresis motor* is a smooth cylinder of magnetically hard steel, without windings or teeth. It is placed inside a slotted stator carrying distributed windings designed to produce as nearly as possible a sinusoidal space distribution of flux, since undulations in the flux wave greatly increase the losses. In single-phase motors, the stator windings usually are of the permanent-split-capacitor type, as in Fig. 9.6. The capacitor is chosen so as to result in approximately balanced two-phase conditions within the motor windings. The stator then produces a primarily space-fundamental air-gap field revolving at synchronous speed.

Instantaneous magnetic conditions in the air gap and rotor are indicated in Fig. 9.10a for a two-pole stator. The axis SS' of the stator-mmf wave revolves at synchronous speed. Because of hysteresis, the magnetization of the rotor lags behind the inducing mmf wave, and therefore the axis RR' of the rotor flux wave lags behind the axis of the stator-mmf wave by the hysteretic lag angle δ (Fig. 9.10a). If the rotor is stationary, starting torque is produced proportional to the product of the fundamental components of the stator mmf and rotor flux and the sine of the torque angle δ. The rotor then accelerates if the torque of the load is less than the developed torque of the motor.

As long as the rotor is turning at less than synchronous speed, each region of the rotor is subjected to a repetitive hysteresis cycle at slip frequency. While the rotor accelerates, the lag angle δ remains constant if the flux is constant, since the angle δ

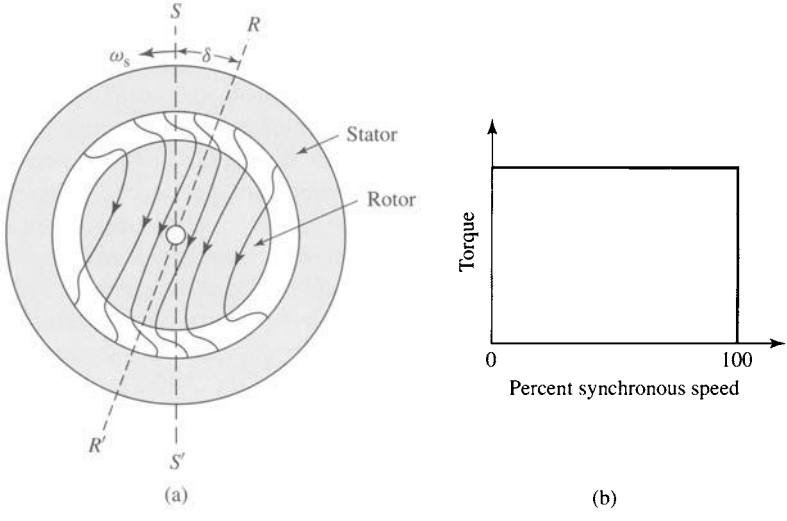

Figure 9.10 (a) General nature of the magnetic field in the air gap and rotor of a hysteresis motor; (b) idealized torque-speed characteristic.

depends merely on the hysteresis loop of the rotor material and is independent of the rate at which the loop is traversed. The motor therefore develops constant torque right up to synchronous speed, as shown in the idealized torque-speed characteristic of Fig. 9.10b. This feature is one of the advantages of the hysteresis motor. In contrast with a reluctance motor, which must "snap" its load into synchronism from an induction-motor torque-speed characteristic, a hysteresis motor can synchronize any load which it can accelerate, no matter how great the inertia. After reaching synchronism, the motor continues to run at synchronous speed and adjusts its torque angle so as to develop the torque required by the load.

The hysteresis motor is inherently quiet and produces smooth rotation of its load. Furthermore, the rotor takes on the same number of poles as the stator field. The motor lends itself to multispeed synchronous operation when the stator is wound with several sets of windings and utilizes pole-changing connections. The hysteresis motor can accelerate and synchronize high-inertia loads because its torque is uniform from standstill to synchronous speed.

9.3 REVOLVING-FIELD THEORY OF SINGLE-PHASE INDUCTION MOTORS

As discussed in Section 9.1, the stator-mmf wave of a single-phase induction motor can be shown to be equivalent to two constant-amplitude mmf waves revolving at synchronous speed in opposite directions. Each of these component stator-mmf waves induces its own component rotor currents and produces induction-motor action just as in a balanced polyphase motor. This double-revolving-field concept not only is useful for qualitative visualization but also can be developed into a quantitative theory applicable to a wide variety of induction-motor types. We will not discuss the full quantitative theory here.[1] However, we will consider the simpler, but important case of a single-phase induction motor running on only its main winding.

Consider conditions with the rotor stationary and only the main stator winding excited. The motor then is equivalent to a transformer with its secondary short-circuited. The equivalent circuit is shown in Fig. 9.11a, where $R_{1,\text{main}}$ and $X_{1,\text{main}}$ are, respectively, the resistance and leakage reactance of the main winding, $X_{m,\text{main}}$ is the magnetizing reactance, and $R_{2,\text{main}}$ and $X_{2,\text{main}}$ are the standstill values of the rotor resistance and leakage reactance referred to the main stator winding by use of the appropriate turns ratio. Core loss, which is omitted here, will be accounted for later as if it were a rotational loss. The applied voltage is $\hat{V}$, and the main-winding current is $\hat{I}_{\text{main}}$. The voltage $\hat{E}_{\text{main}}$ is the counter emf generated in the main winding by the stationary pulsating air-gap flux wave produced by the combined action of the stator and rotor currents.

In accordance with the double-revolving-field concept of Section 9.1, the stator mmf can be resolved into half-amplitude forward and backward rotating fields. At

[1] For an extensive treatment of single-phase motors, see, for example, C. B. Veinott, *Fractional- and Subfractional-Horsepower Electric Motors*, McGraw-Hill, New York, 1970.

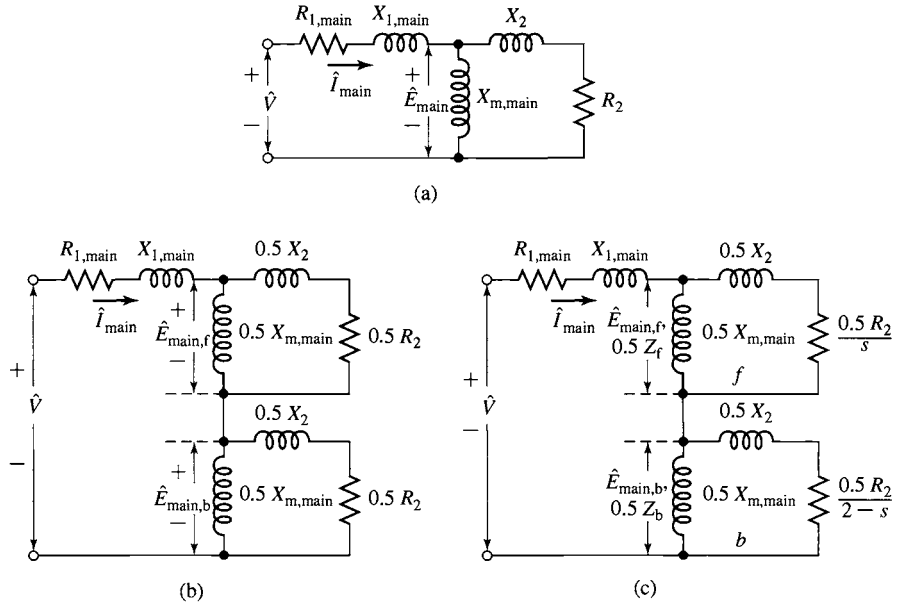

Figure 9.11 Equivalent circuits for a single-phase induction motor: (a) rotor blocked; (b) rotor blocked, showing effects of forward and backward fields; (c) running conditions.

standstill the amplitudes of the forward and backward resultant air-gap flux waves both equal half the amplitude of the pulsating field. In Fig. 9.11b the portion of the equivalent circuit representing the effects of the air-gap flux is split into two equal portions, representing the effects of the forward and backward fields, respectively.

Now consider conditions after the motor has been brought up to speed by some auxiliary means and is running on only its main winding in the direction of the forward field at a per-unit slip s. The rotor currents induced by the forward field are of slip frequency sf_e, where f_e is the stator applied electrical frequency. Just as in any polyphase motor with a symmetric polyphase or squirrel-cage rotor, these rotor currents produce an mmf wave traveling forward at slip speed with respect to the rotor and therefore at synchronous speed with respect to the stator. The resultant of the forward waves of stator and rotor mmf creates a resultant forward wave of air-gap flux, which generates a counter emf $\hat{E}_{main,f}$ in the main winding of the stator. The reflected effect of the rotor as viewed from the stator is like that in a polyphase motor and can be represented by an impedance $0.5R_{2,main}/s + j0.5X_{2,main}$ in parallel with $j0.5X_{m,main}$ as in the portion of the equivalent circuit of Fig. 9.11c labeled 'f'. The factors of 0.5 come from the resolution of the pulsating stator mmf into forward and backward components.

Now consider conditions with respect to the backward field. The rotor is still turning at a slip s with respect to the forward field, and its per-unit speed n in the

direction of the forward field is $n = 1 - s$. The relative speed of the rotor with respect to the backward field is $1 + n$, or its slip with respect to the backward field is $1 + n = 2 - s$. The backward field then induces rotor currents whose frequency is $(2 - s)f_e$. For small slips, these rotor currents are of almost twice stator frequency.

At a small slip, an oscilloscope trace of rotor current will therefore show a high-frequency component from the backward field superposed on a low-frequency component from the forward field. As viewed from the stator, the rotor-mmf wave of the backward-field induced rotor current travels at synchronous speed but in the backward direction. The equivalent-circuit representing these internal reactions from the viewpoint of the stator is like that of a polyphase motor whose slip is $2 - s$ and is shown in the portion of the equivalent circuit (Fig. 9.11c) labeled 'b'. As with the forward field, the factors of 0.5 come from the resolution of the pulsating stator mmf into forward and backward components. The voltage $\hat{E}_{\text{main,b}}$ across the parallel combination representing the backward field is the counter emf generated in the main winding of the stator by the resultant backward field.

By use of the equivalent circuit of Fig. 9.11c, the stator current, power input, and power factor can be computed for any assumed value of slip when the applied voltage and the motor impedances are known. To simplify the notation, let

$$Z_f \equiv R_f + jX_f \equiv \left(\frac{R_{2,\text{main}}}{s} + jX_{2,\text{main}}\right) \text{ in parallel with } jX_{\text{m,main}} \tag{9.4}$$

and

$$Z_b \equiv R_b + jX_b \equiv \left(\frac{R_{2,\text{main}}}{2 - s} + jX_{2,\text{main}}\right) \text{ in parallel with } jX_{\text{m,main}} \tag{9.5}$$

The impedances representing the reactions of the forward and backward fields from the viewpoint of the single-phase main stator winding are $0.5Z_f$ and $0.5Z_b$, respectively, in Fig. 9.11c.

Examination of the equivalent circuit (Fig. 9.11c) confirms the conclusion, reached by qualitative reasoning in Section 9.1 (Fig. 9.2b), that the forward air-gap flux wave increases and the backward wave decreases when the rotor is set in motion. When the motor is running at a small slip, the reflected effect of the rotor resistance in the forward field, $0.5R_{2,\text{main}}/s$, is much larger than its standstill value, while the corresponding effect in the backward field, $0.5R_{2,\text{main}}/(2 - s)$, is smaller. The forward-field impedance therefore is larger than its standstill value, while that of the backward field is smaller. The forward-field counter emf $\hat{E}_{\text{main,f}}$ therefore is larger than its standstill value, while the backward-field counter emf $\hat{E}_{\text{main,b}}$ is smaller; i.e., the forward air-gap flux wave increases, while the backward flux wave decreases.

Mechanical power and torque can be computed by application of the torque and power relations developed for polyphase motors in Chapter 6. The torques produced by the forward and backward fields can each be treated in this manner. The interactions of the oppositely rotating flux and mmf waves cause torque pulsations at twice stator frequency but produce no average torque.

As in Eq. 6.25, the electromagnetic torque $T_{\text{main,f}}$ of the forward field in newton-meters equals $1/\omega_s$ times the power $P_{\text{gap,f}}$ in watts delivered by the stator winding to the forward field, where ω_s is the synchronous angular velocity in mechanical radians per second; thus

$$T_{\text{main,f}} = \frac{1}{\omega_s} P_{\text{gap,f}} \tag{9.6}$$

When the magnetizing impedance is treated as purely inductive, $P_{\text{gap,f}}$ is the power absorbed by the impedance $0.5Z_f$; that is,

$$P_{\text{gap,f}} = I^2(0.5R_f) \tag{9.7}$$

where R_f is the resistive component of the forward-field impedance defined in Eq. 9.4.

Similarly, the internal torque $T_{\text{main,b}}$ of the backward field is

$$T_{\text{main,b}} = \frac{1}{\omega_s} P_{\text{gap,b}} \tag{9.8}$$

where $P_{\text{gap,b}}$ is the power delivered by the stator winding to the backward field, or

$$P_{\text{gap,b}} = I^2(0.5R_b) \tag{9.9}$$

where R_b is the resistive component of the backward-field impedance Z_b defined in Eq. 9.5.

The torque of the backward field is in the opposite direction to that of the forward field, and therefore the net internal torque T_{mech} is

$$T_{\text{mech}} = T_{\text{main,f}} - T_{\text{main,b}} = \frac{1}{\omega_s}(P_{\text{gap,f}} - P_{\text{gap,b}}) \tag{9.10}$$

Since the rotor currents produced by the two component air-gap fields are of different frequencies, the total rotor I^2R loss is the numerical sum of the losses caused by each field. In general, as shown by comparison of Eqs. 6.17 and 6.19, the rotor I^2R loss caused by a rotating field equals the slip of the field times the power absorbed from the stator. Thus

$$\text{Forward-field rotor } I^2R = sP_{\text{gap,f}} \tag{9.11}$$

$$\text{Backward-field rotor } I^2R = (2 - s)P_{\text{gap,b}} \tag{9.12}$$

$$\text{Total rotor } I^2R = sP_{\text{gap,f}} + (2 - s)P_{\text{gap,b}} \tag{9.13}$$

Since power is torque times angular velocity and the angular velocity of the rotor is $(1 - s)\omega_s$, using Eq. 9.10, the internal power P_{mech} converted to mechanical form, in watts, is

$$P_{\text{mech}} = (1 - s)\omega_s T_{\text{mech}} = (1 - s)(P_{\text{gap,f}} - P_{\text{gap,b}}) \tag{9.14}$$

As in the polyphase motor, the internal torque T_{mech} and internal power P_{mech} are not the output values because rotational losses remain to be accounted for. It is obviously correct to subtract friction and windage losses from T_{mech} or P_{mech} and it

is usually assumed that core losses can be treated in the same manner. For the small changes in speed encountered in normal operation, the rotational losses are often assumed to be constant.[2]

EXAMPLE 9.2

A $\frac{1}{4}$-hp, 110-V, 60-Hz, four-pole, capacitor-start motor has the following equivalent circuit parameter values (in Ω) and losses:

$$R_{1,\text{main}} = 2.02 \qquad X_{1,\text{main}} = 2.79 \qquad R_{2,\text{main}} = 4.12$$

$$X_{2,\text{main}} = 2.12 \qquad X_{\text{m,main}} = 66.8$$

$$\text{Core loss} = 24 \text{ W} \qquad \text{Friction and windage loss} = 13 \text{ W}$$

For a slip of 0.05, determine the stator current, power factor, power output, speed, torque, and efficiency when this motor is running as a single-phase motor at rated voltage and frequency with its starting winding open.

■ Solution

The first step is to determine the values of the forward- and backward-field impedances at the assigned value of slip. The following relations, derived from Eq. 9.4, simplify the computations of the forward-field impedance Z_f:

$$R_f = \left(\frac{X_{\text{m,main}}^2}{X_{22}}\right) \frac{1}{sQ_{2,\text{main}} + 1/(sQ_{2,\text{main}})} \qquad X_f = \frac{X_{2,\text{main}}X_{\text{m,main}}}{X_{22}} + \frac{R_f}{sQ_{2,\text{main}}}$$

where

$$X_{22} = X_{2,\text{main}} + X_{\text{m,main}} \qquad \text{and} \qquad Q_{2,\text{main}} = \frac{X_{22}}{R_{2,\text{main}}}$$

Substitution of numerical values gives, for $s = 0.05$,

$$Z_f = R_f + jX_f = 31.9 + j40.3\ \Omega$$

Corresponding relations for the backward-field impedance Z_b are obtained by substituting $2 - s$ for s in these equations. When $(2 - s)Q_{2,\text{main}}$ is greater than 10, as is usually the case, less than 1 percent error results from use of the following approximate forms:

$$R_b = \frac{R_{2,\text{main}}}{2 - s}\left(\frac{X_{\text{m,main}}}{X_{22}}\right)^2 \qquad X_b = \frac{X_{2,\text{main}}X_{\text{m,main}}}{X_{22}} + \frac{R_b}{(2 - s)Q_{2,\text{main}}}$$

Substitution of numerical values gives, for $s = 0.05$,

$$Z_b = R_b + jX_b = 1.98 + j2.12\ \Omega$$

[2] For a treatment of the experimental determination of motor constants and losses, see Veinott, op. cit., Chapter 18.

Addition of the series elements in the equivalent circuit of Fig. 9.11c gives

$$\begin{aligned} R_{1,\text{main}} + jX_{1,\text{main}} &= 2.02 + j2.79 \\ 0.5(R_\text{f} + jX_\text{f}) &= 15.95 + j20.15 \\ \underline{0.5(R_\text{b} + jX_\text{b})} &= \underline{0.99 + j1.06} \\ \text{Total Input } Z &= 18.96 + j24.00 = 30.6\angle 51.7^\circ \end{aligned}$$

$$\text{Stator current } I = \frac{V}{Z} = \frac{110}{30.6} = 3.59 \text{ A}$$

$$\text{Power factor} = \cos(51.7^\circ) = 0.620$$

$$\text{Power input} = P_\text{in} = VI \times \text{power factor} = 110 \times 3.59 \times 0.620 = 244 \text{ W}$$

The power absorbed by the forward field (Eq. 9.7) is

$$P_{\text{gap,f}} = I^2(0.5R_\text{f}) = 3.59^2 \times 15.95 = 206 \text{ W}$$

The power absorbed by the backward field (Eq. 9.9) is

$$P_{\text{gap,b}} = I^2(0.5R_\text{b}) = 3.59^2 \times 0.99 = 12.8 \text{ W}$$

The internal mechanical power (Eq. 9.14) is

$$P_\text{mech} = (1 - s)(P_{\text{gap,f}} - P_{\text{gap,b}}) = 0.95(206 - 13) = 184 \text{ W}$$

Assuming that the core loss can be combined with the friction and windage loss, the rotational loss becomes $24 + 13 = 37$ W and the shaft output power is the difference. Thus

$$P_\text{shaft} = 184 - 37 = 147 \text{ W} = 0.197 \text{ hp}$$

From Eq. 4.40, the synchronous speed in rad/sec is given by

$$\omega_\text{s} = \left(\frac{2}{\text{poles}}\right)\omega_\text{e} = \left(\frac{2}{4}\right)120\pi = 188.5 \text{ rad/sec}$$

or in terms of r/min from Eq. 4.41

$$n_s = \left(\frac{120}{\text{poles}}\right)f_\text{e} = \left(\frac{120}{4}\right)60 = 1800 \text{ r/min}$$

$$\begin{aligned} \text{Rotor speed} &= (1 - s)(\text{synchronous speed}) \\ &= 0.95 \times 1800 = 1710 \text{ r/min} \end{aligned}$$

and

$$\omega_\text{m} = 0.95 \times 188.5 = 179 \text{ rad/sec}$$

The torque can be found from Eq. 9.14.

$$T_\text{shaft} = \frac{P_\text{shaft}}{\omega_\text{m}} = \frac{147}{179} = 0.821 \text{ N} \cdot \text{m}$$

and the efficiency is

$$\eta = \frac{P_{\text{shaft}}}{P_{\text{in}}} = \frac{147}{244} = 0.602 = 60.2\%$$

As a check on the power bookkeeping, compute the losses:

$$I^2R_{1,\text{main}} = (3.59)^2(2.02) = 26.0$$

$$\text{Forward-field rotor } I^2R \text{ (Eq. 9.11)} = 0.05 \times 206 = 10.3$$

$$\text{Backward-field rotor } I^2R \text{ (Eq. 9.12)} = 1.95 \times 12.8 = 25.0$$

$$\text{Rotational losses} = \underline{37.0}$$

$$98.3\text{ W}$$

From $P_{\text{in}} - P_{\text{shaft}}$, the total losses = 97 W which checks within accuracy of computations.

Practice Problem 9.2

Assume the motor of Example 9.2 to be operating at a slip of 0.065 and at rated voltage and frequency. Determine (*a*) the stator current and power factor and (*b*) the power output.

Solution

a. 4.0 A, power factor = 0.70 lagging
b. 190 W

Examination of the order of magnitude of the numerical values in Example 9.2 suggests approximations which usually can be made. These approximations pertain particularly to the backward-field impedance. Note that the impedance $0.5(R_b + jX_b)$ is only about 5 percent of the total motor impedance for a slip near full load. Consequently, an approximation as large as 20 percent of this impedance would cause only about 1 percent error in the motor current. Although, strictly speaking, the backward-field impedance is a function of slip, very little error usually results from computing its value at any convenient slip in the normal running region, e.g., 5 percent, and then assuming R_b and X_b to be constants.

Corresponding to a slightly greater approximation, the shunting effect of $jX_{m,\text{main}}$ on the backward-field impedance can often be neglected, whence

$$Z_b \approx \frac{R_{2,\text{main}}}{2 - s} + jX_{2,\text{main}} \tag{9.15}$$

This equation gives values of the backward-field resistance that are a few percent high, as can be seen by comparison with the exact expression given in Example 9.2. Neglecting s in Eq. 9.15 would tend to give values of the backward-field resistance that would be too low, and therefore such an approximation would tend to counteract the error in Eq. 9.15. Consequently, for small slips

$$Z_b \approx \frac{R_{2,\text{main}}}{2} + jX_{2,\text{main}} \tag{9.16}$$

In a polyphase motor (Section 6.5), the maximum internal torque and the slip at which it occurs can easily be expressed in terms of the motor parameters; the maximum internal torque is independent of rotor resistance. No such simple expressions exist for a single-phase motor. The single-phase problem is much more involved because of the presence of the backward field, the effect of which is twofold: (1) it absorbs some of the applied voltage, thus reducing the voltage available for the forward field and decreasing the forward torque developed; and (2) the backward field produces negative torque, reducing the effective developed torque. Both of these effects depend on rotor resistance as well as leakage reactance. Consequently, unlike the polyphase motor, the maximum internal torque of a single-phase motor is influenced by rotor resistance; increasing the rotor resistance decreases the maximum torque and increases the slip at which maximum torque occurs.

Principally because of the effects of the backward field, a single-phase induction motor is somewhat inferior to a polyphase motor using the same rotor and the same stator core. The single-phase motor has a lower maximum torque which occurs at a lower slip. For the same torque, the single-phase motor has a higher slip and greater losses, largely because of the backward-field rotor I^2R loss. The volt-ampere input to the single-phase motor is greater, principally because of the power and reactive volt-amperes consumed by the backward field. The stator I^2R loss also is somewhat higher in the single-phase motor, because one phase, rather than several, must carry all the current. Because of the greater losses, the efficiency is lower, and the temperature rise for the same torque is higher. A larger frame size must be used for a single-phase motor than for a polyphase motor of the same power and speed rating. Because of the larger frame size, the maximum torque can be made comparable with that of a physically smaller but equally rated polyphase motor. In spite of the larger frame size and the necessity for auxiliary starting arrangements, general-purpose single-phase motors in the standard fractional-kilowatt ratings cost approximately the same as correspondingly rated polyphase motors because of the much greater volume of production of the former.

9.4 TWO-PHASE INDUCTION MOTORS

As we have seen, most single-phase induction motors are actually constructed in the form of two-phase motors, with two stator windings in space quadrature. The main and auxiliary windings are typically quite different, with a different number of turns, wire size, and turns distribution. This difference, in combination with the capacitor that is typically used in series with the auxiliary winding, guarantees that the mmfs produced by the two winding currents will be quite unbalanced; at best they may be balanced at one specific operating point. We will thus discuss various analytical techniques for two-phase motors, both to expand our understanding and insight into machine performance and also to develop techniques for the analysis of single- and two-phase motors.

Under balanced operating conditions, a symmetrical two-phase motor can be analyzed using techniques developed in Chapter 6 for three-phase motors, modified

only slightly to take into account the fact that there are two phases rather than three. In this section, we will first discuss one technique that can be used to analyze a symmetrical two-phase motor operating under unbalanced operating conditions. We will then formally derive an analytical model for an unsymmetrical two-phase motor that can be applied to the general case single-phase motors operating off both their main and auxiliary windings.

9.4.1 Unbalanced Operation of Symmetrical Two-Phase Machines; The Symmetrical-Component Concept

When operating from the main winding alone, the single-phase motor is the extreme case of a motor operating under unbalanced stator-current conditions. In some cases, unbalanced voltages or currents are produced in the supply network to a motor, e.g., when a line fuse is blown. In other cases, unbalanced voltages are produced by the starting impedances of single-phase motors, as described in Section 9.2. The purpose of this section is to develop the symmetrical-component theory of two-phase induction motors from the double-revolving-field concept and to show how the theory can be applied to a variety of problems involving induction motors having two stator windings in space quadrature.

First consider in review what happens when balanced two-phase voltages are applied to the stator terminals of a two-phase machine having a uniform air gap, a symmetrical polyphase or cage rotor, and two identical stator windings α and β in space quadrature. The stator currents are equal in magnitude and in time quadrature. When the current in winding α is at its instantaneous maximum, the current in winding β is zero and the stator-mmf wave is centered on the axis of winding α. Similarly, the stator-mmf wave is centered on the axis of winding β at the instant when the current in winding β is at its instantaneous maximum. The stator-mmf wave therefore travels 90 electrical degrees in space in a time interval corresponding to a 90° phase change of the applied voltage, with the direction of its travel depending on the phase sequence of the currents. A more complete analysis in the manner of Section 4.5 shows that the traveling wave has constant amplitude and constant angular velocity. This fact is, of course, the basis for the theory of the balanced operation of induction machines.

The behavior of the motor for balanced two-phase applied voltages of either phase sequence can be readily determined. Thus, if the rotor is turning at a slip s in the direction from winding α toward winding β, the terminal impedance per phase is given by the equivalent circuit of Fig. 9.12a when the applied voltage $\hat{V}_\beta$ lags the applied voltage $\hat{V}_\alpha$ by 90°. Throughout the rest of this treatment, this phase sequence is called *positive sequence* and is designated by the subscript 'f' since positive-sequence currents result in a forward field. With the rotor running at the same speed and in the same direction, the terminal impedance per phase is given by the equivalent circuit of Fig. 9.12b when $\hat{V}_\beta$ leads $\hat{V}_\alpha$ by 90°. This phase sequence is called *negative sequence* and is designated by subscript 'b', since negative-sequence currents produce a backward field.

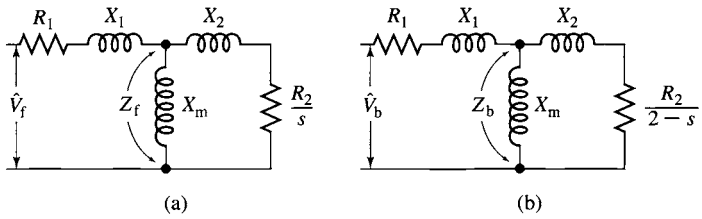

Figure 9.12 Single-phase equivalent circuits for a two-phase motor under unbalanced conditions: (a) forward field and (b) backward field.

Suppose now that *two* balanced two-phase voltage sources of *opposite phase sequence* are connected in series and applied simultaneously to the motor, as indicated in Fig. 9.13a, where phasor voltages $\hat{V}_f$ and $j\hat{V}_f$ applied, respectively, to windings α and β form a balanced system of positive sequence, and phasor voltages $\hat{V}_b$ and $-j\hat{V}_b$ form another balanced system but of negative sequence.

The resultant voltage V_α applied to winding α is, as a phasor,

$$\hat{V}_\alpha = \hat{V}_f + \hat{V}_b \tag{9.17}$$

and that applied to winding β is

$$\hat{V}_\beta = j\hat{V}_f - j\hat{V}_b \tag{9.18}$$

Fig. 9.13b shows a generalized phasor diagram in which the forward, or positive-sequence, system is given by the phasors $\hat{V}_f$ and $j\hat{V}_f$ and the backward, or negative-sequence, system is given by the phasors $\hat{V}_b$ and $-j\hat{V}_b$. The resultant voltages, given by the phasors $\hat{V}_\alpha$ and $\hat{V}_\beta$ are not, in general, either equal in magnitude or in time

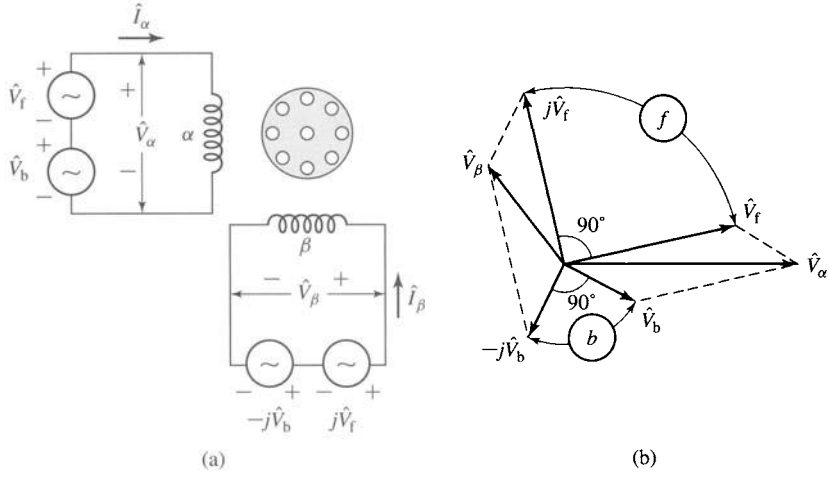

Figure 9.13 Synthesis of an unbalanced two-phase system from the sum of two balanced systems of opposite phase sequence.

quadrature. From this discussion we see that an unbalanced two-phase system of applied voltages V_α and V_β can be synthesized by combining two balanced voltage sets of opposite phase sequence.

The symmetrical-component systems are, however, much easier to work with than their unbalanced resultant system. Thus, it is easy to compute the component currents produced by each symmetrical-component system of applied voltages because the induction motor operates as a balanced two-phase motor for each component system. By superposition, the actual current in a winding then is the sum of its components. Thus, if $\hat{I}_f$ and $\hat{I}_b$ are, respectively, the positive- and negative-sequence component phasor currents in winding α, then the corresponding positive- and negative-sequence component phasor currents in winding β are, respectively, $j\hat{I}_f$ and $-j\hat{I}_b$, and the actual winding currents $\hat{I}_\alpha$ and $\hat{I}_\beta$ are

$$\hat{I}_\alpha = \hat{I}_f + \hat{I}_b \tag{9.19}$$

$$\hat{I}_\beta = j\hat{I}_f - j\hat{I}_b \tag{9.20}$$

The inverse operation of finding the symmetrical components of specified voltages or currents must be performed often. Solution of Eqs. 9.17 and 9.18 for the phasor components $\hat{V}_f$ and $\hat{V}_b$ in terms of known phasor voltages $\hat{V}_\alpha$ and $\hat{V}_\beta$ gives

$$\hat{V}_f = \frac{1}{2}(\hat{V}_\alpha - j\hat{V}_\beta) \tag{9.21}$$

$$\hat{V}_b = \frac{1}{2}(\hat{V}_\alpha + j\hat{V}_\beta) \tag{9.22}$$

These operations are illustrated in the phasor diagram of Fig. 9.14. Obviously, similar relations give the phasor symmetrical components $\hat{I}_f$ and $\hat{I}_b$ of the current in winding α in terms of specified phasor currents $\hat{I}_m$ and $\hat{I}_a$ in the two phases; thus

$$\hat{I}_f = \frac{1}{2}(\hat{I}_\alpha - j\hat{I}_\beta) \tag{9.23}$$

$$\hat{I}_b = \frac{1}{2}(\hat{I}_\alpha + j\hat{I}_\beta) \tag{9.24}$$

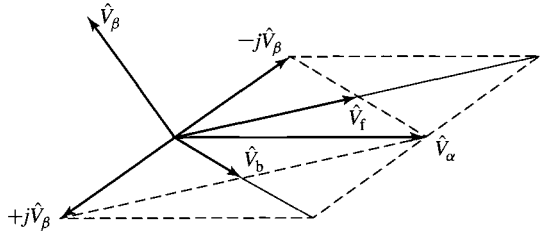

Figure 9.14 Resolution of unbalanced two-phase voltages into symmetrical components.

EXAMPLE 9.3

The equivalent-circuit parameters of a 5-hp 220-V 60-Hz four-pole two-phase squirrel-cage induction motor in ohms per phase are

$$R_1 = 0.534 \qquad X_1 = 2.45 \qquad X_m = 70.1 \qquad R_2 = 0.956 \qquad X_2 = 2.96$$

This motor is operated from an unbalanced two-phase 60-Hz source whose phase voltages are, respectively, 230 and 210 V, the smaller voltage leading the larger by 80°. For a slip of 0.05, find (*a*) the positive- and negative-sequence components of the applied voltages, (*b*) the positive- and negative-sequence components of the stator-phase currents, (*c*) the effective values of the phase currents, and (*d*) the internal mechanical power.

■ Solution

We will solve this example using MATLAB.†

a. Let $\hat{V}_\alpha$ and $\hat{V}_\beta$ denote the voltages applied to the two phases, respectively. Then

$$\hat{V}_\alpha = 230\angle 0^\circ = 230 + j0 \text{ V}$$

$$\hat{V}_\beta = 210\angle 80^\circ = 36.4 + j207 \text{ V}$$

From Eqs. 9.21 and 9.22 the forward and backward components of voltages are, respectively,

$$\hat{V}_f = 218.4 - j18.2 = 219.2\angle -4.8^\circ \text{ V}$$

$$\hat{V}_b = 11.6 + j18.2 = 21.6\angle 57.5^\circ \text{ V}$$

b. Because of the ease with which MATLAB handles complex numbers, there is no need to use approximations such as are derived in Example 9.2. Rather, the forward- and backward-field input impedances of the motor can be calculated from the equivalent circuits of Figs. 9.12a and b. Dividing the forward-field voltage by the forward-field input impedance gives

$$\hat{I}_f = \frac{\hat{V}_f}{R_1 + jX_1 + Z_f} = 9.3 - j6.3 = 11.2\angle -34.2^\circ \text{ A}$$

Similarly, dividing the backward-field voltage by the backward-field input impedance gives

$$\hat{I}_b = \frac{\hat{V}_b}{R_1 + jX_1 + Z_b} = 3.7 - j1.5 = 4.0\angle -21.9^\circ \text{ A}$$

c. The winding currents can be calculated from Eqs. 9.19 and 9.20

$$\hat{I}_\alpha = \hat{I}_f + \hat{I}_b = 13.0 - j7.8 = 15.2\angle -31.0^\circ \text{ A}$$

$$\hat{I}_\beta = j\hat{I}_f - j\hat{I}_b = 4.8 + j5.6 = 7.4\angle 49.1^\circ \text{ A}$$

Note that the winding currents are much more unbalanced than the applied voltages. Even though the motor is not overloaded insofar as shaft load is concerned, the losses are

† MATLAB is a registered trademark of The MathWorks, Inc.

appreciably increased by the current unbalance, and the stator winding with the greatest current may overheat.

d. The power delivered across the air gap by the forward field is equal to the forward-field equivalent-circuit input power minus the corresponding stator loss

$$P_{\text{gap,f}} = 2\left(\text{Re}[\hat{V}_\text{f}\hat{I}_\text{f}^*] - I_\text{f}^2 R_1\right) = 4149\ \text{W}$$

where the factor of 2 accounts for the fact that this is a two-phase motor. Similarly, the power delivered to the backward field is

$$P_{\text{gap,b}} = 2\left(\text{Re}[\hat{V}_\text{b}\hat{I}_\text{b}^*] - I_\text{b}^2 R_1\right) = 14.5\ \text{W}$$

Here, the symbol Re[ ] indicates the real part of a complex number, and the superscript * indicates the complex conjugate.

Finally, from Eq. 9.14, the internal mechanical power developed is equal to $(1 - s)$ times the total air-gap power or

$$P_{\text{mech}} = (1 - s)(P_{\text{gap,f}} - P_{\text{gap,b}}) = 3927\ \text{W}$$

If the core losses, friction and windage, and stray load losses are known, the shaft output can be found by subtracting them from the internal power. The friction and windage losses depend solely on the speed and are the same as they would be for balanced operation at the same speed. The core and stray load losses, however, are somewhat greater than they would be for balanced operation with the same positive-sequence voltage and current. The increase is caused principally by the $(2 - s)$-frequency core and stray losses in the rotor caused by the backward field.

Here is the MATLAB script:

```
clc
clear

% Useful constants
f = 60; %60 Hz system
omega = 2*pi*f;
s = 0.05; % slip

% Parameters

R1 = 0.534;
X1 = 2.45;
Xm = 70.1;
R2 = 0.956;
X2 = 2.96;

% Winding voltages

Valpha = 230;
Vbeta = 210 * exp(j*80*pi/180);

%(a) Calculate Vf and Vb from Equations and 9-21 and 9-22

Vf = 0.5*(Valpha - j*Vbeta);
Vb = 0.5*(Valpha + j*Vbeta);
```

```
magVf = abs(Vf);
angleVf = angle(Vf)*180/pi;

magVb = abs(Vb);
angleVb = angle(Vb)*180/pi;

fprintf('\n(a)')
fprintf('\n Vf = %.1f + j %.1f = %.1f at angle %.1f degrees V', ...
 real(Vf),imag(Vf),magVf,angleVf);
fprintf('\n Vb = %.1f + j %.1f = %.1f at angle %.1f degrees V\n', ...
 real(Vb),imag(Vb),magVb,angleVb);

%(b) First calculate the forward-field input impedance of the motor from
% the equivalent circuit of Fig. 9-12(a).

Zforward = R1 + j*X1 + j*Xm*(R2/s+j*X2)/(R2/s+j*(X2+Xm));

%Now calculate the forward-field current.

If = Vf/Zforward;

magIf = abs(If);
angleIf = angle(If)*180/pi;

% Next calculate the backward-field input impedance of the motor from
% Fig. 9-12(b).

Zback = R1 + j*X1 + j*Xm*(R2/(2-s)+j*X2)/(R2/(2-s)+j*(X2+Xm));

%Now calculate the backward-field current.

Ib = Vb/Zback;

magIb = abs(Ib);
angleIb = angle(Ib)*180/pi;

fprintf('\n(b)')
fprintf('\n If = %.1f + j %.1f = %.1f at angle %.1f degrees A', ...
 real(If),imag(If),magIf,angleIf);
fprintf('\n Ib = %.1f + j %.1f = %.1f at angle %.1f degrees A\n', ...
 real(Ib),imag(Ib),magIb,angleIb);

%(c) Calculate the winding currents from Eqs. 9-19 and 9-20

Ialpha = If + Ib;

Ibeta = j*(If - Ib);

magIalpha = abs(Ialpha);
angleIalpha = angle(Ialpha)*180/pi;

magIbeta = abs(Ibeta);
angleIbeta = angle(Ibeta)*180/pi;

fprintf('\n(c)')
fprintf('\n Ialpha = %.1f + j %.1f = %.1f at angle %.1f degrees A', ...
 real(Ialpha),imag(Ialpha),magIalpha,angleIalpha);
fprintf('\n Ibeta = %.1f + j %.1f = %.1f at angle %.1f degrees A\n', ...
 real(Ibeta),imag(Ibeta),magIbeta,angleIbeta);
```

```
%(d) Power delivered to the forward field is equal to the
% forward-field input power less the stator-winding I^2R loss
Pgf = 2*(real(Vf*conj(If)) - R1*magIf^2);
% Power delivered to the backward field is equal to the
% backward-field input power less the stator-winding I^2R loss
Pgb = 2*(real(Vb*conj(Ib)) - R1*magIb^2);
% The electromagnetic power is equal to (1-s) times the
% net air-gap power
Pmech = (1-s)*(Pgf - Pgb);
fprintf('\n(d)')
fprintf('\n Power to forward field = %.1f W',Pgf)
fprintf('\n Power to backward field = %.1f W',Pgb)
fprintf('\n Pmech = %.1f W\n',Pmech)
fprintf('\n')
```

Practice Problem 9.3

For the motor of Example 9.3, use MATLAB to produce a plot of the internal mechanical power as a function of slip as the slip varies from $s = 0.04$ to $s = 0.05$ for the unbalanced voltages assumed in the example. On the same axes (using dashed lines), plot the internal mechanical power for balanced two-phase voltages of 220-V magnitude and 90° phase shift.

Solution

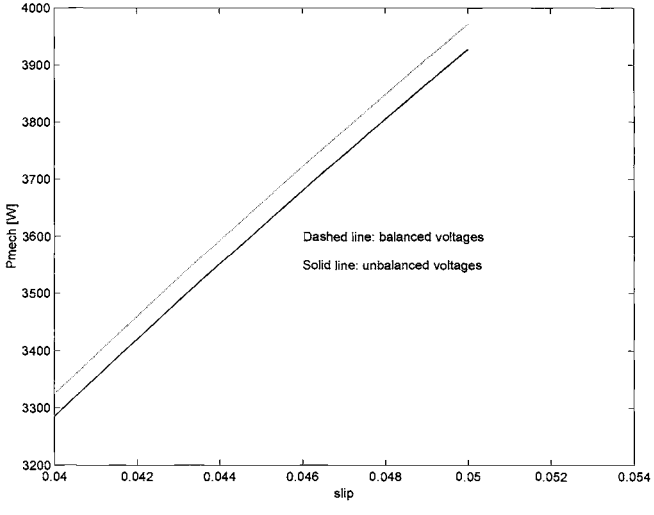

Figure 9.15 MATLAB plot for Practice Problem 9.3.

9.4.2 The General Case: Unsymmetrical Two-Phase Induction Machines

As we have discussed, a single-phase induction motor with a main and auxiliary winding is an example of an unsymmetrical two-phase induction motor. In this section we will develop a model for such a two-phase motor, using notation appropriate to the single-phase motor. We will assume, as is commonly the case, that the windings are in space quadrature but that they are unsymmetrical in that they may have a different number of turns, a different winding distribution, and so on.

Our analytical approach is to represent the rotor by an equivalent two-phase winding as shown in schematic form in Fig. 9.16 and to start with flux-linkage/current relationships for the rotor and stator of the form

$$\begin{bmatrix} \lambda_{main} \\ \lambda_{aux} \\ \lambda_{r1} \\ \lambda_{r2} \end{bmatrix} = \begin{bmatrix} L_{main} & 0 & \mathcal{L}_{main,r1}(\theta_{me}) & \mathcal{L}_{main,r2}(\theta_{me}) \\ 0 & L_{aux} & \mathcal{L}_{aux,r1}(\theta_{me}) & \mathcal{L}_{aux,r2}(\theta_{me}) \\ \mathcal{L}_{main,r1}(\theta_{me}) & \mathcal{L}_{aux,r1}(\theta_{me}) & L_r & 0 \\ \mathcal{L}_{main,r2}(\theta_{me}) & \mathcal{L}_{aux,r2}(\theta_{me}) & 0 & L_r \end{bmatrix} \begin{bmatrix} i_{main} \\ i_{aux} \\ i_{r1} \\ i_{r2} \end{bmatrix} \tag{9.25}$$

where θ_{me} is the rotor angle measured in electrical radians.

L_{main} = Self-inductance of the main winding

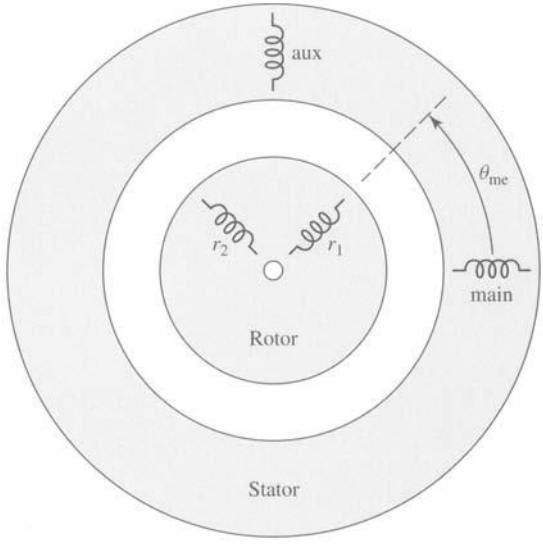

Figure 9.16 Schematic representation of a two-phase induction motor with an equivalent two-phase rotor.

L_{aux} = Self-inductance of the auxiliary winding

L_r = Self-inductance of the equivalent rotor windings

$\mathcal{L}_{main,r1}(\theta_{me})$ = Mutual inductance between the main winding and equivalent rotor winding 1

$\mathcal{L}_{main,r2}(\theta_{me})$ = Mutual inductance between the main winding and equivalent rotor winding 2

$\mathcal{L}_{aux,r1}(\theta_{me})$ = Mutual inductance between the auxiliary winding and rotor winding 1

$\mathcal{L}_{aux,r2}(\theta_{me})$ = Mutual inductance between the auxiliary winding and rotor winding 2

Assuming a sinusoidal distribution of air-gap flux, the mutual inductances between the main winding and the rotor will be of the form

$$\mathcal{L}_{main,r1}(\theta_{me}) = L_{main,r} \cos \theta_{me} \tag{9.26}$$

and

$$\mathcal{L}_{main,r2}(\theta_{me}) = -L_{main,r} \sin \theta_{me} \tag{9.27}$$

where $L_{main,r}$ is the amplitude of the mutual inductance.

The mutual inductances between the auxiliary winding will be of the same form with the exception that the auxiliary winding is displaced by 90 electrical degrees in space from the main winding. Hence we can write

$$\mathcal{L}_{aux,r1}(\theta_{me}) = L_{aux,r} \sin \theta_{me} \tag{9.28}$$

and

$$\mathcal{L}_{aux,r2}(\theta_{me}) = L_{aux,r} \cos \theta_{me} \tag{9.29}$$

Note that the auxiliary winding will typically have a different number of turns (and perhaps a different winding distribution) from that of the main winding. Thus, for modeling purposes, it is often convenient to write

$$L_{aux,r} = a\, L_{main,r} \tag{9.30}$$

where

$$a = \text{Turns ratio} = \frac{\text{Effective turns of auxiliary winding}}{\text{Effective turns of main winding}} \tag{9.31}$$

Similarly, if we write the self-inductance of the magnetizing branch as the sum of a leakage inductance $L_{main,l}$ and a magnetizing inductance L_m

$$L_{main} = L_{main,l} + L_m \tag{9.32}$$

then the self-inductance of the auxiliary winding can be written in the form

$$L_{aux} = L_{aux,l} + a^2\, L_m \tag{9.33}$$

The voltage equations for this machine can be written in terms of the winding currents and flux linkages as

$$v_{main} = i_{main} R_{main} + \frac{d\lambda_{main}}{dt} \tag{9.34}$$

$$v_{aux} = i_{aux} R_{aux} + \frac{d\lambda_{aux}}{dt} \tag{9.35}$$

$$v_{r1} = 0 = i_{r1} R_r + \frac{d\lambda_{r1}}{dt} \tag{9.36}$$

$$v_{r2} = 0 = i_{r2} R_r + \frac{d\lambda_{r2}}{dt} \tag{9.37}$$

where R_{main}, R_{aux} and R_r are the resistances of the main, auxiliary, and rotor windings, respectively. Note that the rotor-winding voltages are set equal to zero because the rotor windings of an induction motor are internally shorted.

When modeling a split-phase induction motor (Section 9.2.1) the main and auxiliary windings are simply connected in parallel, and thus v_{main} and v_{aux} are both set equal to the single-phase supply voltage when the motor is started. Following the time that the auxiliary winding is disconnected, the auxiliary-winding current is zero, and the motor is represented by a reduced-order model which includes only the main winding and the two equivalent rotor windings.

When modeling the various capacitor motors of Section 9.2.2, the circuit equations must take into account the fact that, while the main winding is connected directly to the single-phase supply, a capacitor is connected between the supply and the auxiliary-winding terminals. Depending upon the type of motor being modeled, the auxiliary winding may or may not be switched out as the motor comes up to speed.

Finally, the techniques of Section 3.5 can be used to show that the electromagnetic torque of this motor can be written as

$$\begin{aligned} T_{mech} &= i_{main} i_{r1} \frac{d\mathcal{L}_{main,r1}(\theta_{me})}{d\theta_m} + i_{main} i_{r2} \frac{d\mathcal{L}_{main,r2}(\theta_{me})}{d\theta_m} \\ &\quad + i_{aux} i_{r1} \frac{d\mathcal{L}_{aux,r1}(\theta_{me})}{d\theta_m} + i_{aux} i_{r2} \frac{d\mathcal{L}_{aux,r2}(\theta_{me})}{d\theta_m} \\ &= \left(\frac{\text{poles}}{2}\right) [-L_{main,r} (i_{main} i_{r1} \sin\theta_{me} + i_{main} i_{r2} \cos\theta_{me}) \\ &\quad + L_{aux,r} (i_{aux} i_{r1} \cos\theta_{me} - i_{aux} i_{r2} \sin\theta_{me})] \end{aligned} \tag{9.38}$$

where $\theta_m = (2/\text{poles})\theta_{me}$ is the rotor angle in radians.

Analogous to the development of the equivalent circuits derived in Chapter 6 for polyphase induction machines and earlier in this chapter for single-phase machines, the equations derived in this section can be further developed by assuming steady-state operation, with constant mechanical speed ω_{me}, corresponding to a slip s, and constant electrical supply frequency ω_e. Consistent with this assumption the rotor currents will be at frequencies $\omega_r = \omega_e - \omega_{me} = s\omega_e$ (produced by the stator positive-sequence field) and $\omega_r = \omega_e + \omega_{me} = (2-s)\omega_e$ (produced by the stator negative-sequence field).

After considerable algebraic manipulation, which includes using Eqs. 9.36 and 9.37 to eliminate the rotor currents, the main- and auxiliary-winding flux-linkage/current relationships of Eq. 9.25 can be written as phasor equations

$$\hat{\lambda}_{\text{main}} = \left[L_{\text{main}} - jL_{\text{main,r}}^2(\hat{K}^+ + \hat{K}^-)\right]\hat{I}_{\text{main}} + L_{\text{main,r}}L_{\text{aux,r}}(\hat{K}^+ - \hat{K}^-)\hat{I}_{\text{aux}} \tag{9.39}$$

and

$$\hat{\lambda}_{\text{aux}} = -L_{\text{main,r}}L_{\text{aux,r}}(\hat{K}^+ - \hat{K}^-)\hat{I}_{\text{main}} + \left[L_{\text{aux}} - jL_{\text{aux,r}}^2(\hat{K}^+ + \hat{K}^-)\right]\hat{I}_{\text{aux}} \tag{9.40}$$

where

$$\hat{K}^+ = \frac{s\omega_e}{2(R_r + js\omega_e L_r)} \tag{9.41}$$

and

$$\hat{K}^+ = \frac{(2-s)\omega_e}{2(R_r + j(2-s)\omega_e L_r)} \tag{9.42}$$

Similarly, the voltage equations, Eqs. 9.34 and 9.35 become

$$\hat{V}_{\text{main}} = \hat{I}_{\text{main}}R_{\text{main}} + j\omega_e\hat{\lambda}_{\text{main}} \tag{9.43}$$

$$\hat{V}_{\text{aux}} = \hat{I}_{\text{aux}}R_{\text{aux}} + j\omega_e\hat{\lambda}_{\text{aux}} \tag{9.44}$$

The rotor currents will each consist of positive- and negative-sequence components. The complex amplitudes of the positive sequence components (at frequency $s\omega_e$) are given by

$$\hat{I}_{r1}^+ = \frac{-js\omega_e[L_{\text{main,r}}\hat{I}_{\text{main}} + jL_{\text{aux,r}}\hat{I}_{\text{aux}}]}{2(R_r + js\omega_e L_r)} \tag{9.45}$$

and

$$\hat{I}_{r2}^+ = -j\hat{I}_{r1}^+ \tag{9.46}$$

while the complex amplitudes of the negative sequence components (at frequency $(2-s)\omega_e$) are given by

$$\hat{I}_{r1}^- = \frac{-j(2-s)\omega_e[L_{\text{main,r}}\hat{I}_{\text{main}} - jL_{\text{aux,r}}\hat{I}_{\text{aux}}]}{2(R_r + j(2-s)\omega_e L_r)} \tag{9.47}$$

and

$$\hat{I}_{r2}^- = j\hat{I}_{r1}^- \tag{9.48}$$

Finally, again after careful algebraic manipulation, the time-averaged electromagnetic torque can be shown to be given by

$$<T_{\text{mech}}> = \left(\frac{\text{poles}}{2}\right)\text{Re}\left[(L_{\text{main,r}}^2\hat{I}_{\text{main}}\hat{I}_{\text{main}}^* + L_{\text{aux,r}}^2\hat{I}_{\text{aux}}\hat{I}_{\text{aux}}^*)(\hat{K}^+ - \hat{K}^-)^*\right.$$
$$\left. + jL_{\text{main,r}}L_{\text{aux,r}}(\hat{I}_{\text{main}}^*\hat{I}_{\text{aux}} - \hat{I}_{\text{main}}\hat{I}_{\text{aux}}^*)(\hat{K}^+ + \hat{K}^-)^*\right] \tag{9.49}$$

where the symbol Re[ ] again indicates the real part of a complex number and the superscript * indicates the complex conjugate. Note that Eq. 9.49 is derived based upon the assumption that the various currents are expressed as rms quantities.

EXAMPLE 9.4

Consider the case of a symmetrical two-phase motor such as is discussed in Section 9.4.1. In this case, Eqs. 9.25 through 9.37 simplify with equal self and mutual inductances and resistances for the two windings. Using the notation of Section 9.4.1, 'α' and 'β' replacing 'main' and 'aux', the flux-linkage/current relationships of Eq. 9.39 and 9.40 become

$$\hat{\lambda}_\alpha = \left[L_\alpha - jL_{\alpha,r}^2(\hat{K}^+ + \hat{K}^-)\right]\hat{I}_\alpha + L_{\alpha,r}^2(\hat{K}^+ - \hat{K}^-)\hat{I}_\beta$$

$$\hat{\lambda}_\beta = -L_{\alpha,r}^2(\hat{K}^+ - \hat{K}^-)\hat{I}_\alpha + \left[L_\alpha - jL_{\alpha,r}^2(\hat{K}^+ + \hat{K}^-)\right]\hat{I}_\beta$$

and the voltage equations (Eqs. 9.43 and 9.44) become

$$\hat{V}_\alpha = \hat{I}_\alpha R_\alpha + j\omega_e\hat{\lambda}_\alpha$$

$$\hat{V}_\beta = \hat{I}_\beta R_\alpha + j\omega_e\hat{\lambda}_\beta$$

Show that when operated from a positive sequence set of voltages such that $\hat{V}_\beta = -jV_\alpha$ the single-phase equivalent circuit is that of the forward-field (positive-sequence) equivalent circuit of Fig. 9.12a.

■ Solution

Substitution of the positive-sequence voltages in the above equations and solution for the impedance $Z_\alpha = \hat{V}_\alpha/\hat{I}_\alpha$ gives

$$Z_\alpha = R_\alpha + j\omega_e L_\alpha + \frac{(\omega_e L_{\alpha,r})^2}{(R_r/s + j\omega_e L_r)}$$

$$= R_\alpha + jX_\alpha + \frac{X_{\alpha,r}^2}{(R_r/s + jX_r)}$$

This equation can be rewritten as

$$Z_\alpha = R_\alpha + j(X_\alpha - X_{\alpha,r}) + \frac{jX_{\alpha,r}[j(X_r - X_{\alpha,r}) + R_r/s]}{(R_r/s + jX_r)}$$

Setting $R_\alpha \Rightarrow R_1$, $(X_\alpha - X_{\alpha,r}) \Rightarrow X_1$, $X_{\alpha,r} \Rightarrow X_m$, $(X_r - X_{\alpha,r}) \Rightarrow X_2$, and $R_r \Rightarrow R_2$, we see that this equation does indeed represent an equivalent circuit of the form of Fig. 9.12a.

Practice Problem 9.4

Analogous to the calculation of Example 9.4, show that when operated from a negative sequence set of voltages such that $\hat{V}_\beta = jV_\alpha$ the single-phase equivalent circuit is that of the backward-field (negative-sequence) equivalent circuit of Fig. 9.12b.

Solution

Under negative-sequence conditions, the impedance Z_α is equal to

$$Z_\alpha = R_\alpha + j\omega_e L_\alpha + \frac{(\omega_e L_{\alpha,r})^2}{(R_r/(2-s) + j\omega_e L_r)}$$

$$= R_\alpha + jX_\alpha + \frac{X_{\alpha,r}^2}{(R_r/(2-s) + jX_r)}$$

As in Example 9.4, this can be shown to correspond to an equivalent circuit of the form of Fig. 9.12b.

EXAMPLE 9.5

A two-pole, single-phase induction motor has the following parameters

$$L_{main} = 80.6 \text{ mH} \qquad R_{main} = 0.58\ \Omega$$

$$L_{aux} = 196 \text{ mH} \qquad R_{aux} = 3.37\ \Omega$$

$$L_r = 4.7\ \mu\text{H} \qquad R_r = 37.6\ \mu\Omega$$

$$L_{main,r} = 0.588 \text{ mH} \qquad L_{aux,r} = 0.909 \text{ mH}$$

It is operated from a single-phase, 230-V rms, 60-Hz source as a permanent-split-capacitor motor with a 35 μF capacitor connected in series with the auxiliary winding. In order to achieve the required phase shift of the auxiliary-winding current, the windings must be connected with the polarities shown in Fig. 9.17. The motor has a rotational losses of 40 W and 105 W of core loss.

Consider motor operation at 3500 r/min.

a. Find the main-winding, auxiliary-winding and source currents and the magnitude of the capacitor voltage.
b. Find the time-averaged electromagnetic torque and shaft output power.

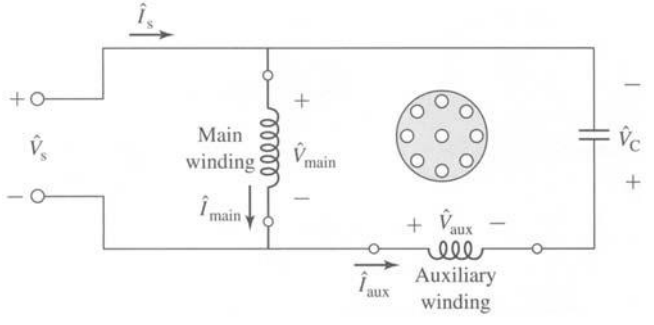

Figure 9.17 Permanent-split-capacitor induction-motor connections for Example 9.5.

c. Calculate the motor input power and its electrical efficiency. Note that since core loss isn't explicitly accounted for in the model derived in this section, you may simply consider it as an additional component of the input power.
d. Plot the motor time-averaged electromagnetic torque as a function of speed from standstill to synchronous speed.

■ Solution

MATLAB, with its ease of handling complex numbers, is ideal for the solution of this problem.

a. The main winding of this motor is directly connected to the single-phase source. Thus we directly set $\hat{V}_{main} = \hat{V}_s$. However, the auxiliary winding is connected to the single-phase source through a capacitor and its polarity is reversed. Thus we must write

$$\hat{V}_{aux} + \hat{V}_C = -\hat{V}_s$$

where the capacitor voltage is given by

$$\hat{V}_C = j\hat{I}_{aux}X_C$$

Here the capacitor impedance X_C is equal to

$$X_C = -\frac{1}{(\omega_e C)} = -\frac{1}{(120\pi \times 35 \times 10^{-6})} = -75.8\ \Omega$$

Setting $\hat{V}_s = V_0 = 230$ V and substituting these expressions into Eqs. 9.43 and 9.44 and using Eqs. 9.39 and 9.40 then gives the following matrix equation for the main- and auxiliary-winding currents.

$$\begin{bmatrix} (R_{main} + j\omega_e\hat{A}_1) & j\omega_e\hat{A}_2 \\ -j\omega_e\hat{A}_2 & (R_{aux} + jX_c + j\omega_e\hat{A}_3) \end{bmatrix} \begin{bmatrix} \hat{I}_{main} \\ \hat{I}_{aux} \end{bmatrix} = \begin{bmatrix} V_0 \\ -V_0 \end{bmatrix}$$

where

$$\hat{A}_1 = L_{main} - jL^2_{main,r}(\hat{K}^+ + \hat{K}^-)$$
$$\hat{A}_2 = L_{main,r}L_{aux,r}(\hat{K}^+ - \hat{K}^-)$$

and

$$\hat{A}_3 = L_{aux} - jL^2_{aux,r}(\hat{K}^+ + \hat{K}^-)$$

The parameters $\hat{K}^+$ and $\hat{K}^-$ can be found from Eqs. 9.41 and 9.42 once the slip is found using Eq. 6.1

$$s = \frac{n_s - n}{n_s} == \frac{3600 - 3500}{3600} = 0.278$$

This matrix equation can be readily solved using MATLAB with the result

$$\hat{I}_{main} = 15.9\angle -37.6^\circ\ \text{A}$$
$$\hat{I}_{aux} = 5.20\angle -150.7^\circ\ \text{A}$$

and

$$\hat{I}_s = 18.5\angle -22.7^\circ \text{ A}$$

The magnitude of the capacitor voltage is

$$|\hat{V}_C| = |\hat{I}_{aux} X_C| = 374 \text{ V}$$

b. Using MATLAB the time-averaged electromagnetic torque can be found from Eq. 9.49 to be

$$<T_{mech}> = 9.74 \text{ N} \cdot \text{m}$$

The shaft power can then be found by subtracting the rotational losses P_{rot} from the air-gap power

$$\begin{aligned} P_{shaft} &= \omega_m <T_{mech}> - P_{rot} \\ &= \left(\frac{2}{\text{poles}}\right)(1-s)\omega_e(<T_{mech}>) - P_{rot} \\ &= 3532 \text{ W} \end{aligned}$$

c. The power input to the main winding can be found as

$$P_{main} = \text{Re}\left[V_0 \hat{I}^*_{main}\right] = 2893 \text{ W}$$

and that into the auxiliary winding, including the capacitor (which dissipates no power)

$$P_{aux} = \text{Re}\left[-V_0 \hat{I}^*_{aux}\right] = 1043 \text{ W}$$

The total input power, including the core loss power P_{core} is found as

$$P_{in} = P_{main} + P_{aux} + P_{core} = 4041 \text{ W}$$

Finally, the efficiency can be determined

$$\eta = \frac{P_{shaft}}{P_{in}} == 0.874 = 87.4\%$$

d. The plot of $<T_{mech}>$ versus speed generated by MATLAB is found in Fig. 9.18.

Here is the MATLAB script:

```
clc
clear

% Source parameters
V0 = 230;
omegae = 120*pi;

% Motor parameters
poles = 2;
Lmain = .0806;
Rmain = 0.58;
Laux = 0.196;
Raux = 3.37;
Lr = 4.7e-6;
```

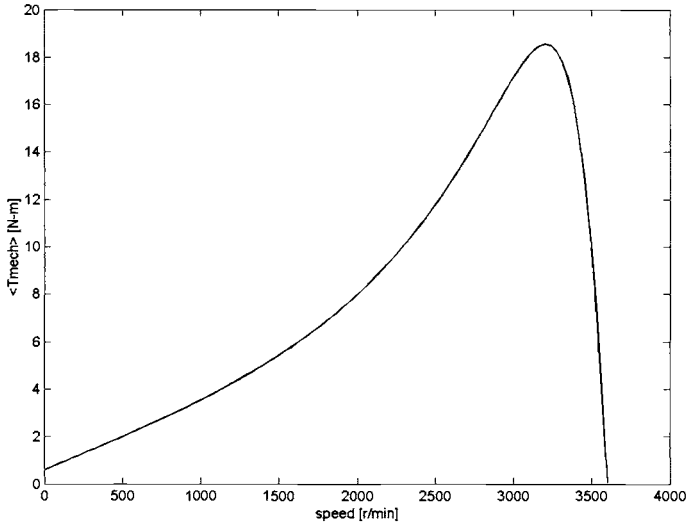

Figure 9.18 Time-averaged electromagnetic torque versus speed for the single-phase induction motor of Example 9.5.

```
Rr = 37.6e-6;
Lmainr = 5.88e-4;
Lauxr = 9.09e-4;
C = 35e-6;
Xc = -1/(omegae*C);
Prot = 40;
Pcore = 105;

% Run through program twice. If calcswitch = 1, then
% calculate at speed of 3500 r/min only. The second time
% program will produce the plot for part (d).

for calcswitch = 1:2

if calcswitch == 1
  mmax = 1;
else
   mmax = 101;
end

for m = 1:mmax

if calcswitch == 1
   speed(m) = 3500;
else
   speed(m) = 3599*(m-1)/100;
end
```

```
% Calculate the slip
ns = (2/poles)*3600;
s = (ns-speed(m))/ns;

% part (a)
% Calculate the various complex constants
Kplus = s*omegae/(2*(Rr + j*s*omegae*Lr));
Kminus = (2-s)*omegae/(2*(Rr + j*(2-s)*omegae*Lr));
A1 = Lmain - j*Lmainr^2*(Kplus+Kminus);
A2 = Lmainr*Lauxr*(Kplus-Kminus);
A3 = Laux - j*Lauxr^2*(Kplus+Kminus);

% Set up the matrix
M(1,1) = Rmain + j*omegae*A1;
M(1,2) = j*omegae*A2;
M(2,1) = -j*omegae*A2;
M(2,2) = Raux + j*Xc+ j*omegae*A3;

% Here is the voltage vector
V = [V0 ; -V0];

% Now find the current matrix

I = M\V;

Imain = I(1);
Iaux = I(2);
Is = Imain-Iaux;

magImain = abs(Imain);
angleImain = angle(Imain)*180/pi;
magIaux = abs(Iaux);
angleIaux = angle(Iaux)*180/pi;
magIs = abs(Is);
angleIs = angle(Is)*180/pi;

%Capacitor voltage
Vcap = Iaux*Xc;
magVcap = abs(Vcap);

% part (b)
Tmech1 = conj(Kplus-Kminus);
Tmech1 = Tmech1*(Lmainr^2*Imain*conj(Imain)+Lauxr^2*Iaux*conj(Iaux));
Tmech2 = j*Lmainr*Lauxr*conj(Kplus+Kminus);
Tmech2 = Tmech2*(conj(Imain)*Iaux-Imain*conj(Iaux));
Tmech(m) = (poles/2)*real(Tmech1+Tmech2);
Pshaft = (2/poles)*(1-s)*omegae*Tmech(m)-Prot;

%part (c)
Pmain = real(V0*conj(Imain));
Paux = real(-V0*conj(Iaux));
```

```
Pin = Pmain+Paux+Pcore;
eta = Pshaft/Pin;

if calcswitch == 1
  fprintf('part (a):')
  fprintf('\n  Imain = %g A at angle %g degrees',magImain,angleImain)
  fprintf('\n  Iaux = %g A at angle %g degrees',magIaux,angleIaux)
  fprintf('\n  Is = %g A at angle %g degrees',magIs,angleIs)
  fprintf('\n  Vcap = %g V\n',magVcap)
  fprintf('\npart (b):')
  fprintf('\n  Tmech = %g N-m',Tmech)
  fprintf('\n  Pshaft = %g W\n',Pshaft)
  fprintf('\npart (c):')
  fprintf('\n  Pmain = %g W',Pmain)
  fprintf('\n  Paux = %g W',Paux)
  fprintf('\n  Pin = %g W',Pin)
  fprintf('\n  eta = %g percent\n\n',100*eta)
else
  plot(speed,Tmech)
  xlabel('speed [r/min]')
  ylabel('<Tmech> [N-m]')

end

end %end of for m loop
end %end of for calcswitch loop
```

Practice Problem 9.5

(*a*) Calculate the efficiency of the single-phase induction motor of Example 9.5 operating at a speed of 3475 r/min. (*b*) Search over the range of capacitor values from 25 μF to 45 μF to find the capacitor value which will give the maximum efficiency at this speed and the corresponding efficiency.

Solution

a. 86.4%
b. 41.8 μF, 86.6%

9.5 SUMMARY

One theme of this chapter is a continuation of the induction-machine theory of Chapter 6 and its application to the single-phase induction motor. This theory is expanded by a step-by-step reasoning process from the simple revolving-field theory of the symmetrical polyphase induction motor. The basic concept is the resolution of the stator-mmf wave into two constant-amplitude traveling waves revolving around the air gap at synchronous speed in opposite directions. If the slip for the forward field is s,

then that for the backward field is $(2 - s)$. Each of these component fields produces induction-motor action, just as in a symmetrical polyphase motor. From the viewpoint of the stator, the reflected effects of the rotor can be visualized and expressed quantitatively in terms of simple equivalent circuits. The ease with which the internal reactions can be accounted for in this manner is the essential reason for the usefulness of the double-revolving-field theory.

For a single-phase winding, the forward- and backward-component mmf waves are equal, and their amplitude is half the maximum value of the peak of the stationary pulsating mmf produced by the winding. The resolution of the stator mmf into its forward and backward components then leads to the physical concept of the single-phase motor described in Section 9.1 and finally to the quantitative theory developed in Section 9.3 and to the equivalent circuits of Fig. 9.11.

In most cases, single-phase induction motors are actually two-phase motors with unsymmetrical windings operated off of a single phase source. Thus to complete our understanding of single-phase induction motors, it is necessary to examine the performance of two-phase motors. Hence, the next step is the application of the double-revolving-field picture to a symmetrical two-phase motor with unbalanced applied voltages, as in Section 9.4.1. This investigation leads to the symmetrical-component concept, whereby an unbalanced two-phase system of currents or voltages can be resolved into the sum of two balanced two-phase component systems of opposite phase sequence. Resolution of the currents into symmetrical-component systems is equivalent to resolving the stator-mmf wave into its forward and backward components, and therefore the internal reactions of the rotor for each symmetrical-component system are the same as those which we have already investigated. A very similar reasoning process, not considered here, leads to the well-known three-phase symmetrical-component method for treating problems involving unbalanced operation of three-phase rotating machines. The ease with which the rotating machine can be analyzed in terms of revolving-field theory is the chief reason for the usefulness of the symmetrical-component method.

Finally, the chapter ends in Section 9.4.2 with the development of an analytical theory for the general case of a two-phase induction motor with unsymmetrical windings. This theory permits us to analyze the operation of single-phase motors running off both their main and auxiliary windings.

9.6 PROBLEMS

9.1 A 1-kW, 120-V, 60-Hz capacitor-start motor has the following parameters for the main and auxiliary windings (at starting):

$$Z_{\text{main}} = 4.82 + j7.25\ \Omega \quad \text{main winding}$$
$$Z_{\text{aux}} = 7.95 + j9.21\ \Omega \quad \text{auxiliary winding}$$

a. Find the magnitude and the phase angles of the currents in the two windings when rated voltage is applied to the motor under starting conditions.

b. Find the value of starting capacitance that will place the main- and auxiliary-winding currents in time quadrature at starting.

c. Repeat part (a) when the capacitance of part (b) is inserted in series with the auxiliary winding.

9.2 Repeat Problem 9.1 if the motor is operated from a 120-V, 50-Hz source.

9.3 Given the applied electrical frequency and the corresponding impedances Z_{main} and Z_{aux} of the main and auxiliary windings at starting, write a MATLAB script to calculate the value of the capacitance, which, when connected in series with the starting winding, will produce a starting winding current which will lead that of the main winding by 90°.

9.4 Repeat Example 9.2 for slip of 0.045.

9.5 A 500-W, four-pole, 115-V, 60-Hz single-phase induction motor has the following parameters (resistances and reactances in Ω/phase):

$$R_{1,main} = 1.68 \quad R_{2,main} = 2.96$$

$$X_{1,main} = 1.87 \quad X_{m,main} = 60.6 \quad X_{2,main} = 1.72$$

$$\text{Core loss} = 38 \text{ W} \quad \text{Friction and windage} = 11.8 \text{ W}$$

Find the speed, stator current, torque, power output, and efficiency when the motor is operating at rated voltage and a slip of 4.2 percent.

9.6 Write a MATLAB script to produce plots of the speed and efficiency of the single-phase motor of Problem 9.5 as a function of output power over the range $0 \leq P_{out} \leq 500$ W.

9.7 At standstill the rms currents in the main and auxiliary windings of a four-pole, capacitor-start induction motor are $I_{main} = 20.7$ A and $I_{aux} = 11.1$ A respectively. The auxiliary-winding current leads the main-winding current by 53°. The effective turns per pole (i.e., the number of turns corrected for the effects of winding distribution) are $N_{main} = 42$ and $N_{aux} = 68$. The windings are in space quadrature.

a. Determine the peak amplitudes of the forward and backward stator-mmf waves.

b. Suppose it were possible to adjust the magnitude and phase of the auxiliary-winding current. What magnitude and phase would produce a purely forward mmf wave?

9.8 Derive an expression in terms of $Q_{2,main}$ for the nonzero speed of a single-phase induction motor at which the internal torque is zero. (See Example 9.2.)

9.9 The equivalent-circuit parameters of an 8-kW, 230-V, 60-Hz, four-pole, two-phase, squirrel-cage induction motor in ohms per phase are

$$R_1 = 0.253 \quad X_1 = 1.14 \quad X_m = 32.7 \quad R_2 = 0.446 \quad X_2 = 1.30$$

This motor is operated from an unbalanced two-phase, 60-Hz source whose phase voltages are, respectively, 223 and 190 V, the smaller voltage leading the larger by 73°. For a slip of 0.045, find

a. the phase currents in each of the windings and

b. the internal mechanical power.

9.10 Consider the two-phase motor of Example 9.3.

a. Find the starting torque for the conditions specified in the example.

b. Compare the result of part (a) with the starting torque which the motor would produce if 220-V, balanced two-phase voltages were applied to the motor.

c. Show that if the stator voltages $\hat{V}_\alpha$ and $\hat{V}_{\text{beta}}$ of a two-phase induction motor are in time quadrature but unequal in magnitude, the starting torque is the same as that developed when balanced two-phase voltages of magnitude $\sqrt{V_\alpha V_\beta}$ are applied.

9.11 The induction motor of Problem 9.9 is supplied from an unbalanced two-phase source by a four-wire feeder having an impedance $Z = 0.32 + j1.5\ \Omega$/phase. The source voltages can be expressed as

$$\hat{V}_\alpha = 235\angle 0^\circ \quad \hat{V}_\alpha = 212\angle 78^\circ$$

For a slip of 5 percent, show that the induction-motor terminal voltages correspond more nearly to a balanced two-phase set than do those of the source.

9.12 The equivalent-circuit parameters in ohms per phase referred to the stator for a two-phase, 1.0 kW, 220-V, four-pole, 60-Hz, squirrel-cage induction motor are given below. The no-load rotational loss is 65 W.

$$R_1 = 0.78 \quad R_2 = 4.2 \quad X_1 = X_2 = 5.3 \quad X_m = 93$$

a. The voltage applied to phase α is $220\angle 0^\circ$ V and that applied to phase β is $220\angle 65^\circ$ V. Find the net air-gap torque at a slip $s = 0.035$.

b. What is the starting torque with the applied voltages of part (a)?

c. The applied voltages are readjusted so that $\hat{V}_\alpha = 220\angle 65^\circ$ V and $\hat{V}_\beta = 220\angle 90^\circ$ V. Full load on the machine occurs at $s = 0.048$. At what slip does maximum internal torque occur? What is the value of the maximum torque?

d. While the motor is running as in part (c), phase β is open-circuited. What is the power output of the machine at a slip $s = 0.04$?

e. What voltage appears across the open phase-β terminals under the conditions of part (d)?

9.13 A 120-V, 60-Hz, capacitor-run, two-pole, single-phase induction motor has the following parameters:

$$L_{\text{main}} = 47.2\ \text{mH} \qquad R_{\text{main}} = 0.38\ \Omega$$

$$L_{\text{aux}} = 102\ \text{mH} \qquad R_{\text{aux}} = 1.78\ \Omega$$

$$L_{\text{r}} = 2.35\ \mu\text{H} \qquad R_{\text{r}} = 17.2\ \mu\Omega$$

$$L_{\text{main,r}} = 0.342\ \text{mH} \qquad L_{\text{aux,r}} = 0.530\ \text{mH}$$

You may assume that the motor has 48 W of core loss and 23 W of rotational losses. The motor windings are connected with the polarity shown in Fig. 9.17 with a 40 μF run capacitor.

a. Calculate the motor starting torque.

With the motor operating at a speed of 3490 r/min, calculate

b. the main and auxiliary-winding currents,

c. the total line current and the motor power factor,

d. the output power and

e. the electrical input power and the efficiency.

Note that this problem is most easily solved using MATLAB.

9.14 Consider the single-phase motor of Problem 9.13. Write a MATLAB script to search over the range of capacitor values from 25 μF to 75 μF to find the value which will maximize the motor efficiency at a motor speed of 3490 r/min. What is the corresponding maximum efficiency?

9.15 In order to raise the starting torque, the single-phase induction motor of Problem 9.13 is to be converted to a capacitor-start, capacitor-run motor. Write a MATLAB script to find the minimum value of starting capacitance required to raise the starting torque to 0.5 N · m.

9.16 Consider the single-phase induction motor of Example 9.5 operating over the speed range 3350 r/min to 3580 r/min.

a. Use MATLAB to plot the output power over the given speed range.

b. Plot the efficiency of the motor over this speed range.

c. On the same plot as that of part (b), plot the motor efficiency if the run capacitor is increased to 45 μF.

CHAPTER 10

Introduction to Power Electronics

Until the last few decades of the twentieth century, ac machines tended to be employed primarily as single-speed devices. Typically they were operated from fixed-frequency sources (in most cases this was the 50- or 60-Hz power grid). In the case of motors, control of motor speed requires a variable-frequency source, and such sources were not readily available. Thus, applications requiring variable speed were serviced by dc machines, which can provide highly flexible speed control, although at some cost since they are more complex, more expensive, and require more maintenance than their ac counterparts.

The availability of solid-state power switches changed this picture immensely. It is now possible to build power electronics capable of supplying the variable-voltage/current, variable-frequency drive required to achieve variable-speed performance from ac machines. Ac machines have now replaced dc machines in many traditional applications, and a wide range of new applications have been developed.

As is the case with electromechanics and electric machinery, power electronics is a discipline which can be mastered only through significant study. Many books have been written on this subject, a few of which are listed in the bibliography at the end of this chapter. It is clear that a single chapter in a book on electric machinery cannot begin to do justice to this topic. Thus our objectives here are limited. Our goal is to provide an overview of power electronics and to show how the basic building blocks can be assembled into drive systems for ac and dc machines. We will not focus much attention on the detailed characteristics of particular devices or on the many details required to design practical drive systems. In Chapter 11, we will build on the discussion of this chapter to examine the characteristics of some common drive systems.

10.1 POWER SWITCHES

Common to all power-electronic systems are switching devices. Ideally, these devices control current much like valves control the flow of fluids: turn them "ON," and they present no resistances to the flow of current; turn them "OFF," and no current flow is possible. Of course, practical switches are not ideal, and their specific characteristics significantly affect their applicability in any given situation. Fortunately, the essential performance of most power-electronic circuits can be understood assuming the switches to be ideal. This is the approach which we will adopt in this book. In this section we will briefly discuss some of the common switching devices and present simplified, idealized models for them.

10.1.1 Diodes

Diodes constitute the simplest of power switches. The general form of the v-i characteristics of a diode is shown in Fig. 10.1.

The essential features of a diode are captured in the idealized v-i characteristic of Fig. 10.2a. The symbol used to represent a diode is shown in Fig. 10.2b along with the reference directions for the current i and voltage v. Based upon terminology developed when rectifier diodes were electron tubes, diode current flows into the *anode* and flows out of the *cathode*.

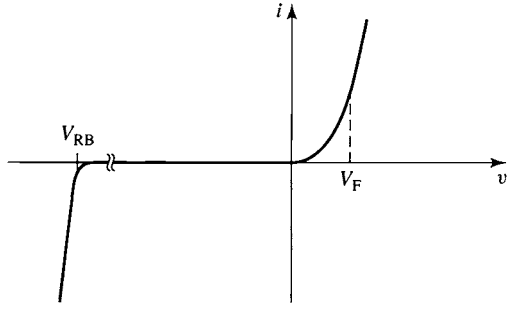

Figure 10.1 v-i characteristic of a diode.

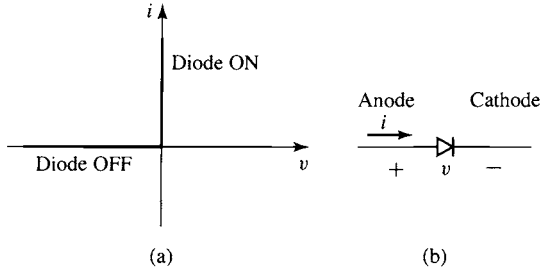

Figure 10.2 (a) v-i characteristic of an ideal diode. (b) Diode symbol.

We can see that the ideal diode blocks current flow when the voltage is negative ($i = 0$ for $v < 0$) and passes positive current without voltage drop ($v = 0$ for $i \geq 0$). We will refer to the negative-voltage region as the diode's OFF state and the positive-current region as the diode's ON state. Comparison with the v-i characteristic shows that a practical diode varies from an ideal diode in that:

- There is a finite *forward voltage drop,* labeled V_F in Fig. 10.1, for positive current flow. For low-power devices, this voltage range is typically on the order of 0.6–0.7 V while for high-power devices it can exceed 3 V.
- Corresponding to this voltage drop is a power dissipation. Practical diodes have a maximum power dissipation (and a corresponding maximum current) which must not be exceeded.
- A practical diode is limited in the negative voltage it can withstand. Known as the *reverse-breakdown voltage* and labeled V_{RB} in Fig. 10.1, this is the maximum reverse voltage that can be applied to the diode before it starts to conduct reverse current.

The diode is the simplest power switch in that it cannot be controlled; it simply turns ON when positive current begins to flow and turns OFF when the current attempts to reverse. In spite of this simple behavior, it is used in a wide variety of applications, the most common of which is as a rectifier to convert ac to dc.

The basic performance of a diode can be illustrated by the simple example shown in Example 10.1.

EXAMPLE 10.1

Consider the *half-wave rectifier* circuit of Fig. 10.3a in which a resistor R is supplied by a voltage source $v_s(t) = V_0 \sin \omega t$ through a diode. Assume the diode to be ideal. (*a*) Find the resistor voltage $v_R(t)$ and current $i_R(t)$. (*b*) Find the dc average resistor voltage V_{dc} and current I_{dc}.

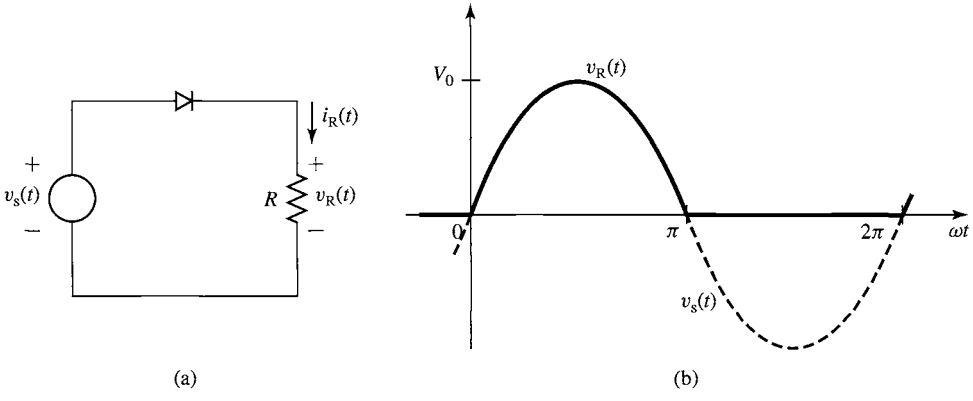

Figure 10.3 (a) Half-wave rectifier circuit for Example 10.1. (b) Resistor voltage.

■ Solution

a. This is a nonlinear problem in that it is not possible to write an analytic expression for the v-i characteristic of the ideal diode. However, it can readily be solved using the *method-of-assumed-states* in which, for any given value of the source voltage, the diode is alternately assumed to be ON (a short-circuit) or OFF (an open-circuit) and the current is found. One of the two solutions will violate the v-i characteristic of the diode (i.e., there will be negative current flow through the short-circuit or positive voltage across the open-circuit) and must be discarded; the remaining solution will be the correct one.

Following the above procedure, we find that the solution is given by

$$v_R(t) = \begin{cases} v_s(t) = V_0 \sin \omega t & v_s(t) \geq 0 \\ 0 & v_s(t) < 0 \end{cases}$$

This voltage is plotted in Fig. 10.3b. The current is identical in form and is found simply as $i_R(t) = v_R(t)/R$. The terminology *half-wave rectification* is applied to this system because voltage is applied to the resistor during only the half cycle for which the supply voltage waveform is positive.

b. The dc or average value of the voltage waveform is equal to

$$V_{dc} = \frac{\omega}{\pi} \int_0^{\frac{\pi}{\omega}} V_0 \sin(\omega t)\, dt = \frac{V_0}{\pi}$$

and hence the dc current through the resistor is equal to

$$I_{dc} = \frac{V_0}{\pi R}$$

Practice Problem 10.1

Calculate the average voltage across the resistor of Fig. 10.3 if the sinusoidal voltage source of Example 10.1 is replaced by a source of the same frequency but which produces a square wave of zero average value and peak-peak amplitude $2V_0$.

Solution

$$V_{dc} = \frac{V_0}{2}$$

10.1.2 Silicon Controlled Rectifiers and TRIACs

The characteristics of a *silicon controlled rectifier,* or *SCR,* also referred to as a *thyristor,* are similar to those of a diode. However, in addition to an anode and a cathode, the SCR has a third terminal known as the *gate*. Figure 10.4 shows the form of the v-i characteristics of a typical SCR.

As is the case with a diode, the SCR will turn ON only if the anode is positive with respect to the cathode. Unlike a diode, the SCR also requires a pulse of current i_G into the gate to turn ON. Note however that once the SCR turns ON, the gate signal

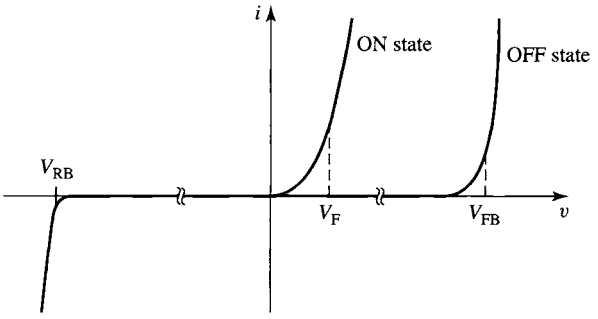

Figure 10.4 *v-i* characteristic of an SCR.

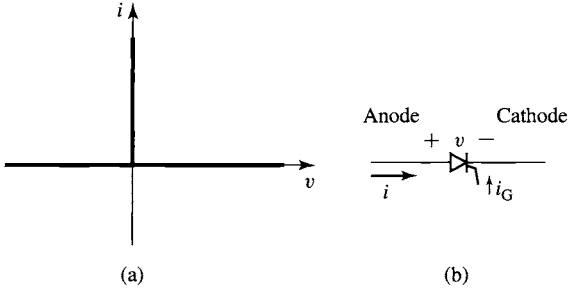

Figure 10.5 (a) Idealized SCR *v-i* characteristic. (b) SCR symbol.

can be removed and the SCR will remain ON until the SCR current drops below a small value referred to as the *holding current,* at which point it will turn OFF just as a diode does.

As can be seen from Fig. 10.4, the ON-state characteristic of an SCR is similar to that of a diode, with a forward voltage drop V_F and a reverse-breakdown voltage V_{RB}. When the SCR is OFF, it does not conduct current over its normal operating range of positive voltage. However it will conduct if this voltage exceeds a characteristic voltage, labeled V_{FB} in the figure and known as the *forward-breakdown voltage.* As is the case for a diode, a practical SCR is limited in its current-carrying capability.

For our purposes, we will simplify these characteristics and assume the SCR to have the idealized characteristics of Fig. 10.5a. Our idealized SCR appears as an open-circuit when it is OFF and a short-circuit when it is ON. It also has a holding current of zero; i.e., it will remain ON until the current drops to zero and attempts to go negative. The symbol used to represent an SCR is shown in Fig. 10.5b.

Care must be taken in the design of gate-drive circuitry to insure that an SCR turns on properly; e.g., the gate pulse must inject enough charge to fully turn on the SCR, and so forth. Similarly, an additional circuit, typically referred to as a *snubber* circuit, may be required to protect an SCR from being turned on inadvertently, such as might occur if the rate of rise of the anode-to-cathode voltage is excessive. Although

these details must be properly accounted for to achieve successful SCR performance in practical circuits, they are not essential for the present discussion.

The basic performance of an SCR can be understood from the following example.

EXAMPLE 10.2

Consider the *half-wave rectifier* circuit of Fig. 10.6 in which a resistor R is supplied by a voltage source $v_s(t) = V_0 \sin \omega t$ through an SCR. Note that this is identical to the circuit of Example 10.1, with the exception that the diode has been replaced by an SCR.

Assume that a pulse of gate current is applied to the SCR at time t_0 ($0 \leq t_0 < \pi/\omega$) following each zero-crossing of the source voltage, as shown in Fig. 10.7a. It is common to describe this *firing-delay time* in terms of a *firing-delay angle*, $\alpha_0 \equiv \omega t_0$. Find the resistor voltage $v_R(t)$ as a function of α_0. Assume the SCR to be ideal and that the gate pulses supply sufficient charge to properly turn ON the SCR.

■ Solution

The solution follows that of Example 10.1 with the exception that, independent of the polarity of the voltage across it, once the SCR turns OFF, it will remain OFF until both the SCR voltage becomes positive and a pulse of gate current is applied. Once a gate pulse has been applied, the method-of-assumed-states can be used to solve for the state of the SCR.

Following the above procedure, we find the solution is given by

$$v_R(t) = \begin{cases} 0 & v_s(t) \geq 0 \quad \text{(prior to the gate pulse)} \\ v_s(t) = V_0 \sin \omega t & v_s(t) \geq 0 \quad \text{(following the gate pulse)} \\ 0 & v_s(t) < 0 \end{cases}$$

This voltage is plotted in Fig. 10.7b. Note that this system produces a half-wave rectified voltage similar to that of the diode system of Example 10.1. However, in this case, the dc value of the rectified voltage can be controlled by controlling the timing of the gate pulse. Specifically, it is given by

$$V_{dc} = \frac{V_0}{2\pi}(1 + \cos \alpha_0)$$

Note that when there is no delay in firing the SCR ($\alpha_0 = 0$), this system produces a dc voltage of V_0/π, equal to that of the diode rectifier system of Example 10.1. However, as the gate pulse of the SCR is delayed (i.e., by increasing α_0), the dc voltage can be reduced. In fact, by delaying the gate pulse a full half cycle ($\alpha_0 = \pi$) the dc voltage can be reduced to

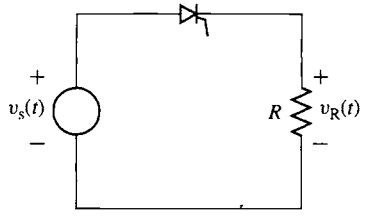

Figure 10.6 Half-wave SCR rectifier circuit for Example 10.2.

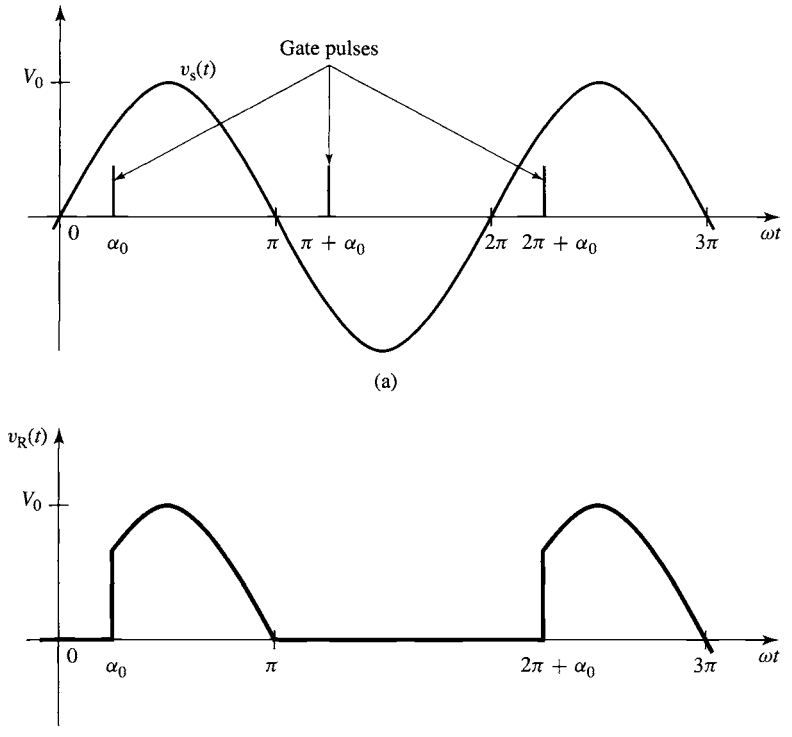

Figure 10.7 (a) Gate pulses for Example 10.2. (b) Resistor voltage.

zero. This system is known as a *phase-controlled rectifier* because the dc output voltage can be varied by controlling the phase angle of the gate pulse relative to the zero crossing of the source voltage.

Practice Problem 10.2

Calculate the resistor average voltage as a function of the delay angle α_0 if the sinusoidal source of Example 10.2 is replaced by a source of the same frequency, but which produces a square wave of zero average value and peak-peak amplitude $2V_0$.

Solution

$$V_{dc} = \frac{V_0}{2}\left(1 - \frac{\alpha_0}{\pi}\right)$$

Example 10.2 shows that the SCR provides a significant advantage over the diode in systems where voltage control is desired. However, this advantage comes at the additional expense of the SCR as well as the circuitry required to produce the gate pulses used to fire the SCR.

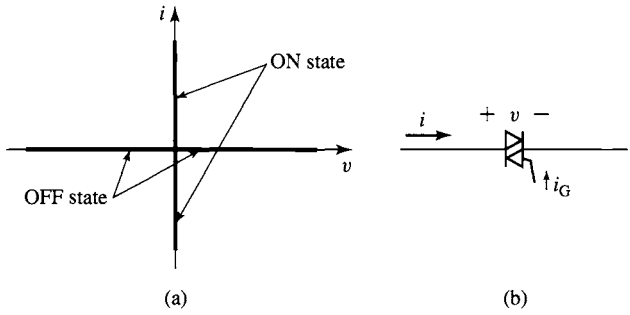

Figure 10.8 (a) Idealized TRIAC *v-i* characteristic. (b) TRIAC symbol.

Another phase-controlled device is the *TRIAC*, which behaves much like two back-to-back SCRs sharing a common gate. The idealized *v-i* characteristic of a TRIAC is shown in Fig. 10.8a and its symbol in Fig. 10.8b. As with an SCR, TRIACs can be turned ON by the application of a pulse of current at their gate. Unlike an SCR, provided the current pulses inject sufficient charge, both positive and negative gate current pulses can be used to turn ON a TRIAC.

The use of a TRIAC is illustrated in the following example.

EXAMPLE 10.3

Consider the circuit of Fig. 10.9 in which the SCR of Example 10.2 has been replaced by a TRIAC.

Assume again that a short gate pulse is applied to the SCR at a delay angle α_0 ($0 \leq \alpha_0 < \pi$) following each zero-crossing of the source voltage, as shown in Fig. 10.10a. Find the resistor voltage $v_R(t)$ and its rms value $V_{R,rms}$ as a function of α_0. Assume the TRIAC to be ideal and that the gate pulses inject sufficient charge to properly turn it ON.

■ Solution

The solution to this example is similar to that of Example 10.2 with the exception that the TRIAC, which will permit current to flow in both directions, turns on each half cycle of the source-voltage waveform.

$$v_R(t) = \begin{cases} 0 & \text{(prior to the gate pulse)} \\ v_s(t) = V_0 \sin \omega t & \text{(following the gate pulse)} \end{cases}$$

Unlike the rectification of Example 10.2, in this case the resistor voltage, shown in Fig. 10.10b, has no dc component. However, its rms value varies with α_0:

$$V_{R,rms} = V_0 \sqrt{\left(\frac{\omega}{\pi} \int_{\frac{\alpha_0}{\omega}}^{\frac{\pi}{\omega}} \sin^2(\omega t)\, dt \right)}$$

$$= V_0 \sqrt{\left(\frac{1}{2} - \frac{\alpha_0}{2\pi} + \frac{1}{4\pi} \sin(2\alpha_0) \right)}$$

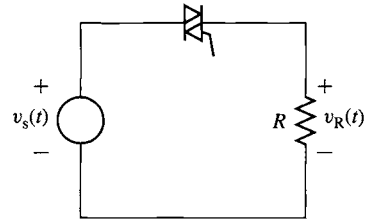

Figure 10.9 Circuit for Example 10.3.

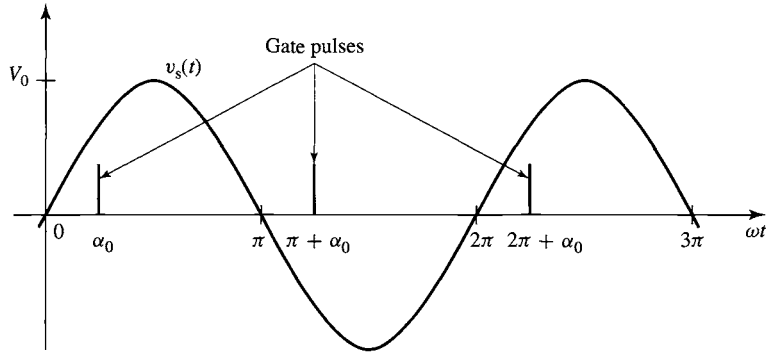

(a)

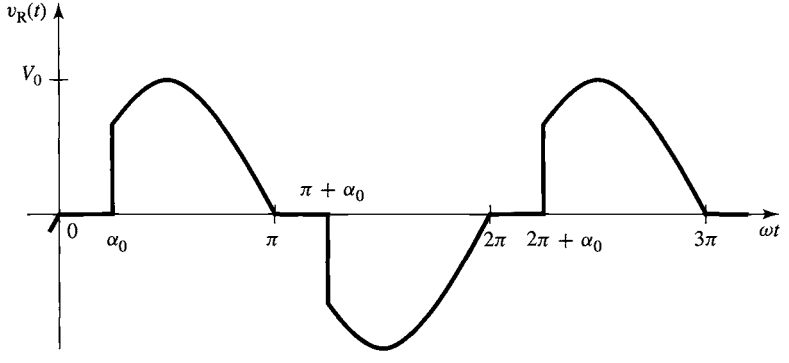

(b)

Figure 10.10 (a) Gate pulses for Example 10.3. (b) Resistor voltage.

Notice that when $\alpha_0 = 0$, the TRIAC is ON all the time and it appears that the resistor is connected directly to the voltage source. In this case, $V_{R,rms} = V_0/\sqrt{2}$ as expected. As α_0 is increased to π, the rms voltage decreases towards zero.

This simple type of controller can be applied to an electric light bulb (in which case it serves as *light dimmer*) as well as to a resistive heater. It is also used to vary the speed of a

universal motor and finds widespread application as a speed-controller in small ac hand tools, such as hand drills, as well as in small appliances, such as electric mixers, where continuous speed variation is desired.

Practice Problem 10.3

Find the rms resistor voltage for the system of Example 10.3 if the sinusoidal source has been replaced by a source of the same frequency but which produces a square wave of zero average value and peak-peak amplitude $2V_0$.

Solution

$$V_{R,rms} = V_0 \sqrt{\left(1 - \frac{\alpha_0}{\pi}\right)}$$

10.1.3 Transistors

For power-electronic circuits where control of voltages and currents is required, power transistors have become a common choice for the controllable switch. Although a number of types are available, we will consider only two: the *metal-oxide-semiconductor field effect transistor* (*MOSFET*) and the *insulated-gate bipolar transistor* (*IGBT*).

MOSFETs and IGBTs are both three-terminal devices. Figure 10.11a shows the symbols for n- and p-channel MOSFETs, while Fig. 10.11b shows the symbol for n- and p-channel IGBTs. In the case of the MOSFET, the three terminals are referred to as the *source, drain,* and *gate,* while in the case of the IGBT the corresponding

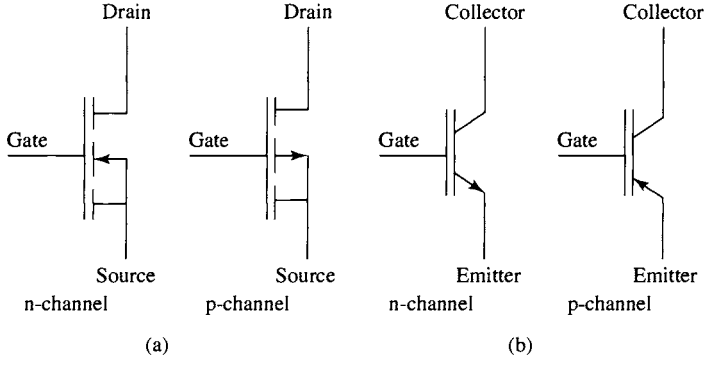

Figure 10.11 (a) Symbols for n- and p-channel MOSFETs. (b) Symbols for n- and p-channel IGBTs.

terminals are the *emitter, collector,* and *gate*. For the MOSFET, the control signal is the gate-source voltage, v_{GS}. For the IGBT, it is the gate-emitter voltage, v_{GE}. In both the MOSFET and the IGBT, the gate electrode is capacitively coupled to the remainder of the device and appears as an open circuit at dc, drawing no current, and drawing only a small capacitive current under ac operation.

Figure 10.12a shows the *v-i* characteristic of a typical n-channel MOSFET. The characteristic of the corresponding p-channel device looks the same, with the exception that the signs of the voltages and the currents are reversed. Thus, in an n-channel device, current flows from the drain to the source when the drain-source and

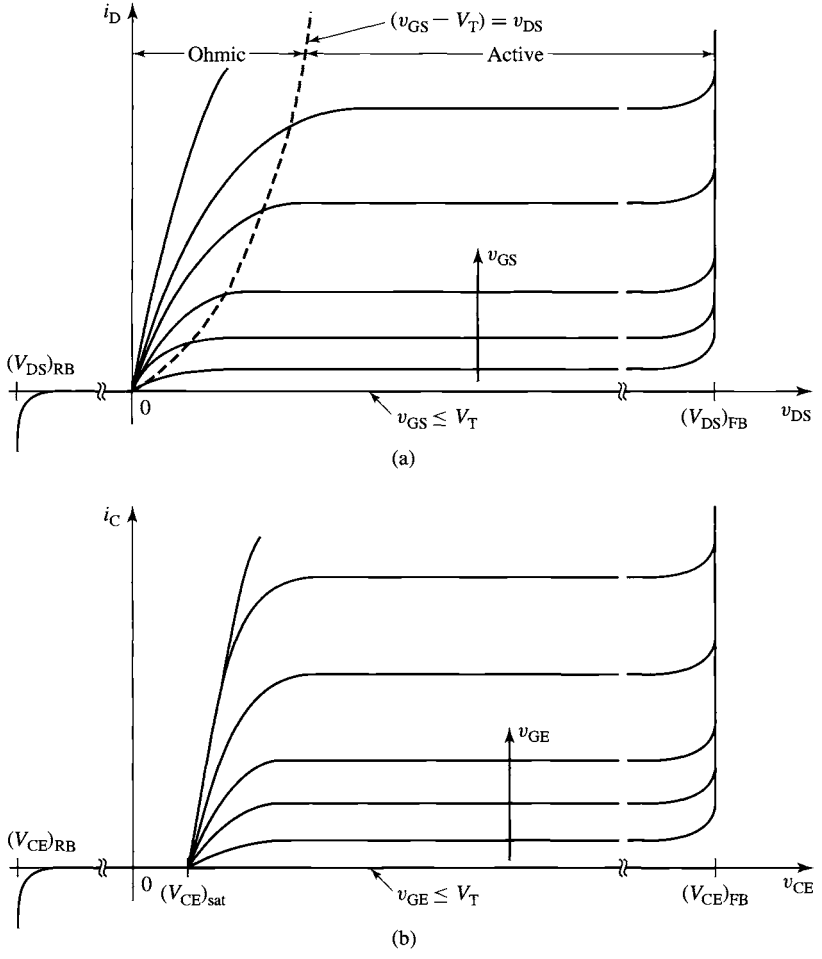

Figure 10.12 (a) Typical *v-i* characteristic for an n-channel MOSFET. (b) Typical *v-i* characteristic for an n-channel IGBT.

gate-source voltages are positive, while in a p-channel device current flows from the source to the drain when the drain-source and gate-source voltages are negative.

Note the following features of the MOSFET and IGBT characteristics:

- In the case of the MOSFET, for positive drain-source voltage v_{DS}, no drain current will flow for values of v_{GS} less than a *threshold voltage* which we will refer to by the symbol V_T. Once v_{GS} exceeds V_T, the drain current i_D increases as v_{GS} is increased.

  In the case of the IGBT, for positive collector-emitter voltage v_{CE}, no collector current will flow for values of v_{GE} less than a threshold voltage V_T. Once v_{GE} exceeds V_T, the collector current i_C increases as v_{GE} is increased.
- In the case of the MOSFET, no drain current flows for negative drain-source voltage.

  In the case of the IGBT, no collector current flows for negative collector-emitter voltage.
- Finally, the MOSFET will fail if the drain-source voltage exceeds its breakdown limits; in Fig. 10.12a, the forward breakdown voltage is indicated by the symbol $(V_{DS})_{FB}$ while the reverse breakdown voltage is indicated by the symbol $(V_{DS})_{RB}$.

  Similarly, the IGBT will fail if the collector-emitter voltage exceeds its breakdown values; in Fig. 10.12b, the forward breakdown voltage is indicated by the symbol $(V_{CE})_{FB}$ while the reverse breakdown voltage is indicated by the symbol $(V_{CE})_{RB}$.
- Although not shown in the figure, a MOSFET will fail due to excessive gate-source voltage as well as excessive drain current which leads to excessive power dissipation in the device. Similarly an IGBT will fail due to excessive gate-emitter voltage and excessive collector current.

Note that for small values of v_{CE}, the IGBT voltage approaches a constant value, independent of the drain current. This *saturation voltage,* labeled $(V_{CE})_{sat}$ in the figure, is on the order of a volt or less in small devices and a few volts in high-power devices. Correspondingly, in the MOSFET, for small values of v_{DS}, v_{DS} is proportional to the drain current and the MOSFET behaves as a small resistance whose value decreases with increasing v_{GS}.

Fortunately, for our purposes, the details of these characteristics are not important. As we will see in the following example, with a sufficient large gate signal, the voltage drop across both the MOSFET and the IGBT can be made quite small. In this case, these devices can be modeled as a short circuit between the drain and the source in the case of the MOSFET and between the collector and the emitter in the case of the IGBT. Note, however, these "switches" when closed carry only unidirectional current, and hence we will model them as a switch in series with an ideal diode. This *ideal-switch model* is shown in Fig. 10.13a.

In many cases, these devices are commonly protected by reverse-biased protection diodes connected between the drain and the source (in the case of a MOSFET) or between the collector and emitter (in the case of an IGBT). These protection

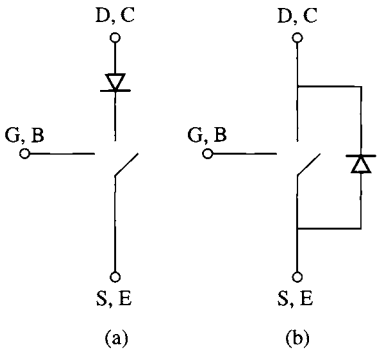

Figure 10.13 (a) Ideal-switch model for a MOSFET or an IGBT showing the series ideal diode which represents the unidirectional-current device characteristic. (b) Ideal-switch model for devices which include a reverse-biased protection diode. The symbols G, D, and S apply to the MOSFET while the symbols B, C, and E apply to the IBGT.

devices are often included as integral components within the device package. If these protection diodes are included, there is actually no need to include the series diode, in which case the model can be reduced to that of Fig. 10.13b.

EXAMPLE 10.4

Consider the circuit of Fig. 10.14a. Here we see an IGBT which is to be used to control the current through the resistor R as supplied from a dc source V_0. Assume that the IGBT characteristics are those of Fig. 10.12b and that V_0 is significantly greater than the saturation voltage. Show a graphical procedure that can be used to find v_{CE} as a function of v_{GE}.

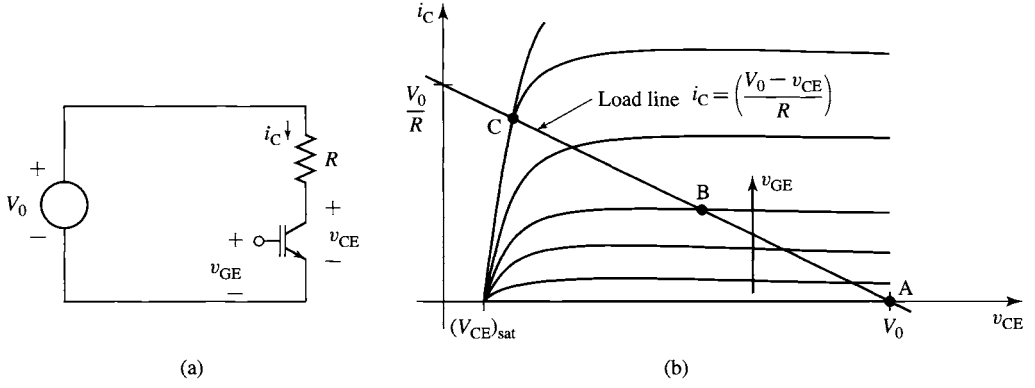

Figure 10.14 (a) Circuit for Example 10.4. (b) IGBT characteristic showing load line and operating point.

■ Solution

Writing KVL for the circuit of Fig. 10.14a gives

$$V_0 = i_C R + v_{CE}$$

Solving for i_C gives

$$i_C = \frac{(V_0 - v_{CE})}{R}$$

Note that this linear relationship, referred to as the *load line*, represents a constraint imposed by the external circuit on the relationship between the IGBT terminal variables i_C and v_{CE}. The corresponding constraint imposed by the IGBT itself is given by the v-i characteristic of Fig. 10.12b.

The operating point of the circuit is that point at which both these constraints are simultaneously satisfied. It can be found most easily by plotting the load line on the v-i relationship of the IGBT. This is done in Fig. 10.14b. The operating point is then found from the intersection of the load line with the v-i characteristic of the IGBT.

Consider the operating point labeled A in Fig. 10.14b. This is the operating point corresponding to values of v_{GE} less than or equal to the threshold voltage V_T. Under these conditions, the IGBT is OFF, there is no collector current, and hence $v_{CE} = V_0$. As v_{GE} is increased past V_T, collector current begins to flow, the operating point begins to climb up the load line, and v_{CE} decreases; the operating point labeled B is a typical example.

Note however that as v_{GE} is further increased, the operating point approaches that portion of the IGBT characteristic for which the curves crowd together (see the operating point labeled C in Fig. 10.14b). Once this point is reached, any further increase in v_{GE} will result in only a minimal decrease in v_{CE}. Under this condition, the voltage across the IGBT is approximately equal to the saturation voltage $(V_{CE})_{sat}$.

If the IGBT of this example were to be replaced by a MOSFET the result would be similar. As the gate-source voltage v_{GS} is increased, a point is reached where the voltage drop across approaches a small constant value. This can be seen by plotting the load line on the MOSFET characteristic of Fig. 10.12a.

The load line intersects the vertical axis at a collector current of $i_C = V_0/R$. Note that the larger the resistance, the lower this intersection and hence the smaller the value of v_{GE} required to saturate the transistor. Thus, in systems where the transistor is to be used as a switch, it is necessary to insure that the device is capable of carrying the required current and that the gate-drive circuit is capable of supplying sufficient drive to the gate.

Example 10.4 shows that when a sufficiently large gate voltage is applied, the voltage drop across a power transistor can be reduced to a small value. Under these conditions, the IGBT will look like a constant voltage while the MOSFET will appear as a small resistance. In either case, the voltage drop will be small, and it is sufficient to approximate it as a closed switch (i.e., the transistor will be ON). When the gate drive is removed (i.e., reduced below V_T), the switch will open and the transistor will turn OFF.

10.2 RECTIFICATION: CONVERSION OF AC TO DC

The power input to many motor-drive systems comes from a constant-voltage, constant-frequency source (e.g., a 50- or 60-Hz power system), while the output must provide variable-voltage and/or variable-frequency power to the motor. Typically such systems convert power in two stages: the input ac is first *rectified* to dc, and the dc is then converted to the desired ac output waveform. We will thus begin with a discussion of rectifier circuits. We will then discuss inverters, which convert dc to ac, in Section 10.3.

10.2.1 Single-Phase, Full-Wave Diode Bridge

Example 10.1 illustrates a half-wave rectifier circuit. Such rectification is typically used only in small, low-cost, low-power applications. Full-wave rectifiers are much more common. Consider the *full-wave rectifier* circuit of Fig. 10.15a. Here the resistor R is supplied from a voltage source $v_s(t) = V_0 \sin \omega t$ through four diodes connected in a *full-wave bridge* configuration.

If we assume the diodes to be ideal, we can use the method-of-assumed states to show that the allowable diode states are:

Diodes D1 and D3 ON, diodes D2 and D4 OFF for $v_s(t) > 0$
Diodes D2 and D4 ON, diodes D1 and D3 OFF for $v_s(t) < 0$

The resistor voltage, plotted in Fig. 10.15b, is then given by

$$v_R(t) = \begin{cases} v_s(t) = V_0 \sin \omega t & v_s(t) \geq 0 \\ -v_s(t) = -V_0 \sin \omega t & v_s(t) < 0 \end{cases} \tag{10.1}$$

Now notice that the resistor voltage is positive for both polarities of the source voltage, hence the terminology *full-wave rectification*. The dc or average value of this waveform can be seen to be twice that of the half-wave rectified waveform of Example 10.1.

$$V_{dc} = \left(\frac{2}{\pi}\right) V_0 \tag{10.2}$$

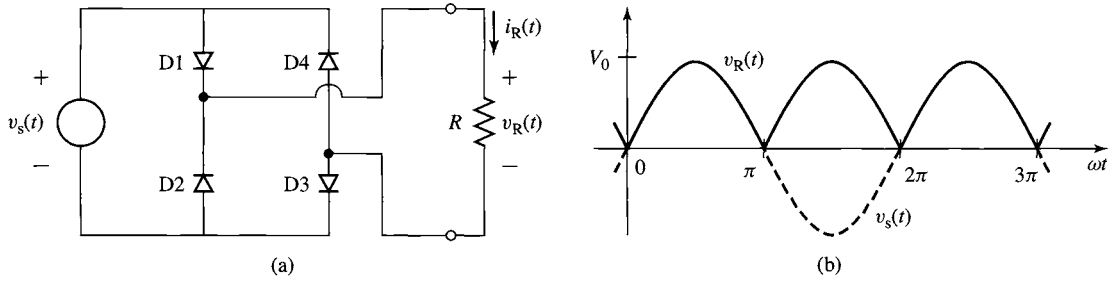

Figure 10.15 (a) Full-wave bridge rectifier. (b) Resistor voltage.

The rectified waveforms of Figs. 10.3b and 10.15b are clearly not the sort of "dc" waveforms that are considered desirable for most applications. Rather, to be most useful, the rectified dc should be relatively constant and ripple free. Such a waveform can be achieved using a filter capacitor, as illustrated in Example 10.5.

EXAMPLE 10.5

As shown in Fig. 10.16, a filter capacitor has been added in parallel with the load resistor in the full-wave rectifier system of Fig. 10.15. For the purposes of this example, assume that $v_s(t) = V_0 \sin \omega t$ with $V_0 = \sqrt{2}\,(120)$ V, $\omega = (2\pi)60 \approx 377$ rad/sec and that $R = 10\ \Omega$ and $C = 10^4\ \mu$F. Plot the resistor voltage, $v_R(t)$, current, $i_R(t)$, and the total bridge current, $i_B(t)$.

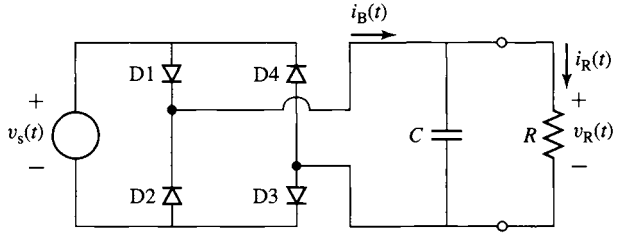

Figure 10.16 Full-wave bridge rectifier with capacitive filter for Example 10.5.

■ Solution

The addition of the filter capacitor will tend to maintain the resistor voltage $v_R(t)$ as the source voltage drops. The diodes will remain ON as long as the bridge output current remains positive and will switch OFF when this current starts to reverse.

This example can be readily solved using MATLAB.† Figure 10.17a shows the resistor voltage $v_R(t)$ plotted along with the rectified source voltage. During the time that the bridge is ON, i.e., one pair of diodes is conducting, the resistor voltage is equal to the rectified source voltage. When the bridge is OFF, the resistor voltage decays exponentially.

Notice that because the capacitor is relatively large (the RC time constant is 100 msec as compared to the period of the rectified source voltage, which is slightly over 8.3 msec) the diodes conduct only for a short amount of time around the peak of the rectified-source-voltage waveform. This can be readily seen from the expanded plots of the resistor current and the bridge current in Fig. 10.17b. Although the resistor current remains continuous and relatively constant, varying between 15.8 and 17 A, the bridge output current consists essentially of a

† MATLAB is a registered trademark of The MathWorks, Inc.

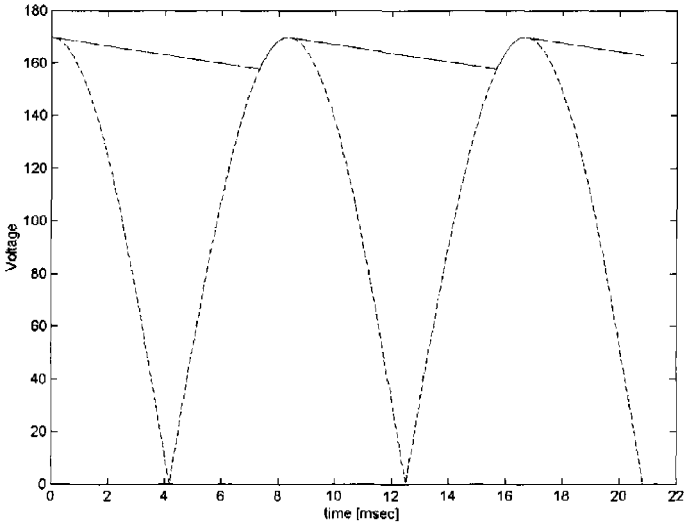

(a)

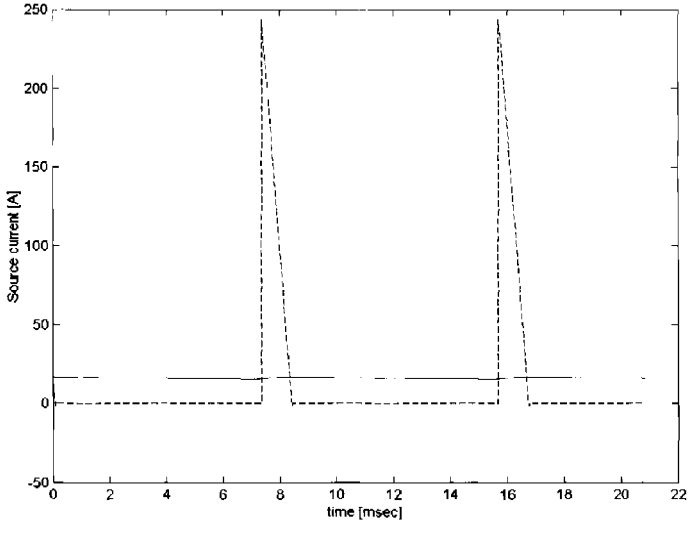

(b)

Figure 10.17 Example 10.5. (a) Resistor voltage and rectified source voltage (dashed). (b) Resistor current and total bridge current (dashed).

current pulse which flows for less than 0.9 msec near the peak of the rectified voltage waveform and has a peak value of 250 A. It should be pointed out that the peak current in a practical circuit will be smaller than 250 A, being limited by circuit impedances, diode drops, and so on.

Using MATLAB, it is possible to calculate the rms value of the resistor current to be 16.4 A while that of the bridge current is 51.8 A. We see therefore that the bridge diodes in such a system must be rated for rms currents significantly in excess of that of the load. The data sheets for power-supply diodes typically indicate their rms current ratings, specifically with these sorts of applications in mind. Such peaked supply currents are characteristic of rectifier circuits with capacitive loads and can significantly affect the voltage waveforms on ac power systems when they become a significant fraction of the overall system load.

The *ripple voltage* in the resistor voltage is defined as the difference between its maximum and minimum values. In this example, the maximum value is equal to the peak value of the source voltage, or 169.7 V. The minimum value can be found from the MATLAB solution to be 157.8 V. Thus the ripple voltage is 11.9 V. Clearly the ripple voltage can be decreased by increasing the value of the filter capacitor. Note however that this comes at the expense of increased cost as well as shorter current pulses and higher rms current through the rectifier diodes.

Here is the MATLAB script for Example 10.5.

```
clc
clear

%parameters
omega = 2*pi*60;
R = 10;
C = 0.01;
V0 = 120*sqrt(2);
tau = R*C;
Nmax = 800;

% diode = 1 when rectifier bridge is conducting
diode = 1;

%Here is the loop that does the work.
for n = 1:Nmax+1
   t(n) = (2.5*pi/omega)*(n-1)/Nmax; %time
   vs(n) = V0*cos(omega*t(n)); %source voltage
   vrect(n) = abs(vs(n)); %full-wave rectified source voltage

%Calculations if the rectifier bridge is ON
if diode == 1

%If the bridge is ON, the resistor voltage is equal to the rectified
%source voltage.
vR(n) = vrect(n);
%Check the total current out of rectifiers
if (omega*t(n)) <= pi/2.
iB(n) = vR(n)/R - V0*C*omega*sin(omega*t(n));
elseif (omega*t(n)) <= 3.*pi/2.
```

```
iB(n) = vR(n)/R + V0*C*omega*sin(omega*t(n));
else
iB(n) = vR(n)/R - V0*C*omega*sin(omega*t(n));
end

%If the current tries to go negative, the diodes will switch OFF
if iB(n) < 0;
diode = 0;
toff = t(n);
Voff = vrect(n);
end
   else
%When the diodes are off, the resistor/capacitor voltage decays
%exponentially.
vR(n) = Voff*exp(-(t(n)-toff)/tau);
iB(n) = 0;
if (vrect(n) - vR(n)) > 0;
diode = 1;
end
   end
end

%Calculate the resistor current
iR = vR/R;

%Now plot vR as a solid line and vrect as a dashed line
plot(1000*t,vR)
xlabel('time [msec]')
ylabel('Voltage [V]')
axis ([0 22 0 180])
hold
plot(1000*t,vrect,'  ')
hold

fprintf('\nHit any key to continue\n')
pause

%Now plot iR as a solid line and iL as a dashed line
plot(1000*t,iR)
xlabel('time [msec]')
ylabel('Source current [A]')
axis ([0 22 -50 250])
hold
plot(1000*t,iB,'--')
hold
```

Practice Problem 10.4

Use MATLAB to calculate the ripple voltage and rms diode current for the system of Example 10.5 for (*a*) $C = 5 \times 10^4$ μF and (*b*) $C = 5 \times 10^3$ μF. (Hint: Note that the rms current must be calculated over an integral number of cycles of the current waveform).

Solution

a. 2.64 V and 79.6 A rms
b. 21.6 V and 42.8 A rms

In Example 10.5 we have seen that a capacitor can significantly decrease the ripple voltage across a resistive load. However, this comes at the cost of large bridge current pulses since the current must be delivered to the capacitor in the short time period during which the rectified source voltage is near its peak value.

Figure 10.18 shows the addition of an inductor L at the output of the bridge, in series with the filter capacitor and its load. If the impedance of the inductor is chosen to be large compared to that of the capacitor/load combination at the frequency of the rectified source voltage, very little of the ac component of the rectified source voltage will appear across the capacitor, and thus the resultant L-C filter will produce low voltage ripple while drawing a relatively constant current from the diode bridge.

We have seen how the addition of a filter capacitor across a dc load can significantly reduce the ripple voltage seen by the load. In fact, the addition of significant capacitance can "stiffen" the rectified voltage to the point that it appears as a constant-voltage dc source to a load. In an analogous fashion, an inductor in series with a load will reduce the current ripple out of a rectifier. Under these conditions, the rectified source will appear as a constant-current dc source to a load.

The combination of a rectifier and an inductor at the output to supply a constant dc current to a load is of significant importance in power-electronic applications. It can be used, for example, as the front end of a current-source inverter which can be used to supply ac current waveforms to a load. We will investigate the behavior of such rectifier systems in the next section.

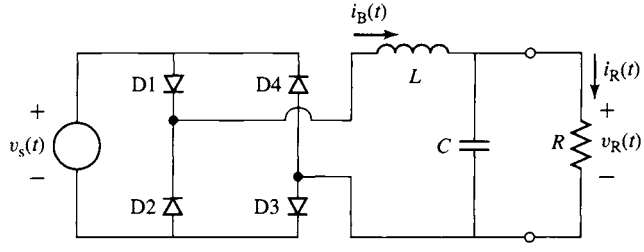

Figure 10.18 Full-wave bridge rectifier with an L-C filter supplying a resistive load.

10.2.2 Single-Phase Rectifier with Inductive Load

In this section we will examine the performance of a single-phase rectifier driving an inductive load. This situation covers both the case where the inductor is included as part of the rectifier system as a filter to smooth out current pulses as well as the case where the load itself is primarily inductive.

Let us examine first the half-wave rectifier circuit of Fig. 10.19. Here, the load consists of an inductor L in series with a resistor R. The source voltage is equal to $v_s(t) = V_0 \cos \omega t$.

Consider first the case where L is small ($\omega L \ll R$). In this case, the load looks essentially resistive and the load current $i_L(t)$ will vary only slightly from the current for a purely resistive load as seen in Example 10.1. This current, obtained from a detailed analytical solution, is plotted in Fig. 10.20a, along with the current for a purely resistive load.

Note that the effect of the inductance is to decrease both the initial rate of rise of the current and the peak current. More significantly, the diode *conduction angle* increases; current flows for longer than the half-period that is the case for a purely resistive load. As can be seen in Fig. 10.20a, this effect increases as the inductance is increased; current flows for a greater fraction of the cycle, and the peak current as well as the current ripple is reduced.

Figure 10.20b, which shows the inductor voltage, illustrates an important point that applies to all situations in which an inductor is subjected to steady-state, periodic conditions: *the time-averaged voltage across the inductor must equal zero.* This can be readily seen from the basic v-i relationship for an inductor

$$v = L\frac{di}{dt} \tag{10.3}$$

If we consider the operation of an inductor over a period of the excitation frequency and recognize that, under steady-state conditions, the change in the inductor current over that period must equal zero (i.e., it must have the same value at time t at the beginning of the period as it does one period later at time $t + T$), then we can write

$$i(t + T) - i(T) = 0 = \frac{1}{L}\int_t^{t+T} v\, dt \tag{10.4}$$

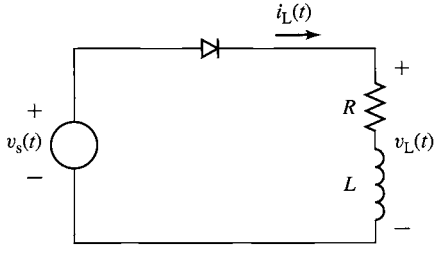

Figure 10.19 Half-wave rectifier with an inductive load.

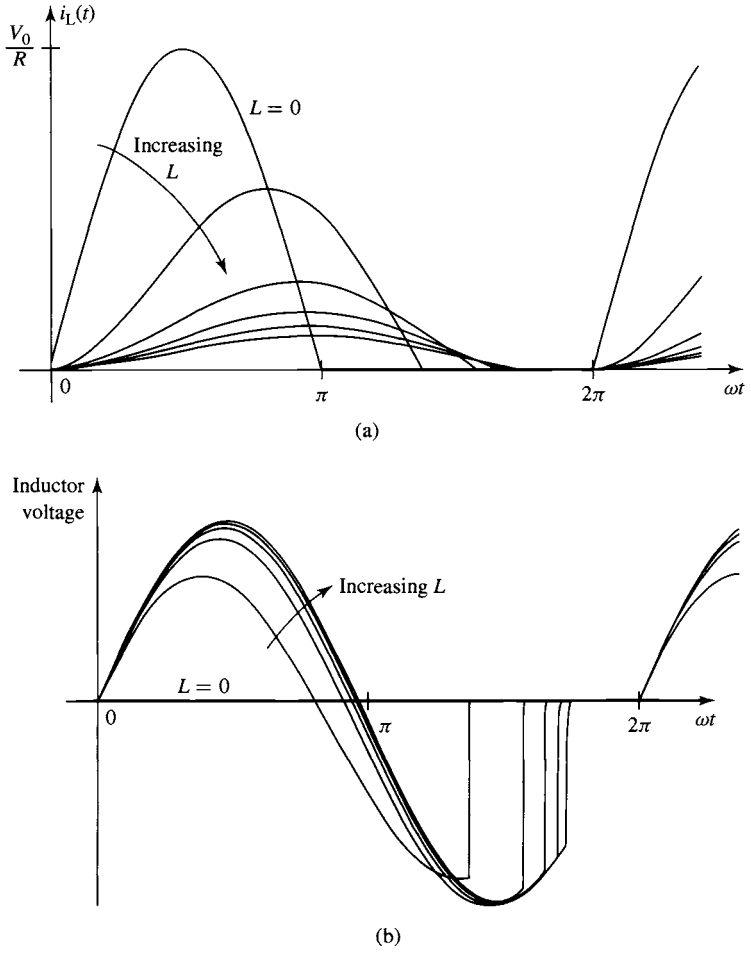

Figure 10.20 Effect of increasing the series inductance in the circuit of Fig. 10.19 on (a) the load current and (b) the inductor voltage.

from which we can see that the net volt-seconds (and correspondingly the average voltage) across the inductor during a cycle must equal zero

$$\int_t^{t+T} v\,dt = 0 \tag{10.5}$$

For this half-wave rectifier, note that as the inductance increases both the ripple current and the dc current will decrease. In fact, for large inductance ($\omega L \gg R$) the dc load current will tend towards zero. This can be easily seen by the following

argument:

As the inductance increases, the conduction angle of the diode will increase from 180° and approach 360° for large values of L.

In the limit of a 360° conduction angle, the diode can be replaced by a continuous short circuit, in which case the circuit reduces to the ac voltage source connected directly across the series combination of the resistor and the inductor.

Under this situation, no dc current will flow since the source is purely ac. In addition, since the impedance $Z = R + j\omega L$ becomes large with large L, the ac (ripple) current will also tend to zero.

Figure 10.21a shows a simple modification which can be made to the half-wave rectifier circuit of Fig. 10.19. The *free-wheeling diode* D2 serves as an alternate path for inductor current.

To understand the behavior of this circuit, consider the condition when the source voltage is positive, and the rectifier diode D1 is ON. The equivalent circuit for this operating condition is shown in Fig. 10.21b. Note that under this condition, the voltage across diode D2 is equal to the negative of the source voltage and diode D2 is turned OFF.

This operating condition will remain in effect as long as the source voltage is positive. However, as soon as the source voltage begins to go negative, the voltage across diode D2 will begin to go positive and it will turn ON. Since the load is

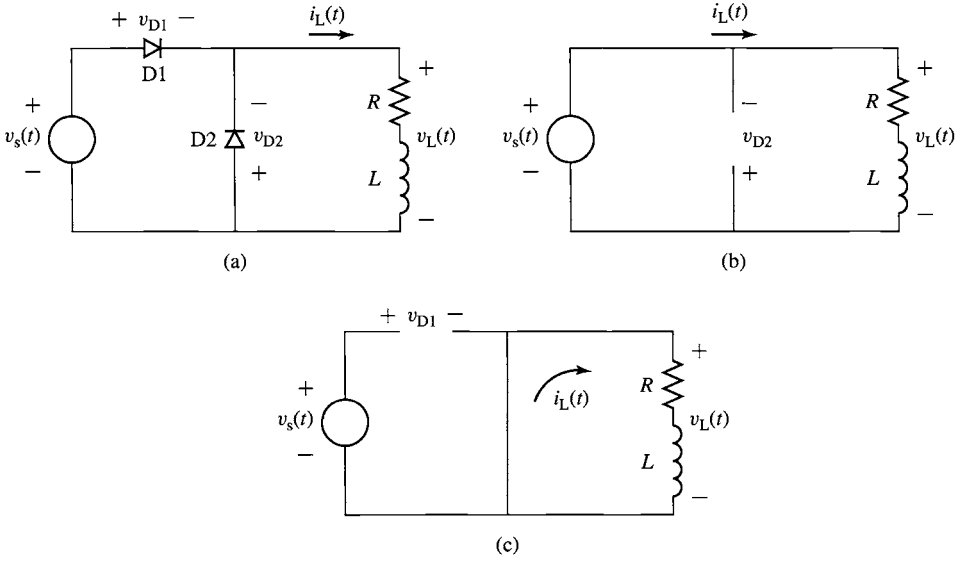

Figure 10.21 (a) Half-wave rectifier with an inductive load and a free-wheeling diode. (b) Equivalent circuit when $v_s(t) > 0$ and diode D1 is conducting. (c) Equivalent circuit when $v_s(t) < 0$ and the free-wheeling diode D2 is conducting.

inductive, a positive load current will be flowing at this time, and that load current will immediately transfer to the short circuit corresponding to diode D2. At the same time, the current through diode D1 will immediately drop to zero, diode D1 will be reverse biased by the source voltage, and it will turn OFF. This operating condition is shown in Fig. 10.21c. Thus, the diodes in this circuit alternately switch ON and OFF each half cycle: D1 is ON when $v_s(t)$ is positive, and D2 is ON when it is negative.

Based upon this discussion, we see that the voltage $v_L(t)$ across the load (equal to the negative of the voltage across diode D2) is a half-wave rectified version of $v_s(t)$ as seen in Fig. 10.22a. As shown in Example 10.1, the average of this voltage is $V_{dc} = V_0/\pi$. Furthermore, the average of the steady-state voltage across the inductor must equal zero, and hence the average of the voltage $v_L(t)$ will appear across the resistor. Thus the dc load current will equal $V_0/(\pi R)$. This value is independent of the inductor value and hence does not approach zero as the inductance is increased.

Figure 10.22b shows the diode and load currents for a relatively small value of inductance ($\omega L < R$), and Fig. 10.22c shows these same currents for a large inductance $\omega L \gg R$. In each case we see the load current, which must be continuous due to the presence of the inductor, instantaneously switching between the diodes depending on the polarity of the source voltage. We also see that during the time diode D1 is ON, the load current increases due to the application of the sinusoidal source voltage, while during the time diode D2 is ON, the load current simply decays with the L/R time constant of the load itself.

As expected, in each case the average current through the load is equal to $V_0/(\pi R)$. In fact, the presence of a large inductor can be seen to reduce the ripple current to the point that the load current is essentially a dc current equal to this value.

Let us now consider the case where the half-wave bridge of Fig. 10.19 is replaced by a full-wave bridge as in Fig. 10.23a. In this circuit, the voltage applied to the load is the full-wave-rectified source voltage as shown in Fig. 10.15 and the average (dc) voltage applied to the load will equal $2V_0/\pi$. Here again, the presence of the inductor will tend to reduce the ac ripple. Figure 10.24, again obtained from a detailed analytical solution, shows the current through the resistor as the inductance is increased.

If we assume a large inductor ($\omega L \gg R$), the load current will be relatively ripple free and constant. It is therefore common practice to analyze the performance of this circuit by replacing the inductor by a dc current source I_{dc} as shown in Fig. 10.23b, where $I_{dc} = 2V_0/(\pi R)$. This is a commonly used technique in the analysis of power-electronic circuits which greatly simplifies their analysis.

Under this assumption, we can easily show that the diode and source currents of this circuit are given by waveforms of Fig. 10.25. Figure 10.25a shows the current through one pair of diodes (e.g., diodes D1 and D3), and Fig. 10.25b shows the source current $i_s(t)$. The essentially constant load current I_{dc} flows through each pair of diodes for one half cycle and appears as a square wave of amplitude I_{dc} at the source.

In a fashion similar to that which we saw in the half-wave rectifier circuit with the free-wheeling diode, here a pair of diodes (e.g., diodes D1 and D3) are carrying current when the source voltage reverses, turning ON the other pair of diodes and switching OFF the pair that were previously conducting. In this fashion, the load current remains continuous and simply switches between the diode pairs.

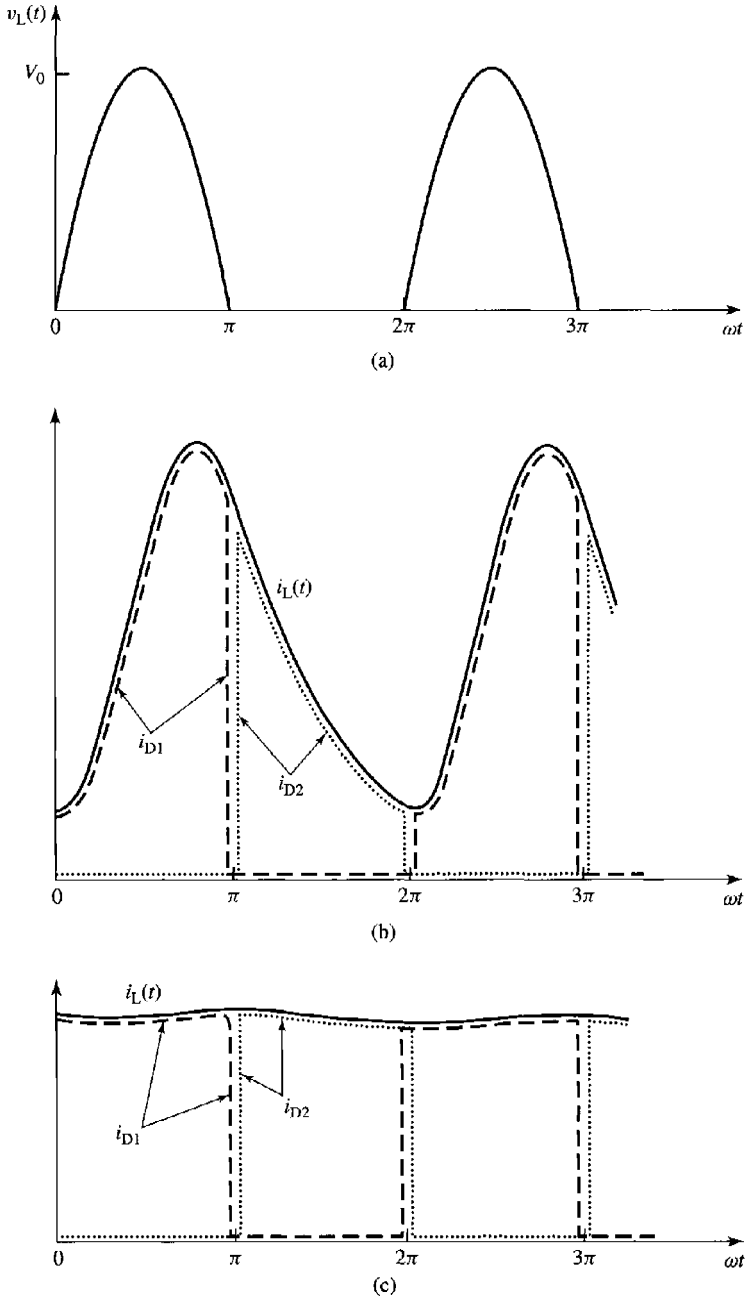

Figure 10.22 (a) Voltage applied to the load by the circuit of Fig. 10.21. (b) Load and diode currents for small L. (c) Load and diode currents for large L.

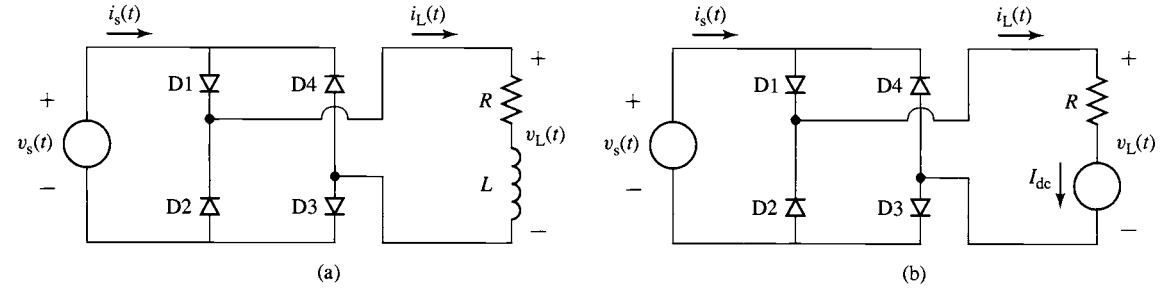

Figure 10.23 (a) Full-wave rectifier with an inductive load. (b) Full-wave rectifier with the inductor replaced by a dc current source.

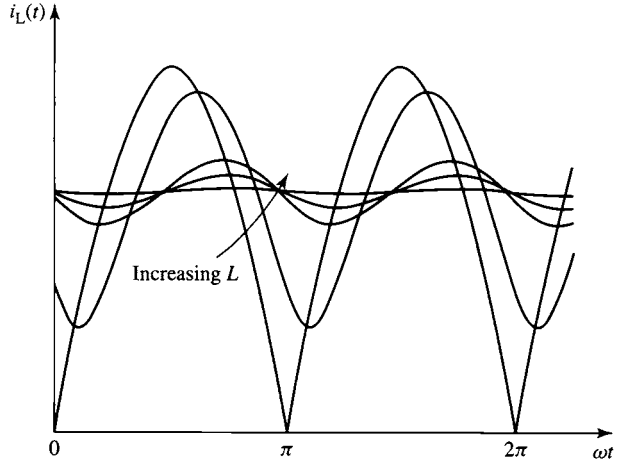

Figure 10.24 Effect of increasing the series inductance in the circuit of Fig. 10.23a on the load current.

10.2.3 Effects of Commutating Inductance

Our analysis and the current waveforms of Fig. 10.25 show that the current commutes instantaneously from one diode pair to the next. In practical circuits, due to the presence of source inductance, *commutation* of the current between the diode pairs does not occur instantaneously. The effect of source inductance, typically referred to as *commutating inductance,* will be examined by studying the circuit of Fig. 10.26 in which a source inductance L_s has been added in series with the voltage source in the full-wave rectifier circuit of Fig. 10.23b. We have again assumed that the load time constant is large ($\omega L/R \gg 1$) and have replaced the inductor with a dc current source I_{dc}.

Figure 10.27a shows the situation which occurs when diodes D2 and D4 are ON and carrying current I_{dc} and when $v_s < 0$. Commutation begins when v_s reaches zero and begins to go positive, turning ON diodes D1 and D3. Note that *because the current in the source inductance L_s cannot change instantaneously,* the circuit condition at

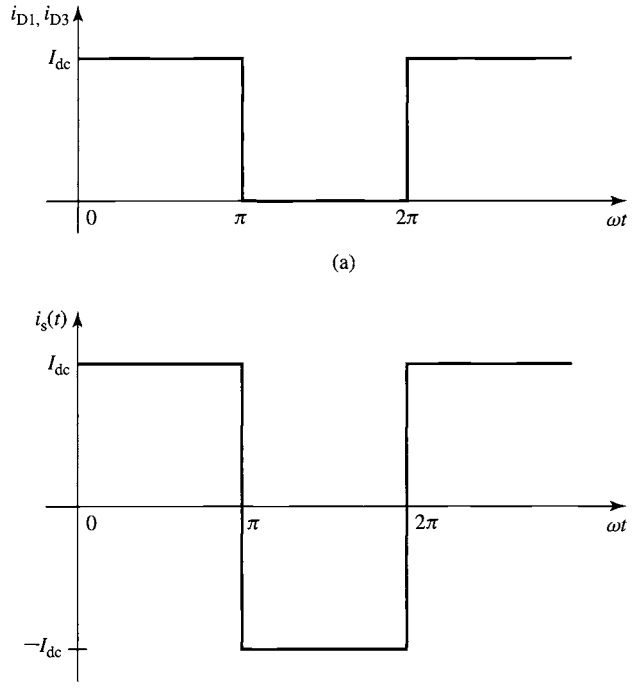

Figure 10.25 (a) Current through diodes D1 and D3 and (b) source current for the circuit of Fig. 10.23, both in the limit of large inductance.

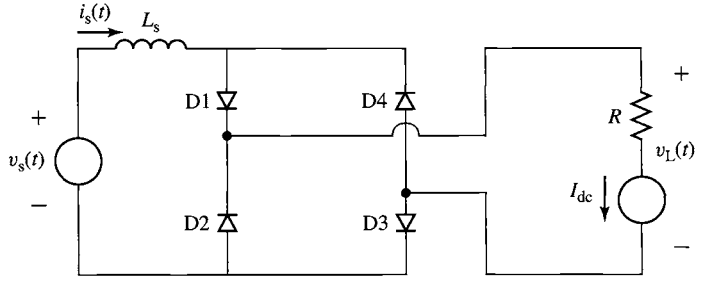

Figure 10.26 Full-wave bridge rectifier with source inductance. Dc load current assumed.

this time is described by Fig. 10.27b: the current through L_s is equal to $-I_{dc}$, the current through diodes D2 and D4 is equal to I_{dc}, while the current through diodes D1 and D3 is zero.

Under this condition with all four diodes ON, the source voltage $v_s(t)$ appears directly across the source inductance L_s. Noting that commutation starts at the time

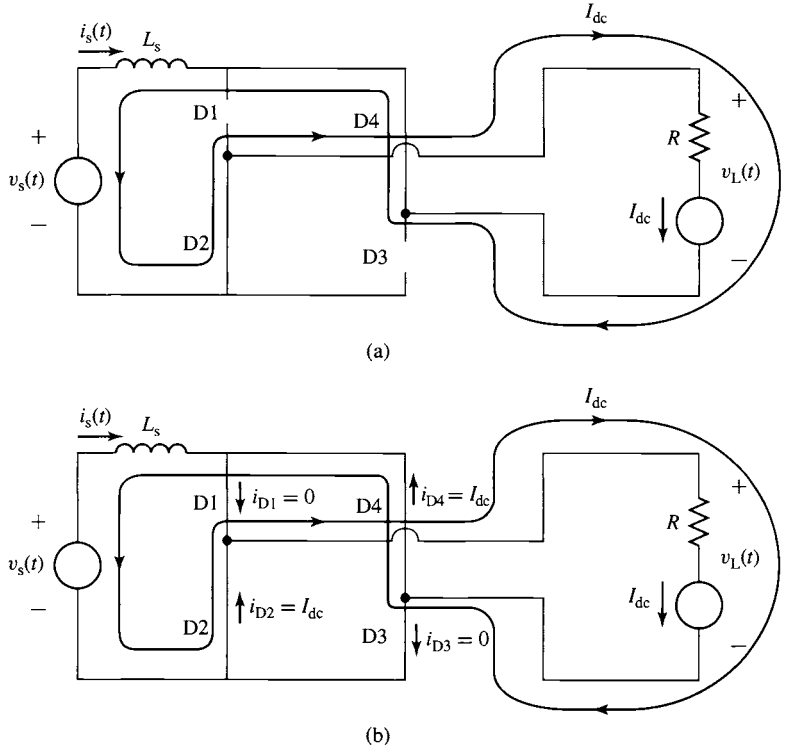

Figure 10.27 (a) Condition of the full-wave circuit of Fig. 10.26 immediately before diodes D1 and D3 turn ON. (b) Condition immediately after diodes D1 and D3 turn ON.

when $v_s(t) = 0$, the current through L_s can be written as

$$i_s(t) = -I_{dc} + \frac{1}{L_s}\int_0^t v_s(t)\,dt$$

$$= -I_{dc} + \left(\frac{V_0}{\omega L_s}\right)(1 - \cos \omega t) \tag{10.6}$$

Noting that $i_s = i_{D1} - i_{D4}$, that $i_{D1} + i_{D2} = I_{dc}$ and, that by symmetry, $i_{D4} = i_{D2}$, we can write that

$$i_{D2} = \frac{I_{dc} - i_s(t)}{2} \tag{10.7}$$

Diode D2 (and similarly diode D4) will turn OFF when i_{D2} reaches zero, which will occur when $i_s(t) = I_{dc}$. In other words, commutation will be completed at time t_c, when the current through L_s has completely reversed polarity and when all of the load current is flowing through diodes D1 and D3.

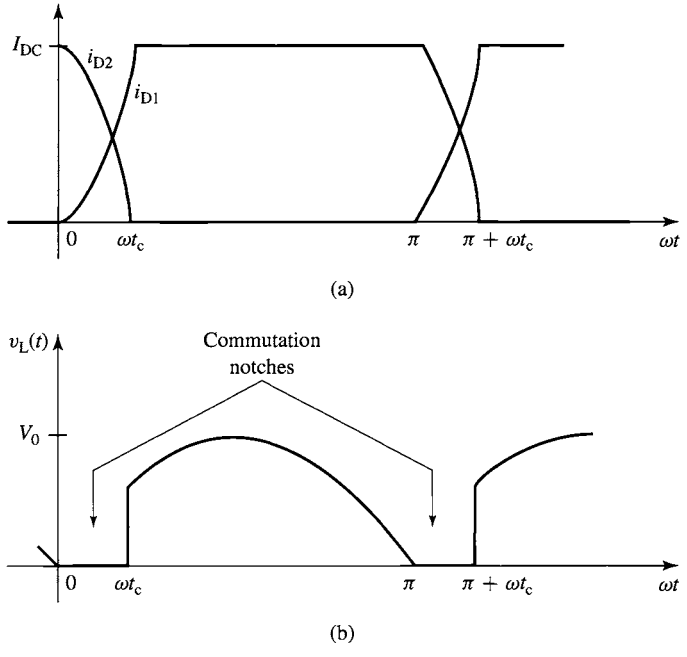

Figure 10.28 (a) Currents through diodes D1 and D2 showing the finite commutation interval. (b) Load voltage showing the commutation notches due to the finite commutation time.

Setting $i_s(t_c) = I_{dc}$ and solving Eq. 10.6 gives an expression for the *commutation interval* t_c as a function of I_{dc}

$$t_c = \frac{1}{\omega} \cos^{-1}\left[1 - \left(\frac{2I_{dc}\omega L_s}{V_0}\right)\right] \tag{10.8}$$

Figure 10.28a shows the currents through diodes D1 and D2 as the current commutates between them. The finite commutation time t_c can clearly be seen. There is a second effect of commutation which can be clearly seen in Fig. 10.28b which shows the rectified load voltage $v_L(t)$. Note that during the time of commutation, with all the diodes on, the rectified load voltage is zero. These intervals of zero voltage on the rectified voltage waveform are known as *commutation notches*.

Comparing the ideal full-wave rectified voltage of Fig. 10.15b to the waveform of Fig. 10.28b, we see that the effect of the commutation notches is to reduce the dc output of the rectifier. Specifically, the dc voltage in this case is given by

$$\begin{aligned} V_{dc} &= \left(\frac{\omega}{\pi}\right) \int_{t_c}^{\frac{\pi}{\omega}} V_0 \sin \omega t \, dt \\ &= \frac{V_0}{\pi} (1 + \cos \omega t_c) \end{aligned} \tag{10.9}$$

where t_c is the commutation interval as calculated by Eq. 10.8.

Finally, the dc load current can be calculated as function of t_c

$$I_{dc} = \frac{V_{dc}}{R} = \frac{V_0}{\pi R}(1 + \cos \omega t_c) \tag{10.10}$$

Substituting Eq. 10.8 into Eq. 10.10 gives a closed-form solution for I_{dc}

$$I_{dc} = \frac{2V_0}{\pi R + 2\omega L_s} \tag{10.11}$$

and hence

$$V_{dc} = I_{dc}R = \frac{2V_0}{\pi + \frac{2\omega L_s}{R}} \tag{10.12}$$

We have seen that commutating inductance (which is to a great extent unavoidable in practical circuits) gives rise to a finite commutation time and produces commutation notches in the rectified-voltage waveform which reduces the dc voltage applied to the load.

EXAMPLE 10.6

Consider a full-wave rectifier driving an inductive load as shown in Fig. 10.29. For a 60-Hz, 230-V rms source voltage, $R = 5.6\ \Omega$ and large L ($\omega L \gg R$), plot the dc current through the load I_{dc} and the commutation time t_c as the source inductance L_s varies from 1 to 100 mH.

■ Solution

The solution can be obtained by substitution into Eqs. 10.8 and 10.11. This is easily done using MATLAB, and the plots of I_{dc} and t_c are shown in Figs. 10.30a and b respectively. Note that the maximum achievable dc current, corresponding to $L_s = 0$, is equal to $2V_0/(\pi R) = 37$ A. Thus, commutating inductances on the order of 1 mH can be seen to have little effect on the performance of the rectifier and can be ignored. On the other hand, a commutating inductance of 100 mH can be seen to reduce the dc current to approximately 7 A, significantly reducing the capability of the rectifier circuit.

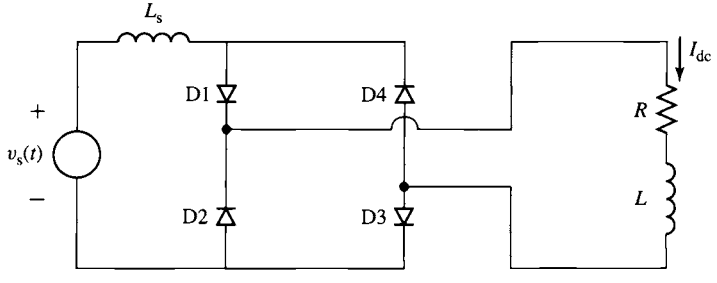

Figure 10.29 Full-wave bridge rectifier with source inductance for Example 10.6.

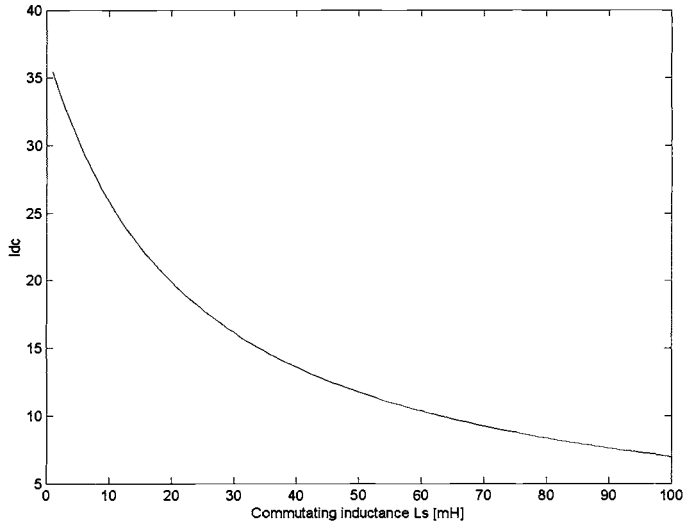

(a)

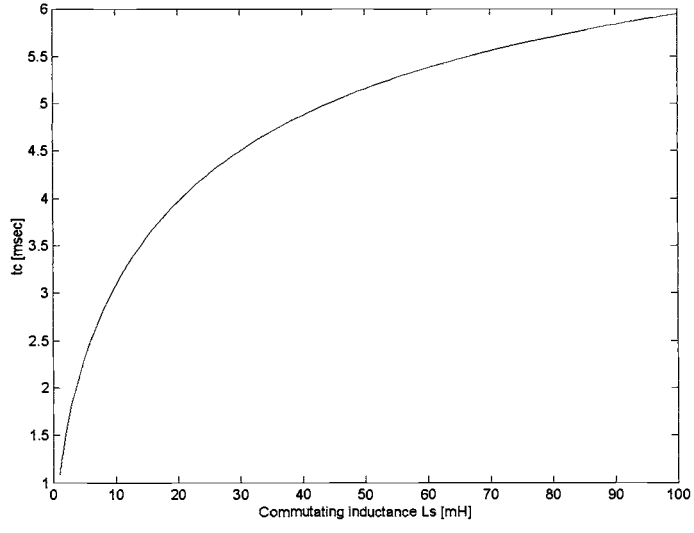

(b)

Figure 10.30 (a) Dc current I_{dc} and (b) commutation time t_c for Example 10.6.

Here is the MATLAB script for Example 10.6.

```
clc
clear

%parameters
omega = 2*pi*60;
R = 5.6;
V0 = 230*sqrt(2);

for n = 1:100
   Ls(n) = n*1e-3;
   Idc(n) = 2*V0/(pi*R + 2*omega*Ls(n));
   tc(n) = (1/omega)*acos(1-(2*Idc(n)*omega*Ls(n))/V0);
end

plot(Ls*1000,Idc)
xlabel('Commutating inductance Ls [mH]')
ylabel('Idc')

fprintf('\nHit any key to continue\n')
pause

plot(Ls*1000,tc*1000)
xlabel('Commutating inductance Ls [mH]')
ylabel('tc [msec]')
```

Practice Problem 10.5

Calculate the commutating inductance and the corresponding commutation time for the circuit of Example 10.6 if the dc load current is observed to be 29.7 A.

Solution

$L_s = 5.7$ mH and $t_c = 2.4$ msec

10.2.4 Single-Phase, Full-Wave, Phase-Controlled Bridge

Figure 10.31 shows a full-wave bridge in which the diodes of Fig. 10.15 have been replaced by SCRs. We will assume that the load inductance L is sufficiently large that the load current is essentially constant at a dc value I_{dc}. We will also ignore any effects of commutating inductance, although they clearly would play the same role in a phase-controlled rectifier system as they do in a diode-rectifier system.

Figure 10.32 shows the source voltage and the timing of the SCR gate pulses under a typical operating condition for this circuit. Here we see that the firing pulses are delayed by an angle α_d after the zero-crossing of the source-voltage waveform, with the firing pulses for SCRs T1 and T3 occuring after the positive-going transition of $v_s(t)$ and those for SCRs T2 and T4 occuring after the negative-going transition.

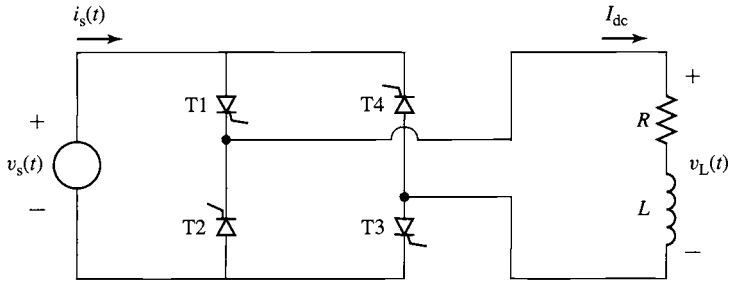

Figure 10.31 Full-wave, phase-controlled SCR bridge.

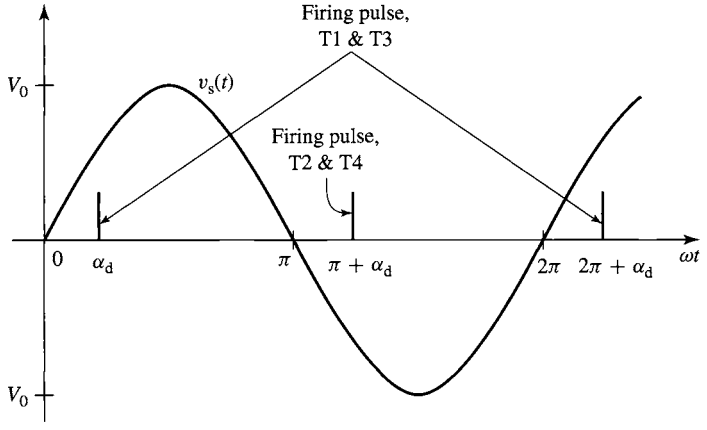

Figure 10.32 Source voltage and firing pulses for the phase-controlled SCR bridge of Fig. 10.31.

Figure 10.33a shows the current through SCRs T1 and T3. Note that these SCRs do not turn ON until they receive firing pulses at angle α_d after they are forward biased following positive-going zero crossing of the source voltage. Furthermore, note that SCRs T2 and T4 do not turn ON following the next zero crossing of the source voltage. Hence, SCRs T1 and T3 remain ON, carrying current until SCRs T2 and T4 are turned ON by gate pulses. Rather, T2 and T4 turn ON only after they receive their respective gate pulses (for example, at angle $\pi + \alpha_d$ in Fig. 10.33). This is an example of *forced commutation,* in that one pair of SCRs does not naturally commutate OFF but rather must be forcibly commutated when the other pair is turned ON.

Figure 10.33b shows the resultant load voltage $v_L(t)$. We see that the load voltage now has a negative component, which will increase as the firing-delay angle α_d is increased. The dc value of this waveform is equal to

$$V_{dc} = \left(\frac{2V_0}{\pi}\right)\cos\alpha_d \quad (0 \le \alpha_d \le \pi) \tag{10.13}$$

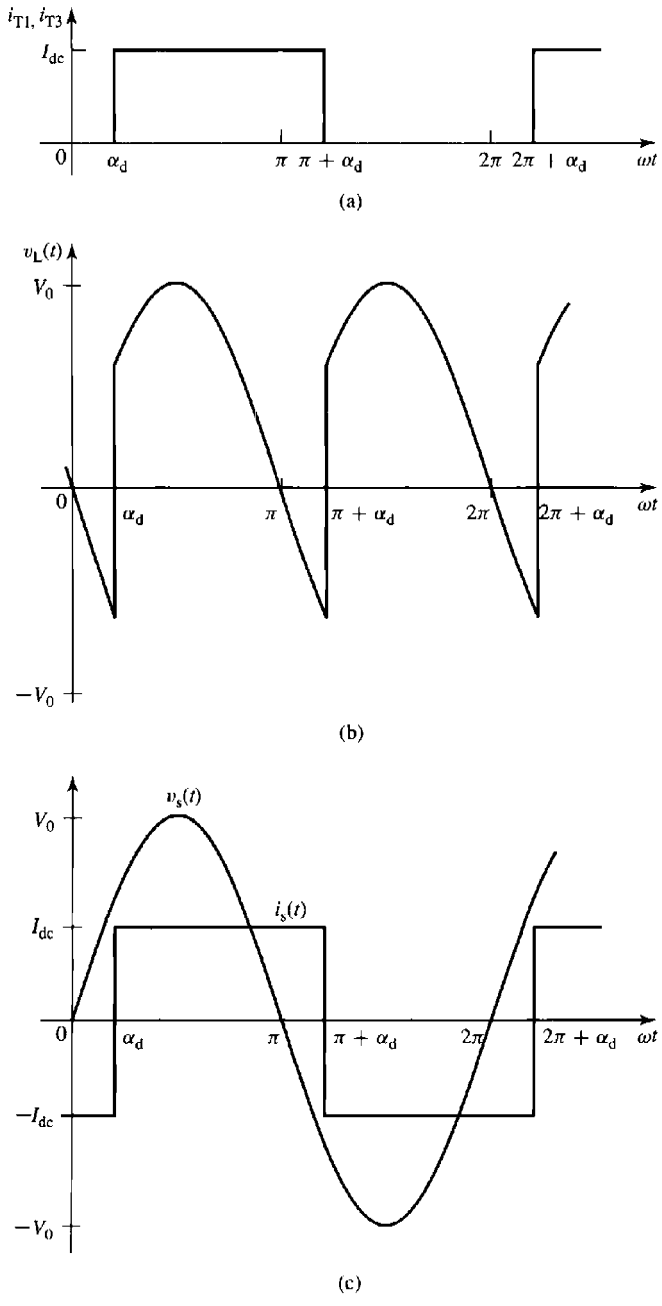

Figure 10.33 Waveforms for the phase-controlled SCR bridge of Fig. 10.31. (a) Current through SCRs T1 and T3. (b) Load voltage. (c) Source voltage and current.

from which the firing-delay angle corresponding to a given value of dc voltage can be seen to be

$$\alpha_d = \cos^{-1}\left(\frac{\pi V_{dc}}{2V_0}\right) \tag{10.14}$$

From Eq. 10.13 we see that the dc voltage applied to the load can vary from $2V_0/\pi$ to $-2V_0/\pi$. This is a rather surprising result in that it is hard to understand how a rectifier bridge can supply negative voltage. However, in this case, it is necessary to recognize that this result applies to an inductive load which maintains positive current flow through the SCRs in spite of the reversal of polarity of the source voltage. If the load were purely resistive, the current through the conducting SCRs would go to zero as the source-voltage reversed polarity, and they would simply turn OFF; no load current would flow until the next pair of SCRs is turned ON.

Figure 10.33c shows the source voltage and current waveforms for the phase-controlled SCR-bridge. We see that the square-wave source current is out of phase with the source voltage. Its fundamental-harmonic is given by

$$i_{s,1}(t) = \left(\frac{4}{\pi}\right) I_{dc} \sin(\omega t - \alpha_d) \tag{10.15}$$

and thus the real power supplied to the load is given by

$$P = V_{dc} I_{dc} = \frac{2}{\pi} V_0 I_{dc} \cos\alpha_d \tag{10.16}$$

and the reactive power supplied is

$$Q = -\frac{2}{\pi} V_0 I_{dc} \sin\alpha_d \tag{10.17}$$

Under steady-state operation at a load current I_{dc}, $V_{dc} = I_{dc}R$ and the steady-state firing-delay angle can be found from Eq. 10.14 to be $\alpha_{ss} = \cos^{-1}(\frac{\pi I_{dc} R}{2V_0})$. Under this condition, the real power simply supplies the losses in the resistor and hence $P = I_{dc}^2 R$. It may seem strange to be supplying reactive power to a "dc" load. However, careful analysis will show that this reactive power supplies the energy associated with the small but finite ripple current through the inductor.

If the delay angle is suddenly reduced ($\alpha_d < \alpha_{ss}$), the dc voltage applied to the load will increase (see Eq. 10.13) as will the power supplied to the load (see Eq. 10.16). As a result, I_{dc} will begin to increase and the increased power will increase the energy storage in the inductor. Similarly, if the delay time is suddenly increased ($t_d > t_{d0}$), V_{dc} will decrease (it may even go negative) and the power into the load will decrease, corresponding to a decrease in I_{dc} and a decrease in the energy storage in the inductor.

Note that if $\alpha_d > \pi/2$, V_{dc} will be negative, a condition which will continue until I_{dc} reaches zero at which time the SCR bridge will turn OFF. Under this condition, the real power P will also be negative. Under this condition, power is being supplied from the load to the source and the system is said to be *regenerating*.

EXAMPLE 10.7

A small superconducting magnet has an inductance $L = 1.2$ H. Although the resistance of the magnet itself is essentially zero, the resistance of the external leads is 12.5 mΩ. Current is supplied to the magnet from a 60-Hz, 15-V peak, single-phase source through a phase-controlled SCR bridge as in Fig. 10.31.

a. The magnet is initially operating in the steady state at a dc current of 35 A. Calculate the dc voltage applied to the magnet, the power supplied to the magnet, and the delay angle α_d in msec. Plot the magnet voltage $v_L(t)$.
b. In order to quickly discharge the magnet, the delay angle is suddenly increased to $\alpha_d = 0.9\pi = 162°$. Plot the corresponding magnet voltage. Calculate the time required to discharge the magnet and the maximum power regenerated to the source.

■ Solution

The example is most easily solved using MATLAB, which can easily produce the required plots.

a. Under this steady-state condition, $V_{dc} = I_{dc}R = 35 \times 0.0125 = 0.438$ V. The power supplied to the magnet is equal to $P = V_{dc}I_{dc} = 0.438 \times 35 = 15.3$ W, all of which is going into supplying losses in the lead resistance. The delay angle can be found from Eq. 10.14.

$$\alpha_d = \cos^{-1}\left(\frac{\pi R I_{dc}}{2V_0}\right) = \cos^{-1}\left(\frac{\pi \times 0.0125 \times 35}{2 \times 15}\right)$$
$$= 1.52 \text{ rad} = 87.4°$$

A plot of $v_L(t)$ for this condition is given in Fig. 10.34a.

b. For a delay angle of 0.9π, the dc load voltage will be

$$V_{dc} = \left(\frac{2V_0}{\pi}\right)\cos\alpha_d = \left(\frac{2 \times 15}{\pi}\right)\cos(0.9\pi) = -9.1 \text{ V}$$

A plot of $v_L(t)$ for this condition is given in Fig. 10.34b.

The magnet current i_m can be calculated from the differential equation

$$V_{dc} = i_m R + L\frac{di_m}{dt}$$

subject to the initial condition that $i_m(0) = 35$ A. Thus

$$i_m(t) = \frac{V_{dc}}{R} + \left(i_m(0) - \frac{V_{dc}}{R}\right)e^{-\left(\frac{R}{L}\right)t}$$

From this equation we find that the magnet current will reach zero at time $t = 4.5$ seconds, at which time the bridge will shut off. The power regenerated to the source will be given by $-V_{dc}i_m(t)$. It has a maximum value of $9.1 \times 35 = 318$ W at time $t = 0$.

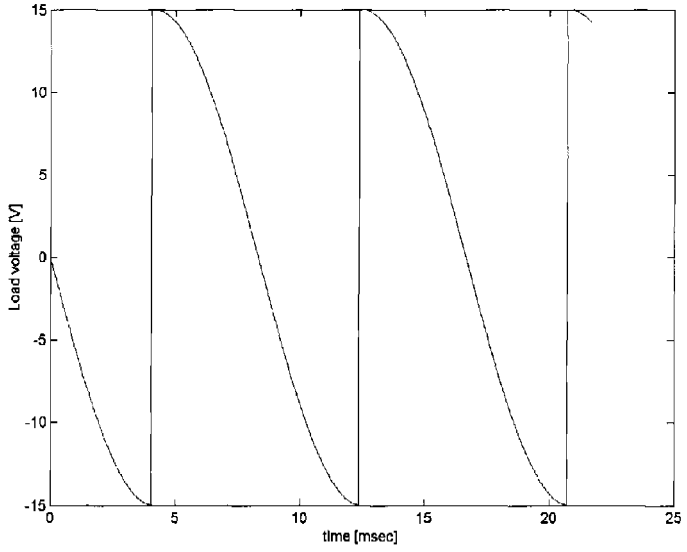

(a)

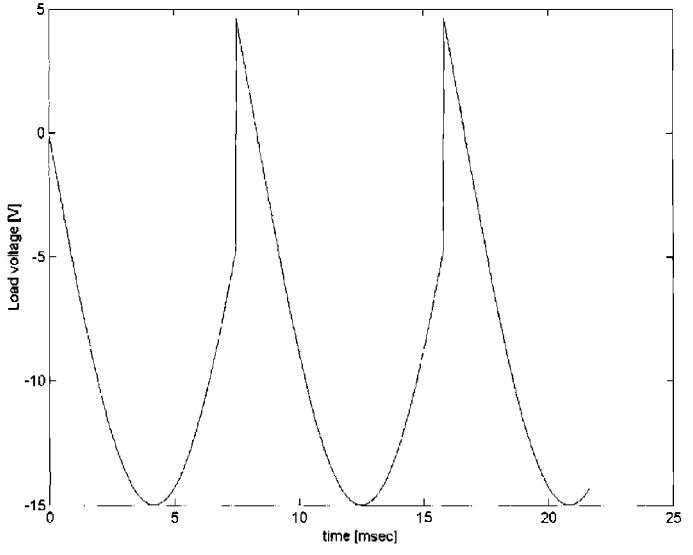

(b)

Figure 10.34 Waveforms for Example 10.7. (a) Magnet-voltage for $\alpha_d = 87.4°$, $V_{dc} = 0.438$ V. (b) Magnet-voltage for $\alpha_d = 162°$, $V_{dc} = -9.1$ V.

Here is the MATLAB script for Example 10.7.

```
clc
clear

% system parameters
R = 12.5e-3;
L = 1.2;
V0 = 15;
omega = 120*pi;

% part (a)

% dc current
Idc = 35;

% dc voltage
Vdc_a = R*Idc;

% Power
P = Vdc_a*Idc;

%Calculate the delay angle
alpha_da = acos(pi*R*Idc/(2*V0));

%Now calculate the load voltage
for n = 1:1300
   theta(n) = 2*pi*(n-1)/1000;
   t(n) = theta(n)/omega;
   vs(n) = V0*sin(theta(n));

   if theta(n) < alpha_da
vL(n) = -vs(n);
   elseif (theta(n) < pi + alpha_da)
vL(n) = vs(n);
   elseif theta(n) < 2*pi + alpha_da
vL(n) = -vs(n);
   elseif theta(n) < 3*pi + alpha_da
vL(n) = vs(n);
   elseif theta(n) < 4*pi + alpha_da
vL(n) = -vs(n);
   else
vL(n) = vs(n);
   end

end

plot(1000*t,vL)
xlabel('time [msec]')
ylabel('Load voltage [V]')

pause

% part (b)
```

```
% delay angle
alpha_db = 0.9*pi;

% Find the new dc voltage
Vdc_b = (2*V0/pi)*cos(alpha_db);

% Time constants
tau = L/R;

% Initial current
im0 = Idc;

% Calculate the time at which the current reaches zero
tzero = -tau*log((-Vdc_b/R)/(im0-Vdc_b/R));

% Now plot the load voltage
for n = 1:1300
   theta(n) = 2*pi*(n-1)/1000;
   t(n) = theta(n)/omega;
   vs(n) = V0*sin(theta(n));

   if theta(n) < alpha_db
vL(n) = -vs(n);
   elseif (theta(n) < pi + alpha_db)
vL(n) = vs(n);
   elseif theta(n) < 2*pi + alpha_db
vL(n) = -vs(n);
   elseif theta(n) < 3*pi + alpha_db
vL(n) = vs(n);
   elseif theta(n) < 4*pi + alpha_db
vL(n) = -vs(n);
   else
vL(n) = vs(n);
   end

end

plot(1000*t,vL)
xlabel('time [msec]')
ylabel('Load voltage [V]')

fprintf('part (a):')
fprintf('\n  Vdc_a = %g [mV]',1000*Vdc_a)
fprintf('\n  Power = %g [W]',P);
fprintf('\n  alpha_d = %g [rad] = %g [degrees]',alpha_da,180*alpha_da/pi)
fprintf('\npart (b):')
fprintf('\n  alpha_d = %g [rad] = %g [degrees]',alpha_db,180*alpha_db/pi)
fprintf('\n  Vdc_b = %g [V]',Vdc_b)
fprintf('\n  Current will reach zero at %g [sec]',tzero)
fprintf('\n')
```

Practice Problem 10.6

The field winding of a small synchronous generator has a resistance of 0.3 Ω and an inductance of 250 mH. It is fed from a 24-V peak, single-phase 60-Hz source through a full-wave phase-controlled SCR bridge. (*a*) Calculate the dc voltage required to achieve a dc current of 18 A through the field winding and the corresponding firing-delay angle. (*b*) Calculate the field current corresponding to a delay angle of 45°.

Solution

a. 5.4 V, 69°
b. 36.0 A

10.2.5 Inductive Load with a Series DC Source

As we have seen in Chapter 9, dc motors can be modeled as dc voltage sources in series with an inductor and a resistor. Thus, it would be useful to briefly investigate the case of a dc voltage source in series with an inductive load.

Let us examine the full-wave, phase-controlled SCR rectifier system of Fig. 10.35. Here we have added a dc source E_{dc} in series with the load. Again assuming that $\omega L \gg R$ so that the load current is essentially dc, we see that the load voltage $v_L(t)$ depends solely on the timing of the SCR gate pulses and hence is unchanged by the presence of the dc voltage source E_{dc}. Thus the dc value of $v_L(t)$ is given by Eq. 10.13 as before.

In the steady-state, the dc current through the load can be found from the net dc voltage across the resistor as

$$I_{dc} = \frac{V_{dc} - E_{dc}}{R} \quad (V_{dc} \geq E_{dc}) \tag{10.18}$$

where V_{dc} is found from Eq. 10.13. Under transient conditions, it is the difference voltage, $V_{dc} - E_{dc}$, that drives a change in the dc current through the series R-L combination, in a fashion similar to that illustrated in Example 10.7.

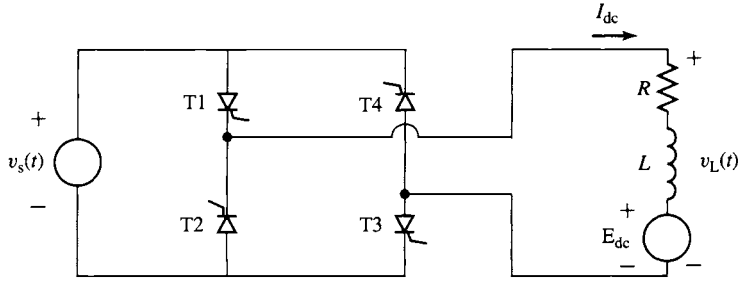

Figure 10.35 Full-wave, phase-controlled SCR bridge with an inductive load including a dc voltage source.

EXAMPLE 10.8

A small permanent-magnet dc motor is to be operated from a phase-controlled bridge. The 60-Hz ac waveform has an rms voltage of 35 volts. The dc motor has an armature resistance of 3.5 Ω and an armature inductance of 17.5 mH. It achieves a no-load speed of 8000 r/min at an armature voltage of 50 V.

Calculate the no-load speed in r/min of the motor as a function of the firing delay angle α_d.

■ Solution

In Section 7.7 we see that the equivalent circuit for a permanent-magnet dc motor consists of a dc source (proportional to motor speed) in series with an inductance and a resistance. Thus, the equivalent circuit of Fig. 10.35 applies directly to the situation of this problem.

From Eq. 7.26, the generated voltage from the dc motor (E_{dc} in Fig. 10.35) is proportional to the speed of the dc motor. Thus,

$$n = \left(\frac{8000}{50}\right) E_{dc} = 160 E_{dc} \text{ r/min}$$

Under steady state operation, the dc voltage drop across the armature inductance will be zero. In addition, at no load, the armature current will be sufficiently small that the voltage drop across the armature resistance can be neglected. Thus, setting $E_{dc} = V_{dc}$ and substituting the expression for V_{dc} from Eq. 10.13 give,

$$E_{dc} = V_{dc} = \left(\frac{2V_0}{\pi}\right) \cos\alpha_d$$

$$= \left(\frac{2\sqrt{2}\,35}{\pi}\right) \cos\alpha_d = 31.5 \cos\alpha_d$$

Note that because the bridge can only supply positive current to the dc motor (and hence, in the steady-state, the dc voltage must be positive), this expression is valid only for $0 \le \alpha_d \le \pi/2$.

Finally, substituting the expression for the speed n in terms of E_{dc} gives

$$n = 160 \times (31.5 \cos\alpha_d) = 5040 \cos\alpha_d \text{ r/min} \quad (0 \le \alpha_d \le \pi/2)$$

Practice Problem 10.7

The dc-motor of Example 10.8 is observed to be operating at a speed of 3530 r/min and drawing a dc current of 1.75 ampere. Calculate the corresponding firing delay angle α_d.

Solution

$$\alpha_d = 0.15\pi \text{ rad} = 27^\circ$$

10.2.6 Three-Phase Bridges

Although many systems with ratings ranging up to five or more kilowatts run off single-phase power, most large systems are supplied from three-phase sources. In general, all of the issues which we have discussed with regard to single-phase,

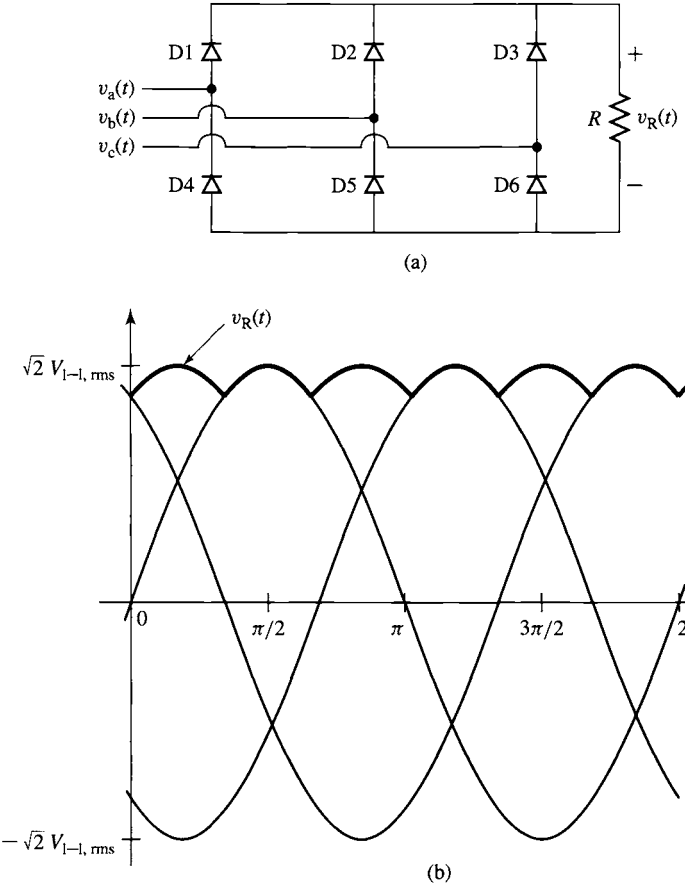

Figure 10.36 (a) Three-phase, six-pulse diode bridge with resistive load. (b) Line-to-line voltages and resistor voltage.

full-wave bridges apply directly to situations with three-phase bridges. As a result, we will discuss three-phase bridges only briefly.

Figure 10.36a shows a system in which a resistor R is supplied from a three-phase source through a *three-phase, six-pulse diode bridge*. Figure 10.36b shows the three-phase line-to-line voltages (peak value $\sqrt{2}V_{l-l,rms}$ where $V_{l-l,rms}$ is the rms value of the line-to-line voltage) and the resistor voltage $v_R(t)$, found using the method-of-assumed-states and assuming that the diodes are ideal.

Note that v_R has six pulses per cycle. Unlike the single-phase, full-wave bridge of Fig. 10.15a, the resistor voltage does not go to zero. Rather, the three-phase diode bridge produces an output voltage equal to the instantaneous maximum of the absolute value of the three line-to-line voltages. The dc average of this voltage (which can

be obtained by integrating over 1/6 of a cycle) is given by

$$V_{dc} = \frac{3\omega}{\pi}\int_0^{\frac{\pi}{3\omega}} -v_{bc}(t)\,dt$$

$$= -\frac{3\omega}{\pi}\int_0^{\frac{\pi}{3\omega}} \sqrt{2}V_{l-l,rms}\sin\left(\omega t - \frac{2\pi}{3}\right)dt$$

$$= \left(\frac{3\sqrt{2}}{\pi}\right)V_{l-l,rms} \qquad (10.19)$$

where $V_{l-l,rms}$ is the rms value of the line-to-line voltage.

Table 10.1 shows the diode-switching sequence for the three-phase bridge of Fig. 10.36a corresponding to a single period of the three-phase voltage of waveforms of Fig. 10.36b. Note that only two diodes are on at any given time and that each diode is on for 1/3 of a cycle (120°).

Analogous to the single-phase, full-wave, phase-controlled SCR bridge of Figs. 10.31 and 10.35, Fig. 10.37 shows a three-phase, phase-controlled SCR bridge. Assuming continuous load current, corresponding for example to the condition $\omega L \gg R$, in which case the load current will be essentially a constant dc current I_{dc}, this bridge is capable of applying a negative voltage to the load and of regenerating power in a fashion directly analogous to the single-phase, full-wave, phase-controlled SCR bridge which we discussed in Section 10.2.4.

Table 10.1 Diode conduction times for the three-phase diode bridge of Fig. 10.36a.

α_d	0–π/3	π/3–2π/3	2π/3–π	π–4π/3	4π/3–5π/3	5π/3–2π
D1	OFF	ON	ON	OFF	OFF	OFF
D2	OFF	OFF	OFF	ON	ON	OFF
D3	ON	OFF	OFF	OFF	OFF	ON
D4	OFF	OFF	OFF	OFF	ON	ON
D5	ON	ON	OFF	OFF	OFF	OFF
D6	OFF	OFF	ON	ON	OFF	OFF

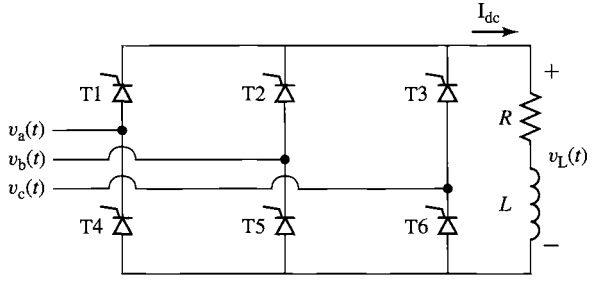

Figure 10.37 Three-phase, phase-controlled SCR bridge circuit with an inductive load.

It is a relatively straightforward matter to show that maximum output voltage of this bridge configuration will occur when the SCRs are turned ON at the times when the diodes in a diode bridge would naturally turn ON. These times can be found from Table 10.1. For example, we see that SCR T5 must be turned ON at angle $\alpha_d = 0$ (i.e., at the positive zero crossing of $v_{ab}(t)$). Similarly, SCR T1 must be turned ON at time $\alpha_d = \pi/3$, and so on.

Thus, one possible scheme for generating the SCR gate pulses is to use the positive-going zero crossing of $v_{ab}(t)$ as a reference from which to synchronize a pulse train running at six times the fundamental frequency (i.e., there will be six uniformly-spaced pulses in each cycle of the applied voltage). SCR T5 would be fired first, followed by SCRs T1, T6, T2, T4, and T3 in that order, each separated by 60° in phase delay.

If the firing pulses are timed to begin immediately following the zero crossing of $v_{ab}(t)$ the load voltage waveform $v_L(t)$ will be that of Fig. 10.36b. If the firing pulses are delayed by an angle α_d, then the load-voltage waveforms will appear as in Fig. 10.38a (for $\alpha_d = 0.1\pi$) and Fig. 10.38b (for $\alpha_d = 0.9\pi$).

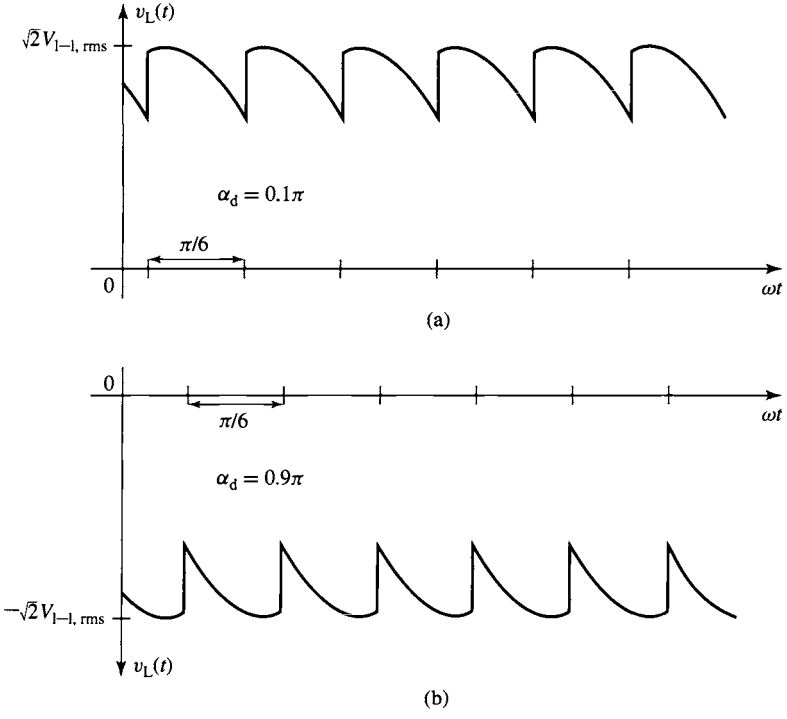

Figure 10.38 Typical load voltages for delayed firing of the SCRs in the three-phase, phase-controlled rectifier of Fig. 10.37; (a) $\alpha_d = 0.1\pi$, (b) $\alpha_d = 0.9\pi$.

The dc average of the output voltage of the phase-controlled bridge can be found as

$$V_{dc} = \frac{3\omega}{\pi} \int_{\frac{\alpha_d}{\omega}}^{\frac{\alpha_d+\pi/3}{\omega}} -v_{bc}(t)\,dt$$

$$= -\frac{3\omega}{\pi} \int_{\frac{\alpha_d}{\omega}}^{\frac{\alpha_d+\pi/3}{\omega}} \sqrt{2}\,V_{l-l,rms} \sin\left(\omega t - \frac{2\pi}{3}\right) dt$$

$$= \left(\frac{3\sqrt{2}}{\pi}\right) V_{l-l,rms} \cos\alpha_d \quad (0 \le \alpha_d \le \pi) \tag{10.20}$$

where $V_{l-l,rms}$ is the rms value of the line-to-line voltage.

EXAMPLE 10.9

A large magnet with an inductance of 14.7 H and resistance of 68 Ω is to be supplied from a 60-Hz, 460-V, three-phase source through a phase-controlled SCR bridge as in Fig. 10.37. Calculate (*a*) the maximum dc voltage $V_{dc,max}$ and current $I_{dc,max}$ which can be supplied from this source and (*b*) the delay angle α_d required to achieve a magnet current of 2.5 A.

■ Solution

a. From Eq. 10.20, the maximum voltage (corresponding to $\alpha_d = 0$) is equal to

$$V_{dc,max} = \left(\frac{3\sqrt{2}}{\pi}\right) V_{l-l,rms} = \left(\frac{3\sqrt{2}}{\pi}\right) 460 = 621 \text{ V}$$

and $I_{dc,max} = V_{dc,max}/R = 9.1$ A

b. The delay angle for a current of 2.5 A, corresponding to $V_{dc} = I_{dc}R = 170$ V, can be found from inverting Eq. 10.20 as

$$\alpha_d = \cos^{-1}\left[\left(\frac{\pi}{3\sqrt{3}}\right)\left(\frac{V_{dc}}{V_{l-l,rms}}\right)\right] = 1.29 \text{ rad} = 74.1°$$

Practice Problem 10.8

Repeat Example 10.9 for the case in which the 60-Hz source is replaced by a 50-Hz, 400-V, three-phase source.

Solution

a. $V_{dc,max} = 540$ V, $I_{dc,max} = 7.94$ V
b. $\alpha_d = 1.25$ rad $= 71.6°$

The derivations for three-phase bridges presented here have ignored issues such as the effect of commutating inductance, which we considered during our examination of single-phase rectifiers. Although the limited scope of our presentation does not

permit us to specifically discuss them here, the effects in three-phase rectifiers are similar to those for single-phase systems and must be considered in the design and analysis of practical three-phase rectifier systems.

10.3 INVERSION: CONVERSION OF DC TO AC

In Section 10.2 we discussed various rectifier configurations that can be used to convert ac to dc. In this section, we will discuss some circuit configurations, referred to as *inverters,* which can be used to convert dc to the variable-frequency, variable-voltage power required for many motor-drive applications. Many such configurations and techniques are available, and we will not attempt to discuss them all. Rather, consistent with the aims of this chapter, we will review some of the common inverter configurations and highlight their basic features and characteristics.

For the purposes of this discussion, we will assume the inverter is preceded by a "stiff" dc source. For example, in Section 10.2, we saw how an LC filter can be used to produce a relatively constant dc output voltage from a rectifier. Thus, as shown in Fig. 10.39a, for our study of inverters we will represent such rectifier systems by a constant dc voltage source V_0, known as the *dc bus voltage* at the inverter input. We will refer to such a system, with a constant-dc input voltage, as a *voltage-source inverter.*

Similarly, we saw that a "large" inductor in series with the rectifier output produces a relatively constant dc current, known as the *dc link current.* We will therefore

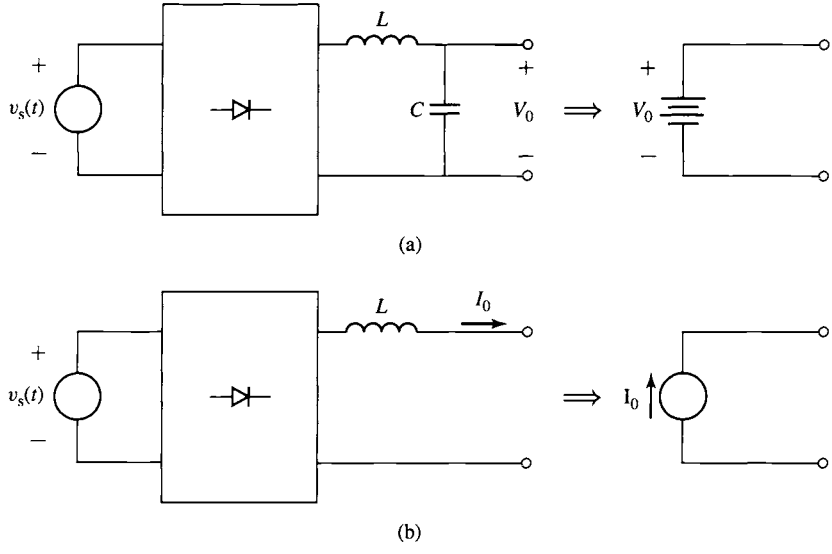

Figure 10.39 Inverter-input representations. (a) Voltage source. (b) Current source.

represent such a rectifier system by a current source I_0 at the inverter input. We will refer to this type of inverter as a *current-source inverter.*

Note that, as we have seen in Section 10.2, the values of these dc sources can be varied by appropriate controls applied to the rectifier stage, such as the timing of gate pulses to SCRs in the rectifier bridge. Control of the magnitude of these sources in conjunction with controls applied to the inverter stage provides the flexibility required to produce a wide variety of output waveforms for various motor-drive applications.

10.3.1 Single-Phase, H-bridge Step-Waveform Inverters

Figure 10.40a shows a single-phase inverter configuration in which a load (consisting here of a series RL combination) is fed from a dc voltage source V_0 through a set of four IGBTs in what is referred to as an *H-bridge* configuration. MOSFETs or other switching devices are equally applicable to this configuration. As we discussed in Section 10.1.3, the IGBTs in this system are used simply as switches. Because the IGBTs in this H-bridge include protection diodes, we can analyze the performance of this circuit by replacing the IGBTs by the ideal-switch model of Fig. 10.13b as shown in Fig. 10.40b.

For our analysis of this inverter, we will assume that the switching times of this inverter (i.e., the length of time the switches remain in a constant state) are much longer than the load time constant L/R. Hence, on the time scale of interest, the load current will simply be equal to V_L/R, with V_L being determined by the state of the switches.

Let us begin our investigation of this inverter configuration assuming that switches S1 and S3 are ON and that i_L is positive, as shown in Fig. 10.41a. Under this condition the load voltage is equal to V_0 and the load current is thus equal to V_0/R.

Let us next assume that switch S1 is turned OFF, while S3 remains ON. This will cause the load current, which cannot change instantaneously due to the presence of the inductor, to commutate from switch S1 to diode D2, as shown in Fig. 10.41b. Note that under this condition, the load voltage is zero and hence there will be zero load current. Note also that this same condition could have been reached by turning switch S3 OFF with S1 remaining ON.

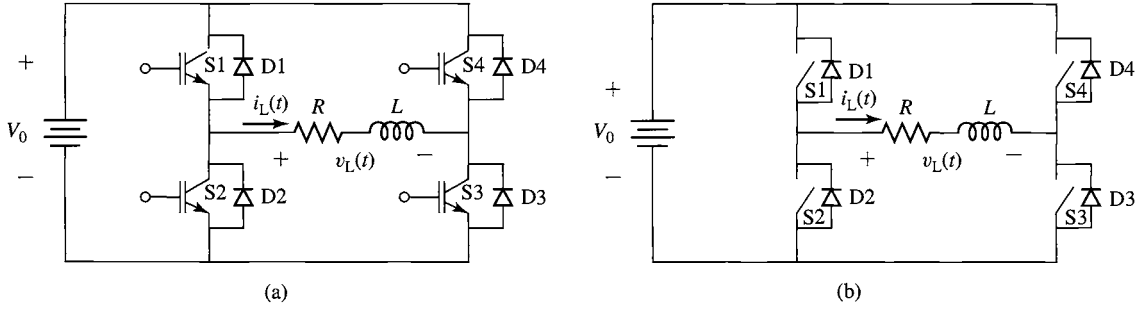

Figure 10.40 Single-phase H-bridge inverter configuration. (a) Typical configuration using IGBTs. (b) Generic configuration using ideal switches.

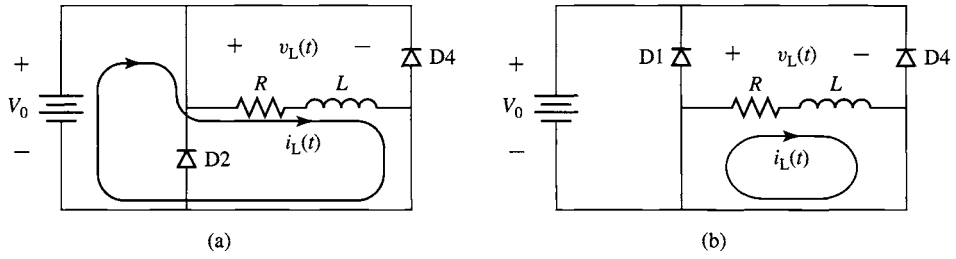

Figure 10.41 Analysis of the H-bridge inverter of Fig. 10.40b. (a) Switches S1 and S3 ON. (b) Switch S3 ON.

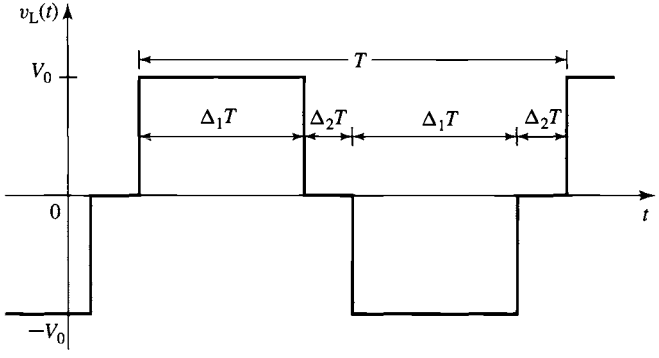

Figure 10.42 Typical output-voltage waveform for the H-bridge of Fig. 10.40.

At this point, it is possible to reverse the load voltage and current by turning ON switches S2 and S4, in which case $V_L = -V_0$ and $i_L = -V_0/R$. Finally, the current can be again brought to zero by turning OFF either switch S2 or switch S4. At this point, one cycle of an applied load-voltage waveform of the form of Fig. 10.42 has been completed.

A typical waveform produced by the switching sequence described above is shown in Fig. 10.42, with an ON time of $\Delta_1 T$ and OFF time of $\Delta_2 T$ ($\Delta_2 = 0.5 - \Delta_1$) for both the positive and negative portions of the cycle. Such a waveform consists of a fundamental ac component of frequency $f_0 = 1/T$, where T is the period of the switching sequence, and components at odd-harmonics frequencies of that fundamental.

The waveform of Fig. 10.42 can be considered a simple one-step approximation to a sinusoidal waveform. Fourier analysis can be used to show that it has a fundamental component of peak amplitude

$$V_{L,1} = \left(\frac{4}{\pi}\right) V_0 \sin(\Delta_1 \pi) \tag{10.21}$$

and n'th-harmonic components ($n = 3, 5, 7, \ldots$) of peak amplitude

$$V_{L,n} = \left(\frac{4}{n\pi}\right) V_0 \sin(n\,\Delta_1\pi) \tag{10.22}$$

Although this stepped waveform appears to be a rather crude approximation to a sinusoid, it clearly contains a significant fundamental component. In many applications it is perfectly adequate as the output voltage of a motor-drive. For example, three-such waveforms, separated by 120° in time phase, could be used to drive a three-phase motor. The fundamental components would combine to produce a rotating flux wave as discussed in Chapter 4. In some motor-drive systems, LC filters, consisting of shunt capacitors operating in conjunction with the motor phase inductances, are used to reduce the harmonic voltages applied to the motor phase windings.

In general, the higher-order harmonics, whose amplitudes vary inversely with their harmonic number, as seen from Eq. 10.22, will produce additional core loss in the stator as well as dissipation in the rotor. Provided that these additional losses are acceptable both from the point of view of motor heating as well as motor efficiency, a drive based upon this switching scheme will be quite adequate for many applications.

EXAMPLE 10.10

A three-phase, H-bridge, voltage-source, step-waveform inverter will be built from three H-bridge inverter stages of the type shown in Fig. 10.40b. Each phase will be identical, with the exception that the switching pattern of each phase will be displaced by 1/3 of a period in time phase. This system will be used to drive a three-phase, four-pole motor with $N_{ph} = 34$ turns per phase and winding factor $k_w = 0.94$. The motor is Y-connected, and the inverters are each connected phase-to-neutral.

For a dc supply voltage of 125 V, a switching period T of 20 msec and with $\Delta_1 = 0.44$, calculate (*a*) the frequency and synchronous speed in rpm of the resultant air-gap flux wave and (*b*) the rms amplitude of the line-to-line voltage applied to the motor.

■ Solution

a. The frequency f_e of the fundamental component of the drive voltage will equal $f_e = 1/T = 50$ Hz. From Eq. 4.41 this will produce an air-gap flux wave which rotates at

$$n_s = \left(\frac{120}{\text{poles}}\right) f_e = \left(\frac{120}{4}\right) 50 = 1500 \text{ r/min}$$

b. The peak of the fundamental component of the applied line-to-neutral voltage can be found from Eq. 10.21.

$$V_{a,peak} = \left(\frac{4}{\pi}\right) V_0 \sin(\Delta_1\pi) = \left(\frac{4}{\pi}\right) 125 \sin(0.44\,\pi) = 156 \text{ V}$$

The resultant rms, line-to-line voltage is thus given by

$$V_{l-l,rms} = \sqrt{\frac{3}{2}}\, V_{a,peak} = 191 \text{ V}$$

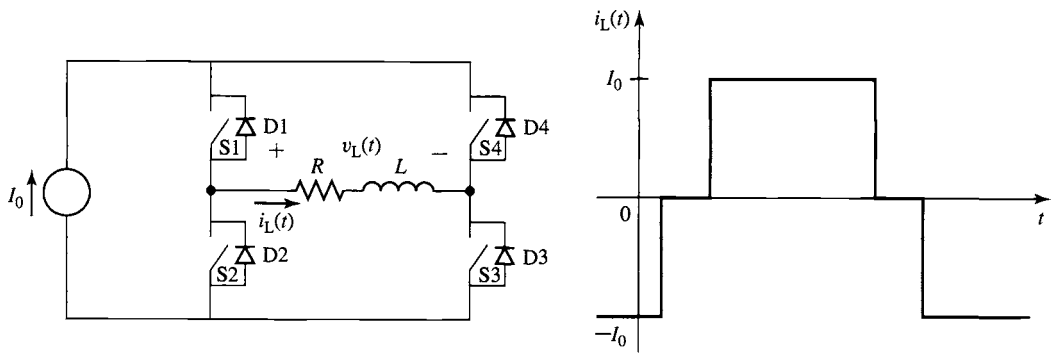

Figure 10.43 (a) H-bridge inverter configuration fed by a current source. (b) Typical stepped load-current waveform.

Practice Problem 10.9

For the three-phase inverter system of Example 10.10, (*a*) find the ON-time fraction Δ_1 for which the 5'th-harmonic component of the applied voltage will be zero. (*b*) Calculate the corresponding peak amplitude of the fundamental-component of the line-to-neutral voltage.

Solution

a. 0.2
b. 93 V

Figure 10.43a shows an H-bridge current-source inverter. This inverter configuration is analogous to the voltage-source configuration of Fig. 10.40. In fact, the discussion of the voltage-source inverter applies directly to the current-source configuration with the exception that the switches control the load current instead of the load voltage. Thus, again assuming that the load time constant (L/R) is much shorter than the switching time, a typical load current waveform would be similar to that shown in Fig. 10.43b.

EXAMPLE 10.11

Determine a switching sequence for the inverter of Fig. 10.43a that will produce the stepped waveform of Fig. 10.43b.

■ Solution

Table 10.2 shows one such switching sequence, starting at time $t = 0$ at which point the load current $i_L(t) = -I_0$.

Note that zero load current is achieved by turning on two switches so as to bypass the load and to directly short the current source. When this is done, the load current will quickly decay to zero, flowing through one of the switches and one of the reverse-polarity diodes. In general, one would not apply such a direct short across the voltage source in a voltage-source inverter

Table 10.2 Switching sequence used to produce the load current waveform of Fig. 10.43b.

$i_L(t)$	S1	S2	S3	S4
$-I_0$	OFF	ON	OFF	ON
0	ON	ON	OFF	OFF
I_0	ON	OFF	ON	OFF
0	OFF	OFF	ON	ON
$-I_0$	OFF	ON	OFF	ON

because the resultant current would most likely greatly exceed the ratings of the switches. However, in the case of a current-source inverter, the switch current cannot exceed that of the current source, and hence the direct short can be (and, in fact, must be) maintained for as long as it is desired to maintain zero load current.

EXAMPLE 10.12

Consider the current-source inverter of Fig. 10.44a. Here the load consists of a sinusoidal voltage source $V_a \cos \omega t$. Assume the inverter switches are controlled such that the load current is a square-wave, also at frequency $f = \omega/(2\pi)$, as shown in Fig. 10.44b. Calculate the time-average power delivered to the load as a function of the delay angle α_d as defined in Fig. 10.44b.

■ Solution

Because the load voltage is sinusoidal, time-average power will only be produced by the fundamental component of the load current. By analogy to Eq. 10.21, with I_0 replacing V_0 and with $\Delta_1 = 0.5$, the amplitude of the fundamental-component of the load current is

$$I_{L,1} = \left(\frac{4}{\pi}\right) I_0$$

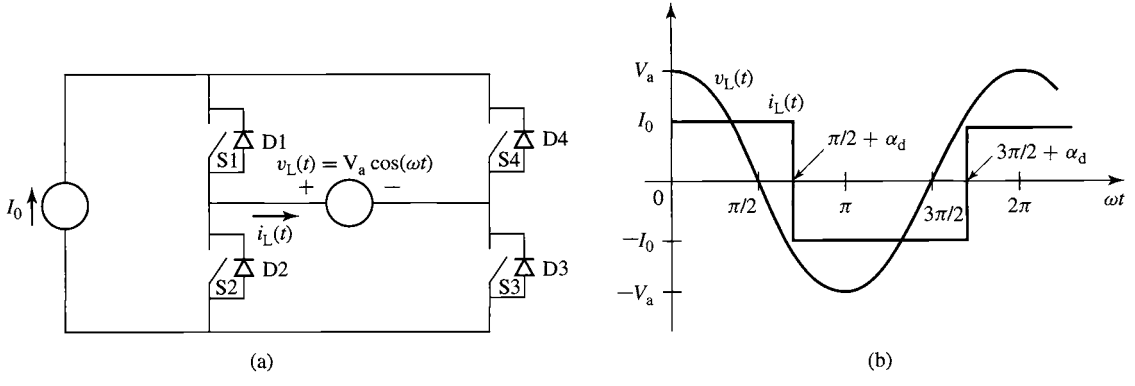

Figure 10.44 (a) Current-source inverter for Example 10.12. (b) Load-current waveform.

and therefore the fundamental component of the load current is equal to

$$i_{L,1}(t) = I_{L,1}\cos(\omega t - \alpha_d) = \left(\frac{4}{\pi}\right) I_0 \cos(\omega t - \alpha_d)$$

The complex amplitude of the load voltage is thus given by $\hat{V}_L = V_a$ and that of the load current is $\hat{I}_L = I_{L,1}e^{-j\alpha_d}$. Thus the time average power is equal to

$$P = \frac{1}{2}\text{Re}[\hat{I}_L \hat{V}_L^*] = \left(\frac{2}{\pi}\right) V_a I_0 \cos\alpha_d$$

By varying the firing-delay angle α_d, the power transferred from the source to the load can be varied. In fact, as α_d is varied over the range $0 \leq \alpha_d \leq \pi$, the power will vary over the range

$$\left(\frac{2}{\pi}\right) V_a I_0 \geq P \geq -\left(\frac{2}{\pi}\right) V_a I_0$$

Note that this inverter can regenerate; i.e., for $\pi/2 < \alpha_d \leq \pi$, $P < 0$ and hence power will flow from the load back into the inverter.

Practice Problem 10.10

The inverter of Example 10.12 is operated with a fixed delay angle $\alpha_d = 0$ but with a variable ON-time fraction Δ_1. Find an expression for the time-average power delivered to the load as a function of Δ_1.

Solution

$$P = \left(\frac{2}{\pi}\right) V_a I_0 \sin(\Delta_1 \pi)$$

10.3.2 Pulse-Width-Modulated Voltage-Source Inverters

Let us again consider the H-bridge configuration of Fig. 10.40b, repeated again in Fig. 10.45. Again, an RL load is fed from a voltage source through the H-bridge. However, in this case, let us assume that the switching time of the inverter is much shorter than the load time constant (L/R).

Consider a typical operating condition as shown in Fig. 10.46. Under this condition, the switches are operated with a period T and a *duty cycle* D $(0 \leq D \leq 1)$. As can be seen from Fig. 10.46a, for a time DT switches S1 and S3 are ON, and the load voltage is V_0. This is followed by a time $(1 - D)T$ during which switches S1 and S3 are OFF, and the current is transferred to diodes D2 and D4, setting the load voltage equal to $-V_0$. The duty cycle D is thus a fraction of the total period, in this case the fraction of the period during which the load voltage is V_0.

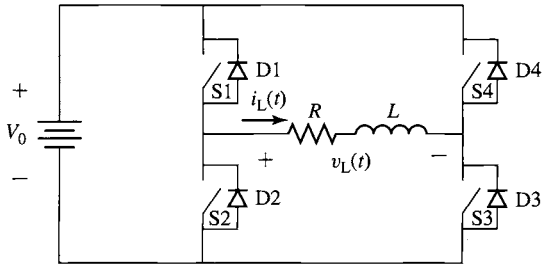

Figure 10.45 Single-phase H-bridge inverter configuration.

Note that although switches S2 and S4 would normally be turned ON after switches S1 and S3 are turned OFF (but not before they are turned OFF, to avoid a direct short across the voltage source) because they are actually semiconductor devices, they will not carry any current unless the load current goes negative. Rather, the current will flow through the protection diodes D1 and D3. Alternatively, if the load current is negative, then the current will be controlled by the operation of switches S2 and S4 in conjunction with diodes D1 and D3. Under this condition, switches S1 and S3 will not carry current.

This type of control is referred to as *pulse-width modulation,* or *PWM,* because it is implemented by varying the width of the voltage pulses applied to the load. As can be seen from Fig. 10.46a, the average voltage applied to the load is equal to

$$(v_L)_{avg} = (2D - 1)V_0 \tag{10.23}$$

As we will now show, varying the duty cycle under PWM control can produce a continuously varying load current.

A typical load-current waveform is shown in Fig. 10.46b. In the steady state, the average current through the inductor will be constant and hence voltage across the inductor must equal zero. Thus, the average load current will equal the average

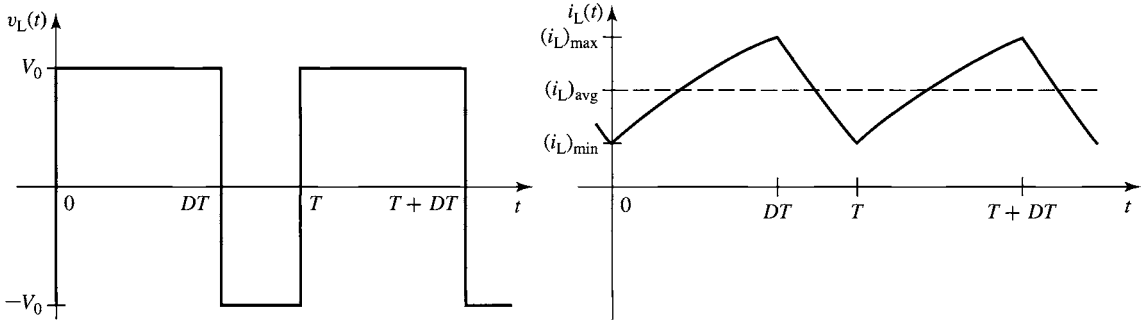

Figure 10.46 Typical (a) voltage and (b) current waveform under PWM operation.

voltage divided by the resistance or

$$(i_L)_{avg} = \frac{(v_L)_{avg}}{R} = \frac{[2D-1]V_0}{R} \tag{10.24}$$

Thus we see that by varying the duty cycle D over the range of 0 to 1, we can vary the load current over the range $-V_0/R \leq (i_L)_{avg} \leq V_0/R$.

Because the current waveform is periodic, the maximum and minimum current, and hence the current ripple, can be easily calculated. Assigning time $t = 0$ to the time switches S1 and S3 are first turned ON and the load current is minimum, the current during this time period will be given by

$$i_L(t) = \frac{V_0}{R} + \left((i_L)_{min} - \frac{V_0}{R}\right) e^{-\frac{t}{\tau}} \quad (0 \leq t \leq DT) \tag{10.25}$$

where $\tau = L/R$. The maximum load current $(i_L)_{max}$ is reached at time DT

$$(i_L)_{max} = \frac{V_0}{R} + \left((i_L)_{min} - \frac{V_0}{R}\right) e^{-\frac{DT}{\tau}} \tag{10.26}$$

After switches S1 and S3 are turned OFF, the load voltage is $-V_0$ and the current is given by

$$i_L(t) = -\frac{V_0}{R} + \left((i_L)_{max} + \frac{V_0}{R}\right) e^{-\frac{(t-DT)}{\tau}} \quad (DT < t \leq T) \tag{10.27}$$

Because the current is periodic with period T, $i_L(t)$ again will be equal to $(i_L)_{min}$ at time T. Thus

$$(i_L)_{min} = -\frac{V_0}{R} + \left((i_L)_{max} + \frac{V_0}{R}\right) e^{-\frac{(T-DT)}{\tau}} \tag{10.28}$$

Solving Eqs. 10.26 and 10.28 gives

$$(i_L)_{min} = -\left(\frac{V_0}{R}\right) \frac{\left[1 - 2e^{\frac{-T(1-D)}{\tau}} + e^{-\frac{T}{\tau}}\right]}{\left(1 - e^{-\frac{T}{\tau}}\right)} \tag{10.29}$$

and

$$(i_L)_{max} = \left(\frac{V_0}{R}\right) \frac{\left[1 - 2e^{\frac{-DT}{\tau}} + e^{-\frac{T}{\tau}}\right]}{\left(1 - e^{-\frac{T}{\tau}}\right)} \tag{10.30}$$

The current ripple Δi_L can be calculated as the difference between the maximum and minimum current.

$$\Delta i_L = (i_L)_{max} - (i_L)_{min} \tag{10.31}$$

In the limit that $T \ll \tau$, this can be written as

$$\Delta i_L \approx \left(\frac{2V_0}{R}\right)\left(\frac{T}{\tau}\right) D(1-D) \tag{10.32}$$

EXAMPLE 10.13

A PWM inverter such as that of Fig. 10.45 is operating from a dc voltage of 48 V and driving a load with $L = 320$ mH and $R = 3.7\ \Omega$. For a switching frequency of 1 kHz, calculate the average load current, the minimum and maximum current, and the current ripple for a duty cycle $D = 0.8$.

■ Solution

From Eq. 10.24, the average load current will equal

$$(i_L)_{avg} = \frac{[2D-1]V_0}{R} = \frac{0.6 \times 48}{3.7} = 7.78\ \text{A}$$

For a frequency of 1 kHz, the period $T = 1$ msec. The time constant $\tau = L/R = 86.5$ msec. $(i_L)_{min}$ and $(i_L)_{max}$ can then be found from Eqs. 10.29 and 10.30 to be $(i_L)_{min} = 7.76$ A and $(i_L)_{max} = 7.81$ A. Thus the current ripple, calculated from Eq. 10.31, is 0.05 A, which is equal to 0.6 percent of the average load current. Alternatively, using the fact that $T/\tau = 0.012 \ll 1$, the current ripple could have been calculated directly from Eq. 10.32

$$\Delta i_L = \left(\frac{2V_0}{R}\right)\left(\frac{T}{\tau}\right)D(1-D) = \left(\frac{2 \times 48}{3.7}\right)\left(\frac{1}{86.5}\right) \times 0.8 \times 0.2 = 0.05\ \text{A}$$

Practice Problem 10.11

Calculate (*a*) the average current and (*b*) the current ripple for the PWM inverter of Example 10.13 if the switching frequency is reduced to 250 Hz.

Solution

a. 7.78 A (unchanged from Example 10.13)
b. 0.19 A

Now let us consider the situation for which the duty cycle is varied with time, i.e., $D = D(t)$. If $D(t)$ varies slowly in comparison to the period T of the switching frequency, from Eq. 10.23, the average load voltage will be equal to

$$(v_L)_{avg} = [2D(t) - 1]V_0 \tag{10.33}$$

and the average load current will be

$$(i_L)_{avg} = \frac{[2D(t) - 1]V_0}{R} \tag{10.34}$$

Figure 10.47a illustrates a method for producing the variable duty cycle for this system. Here we see a saw-tooth waveform which varies between -1 and 1. Also shown is a reference waveform $W_{ref}(t)$ which is constrained to lie within the range -1 and 1. The switches will be controlled in pairs. During the time that $W_{ref}(t)$ is greater than the saw-tooth waveform, switches S1 and S3 will be ON and the load voltage will be V_0. Similarly, when $W_{ref}(t)$ is less than the saw-tooth waveform, switches S2

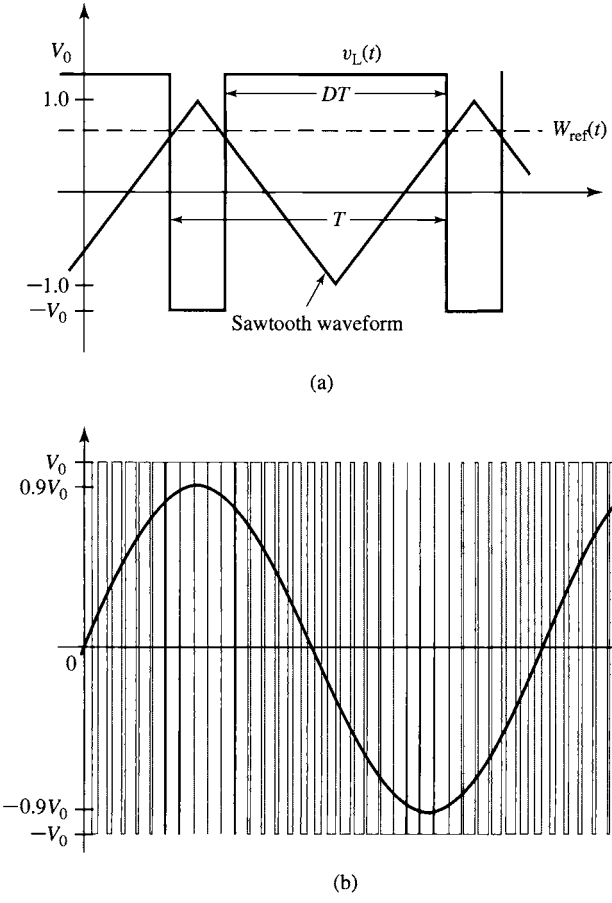

Figure 10.47 (a) Method for producing a variable duty cycle from a reference waveform $W_{ref}(t)$. (b) Load voltage and average load voltage for $W_{ref}(t) = 0.9 \sin \omega t$.

and S4 will be ON and the load voltage will be $-V_0$. Thus,

$$D(t) = \frac{(1 + W_{ref}(t))}{2} \tag{10.35}$$

and thus

$$(v_L)_{avg} = \left[2\left(\frac{1 + W_{ref}(t)}{2}\right) - 1\right] V_0 = W_{ref}(t) V_0 \tag{10.36}$$

Figure 10.47b shows the load voltage $v_L(t)$ for a sinusoidal reference waveform $W_{ref}(t) = 0.9 \sin \omega t$. The average voltage across the load, $(v_L)_{avg} = W_{ref}(t) V_0$, is also shown.

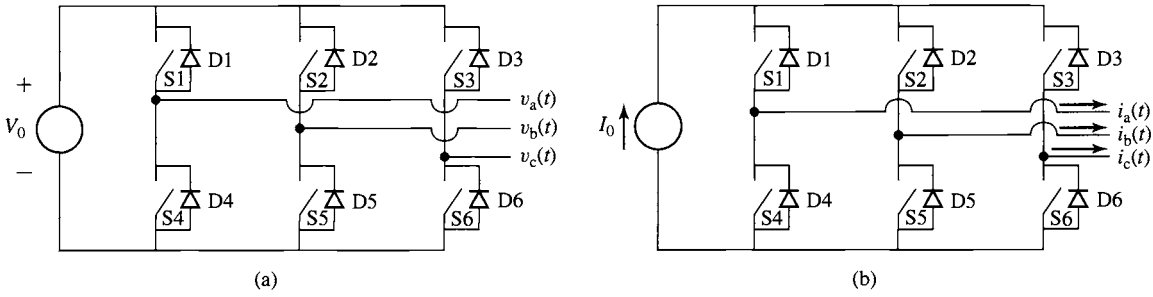

Figure 10.48 Three-phase inverter configurations. (a) Voltage-source. (b) Current-source.

Note that the H-bridge inverter configuration of Fig. 10.43 can be used to produce a PWM current-source inverter. In a fashion directly analogous to the derivation of Eq. 10.36, one can show that such an inverter would produce an average current of the form

$$(i_L)_{avg} = W_{ref}(t)I_0 \tag{10.37}$$

where I_0 is the magnitude of the dc link current feeding the H-bridge. Note, however, that the sudden current swings between I_0 and $-I_0$ associated with such an inverter will produce large voltages should the load have any inductive component. As a result, practical inverters of this type require large capacitive filters to absorb the harmonic components of the PWM current and to protect the load against damage due to voltage-induced insulation failure.

10.3.3 Three-Phase Inverters

Although the single-phase motor drives of Section 10.3.2 demonstrate the important characteristics of inverters, most variable-frequency drives are three phase. Figures 10.48a and 10.48b show the basic configuration of three-phase motor inverters (voltage- and current-source respectively). Here we have shown the switches as ideal switches, recognizing that in a practical implementation, bidirectional capability will be achieved by a combination of a semiconductor switching device, such as an IGBT and a MOSFET, and a reverse-polarity diode.

These configurations can be used to produce both stepped waveforms (either voltage-source or current-source) as well as pulse-width-modulated waveforms. This will be illustrated in the following example.

EXAMPLE 10.14

The three-phase current-source inverter configuration of Fig. 10.48b is to be used to produce a three-phase stepped current waveform of the form shown in Fig 10.49. (*a*) Determine the switch sequence over the period $0 \leq t \leq T$ and (*b*) calculate the fundamental, third, fifth, and seventh harmonics of the phase-*a* current waveform.

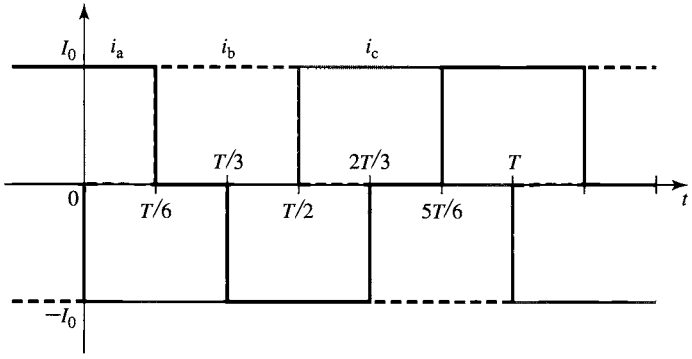

Figure 10.49 Three-phase stepped current waveform for Example 10.14.

■ Solution

a. By observing that switch S1 is ON when the phase-*a* current is positive, switch S4 is ON when it is negative, and so forth, the following table of switching operations can be produced.

t	0–($T/6$)	($T/6$)–($T/3$)	($T/3$)–($T/2$)	($T/2$)–($2T/3$)	($2T/3$)–($5T/6$)	($5T/6$)–T
S1	ON	OFF	OFF	OFF	OFF	ON
S2	OFF	ON	ON	OFF	OFF	OFF
S3	OFF	OFF	OFF	ON	ON	OFF
S4	OFF	OFF	ON	ON	OFF	OFF
S5	OFF	OFF	OFF	OFF	ON	ON
S6	ON	ON	OFF	OFF	OFF	OFF

b. The amplitudes of the harmonic components of the phase current can be determined from Eqs. 10.21 and 10.22 by setting $\Delta_1 = 1/3$. Thus,

$$I_{a,1} = \left(\frac{2\sqrt{3}}{\pi}\right) I_0 \qquad I_{a,3} = 0$$

$$I_{a,5} = -\left(\frac{2\sqrt{3}}{5\pi}\right) I_0 \qquad I_{a,7} = \left(\frac{2\sqrt{3}}{7\pi}\right) I_0$$

10.4 SUMMARY

The goal of this chapter is relatively modest. Our focus has been to introduce some basic principles of power electronics and to illustrate how they can be applied to the design of various power-conditioning circuits that are commonly found in motor drives. Although the discussion in this chapter is neither complete nor extensive, it

is intended to provide the background required to support the various discussions of motor control which are presented in this book.

We began with a brief overview of a few of the available solid-state switching devices: diodes, SCRs, IGBTs and MOSFETs, and so on. We showed that, for the purposes of a preliminary analysis, it is quite sufficient to represent these devices as ideal switches. To emphasize the fact that they typically can pass only unidirectional current, we included ideal diodes in series with these switches. The simplest of these devices is the diode, which has only two terminals and is turned ON and OFF simply by the conditions of the external circuit. The remainder have a third terminal which can be used to turn the device ON and, in the case of transistors such as MOSFETS and IGBTs, OFF again.

A typical variable-frequency, variable-voltage motor-drive system can be considered to consist of three sections. The input section rectifies the power-frequency, fixed-voltage ac input and produces a dc voltage or current. The middle section filters the rectifier output, producing a relatively constant dc current or voltage, depending upon the type of drive under consideration. The output inverter section converts the dc to variable-frequency, variable-voltage ac voltages or currents which can be applied to the terminals of a motor.

The simplest inverters we investigated produce stepped voltage or current waveforms whose amplitude is equal to that of the dc source and whose frequency can be controlled by the timing of the inverter switches. To produce a variable-amplitude output waveform, it is necessary to apply additional control to the rectifier stage to vary the amplitude of the dc bus voltage or link current supplied to the inverter.

We also discussed pulse-width-modulated voltage-source inverters. In this type of inverter, the voltage to the load is switched between V_0 and $-V_0$ such that the average load voltage is determined by the duty cycle of the switching waveform. Loads whose time constant is long compared to the switching time of the inverter will act as filters, and the load current will then be determined by the average load voltage. Pulse-width modulated current-source inverters were also discussed briefly.

The reader should approach the presentation here with great caution. It is important to recognize that a complete treatment of power electronics and motor drives is typically the topic of a multiple-course sequence of study. Although the basic principles discussed here apply to a wide range of motor drives, there are many details which must be included in the design of practical motor drives. Drive circuitry to turn ON the "switches" (gate drives for SCRs, MOSFETs, IGBTs, etc.) must be carefully designed to provide sufficient drive to fully turn on the devices and to provide the proper switching sequences. The typical inverter includes a controller and a protection system which is quite elaborate. Typically, the design of a specific drive is dominated by the current and voltage ratings of available switches devices. This is especially true in the case of high-power drive systems in which switches must be connected in series and/or parallel to achieve the desired power rating. The reader is referred to references in the bibliography for a much more complete discussion of power electronics and inverter systems than has been presented here.

Motor drives based upon the configurations discussed here can be used to control motor speed and motor torque. In the case of ac machines, the application of

power-electronic based motor drives has resulted in performance that was previously available only with dc machines and has led to widespread use of these machines in most applications.

10.5 BIBLIOGRAPHY

This chapter is intended to serve as an introduction to the discipline of power electronics. For readers who wish to study this topic in more depth, this bibliography lists a few of the many textbooks which have been written on this subject.

Bird, B. M., K. G. King, and D. A. G. Pedder, *An Introduction to Power Electronics, 2/e.* New York: John Wiley & Sons, 1993.

Dewan, S. B., and A. Straughen, *Power Semiconductor Circuits.* New York: John Wiley & Sons, 1975.

Hart, D. W., *Introduction to Power Electronics.* Englewood Cliffs, New Jersey: Prentice-Hall, 1998.

Kassakian, J. G., M. F. Schlecht, and G. C. Verghese, *Principles of Power Electronics.* Reading, Massachusetts: Addison-Wesley, 1991.

Mohan, N., T. M. Undeland, and W. P. Robbins, *Power Electronics: Converters, Applications, and Design, 3/e.* New York: John Wiley & Sons, 2002.

Rahsid, M. H., *Power Electronics: Circuits, Devices and Applications, 2/e.* Englewood Cliffs, New Jersey: Prentice-Hall, 1993.

Subrahmanyam, V., *Electric Drives: Concepts and Applications.* New York: McGraw-Hill, 1996.

Thorborg, K., *Power Electronics.* Englewood Cliffs, New Jersey: Prentice Hall International (U.K.) Ltd, 1988.

10.6 PROBLEMS

10.1 Consider the half-wave rectifier circuit of Fig. 10.3a. The circuit is driven by a triangular voltage source $v_s(t)$ of amplitude $V_0 = 9$ V as shown in Fig. 10.50. Assuming the diode to be ideal and for a resistor $R = 1.5$ kΩ:

a. Plot the resistor voltage $v_R(t)$.

b. Calculate the rms value of the resistor voltage.

c. Calculate the time-averaged power dissipation in the resistor.

10.2 Repeat Problem 10.1 assuming the diode to have a fixed 0.6 V voltage drop when it is ON but to be otherwise ideal. In addition, calculate the time-averaged power dissipation in the diode.

10.3 Consider the half-wave SCR rectifier circuit of Fig. 10.6 supplied from the triangular voltage source of Fig. 10.50. Assuming the SCR to be ideal, calculate the rms resistor voltage as a function of the firing-delay time t_d $(0 \leq t_d \leq T/2)$.

10.4 Consider the rectifier system of Example 10.5. Write a MATLAB script to plot the ripple voltage as a function of filter capacitance as the filter

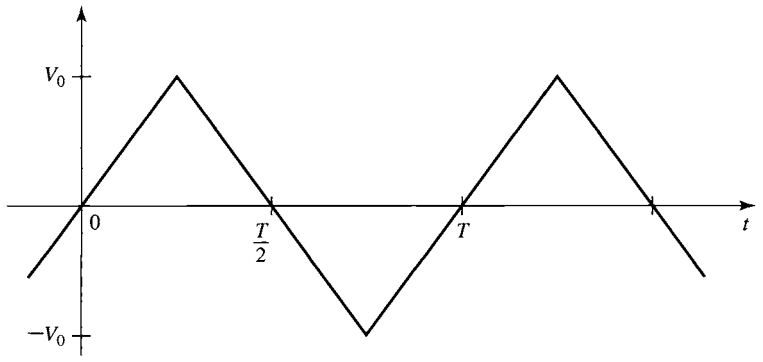

Figure 10.50 Triangular voltage waveform.

capacitance is varied over the range 3000 μF $\leq C \leq 10^5$ μF. Assume the diode to be ideal. Use a log-scale for the capacitance.

10.5 Consider the full-wave rectifier system of Fig. 10.16 with $R = 500\ \Omega$ and $C = 200\ \mu$F. Assume each diode to have a constant voltage drop of 0.7 V when it is ON but to be otherwise ideal. For a 220 V rms, 50 Hz sinusoidal source, write a MATLAB script to calculate

a. the peak voltage across the load resistor.

b. the magnitude of the ripple voltage.

c. the time-averaged power supplied to the load resistor.

d. the time-averaged power dissipation in the diode bridge.

10.6 Consider the half-wave rectifier system of Fig. 10.51. The voltage source is $v_s(t) = V_0 \sin \omega t$ where $V_0 = 15$ V, and the frequency is 100 Hz. For $L = 1$ mH and $R = 1\ \Omega$, plot the inductor current $i_L(t)$ for the first 1-1/2 cycles of the applied waveform assuming the switch closes at time $t = 0$.

10.7 Repeat Problem 10.6, using MATLAB to plot the inductor current for the first 10 cycles following the switch closing at time $t = 0$. (Hint: This problem can be easily solved, using simple Euler integration to solve for the current.)

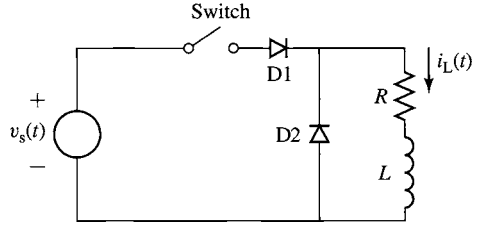

Figure 10.51 Half-wave rectifier system for Problem 10.6.

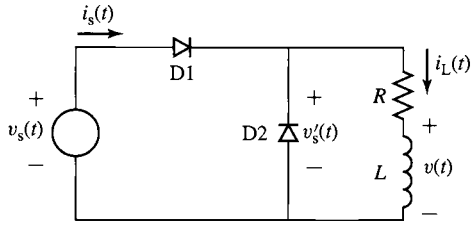

Figure 10.52 Half-wave rectifier system for Problem 10.8.

10.8 Consider the half-wave rectifier system of Fig. 10.52 as L becomes sufficiently large such that $\omega(L/R) \gg 1$, where ω is the supply frequency. In this case, the inductor current will be essentially constant. For $R = 5\ \Omega$ and $v_s(t) = V_0 \sin \omega t$ where $V_0 = 45$ V and $\omega = 100\pi$ rad/sec. Assume the diodes to be ideal.

a. Calculate the average (dc) value V_{dc} of the voltage $v_s'(t)$ across the series resistor/inductor combination.

b. Using the fact that, in the steady state, there will be zero average voltage across the inductor, calculate the dc inductor current I_{dc}.

c. Plot the instantaneous inductor voltage $v(t)$ over one cycle of the supply voltage.

d. Plot the instantaneous source current $i_s(t)$.

10.9 Consider the half-wave, phase-controlled rectifier system of Fig. 10.53. This is essentially the same circuit as that of Problem 10.8 with the exception that diode D1 of Fig. 10.52 has been replaced by an SCR, which you can consider to be ideal. Let $R = 5\ \Omega$ and $v_s(t) = V_0 \sin \omega t$, where $V_0 = 45$ V and $\omega = 100\pi$ rad/sec. Assume that the inductor L is sufficiently large such that $\omega(L/R) \gg 1$ and that the SCR is triggered ON at time t_d $(0 \leq t_d \leq \pi/\omega)$.

a. Find an expression for the average (dc) value V_{dc} of the voltage $v_s'(t)$ across the series resistor/inductor combination as a function of the delay time t_d.

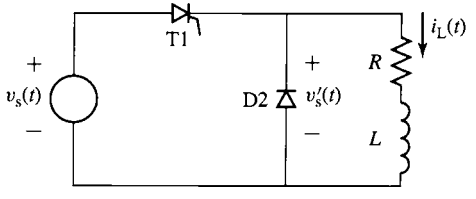

Figure 10.53 Half-wave, phase-controlled rectifier system for Problem 10.9.

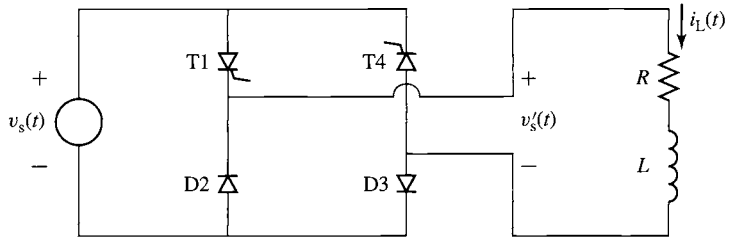

Figure 10.54 Full-wave, phase-controlled rectifier system for Problem 10.10.

b. Using the fact that, in the steady state, there will be zero average voltage across the inductor, find an expression for the dc inductor current I_{dc}, again as a function of the delay time t_d.

c. Plot I_{dc} as a function of t_d for $(0 \leq t_d \leq \pi/\omega)$.

10.10 The half-wave, phase-controlled rectifier system of Problem 10.9 and Fig. 10.53 is to be replaced by the full-wave, phase-controlled system of Fig. 10.54. SCR T1 will be triggered ON at time t_d $(0 \leq t_d \leq \pi/\omega)$, and SCR T4 will be triggered on exactly one half cycle later.

a. Find an expression for the average (dc) value V_{dc} of the voltage $v_s'(t)$ across the series resistor/inductor combination as a function of the delay time t_d.

b. Using the fact that, in the steady state, there will be zero average voltage across the inductor, find an expression for the dc inductor current I_{dc}, again as a function of the delay time t_d.

c. Plot I_{dc} as a function of t_d for $(0 \leq t_d \leq \pi/\omega)$.

d. Plot the source current $i_s(t)$ for one cycle of the source voltage for $t_d = 3$ msec.

10.11 The full-wave, phase-controlled rectifier of Fig. 10.55 is supplying a highly inductive load such that the load current can be assumed to be purely dc, as represented by the current source I_{dc} in the figure. The source voltage is a

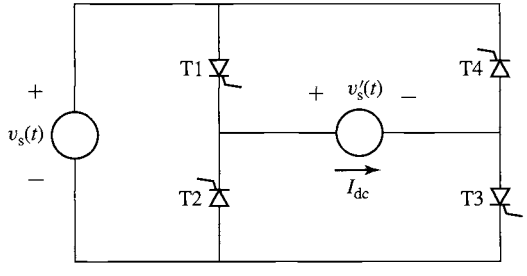

Figure 10.55 Full-wave, phase-controlled rectifier for Problem 10.11.

sinusoid, $v_s(t) = V_0 \sin \omega t$. As shown in Fig. 10.31, SCRs T1 and T3 are triggered together at delay angle α_d ($0 \leq \alpha_d \leq \pi$), and SCRs T2 and T4 are triggered exactly one-half cycle later.

a. For $\alpha_d = \pi/4$:
   (i) Sketch the load voltage $v_s'(t)$.
   (ii) Calculate the average (dc) value V_{dc} of $v_s'(t)$.
   (iii) Calculate the time-averaged power supplied to the load.

b. Repeat part (a) for $\alpha_d = 3\pi/4$.

10.12 A full-wave diode rectifier is fed from a 50-Hz, 220-V rms source whose series inductance is 12 mH. It drives a load with a resistance 8.4 Ω which is sufficiently inductive that the load current can be considered to be essentially dc.

a. Calculate the dc load current I_{dc} and the commutation time t_c.

b. Compare the dc current of part (a) with the dc current which would result if the commutating inductance could be eliminated from the system.

10.13 A 1-kW, 85-V, permanent-magnet dc motor is to be driven from a full-wave, phase-controlled bridge such as is shown in Fig. 10.56. When operating at its rated voltage, the dc-motor has a no-load speed of 1725 r/min and an armature resistance $R_a = 0.82\ \Omega$. A large inductor ($L = 580$ mH) with resistance $R_L = 0.39\ \Omega$ has been inserted in series with the output of the rectifier bridge to reduce the ripple current applied to the motor. The source voltage is a 115-V rms, 60-Hz sinusoid.

With the motor operating at a speed of 1650 r/min, the motor current is measured to be 7.6 A.

a. Calculate the motor input power.

b. Calculate the firing delay angle α_d of the SCR bridge.

10.14 Consider the dc-motor drive system of Problem 10.13. To limit the starting current of the dc motor to twice its rated value, a controller will be used to adjust the initial firing-delay angle of the SCR bridge. Calculate the required firing-delay angle α_d.

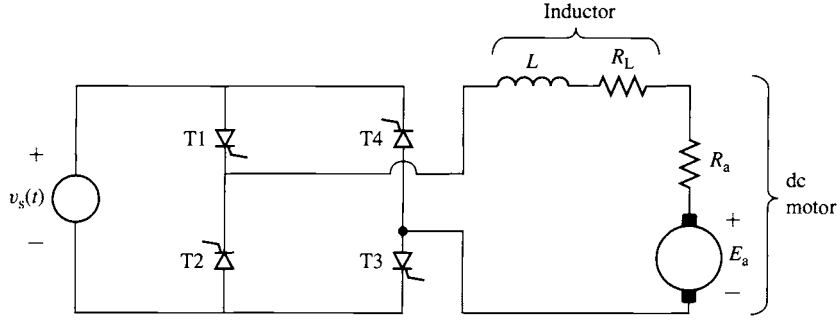

Figure 10.56 Dc motor driven from a full-wave, phase-controlled rectifier. Problem 10.13.

10.15 A three-phase diode bridge is supplied by a three-phase autotransformer such that the line-to-line input voltage to the bridge can be varied from zero to 230 V. The output of the bridge is connected to the shunt field winding of a dc motor. The resistance of this winding is 158 Ω. The autotransformer is adjusted to produce a field current of 1.75 A. Calculate the rms output voltage of the autotransformer.

10.16 A dc-motor shunt field winding of resistance 210 Ω is to be supplied from a 220-V rms, 50-Hz, three-phase source through a three-phase, phase-controlled rectifier. Calculate the delay angle α_d which will result in a field current of 1.1 A.

10.17 A superconducting magnet has an inductance of 4.9 H, a resistance of 3.6 mΩ, and a rated operating current of 80 A. It will be supplied from a 15-V rms, three-phase source through a three-phase, phase-controlled bridge. It is desired to "charge" the magnet at a constant rate to achieve rated current in 25 seconds.

a. Calculate the firing-delay angle α_d required to achieve this objective.

b. Calculate the firing-delay angle required to maintain a constant current of 80 A.

10.18 A voltage-source H-bridge inverter is used to produce the stepped waveform $v(t)$ shown in Fig. 10.57. For $V_0 = 50$ V, $T = 10$ msec and $D = 0.3$:

a. Using Fourier analysis, find the amplitude of the fundamental time-harmonic component of $v(t)$.

b. Use the MATLAB 'fft()' function to find the amplitudes of the first 10 time harmonics of $v(t)$.

10.19 Consider the stepped voltage waveform of Problem 10.18 and Fig. 10.57.

a. Using Fourier analysis, find the value of D ($0 \leq D \leq 0.5$) such that the amplitude of the third-harmonic component of the voltage waveform is zero.

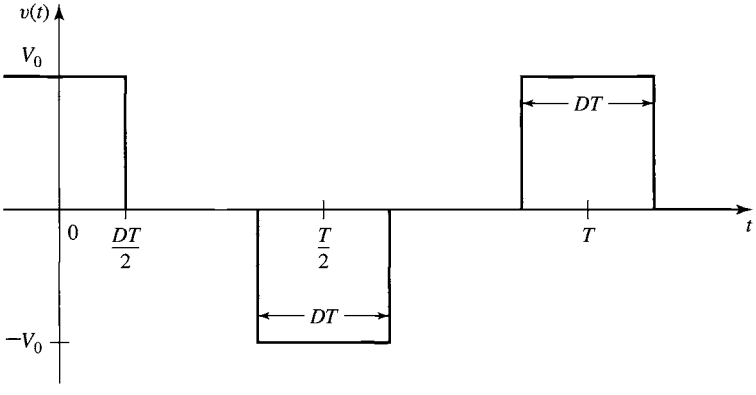

Figure 10.57 Stepped voltage waveform for Problem 10.18.

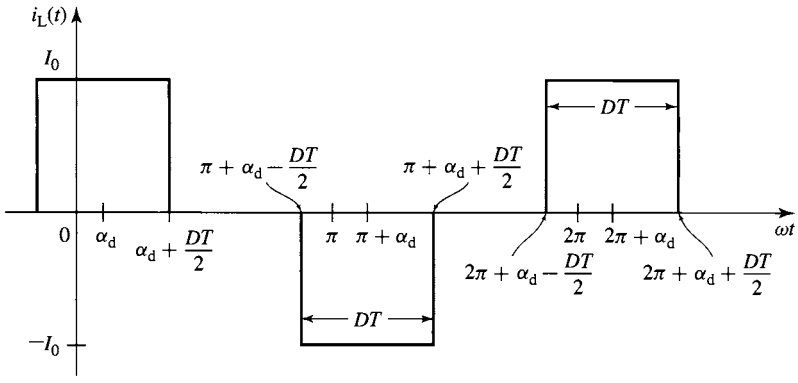

Figure 10.58 Stepped current waveform for Problem 10.20.

b. Use the MATLAB 'fft()' function to find the amplitudes of the first 10 time harmonics of the resulting waveform.

10.20 Consider Example 10.12 in which a current-source inverter is driving a load consisting of a sinusoidal voltage. The inverter is controlled to produce the stepped current waveform shown in Fig. 10.58.

a. Create a table showing the switching sequence required to produce the specified waveform and the time period during which each switch is either ON or OFF.

b. Express the fundamental component of the current waveform in the form

$$i_1(t) = I_1 \cos(\omega t + \phi_1)$$

where I_1 and ϕ_1 are functions of I_0, D and the delay angle α_d.

c. Derive an expression for the time-averaged power delivered to the voltage source $v_L(t) = V_a \cos \omega t$.

10.21 A PWM inverter such as that of Fig. 10.45 is operating from a dc voltage of 75 V and driving a load with $L = 53$ mH and $R = 1.7\ \Omega$. For a switching frequency of 1500 Hz, calculate the average load current, the minimum and maximum current, and the current ripple for a duty cycle $D = 0.7$.

CHAPTER 11

Speed and Torque Control

The objective of this chapter is to discuss various techniques for the control of electric machines. Since an in-depth discussion of this topic is both too extensive for a single chapter and beyond the scope of this book, the presentation here will necessarily be introductory in nature. We will present basic techniques for speed and torque control and will illustrate typical configurations of drive electronics that are used to implement the control algorithms. This chapter will build upon the discussion of power electronics in Chapter 10.

Note that the discussion of this chapter is limited to steady-state operation. The steady-state picture presented here is quite adequate for a wide variety of electric-machine applications. However, the reader is cautioned that system dynamics can play a critical role in some applications, with concerns ranging from speed of response to overall system stability. Although the techniques presented here form the basis for dynamic analyses, the constraints of an introductory textbook are such that a more extensive discussion, including transient and dynamic behavior, is not possible.

In the discussion of torque control for synchronous and induction machines, the techniques of field-oriented or vector control are introduced and the analogy is made with torque control in dc motors. This material is somewhat more sophisticated mathematically than the speed-control discussion and requires application of the dq0 transformations developed in Appendix C. The chapter is written such that this material can be omitted at the discretion of the instructor without detracting from the discussion of speed control.

11.1 CONTROL OF DC MOTORS

Before the widespread application of power-electronic drives to control ac machines, dc motors were by far the machines of choice in applications requiring flexibility of control. Although in recent years ac drives have become quite common, the ease of control of dc machines insure their continued use in many applications.

11.1.1 Speed Control

The three most common speed-control methods for dc motors are adjustment of the flux, usually by means of field-current control, adjustment of the resistance associated with the armature circuit, and adjustment of the armature terminal voltage.

Field-Current Control In part because it involves control at a relatively low power level (the power into the field winding is typically a small fraction of the power into the armature of a dc machine), *field-current control* is frequently used to control the speed of a dc motor with separately excited or shunt field windings. The equivalent circuit for a separately excited dc machine is found in Fig. 7.4a and is repeated in Fig. 11.1. The method is, of course, also applicable to compound motors. The shunt field current can be adjusted by means of a variable resistance in series with the shunt field. Alternatively, the field current can be supplied by power-electronic circuits which can be used to rapidly change the field current in response to a wide variety of control signals.

Figure 11.2a shows in schematic form a switching scheme for pulse-width modulation of the field voltage. This system closely resembles the pulse-width modulation system discussed in Section 10.3.2. It consists of a rectifier which rectifies the ac input voltage, a dc-link capacitor which filters the rectified voltage, producing a dc voltage V_{dc}, and a pulse-width modulator.

In this system, because only a unidirectional field current is required, the pulse-width modulator consists of a single switch and a free-wheeling diode rather than the more complex four-switch arrangement of Fig. 10.45. Assuming both the switch and diode to be ideal, the average voltage across the field winding will be equal to

$$V_f = DV_{dc} \tag{11.1}$$

where D is the duty cycle of the switching waveform; i.e., D is the fraction of time that the switch S is on.

Figure 11.2b shows the resultant field current. Because in the steady-state the average voltage across the inductor must equal zero, the average field current I_f will thus be equal to

$$I_f = \frac{V_f}{R_f} = D\left(\frac{V_{dc}}{R_f}\right) \tag{11.2}$$

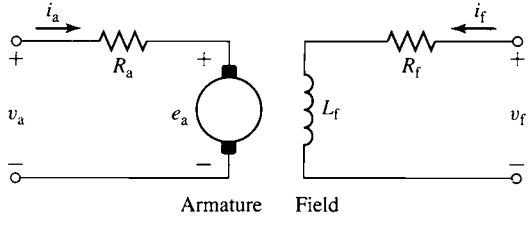

Figure 11.1 Equivalent circuit for a separately excited dc motor.

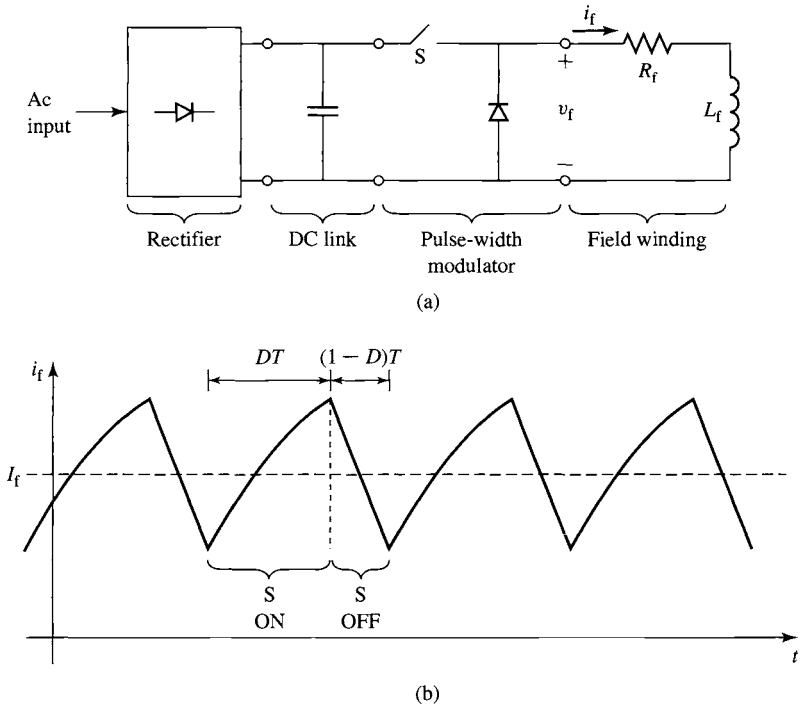

Figure 11.2 (a) Pulse-width modulation system for a dc-machine field winding. (b) Field-current waveform.

Thus, the field current can be controlled simply by controlling the duty cycle of the pulse-width modulator. If the field-winding time constant L_f/R_f is long compared to the switching time, the ripple current Δi_f will be small compared to the average current I_f.

EXAMPLE 11.1

A 25-kW, 3600 r/min, 240-V dc motor has an armature resistance of 47 mΩ and a shunt-field with a resistance of 187 Ω and an inductance of 4.2 H. Calculate (*a*) the average field current I_f and (*b*) the magnitude of the current ripple Δi_f when the field winding is supplied from a 240 V dc source by pulse-width modulation with a duty cycle $D = 0.75$ and a switching period of 1 msec.

■ Solution

a. The average field current is readily found from Eq. 11.2

$$I_f = D\left(\frac{V_{dc}}{R_f}\right) = 0.75\left(\frac{240}{187}\right) = 0.96 \text{ A}$$

b. The field time constant $\tau = L_f/R_f = 22.5$ msec is much longer that the switching period of 1 msec. Thus, the ripple current can be calculated using Eq. 10.32 as

$$\begin{aligned}\Delta i_f &= \left(\frac{2V_{dc}}{R_f}\right)\left(\frac{T}{\tau}\right) D(1-D) \\ &= \left(\frac{2 \times 240}{187}\right)\left(\frac{1}{22.5}\right) 0.75 \times (1-0.75) \\ &= 21.4 \text{ mA}\end{aligned}$$

Practice Problem 11.1

The duty-cycle D of the dc-motor controller of Example 11.1 is suddenly switched from 0.75 to 1.0. Calculate (*a*) the resultant steady-state field current and (*b*) the time constant for the change from the initial value of 1.08 A to the new final value.

Solution

a. 1.28 A
b. 22.5 msec

To examine the effect of field-current control, let us begin with the case of a dc motor driving a load of constant torque T_{load}. From Eqs. 7.9 and 7.14, the generated voltage of a dc motor can be written as

$$E_a = K_f I_f \omega_m \tag{11.3}$$

where I_f is the average field current, ω_m is the angular velocity in rad/sec, and $K_f = K_a \mathcal{P}_d N_f$ is a geometric constant which depends upon the dimensions of the motor, the properties of the magnetic material used to construct the motor, as well as the number of turns in the field winding. Note that strictly speaking, K_f is not constant since it is proportional to the direct-axis permeance, which typically varies as the flux-level in the motor increases to the point that the effects of magnetic saturation become significant.

The electromagnetic torque is given by Eq. 7.16 as

$$T_{mech} = \frac{E_a I_a}{\omega_m} = K_f I_f I_a \tag{11.4}$$

and the armature current can be seen from the equivalent circuit of Fig. 11.1 to be given by

$$I_a = \frac{(V_a - E_a)}{R_a} \tag{11.5}$$

Setting the motor torque equal to T_{load}, Eqs. 11.3 through 11.5 can be solved for ω_m

$$\omega_m = \frac{(V_a - I_a R_a)}{K_f I_f} = \frac{\left(V_a - \frac{T_{load} R_a}{K_f I_f}\right)}{K_f I_f} \tag{11.6}$$

From Eq. 11.6, recognizing that the armature resistance voltage drop $I_a R_a$ is generally quite small in comparison to the armature voltage V_a, we see that for a given load torque, the motor speed will increase with decreasing field current and decrease as the field current is increased. The lowest speed obtainable is that corresponding to maximum field current (the field current is limited by heating considerations); the highest speed is limited mechanically by the mechanical integrity of the rotor and electrically by the effects of armature reaction under weak-field conditions giving rise to poor commutation.

Armature current is typically limited by motor cooling capability. In many dc motors, cooling is aided by a shaft-driven fan whose cooling capacity is a function of motor speed. To examine in an approximate fashion the limitations on the allowable continuous motor output as the speed is changed, we will neglect the influence of changing ventilation and assume that the armature current I_a cannot exceed its rated value, in order to insure that the motor will not overheat. In addition, in our approximate argument we will neglect the effect of rotational losses (which of course also change with motor speed). Because the voltage drop across the armature resistance is relatively small, the speed voltage E_a will remain essentially constant at a value slightly below the applied armature voltage; any change in field current will be compenstated for by a change in motor speed.

Thus under constant-terminal-voltage operation with varying field current, the $E_a I_a$ product, and hence the allowable motor output power, remain substantially constant as the speed is varied. A dc motor controlled in this fashion is referred to as a *constant-power drive*. Torque, however, varies directly with field flux and therefore has its highest allowable value at the highest field current and hence lowest speed. Field-current control is thus best suited to drives requiring increased torque at low speeds. When a motor so controlled is used with a load requiring constant torque over the speed range, the rating and size of the machine are determined by the product of the torque and the highest speed. Such a drive is inherently oversized at the lower speeds, which is the principal economic factor limiting the practical speed range of large motors.

EXAMPLE 11.2

With an armature terminal voltage of 240 V and with a shunt-field current of 0.34 A, the no-load speed of the dc motor of Example 11.1 is found to be 3600 r/min. In this example, the motor is assumed to be driving a load which varies with speed as

$$P_{load} = 22.4 \left(\frac{n}{3600}\right)^3 \text{ kW}$$

where n is the motor speed in r/min. A rheostat is to be installed in series with the shunt field to vary the speed. Assuming the armature terminal voltage to remain constant at 240 V, calculate

the required resistance range if the speed is to be varied between 1800 and 3600 r/min. The effect of rotational losses can be ignored.

■ Solution

The load torque is equal to the load power divided by the motor speed ω_m expressed in rad/sec. First expressing the power in terms of ω_m

$$P_{load} = 22.4\left(\frac{\omega_m}{120\pi}\right)^3 \text{ kW}$$

The load torque is then given by

$$T_{load} = \frac{P_{load}}{\omega_m} = 22.4\left(\frac{\omega_m^2}{(120\pi)^3}\right) = 4.18 \times 10^{-4}\omega_m^2 \text{ N} \cdot \text{m}$$

Thus, at 1800 r/min, $\omega_m = 60\pi$ and $T_{load} = 14.9$ N·m. At 3600 r/min, $\omega_m = 120\pi$ and $T_{load} = 59.4$ N·m.

Before solving for I_f, we must find the value of K_f, which can be found from the no-load data. Specifically, we see that with a terminal voltage of 240-V and at a no-load speed of 3600 r/min ($\omega_m = 120\pi$), the corresponding field current is 0.34 A. Since under no-load conditions $E_a \approx V_a$, we can find K_f from Eq. 11.3 as

$$K_f = \frac{E_a}{I_f\omega_m} = \frac{240}{0.34 \times 120\pi} = 1.87 \text{ V/(A} \cdot \text{rad/sec)}$$

To find the required field current, we can solve Eq.11.6 for I_f

$$I_f = \frac{V_a}{2K_f\omega_m}\left(1 \pm \sqrt{1 - \frac{4\omega_m T_{load} R_a}{V_a^2}}\right)$$

Recognizing that R_a is small and hence that $I_f \approx V_a/(K_f\omega_m)$ we see that the positive sign should be used and thus

$$I_f = \frac{V_a}{2K_f\omega_m}\left(1 + \sqrt{1 - \frac{4\omega_m T_{load} R_a}{V_a^2}}\right)$$

Once the field current has been found, the total field resistance can be found as

$$(R_f)_{total} = \frac{V_a}{I_f} = \frac{240}{I_f}$$

and the required added rheostat resistance can be found by subtracting the resistance of the shunt-field winding (187 Ω) from $(R_f)_{total}$.

This leads to the following table:

r/min	T_{load} [N · m]	I_f [A]	$(R_f)_{total}$ [Ω]	$R_{rheostat}$ [Ω]
1800	14.9	0.678	354	167
3600	59.4	0.334	719	532

Thus, the rheostat must be able to cover the range from 166 Ω to 532 Ω.

Practice Problem 11.2

The rheostat of Example 11.2 is to be replaced by a duty cycle controller operating from the 240-V dc supply. Calculate the duty-cycle range required to achieve operation over the speed range of 1800–3600 r/min as specified in Example 11.2.

Solution

$0.26 \leq D \leq 0.53$

Armature-Circuit Resistance Control *Armature-circuit resistance control* provides a means of obtaining reduced speed by the insertion of external series resistance in the armature circuit. It can be used with series, shunt, and compound motors; for the last two types, the series resistor must be connected between the shunt field and the armature, not between the line and the motor. It is a common method of speed control for series motors and is generally analogous in action to wound-rotor-induction-motor control by the addition of external series rotor resistance.

Depending upon the value of the series armature resistance, the speed may vary significantly with load, since the speed depends on the voltage drop in this resistance and hence on the armature current demanded by the load. For example, a 1200-r/min shunt motor whose speed under load is reduced to 750 r/min by series armature resistance will return to almost 1200-r/min operation if the load is removed because the no-load current produces a voltage drop across the series resistance which is insignificant. The disadvantage of poor speed regulation may not be important in a series motor, which is used only where varying-speed service is required or can be tolerated.

A significant disadvantage of this method of speed control is that the power loss in the external resistor is large, especially when the speed is greatly reduced. In fact, for a constant-torque load, the power input to the motor plus resistor remains constant, while the power output to the load decreases in proportion to the speed. Operating costs are therefore comparatively high for lengthy operation at reduced speeds. Because of its low initial cost however, the series-resistance method (or the variation of it discussed in the next paragraph) will often be attractive economically for applications which require only short-time or intermittent speed reduction. Unlike field-current control, armature-resistance control results in a *constant-torque drive* because both the field-flux and, to a first approximation, the allowable armature current remain constant as speed changes.

A variation of this control scheme is given by the *shunted-armature method*, which may be applied to a series motor, as in Fig. 11.3a, or a shunt motor, as in Fig. 11.3b. In effect, resistors R_1 and R_2 act as a voltage divider applying a reduced voltage to the armature. Greater flexibility is possible because two resistors can now be adjusted to provide the desired performance. For series motors, the no-load speed can be adjusted to a finite, reasonable value, and the scheme is therefore applicable to the production of slow speeds at light loads. For shunt motors, the speed regulation in the low-speed range is appreciably improved because the no-load speed is definitely lower than the value with no controlling resistors.

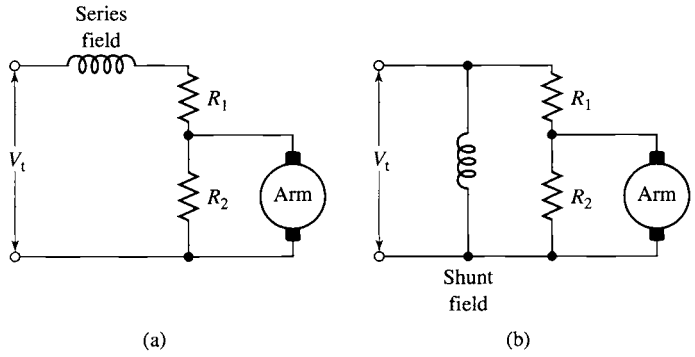

Figure 11.3 Shunted-armature method of speed control applied to (a) a series motor and (b) a shunt motor.

Armature-Terminal Voltage Control *Armature-terminal voltage control* can be readily accomplished with the use of power-electronic systems such as those discussed in Chapter 10. Figure 11.4 shows in somewhat schematic form three possible configurations. In Fig. 11.4a, a phase-controlled rectifier in combination with a dc-link filter capacitor can be used to produce a variable dc-link voltage which can be applied directly to the armature terminals of the dc motor.

In Fig. 11.4b, a constant dc-link voltage is produced by a diode rectifier in combination with a dc-link filter capacitor. The armature terminal voltage is then varied by a pulse-width modulation scheme in which switch S is alternately opened and closed. When switch S is closed, the armature voltage is equal to the dc-link voltage V_{dc}, and when the switch is opened, current transfers to the freewheeling diode, essentially setting the armature voltage to zero. Thus the average armature voltage under this condition is equal to

$$V_a = DV_{dc} \tag{11.7}$$

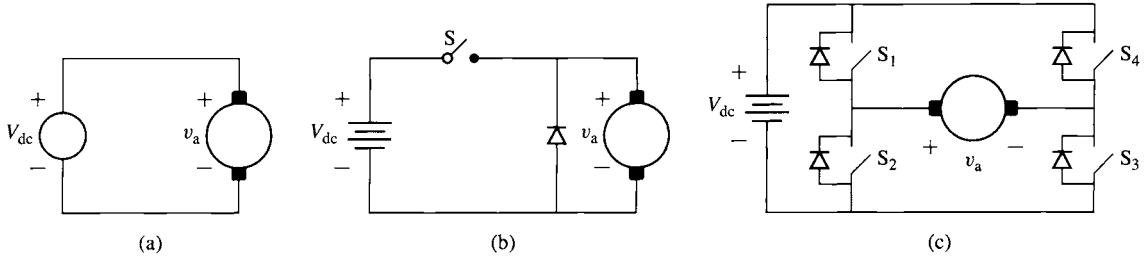

Figure 11.4 Three typical configurations for armature-voltage control. (a) Variable dc-link voltage (produced by a phase-controlled rectifier) applied directly to the dc-motor armature terminals. (b) Constant dc-link voltage with single-polarity pulse-width modulation. (c) Constant dc-link voltage with a full H-bridge.

where

V_a = average armature voltage (V)
V_{dc} = dc-link voltage (V)
D = PWM duty cycle (fraction of time that switch S is closed)

Figure 11.4c shows an H-bridge configuration as is discussed in the context of inverters in Section 10.3.3. Note that if switch S3 is held closed while switch S4 remains open, this configuration reduces to that of Fig. 11.4b. However, the H-bridge configuration is more flexible because it can produce both positive- and negative-polarity armature voltage. For example, with switches S1 and S3 closed, the armature voltage is equal to V_{dc} while with switches S2 and S4 closed, the armature voltage is equal to $-V_{dc}$. Clearly, using such an H-bridge configuration in combination with an appropriate choice of control signals to the switches allows this PWM system to achieve any desired armature voltage in the range $-V_{dc} \leq V_a \leq V_{dc}$.

Armature-voltage control takes advantage of the fact that, because the voltage drop across the armature resistance is relatively small, a change in the armature terminal voltage of a shunt motor is accompanied in the steady state by a substantially equal change in the speed voltage. With constant shunt field current and hence field flux, this change in speed voltage must be accompanied by a proportional change in motor speed. Thus, motor speed can be controlled directly by means of the armature terminal voltage.

EXAMPLE 11.3

A 500-V, 100-hp, 2500 r/min, separately excited dc motor has the following parameters:

Field resistance:	$R_f = 109\ \Omega$
Rated field voltage:	$V_{f0} = 300$ V
Armature resistance:	$R_a = 0.084\ \Omega$
Geometric constant:	$K_f = 0.694$ V/(A · rad/sec)

Assuming the field voltage to be held constant at 300 V, use MATLAB† to plot the motor speed as a function of armature voltage with the motor operating under no-load and also under rated full-load torque as the armature voltage is varied from 250 V to 500 V.

■ Solution

From Eq. 11.4

$$I_a = \frac{T_{mech}}{K_f I_f}$$

and from Eq. 11.5

$$I_a = \frac{V_a - E_a}{R_a} = \frac{V_a - K_f I_f \omega_m}{R_a}$$

† MATLAB is a registered trademark of The MathWorks, Inc.

Hence we can solve for ω_m

$$\omega_m = \frac{V_a - \left(\frac{T_{mech} R_a}{K_f I_f}\right)}{K_f I_f}$$

and the speed in r/min as

$$n = \left(\frac{30}{\pi}\right) \omega_m$$

Finally, the field current is

$$I_f = \frac{V_f}{R_f} = \frac{300}{109} = 2.75 \text{ A}$$

and the rated full-load torque is given by

$$T_{rated} = \frac{P_{rated}}{(\omega_m)_{rated}} = \frac{100 \times 746}{2500 \times \left(\frac{\pi}{30}\right)} = 285 \text{ N} \cdot \text{m}$$

Figure 11.5 is the desired plot. Notice that the speed drops approximately 63 r/min as the torque is increased from zero to full-load, independent of the armature voltage and machine speed.

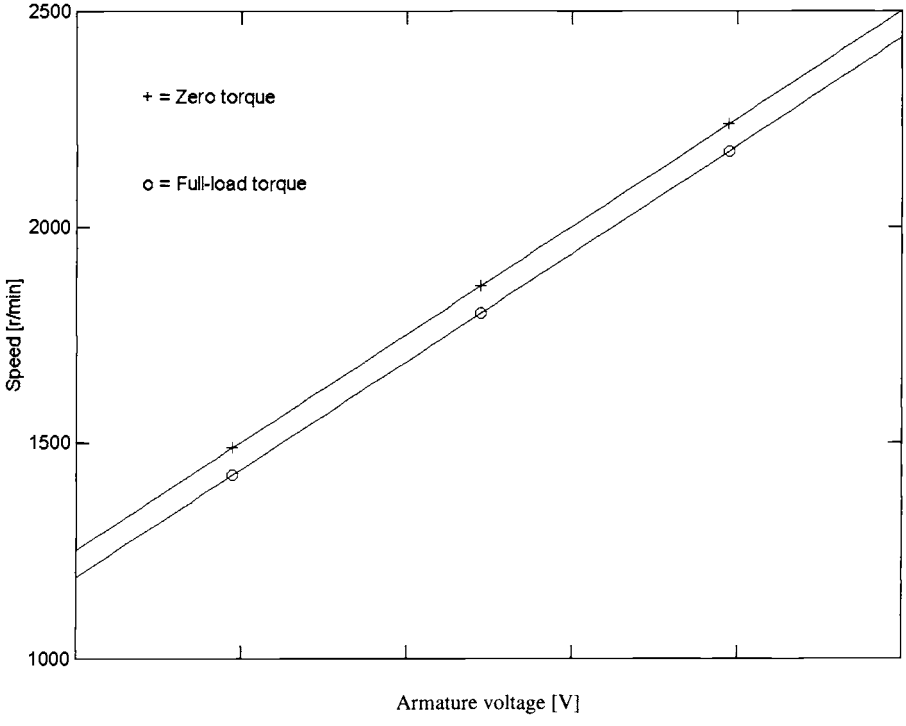

Figure 11.5 A plot of speed versus armature voltage for the dc motor of Example 11.3.

Here is the MATLAB script:

```
clc
clear

% Motor parameters
Rf = 109;
Ra = 0.084;
Kf = 0.694;

% Constant field voltage
Vf = 300;

% Resulting field current
If = Vf/Rf;

% Rated speed in rad/sec
omegarated = 2500*(pi/30);

% Rated power in Watts
Prated = 100*746;

% Rated torque in N-m
Trated = Prated/omegarated;

% Vary the armature voltage from 250 to 500 V
% and calculate speed.

for n=1:101
  Va(n) = 250 * (1 + (n-1)/100);

  % Zero torque
  T = 0;
  omega = (Va(n)- T*Ra/(Kf*If))/(Kf*If);
  NoLoadRPM(n) = omega*30/pi;

  % Full-load torque
  T = Trated;
  omega = (Va(n)- T*Ra/(Kf*If))/(Kf*If);
  FullLoadRPM(n) = omega*30/pi;
end

plot(Va,NoLoadRPM)
hold
plot(Va(20),NoLoadRPM(20),'+')
plot(Va(50),NoLoadRPM(50),'+')
plot(Va(80),NoLoadRPM(80),'+')
plot(Va,FullLoadRPM)
plot(Va(20),FullLoadRPM(20),'o')
plot(Va(50),FullLoadRPM(50),'o')
plot(Va(80),FullLoadRPM(80),'o')
hold

xlabel('Armature voltage [V]')
```

```
ylabel('Speed [r/min]')
text(270,2300,'+ = Zero torque')
text(270,2100,'o = Full-load torque')
```

Practice Problem 11.3

Calculate the change in armature voltage required to maintain the motor of Example 11.3 at a speed of 2000 r/min as the load is changed from zero to full-load torque.

Solution

12.5 V

Frequently the control of motor voltage is combined with field-current control in order to achieve the widest possible speed range. With such dual control, base speed can be defined as the normal-armature-voltage, full-field speed of the motor. Speeds above base speed are obtained by reducing the field current; speeds below base speed are obtained by armature-voltage control. As discussed in connection with field-current control, the range above base speed is that of a constant-power drive. The range below base speed is that of a constant-torque drive because, as in armature-resistance control, the flux and the allowable armature current remain approximately constant. The overall output limitations are therefore as shown in Fig. 11.6a for approximate allowable torque and in Fig. 11.6b for approximate allowable power. The constant-torque characteristic is well suited to many applications in the machine-tool industry, where many loads consist largely of overcoming the friction of moving parts and hence have essentially constant torque requirements.

The speed regulation and the limitations on the speed range above base speed are those already presented with reference to field-current control; the maximum speed thus does not ordinarily exceed four times base speed and preferably not twice base speed. For conventional machines, the lower limit for reliable and stable operation is

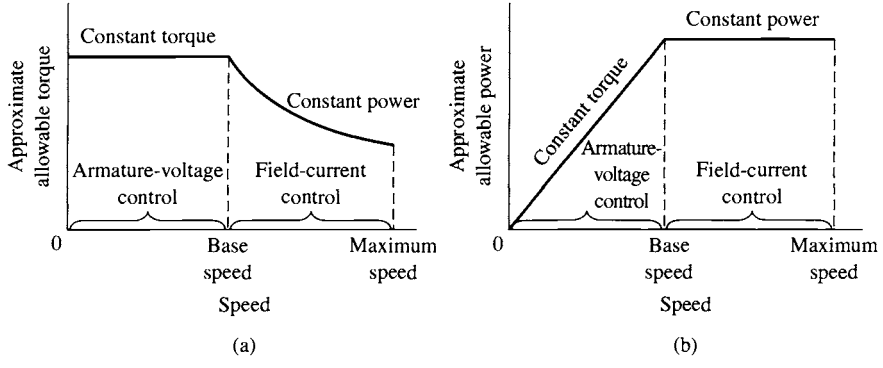

Figure 11.6 (a) Torque and (b) power limitations of combined armature-voltage and field-current methods of speed control.

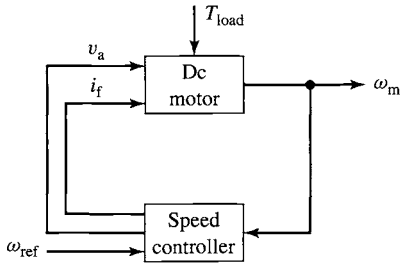

Figure 11.7 Block diagram for a speed-control system for a separately excited or shunt-connected dc motor.

about one-tenth of base speed, corresponding to a total maximum-to-minimum range not exceeding 40:1.

With armature reaction ignored, the decrease in speed from no-load to full-load torque is caused entirely by the full-load armature-resistance voltage drop in the dc generator and motor. This full-load armature-resistance voltage drop is constant over the voltage-control range, since full-load torque and hence full-load current are usually regarded as constant in that range. When measured in r/min, therefore, the speed decrease from no-load to full-load torque is a constant, independent of the no-load speed, as we saw in Example 11.3. The torque-speed curves accordingly are closely approximated by a series of parallel straight lines for the various motor-field adjustments. Note that a speed decrease of, say, 40 r/min from a no-load speed of 1200 r/min is often of little importance; a decrease of 40 r/min from a no-load speed of 120 r/min, however, may at times be of critical importance and require corrective steps in the layout of the system.

Figure 11.7 shows a block diagram of a feedback-control system that can be used to regulate the speed of a separately excited or shunt-connected dc motor. The inputs to the dc-motor block include the armature voltage and the field current as well as the load torque T_{load}. The resultant motor speed ω_m is fed back to a controller block which represents both the control logic and power electronics and which controls the armature voltage and field current applied to the dc motor, based upon a reference speed signal ω_{ref}. Depending upon the design of the controller, with such a scheme it is possible to control the steady-state motor speed to a high degree of accuracy independent of the variations in the load torque.

EXAMPLE 11.4

Figure 11.8 shows the block diagram for a simple speed control system to be applied to the dc motor of Example 11.3. In this controller, the field voltage is held constant (not shown) at its rated value of 300 V. Thus, the control is applied only to the armature voltage and takes the form

$$V_a = V_{a0} + G(\omega_{ref} - \omega_m)$$

where V_{a0} is the armature voltage when $\omega_m = \omega_{ref}$ and G is a multiplicative constant.

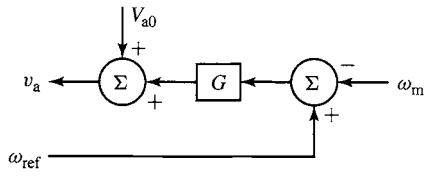

Figure 11.8 Simple dc-motor speed controller for Example 11.4.

With the reference speed set to 2000 r/min ($\omega_{ref} = 2000 \times \pi/30$), calculate V_{a0} and G so that the motor speed is 2000 r/min at no load and drops only by 25 r/min when the torque is increased to its rated full-load value.

■ Solution

As was found in Example 11.3, the field current under this condition will be 2.75 A. At no load, 2000 r/min,

$$V_a \approx E_a = K_f I_f \omega_m = 0.694 \times 2.75 \times 2000 \left(\frac{\pi}{30}\right) = 400 \text{ V}$$

and thus $V_{a0} = 400$ V.

The full load torque was found in Example 11.3 to be $T_{rated} = 285$ N·m and thus the armature current required to achieve rated full-load torque can be found from Eq. 11.4

$$I_a = \frac{T_{rated}}{K_f I_f} = \frac{285}{0.694 \times 2.75} = 149 \text{ A}$$

At a speed of 1975 r/min, E_a will be given by

$$E_a = K_f I_f \omega_m = 0.694 \times 2.75 \times 1975 \left(\frac{\pi}{30}\right) = 395 \text{ V}$$

and thus

$$V_a = E_a + I_a R_a = 395 + 149 \times 0.084 = 408 \text{ V}$$

Solving for G gives

$$G = \frac{V_a - V_{a0}}{\omega_{ref} - \omega_m} = \frac{408 - 400}{(2000 - 1975)\left(\frac{\pi}{30}\right)} = 3.06 \text{ V} \cdot \text{sec/rad}$$

Practice Problem 11.4

If the load torque in Example 11.4 is equal to half of the rated full-load torque, calculate (*a*) the speed of the motor and (*b*) the corresponding load power.

Solution

a. 1988 r/min
b. 29.6 kW

In the case of permanent-magnet dc motors, the field flux is, of course, fixed by the permanent magnet (with the possible exception of any effects of temperature changes on the magnet properties as the motor heats up). From Eqs. 11.3 and 11.4, we see that the voltage generated voltage can be written in the form

$$E_a = K_m \omega_m \tag{11.8}$$

and that the electromagnetic torque can be written as

$$T_{mech} = K_m I_a \tag{11.9}$$

Comparison of Eqs. 11.8 and 11.9 with Eqs. 11.3 and 11.4 show that the analysis of a permanent-magnet dc motor is identical to that of a shunt or separately excited dc motor with the exception that the torque-constant K_m must be substituted for the term $K_f I_f$.

EXAMPLE 11.5

The permanent-magnet dc motor of Example 7.9 has an armature resistance of 1.03 Ω and a torque constant $K_m = 0.22$ V/(rad/sec). Assume the motor to be driving a constant power load of 800 W (including rotational losses), and calculate the motor speed as the armature voltage is varied from 40 to 50 V.

■ Solution

The motor power output (including rotational losses) is given by the product $E_a I_a$ and thus we can write

$$P_{load} = E_a I_a = K_m \omega_m I_a$$

Solving for ω_m gives

$$\omega_m = \frac{P_{load}}{K_m I_a}$$

The armature current can be written as

$$I_a = \frac{(V_a - E_a)}{R_a} = \frac{(V_a - K_m \omega_m)}{R_a}$$

These two equations can be combined to give an equation for ω_m of the form

$$\omega_m^2 - \left(\frac{V_a}{K_m}\right)\omega_m + \frac{P_{load} R_a}{K_m^2} = 0$$

from which we can find

$$\omega_m = \frac{V_a}{2K_m}\left[1 \pm \sqrt{1 - \frac{4P_{load} R_a}{V_a^2}}\right]$$

Recognizing that, if the voltage drop across the armature resistance is small, $V_a \approx E_a = K_m \omega_m$, we pick the positive sign and thus

$$\omega_m = \frac{V_a}{2K_m}\left[1 + \sqrt{1 - \frac{4P_{load} R_a}{V_a^2}}\right]$$

Substituting values, we find that for $V_a = 40$ V, $\omega_m = 169.2$ rad/sec (1616 r/min) and for $V_a = 50$ V, $\omega_m = 217.5$ rad/sec (2077 r/min).

Practice Problem 11.5

Calculate the speed variation (in r/min) of the permanent-magnet dc motor of Example 11.5 if the armature voltage is held constant at 50 V and the load power varies from 100 W to 500 W.

Solution

2077 r/min to 1540 r/min

11.1.2 Torque Control

As we have seen, the electromagnetic torque of a dc motor is proportional to the armature current I_a and is given by

$$T_{mech} = K_f I_f I_a \tag{11.10}$$

in the case of a separately excited or shunt motor and

$$T_{mech} = K_m I_a \tag{11.11}$$

in the case of a permanent-magnet motor.

From these equations we see that torque can be controlled directly by controlling the armature current. Fig. 11.9 shows three possible configurations. In Fig. 11.9a, a phase-controlled rectifier, in combination with a dc-link filter inductor, can be used to create a variable dc-link current which can be applied directly to the armature terminals of the dc motor.

In Fig. 11.9b, a constant dc-link current is produced by a diode rectifier. The armature terminal voltage is then varied by a pulse-width modulation scheme in which switch S is alternately opened and closed. When switch S is opened, the current I_{dc} flows into the dc-motor armature while when switch S is closed, the armature is

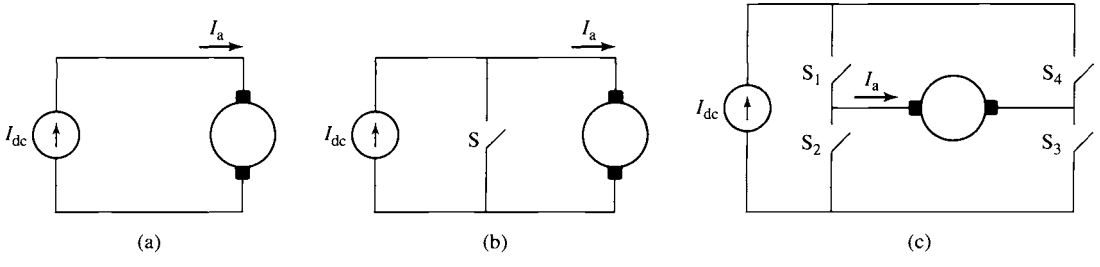

Figure 11.9 Three typical configurations for armature-current control. (a) Variable dc-link current (produced by a phase-controlled rectifier) applied directly to the dc-motor armature terminals. (b) Constant dc-link current with single-polarity pulse-width modulation. (c) Constant dc-link current with a full H-bridge.

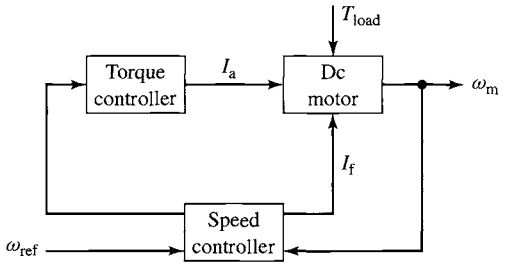

Figure 11.10 Block diagram of a dc-motor speed-control system using direct-control of motor torque.

shorted and I_a decays. Thus, the duty cycle of switch S will control the average current into the armature.

Finally, Fig 11.9c shows an H-bridge configuration as is discussed in the context of inverters in Section 10.3.2. Appropriate control of the four switches S1 through S4 allows this PWM system to achieve any desired armature average current in the range $-I_{dc} \leq I_a \leq I_{dc}$.

Note that in each of the PWM configurations of Fig. 11.9b and c, rapid changes in instantaneous current through the dc machine armature can give rise to large voltage spikes, which can damage the machine insulation as well as give rise to flashover and voltage breakdown of the commutator. In order to eliminate these effects, a practical system must include some sort of filter across the armature terminals (such as a large capacitor) to limit the voltage rise and to provide a low-impedance path for the high-frequency components of the drive current.

Figure 11.10 shows a typical configuration in which the torque control is surrounded by a speed-feedback loop. This looks similar to the speed control of Fig. 11.7. However, instead of controlling the armature voltage, in this case the output of the speed controller is a torque reference signal T_{ref} which in turn serves as the input to the torque controller. One advantage of such a system is that it automatically limits the dc-motor armature current to acceptable levels under all operating conditions, as is shown in Example 11.6.

EXAMPLE 11.6

Consider the 100-hp dc motor of Examples 11.3 and 11.4 to be driving a load whose torque varies linearly with speed such that it equals rated full-load torque (285 N·m) at a speed of 2500 r/min. We will assume the combined moment of inertia of the motor and load to equal 0.92 kg·m^2. The field voltage is to be held constant at 300 V.

a. Calculate the armature voltage and current required to achieve speeds of 2000 and 2500 r/min.
b. Assume that the motor is operated from an armature-voltage controller and that the armature voltage is suddenly switched from its 2000 r/min to its 2500 r/min value. Calculate the resultant motor speed and armature current as a function of time.

c. Assume that the motor is operated from an armature-current controller and that the armature current is suddenly switched from its 2000 r/min to its 2500 r/min value. Calculate the resultant motor speed as a function of time.

■ Solution

a. Neglecting any rotational losses, the armature current can be found from Eq. 11.4 by setting $T_{mech} = T_{load}$

$$I_a = \frac{T_{load}}{K_f I_f}$$

Substituting

$$T_{load} = \left(\frac{n}{n_f}\right) T_{fl}$$

where n is the motor speed in r/min, $n_f = 2500$ r/min and $T_{fl} = 285$ N·m gives

$$I_a = \frac{nT_{fl}}{n_f K_f I_f}$$

Solving for $V_a = E_a + I_a R_a$ then allows us to complete the following table:

r/min	ω_m [rad/sec]	V_a [V]	I_a [A]	T_{load} [N · m]
2000	209	410	119	228
2500	262	513	149	285

b. The dynamic equation governing the speed of the motor is

$$J\frac{d\omega_m}{dt} = T_{mech} - T_{load}$$

Substituting $\omega_m = (\pi/30)n$ and $\omega_r = (\pi/30)n_f$ we can write

$$T_{load} = \left(\frac{T_{fl}}{\omega_f}\right)\omega_m$$

Under armature-voltage control,

$$T_{mech} = K_f I_f I_a = K_f I_f \left(\frac{V_a - E_a}{R_a}\right)$$

$$= K_f I_f \left(\frac{V_a - K_f I_f \omega_m}{R_a}\right)$$

and thus the governing differential equation is

$$J\frac{d\omega_m}{dt} = K_f I_f \left(\frac{V_a - K_f I_f \omega_m}{R_a}\right) - \left(\frac{T_{fl}}{\omega_f}\right)\omega_m$$

or

$$\frac{d\omega_m}{dt} + \frac{1}{J}\left(\frac{T_{fl}}{\omega_f} + \frac{(K_f I_f)^2}{R_a}\right)\omega_m - \frac{K_f I_f V_a}{J R_a}$$

$$= \frac{d\omega_m}{dt} + 48.4\,\omega_m - 24.7 V_a = 0$$

From this differential equation, we see that with the motor initially at $\omega_m = \omega_i = 209$ rad/sec, if the armature voltage V_a is suddenly switched from $V_i = 413$ V to $V_f = 513$ V, the speed will rise exponentially to $\omega_m = \omega_f = 262$ rad/sec as

$$\begin{aligned}\omega_m &= \omega_f + (\omega_i - \omega_f)e^{-t/\tau} \\ &= 262 - 53e^{-t/\tau} \text{ rad/sec}\end{aligned}$$

where $\tau = 1/48.4 = 20.7$ msec. Expressed in terms of r/min

$$n = 2500 - 50e^{-t/\tau} \text{ r/min}$$

The armature current will decrease exponentially with the same 20.7 msec time constant from an initial value of $(V_f - V_i)/R_a = 1190$ A to its final value of 149 A. Thus,

$$I_a = 149 + 1041e^{-t/\tau} \text{ A}$$

Notice that it is unlikely that the supply to the dc motor can supply this large initial current (eight times the rated full-load armature current) and, in addition, the high current and corresponding high torque could potentially cause damage to the dc motor commutator, brushes, and armature winding. Hence, as a practical matter, a practical controller would undoubtedly limit the rate of change of the armature voltage to avoid such sudden steps in voltage, with the result that the speed change would not occur as rapidly as calculated here.

c. The dynamic equation governing the speed of the motor remains the same as that in part (b) as does the equation for the load torque. However, in this case, because the motor is being operated from a current controller, the electromagnetic torque will remain constant at $T_{mech} = T_f = 285$ N·m after the current is switched from its initial value of 119 A to its final value of 149 A.

Thus

$$J\frac{d\omega_m}{dt} = T_{mech} - T_{load} = T_f - \left(\frac{T_f}{\omega_f}\right)\omega_m$$

or

$$\begin{aligned}&\frac{d\omega_m}{dt} + \left(\frac{T_{fl}}{J\omega_f}\right)\omega_m - \frac{T_f}{J} \\ &= \frac{d\omega_m}{dt} + 1.18\omega_m - 310 = 0\end{aligned}$$

In this case, the speed will rise exponentially to $\omega_m = \omega_f = 262$ rad/sec as

$$\begin{aligned}\omega_m &= \omega_f + (\omega_i - \omega_f)e^{-t/\tau} \\ &= 262 - 53e^{-t/\tau} \text{ rad/sec}\end{aligned}$$

where now the time constant $\tau = 1/1.18 = 845$ msec.

Clearly, the change in motor speed under the current controller is much slower. However, at no point during this transient do either the motor current or the motor torque exceed their rated value. In addition, should faster response be desired, the armature current (and hence motor torque) could be set temporarily to a fixed value higher than the rated value (e.g., two or three times rated as compared to the factor of 8 found in part (b)), thus limiting the potential for damage to the motor.

Practice Problem 11.6

Consider the dc motor/load combination of Example 11.6 operating under current (torque) control to be operating in the steady-state at a speed of 2000 r/min at an armature current of 119 A. If the armature current is suddenly switched to 250 A, calculate the time required for the motor to reach a speed of 2500 r/min.

Solution

0.22 sec

11.2 CONTROL OF SYNCHRONOUS MOTORS

11.2.1 Speed Control

As discussed in Chapters 4 and 5, synchronous motors are essentially constant-speed machines, with their speed being determined by the frequency of the armature currents as described by Eqs. 4.40 and 4.41. Specifically, Eq. 4.40 shows that the synchronous angular velocity is proportional to the electrical frequency of the applied armature voltage and inversely proportional to the number of poles in the machine

$$\omega_s = \left(\frac{2}{\text{poles}}\right)\omega_e \tag{11.12}$$

where

ω_s = synchronous spatial angular velocity of the air-gap mmf wave [rad/sec]
$\omega_e = 2\pi f_e$ = angular frequency of the applied electrical excitation [rad/sec]
f_e = applied electrical frequency [Hz]

Clearly, the simplest means of synchronous motor control is speed control via control of the frequency of the applied armature voltage, driving the motor by a polyphase voltage-source inverter such as the three-phase inverter shown in Fig. 11.11. As is discussed in Section 10.3.3, this inverter can either be used to supply stepped ac voltage waveforms of amplitude V_{dc} or the switches can be controlled to produce pulse-width-modulated ac voltage waveforms of variable amplitude. The dc-link voltage V_{dc} can itself be varied, for example, through the use of a phase-controlled rectifier.

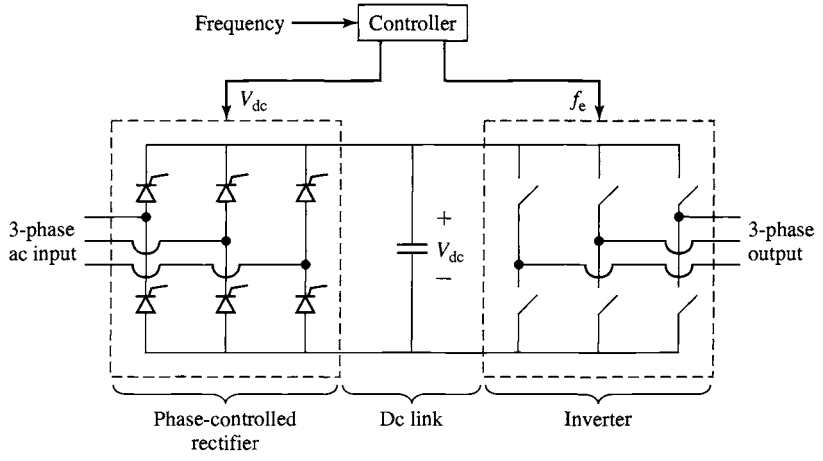

Figure 11.11 Three-phase voltage-source inverter.

The frequency of the inverter output waveforms can of course be varied by controlling the switching frequency of the inverter switches. For ac-machine applications, coupled with this frequency control must be control of the amplitude of the applied voltage, as we will now see.

From Faraday's Law, we know that the air-gap component of the armature voltage in an ac machine is proportional to the peak flux density in the machine and the electrical frequency. Thus, if we neglect the voltage drop across the armature resistance and leakage reactance, we can write

$$V_a = \left(\frac{f_e}{f_{rated}}\right)\left(\frac{B_{peak}}{B_{rated}}\right) V_{rated} \tag{11.13}$$

where V_a is the amplitude of the armature voltage, f_e is the operating frequency, and B_{peak} is the peak air-gap flux density. V_{rated}, f_{rated}, and B_{rated} are the corresponding rated-operating-point values.

Consider a situation in which the frequency of the armature voltage is varied while its amplitude is maintained at its rated value ($V_a = V_{rated}$). Under these conditions, from Eq. 11.13 we see that

$$B_{peak} = \left(\frac{f_{rated}}{f_e}\right) B_{rated} \tag{11.14}$$

Equation 11.14 clearly demonstrates the problem with constant-voltage, variable-frequency operation. Specifically, for a given armature voltage, the machine flux density is inversely proportional to frequency and thus as the frequency is reduced, the flux density will increase. Thus for a typical machine which operates in saturation at rated voltage and frequency, any reduction in frequency will further increase the flux density in the machine. In fact, a significant drop in frequency will increase

the flux density to the point of potential machine damage due both to increased core loss and to the increased machine currents required to support the higher flux density.

As a result, for frequencies less than or equal to rated frequency, it is typical to operate a machine at constant flux density. From Eq. 11.13, with $B_{peak} = B_{rated}$

$$V_a = \left(\frac{f_e}{f_{rated}}\right) V_{rated} \tag{11.15}$$

which can be rewritten as

$$\frac{V_a}{f_e} = \frac{V_{rated}}{f_{rated}} \tag{11.16}$$

From Eq. 11.16, we see that constant-flux operation can be achieved by maintaining a constant ratio of armature voltage to frequency. This is referred to as *constant-volts-per-hertz* (constant V/Hz) operation. It is typically maintained from rated frequency down to the low frequency at which the armature resistance voltage drop becomes a significant component of the applied voltage.

Similarly, we see from Eq. 11.13 that if the machine is operated at frequencies in excess of rated frequency with the voltage at its rated value, the air-gap flux density will drop below its rated value. Thus, in order to maintain the flux density at its rated value, it would be necessary to increase the terminal voltage for frequencies in excess of rated frequency. In order to avoid insulation damage, it is common to maintain the machine terminal voltage at its rated value for frequencies in excess of rated frequency.

The machine terminal current is typically limited by thermal constraints. Thus, provided the machine cooling is not affected by rotor speed, the maximum permissible terminal current will remain constant at its rated value I_{rated}, independent of the applied frequency. As a result, for frequencies below rated frequency, with V_a proportional to f_e, the maximum machine power will be proportional to $f_e V_{rated} I_{rated}$. The maximum torque under these conditions can be found by dividing the power by the rotor speed ω_s, which is also proportional to f_e as can be seen from Eq. 11.12. Thus, we see that the maximum torque is proportional to $V_{rated} I_{rated}$, and hence it is constant at its rated-operating-point value.

Similarly, for frequencies in excess of rated frequency, the maximum power will be constant and equal to $V_{rated} I_{rated}$. The corresponding maximum torque will then vary inversely with machine speed as $V_{rated} I_{rated}/\omega_s$. The maximum operating speed for this operating regime will be determined either by the maximum frequency which can be supplied by the drive electronics or by the maximum speed at which the rotor can be operated without risk of damage due to mechanical concerns such as excessive centrifugal force or to the presence of a resonance in the shaft system.

Figure 11.12 shows a plot of maximum power and maximum torque versus speed for a synchronous motor under variable-frequency operation. The operating regime below rated frequency and speed is referred to as the *constant-torque regime* and that above rated speed is referred to as the *constant-power regime*.

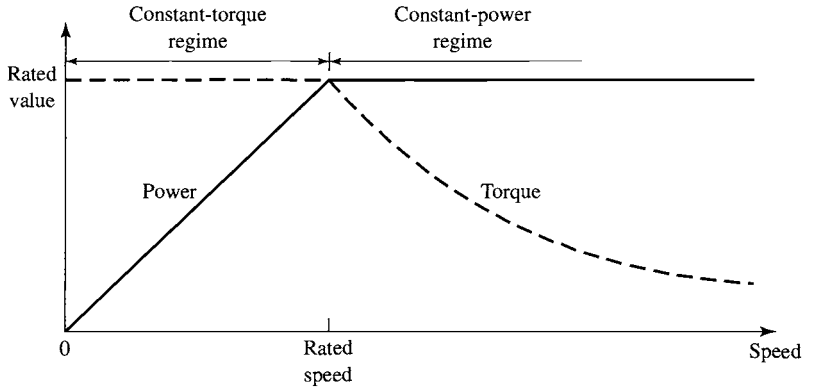

Figure 11.12 Variable-speed operating regimes for a synchronous motor.

EXAMPLE 11.7

The 45-kVA, 220-V, 60-Hz, six-pole, three-phase synchronous machine of Example 5.4 is to be operated as a motor and driven from a variable-frequency, three-phase voltage-source inverter which provides 220 V at 60 Hz and which maintains constant V/Hz as the frequency is reduced. The machine has a saturated synchronous reactance of 0.836 per unit and achieves rated open-circuit voltage at a field current of 2.84 A. For the purposes of this example, assume that the motor losses are negligible.

a. With the motor operating at 60 Hz, 220 V and at rated power, unity power factor, calculate (*i*) the motor speed in r/min and (*ii*) the motor field current.
b. If the inverter frequency is reduced to 50 Hz and the motor load adjusted to rated torque, calculate the (*i*) the resulting motor speed and (*ii*) and the motor field current required to again achieve unity power factor.

■ Solution

a. (*i*) The motor will operate at its synchronous speed which can be found from Eq. 4.41

$$n_s = \left(\frac{120}{\text{poles}}\right) f_e = \left(\frac{120}{6}\right) 60 = 1200 \text{ r/min}$$

(*ii*) As seen in Chapter 5, the field current can be determined from the generated voltage. For motor operation,

$$\hat{E}_{af} = \hat{V}_a - jX_s\hat{I}_a = 1.0 - j0.836 \times 1.0 = 1.30 \angle -39.9°$$

where V_a has been chosen as the reference phasor. Thus the field current is

$$I_f = 1.30 \times 2.84 = 3.69 \text{ A}$$

Note that we have chosen to solve for E_{af} in per unit. A solution in real units would have of course produced the same result.

b. (*i*) When the frequency is reduced from 60 Hz to 50 Hz, the motor speed will drop from 1200 r/min to 1000 r/min.

(*ii*) Let us again consider the equation for the generated voltage

$$\hat{E}_{af} = \hat{V}_a - jX_s\hat{I}_a$$

where here we will assume that the equation is written in real units.

As the inverter frequency is reduced from 60 Hz, the inverter voltage will drop proportionally since the inverter maintains constant V/Hz. Thus we can write

$$V_a = \left(\frac{\omega_m}{\omega_{m0}}\right) V_{a0}$$

where the subscript 0 is used to indicate a 60-Hz value as found in part (a). Reactance is also proportional to frequency and thus

$$X_s = \left(\frac{\omega_m}{\omega_{m0}}\right) X_{s0}$$

The generated voltage is proportional to both the motor speed (and hence the frequency) and the field current, and thus we can write

$$E_{af} = \left(\frac{\omega_m}{\omega_{m0}}\right)\left(\frac{I_f}{I_{f0}}\right) E_{af0}$$

Finally, if we recognize that, to operate at rated torque and unity power factor under this reduced frequency condition, the motor armature current will have to be equal to the value found in part (a), i.e., $I_a = I_{a0}$, we can write the generated voltage equation as

$$\left(\frac{\omega_m}{\omega_{m0}}\right)\left(\frac{I_f}{I_{f0}}\right)\hat{E}_{af0} = \left(\frac{\omega_m}{\omega_{m0}}\right)\hat{V}_{a0} - j\left(\frac{\omega_m}{\omega_{m0}}\right) X_{s0}\hat{I}_{a0}$$

or

$$\left(\frac{I_f}{I_{f0}}\right)\hat{E}_{af0} = \hat{V}_{a0} - jX_{s0}\hat{I}_{a0}$$

Since the subscripted quantities correspond to the solution of part (a), they must satisfy

$$\hat{E}_{af0} = \hat{V}_{a0} - jX_{s0}\hat{I}_{a0}$$

and thus we see that we must have $I_f = I_{f0}$. In other words, the field current for this operating condition is equal to that found in part (a), or $I_f = 3.69$ A.

Practice Problem 11.7

Consider 50-Hz operation of the synchronous motor of Example 11.7, part (b). If the load torque is reduced to 75 percent of rated torque, calculate the field current required to achieve unity power factor.

Solution

3.35 A

Although during steady-state operation the speed of a synchronous motor is determined by the frequency of the drive, speed control by means of frequency control is of limited use in practice. This is due in most part to the fact that it is difficult for the rotor of a synchronous machine to track arbitrary changes in the frequency

of the applied armature voltage. In addition, starting is a major problem, and, as a result, the rotors of synchronous motors are often equipped with a squirrel-cage winding known as an *amortisseur* or *damper winding* similar to the squirrel-cage winding in an induction motor, as shown in Fig. 5.3. Following the application of a polyphase voltage to the armature, the rotor will come up almost to synchronous speed by induction-motor action with the field winding unexcited. If the load and inertia are not too great, the motor will pull into synchronism when the field winding is subsequently energized.

Problems with changing speed result from the fact that, in order to develop torque, the rotor of a synchronous motor must remain in synchronism with the stator flux. Control of synchronous motors can be greatly enhanced by control algorithms in which the stator flux and its relationship to the rotor flux are controlled directly. Such control, which amounts to direct control of torque, is discussed in Section 11.2.2.

11.2.2 Torque Control

Direct torque control in an ac machine, which can be implemented in a number of different ways, is commonly referred to as *field-oriented control* or *vector control*. To facilitate our discussion of field-oriented control, it is helpful to return to the discussion of Section 5.6.1. Under this viewpoint, which is formalized in Appendix C, stator quantities (flux, current, voltage, etc.) are resolved into components which rotate in synchronism with the rotor. *Direct-axis* quantities represent those components which are aligned with the field-winding axis, and *quadrature-axis* components are aligned perpendicular to the field-winding axis.

Section C.2 of Appendix C derives the basic machine relations in dq0 variables for a synchronous machine consisting of a field winding and a three-phase stator winding. The transformed flux-current relationships are found to be

$$\lambda_d = L_d i_d + L_{af} i_f \tag{11.17}$$

$$\lambda_q = L_q i_q \tag{11.18}$$

$$\lambda_f = \frac{3}{2} L_{af}\, i_d + L_{ff} i_f \tag{11.19}$$

where the subscripts d, q, and f refer to armature direct-, quadrature-axis, and field-winding quantities respectively. Note that throughout this chapter we will assume balanced operating conditions, in which case zero-sequence quantities will be zero and hence will be ignored.

The corresponding transformed voltage equations are

$$v_d = R_a i_d + \frac{d\lambda_d}{dt} - \omega_{me}\lambda_q \tag{11.20}$$

$$v_q = R_a i_q + \frac{d\lambda_q}{dt} + \omega_{me}\lambda_d \tag{11.21}$$

$$v_f = R_f i_f + \frac{d\lambda_f}{dt} \tag{11.22}$$

where $\omega_{me} = (\text{poles}/2)\omega_m$ is the electrical angular velocity of the rotor.

Finally, the electromagnetic torque acting on the rotor of a synchronous motor is shown to be (Eq. C.31)

$$T_{\text{mech}} = \frac{3}{2}\left(\frac{\text{poles}}{2}\right)(\lambda_{\text{d}} i_{\text{q}} - \lambda_{\text{q}} i_{\text{d}}) \tag{11.23}$$

Under steady-state, balanced-three-phase operating conditions, $\omega_{\text{me}} = \omega_{\text{e}}$ where ω_{e} is the electrical frequency of the armature voltage and current in rad/sec. Because the armature-produced mmf and flux waves rotate in synchronism with the rotor and hence with respect to the dq reference frame, under these conditions an observer in the dq reference frame will see constant fluxes, and hence one can set $d/dt = 0$.[1]

Letting the subscripts F, D, and Q indicate the corresponding constant values of field-, direct- and quadrature-axis quantities respectively, the flux-current relationships of Eqs. 11.17 through 11.19 then become

$$\lambda_{\text{D}} = L_{\text{d}} i_{\text{D}} + L_{\text{af}} i_{\text{F}} \tag{11.24}$$

$$\lambda_{\text{Q}} = L_{\text{q}} i_{\text{Q}} \tag{11.25}$$

$$\lambda_{\text{F}} = \frac{3}{2} L_{\text{af}} i_{\text{D}} + L_{\text{ff}} i_{\text{F}} \tag{11.26}$$

Armature resistance is typically quite small, and, if we neglect it, the steady-state voltage equations (Eqs. 11.20 through 11.22) then become

$$v_{\text{D}} = -\omega_{\text{e}} \lambda_{\text{Q}} \tag{11.27}$$

$$v_{\text{Q}} = \omega_{\text{e}} \lambda_{\text{D}} \tag{11.28}$$

$$v_{\text{F}} = R_{\text{f}} i_{\text{F}} \tag{11.29}$$

Finally, we can write Eq. 11.23 as

$$T_{\text{mech}} = \frac{3}{2}\left(\frac{\text{poles}}{2}\right)(\lambda_{\text{D}} i_{\text{Q}} - \lambda_{\text{Q}} i_{\text{D}}) \tag{11.30}$$

From this point on, we will focus our attention on machines in which the effects of saliency can be neglected. In this case, the direct- and quadrature-axis synchronous inductances are equal and we can write

$$L_{\text{d}} = L_{\text{q}} = L_{\text{s}} \tag{11.31}$$

where L_{s} is the synchronous inductance. Substitution into Eqs. 11.24 and 11.25 and then into Eq. 11.30 gives

$$\begin{aligned} T_{\text{mech}} &= \frac{3}{2}\left(\frac{\text{poles}}{2}\right)[(L_{\text{s}} i_{\text{D}} + L_{\text{af}} i_{\text{F}}) i_{\text{Q}} - L_{\text{s}} i_{\text{Q}} i_{\text{D}}] \\ &= \frac{3}{2}\left(\frac{\text{poles}}{2}\right) L_{\text{af}} i_{\text{F}} i_{\text{Q}} \end{aligned} \tag{11.32}$$

[1] This can easily be derived formally by substituting expressions for the balanced-three-phase armature currents and voltages into the transformation equations.

Equation 11.32 shows that torque is produced by the interaction of the field flux (proportional to the field current) and the quadrature-axis component of the armature current, in other words the component of armature current that is orthogonal to the field flux. By analogy, we see that the direct-axis component of armature current, which is aligned with the field flux, produces no torque.

This result is fully consistent with the generalized torque expressions which are derived in Chapter 4. Consider for example Eq. 4.73 which expresses the torque in terms of the product of the stator and rotor mmfs (F_s and F_r respectively) and the sine of the angle between them.

$$T = -\left(\frac{\text{poles}}{2}\right)\left(\frac{\mu_0 \pi D l}{2g}\right) F_s F_r \sin \delta_{sr} \tag{11.33}$$

where δ_r is the electrical space angle between the stator and rotor mmfs. This shows clearly that no torque will be produced by the direct-axis component of the armature mmf which, by definition, is that component of the stator mmf which is aligned with that of the field winding on the rotor.

Equation 11.32 shows the torque in a nonsalient synchronous motor is proportional to the product of the field current and the quadrature-axis component of the armature current. This is directly analogous to torque production in a dc machine for which Eqs. 7.10 and 7.13 can be combined to show that the torque is proportional to the product of the field current and the armature current.

The analogy between a nonsalient synchronous machine and dc machine can be further reinforced. Consider Eq. 5.21, which expresses the rms value of the line-to-neutral generated voltage of a synchronous generator as

$$E_{af} = \frac{\omega_e L_{af} i_F}{\sqrt{2}} \tag{11.34}$$

Substitution into Eq. 11.32 gives

$$T_{mech} = \frac{3}{2}\left(\frac{\text{poles}}{\sqrt{2}}\right)\frac{E_{af} i_Q}{\omega_e} \tag{11.35}$$

This is directly analogous to Eq. 7.16 ($T_{mech} = E_a I_a / \omega_m$) for a dc machine in which the torque is proportional to the product of the generated voltage and the armature current.

The brushes and commutator of a dc machine force the commutated armature current and armature flux along the quadrature axis such that $I_d = 0$ and it is the interaction of this quadrature-axis current with the direct-axis field flux that produces the torque.[2] A field-oriented controller which senses the position of the rotor and controls the quadrature-axis component of armature current produces the same effect in a synchronous machine.

[2] In a practical dc motor, the brushes may be adjusted away from this ideal condition somewhat to improve commutation. In this case, some direct-axis flux will be produced, corresponding to a small direct-axis component of armature current.

Although the direct-axis component of the armature current does not play a role in torque production, it does play a role in determining the resultant stator flux and hence the machine terminal voltage, as can be readily shown. Specifically, from the transformation equations of Appendix C,

$$v_a = v_D \cos(\omega_e t) - v_Q \sin(\omega_e t) \tag{11.36}$$

and thus the rms amplitude of the armature voltage is equal to[3]

$$V_a = \sqrt{\frac{v_D^2 + v_Q^2}{2}} = \omega_e \sqrt{\frac{\lambda_D^2 + \lambda_Q^2}{2}}$$

$$= \omega_e \sqrt{\frac{(L_s i_D + L_{af} i_F)^2 + (L_s i_Q)^2}{2}} \tag{11.37}$$

Dividing V_a by the electrical frequency ω_e, we get an expression for rms armature flux linkages

$$(\lambda_a)_{rms} = \sqrt{\frac{\lambda_D^2 + \lambda_Q^2}{2}} = \sqrt{\frac{(L_s i_D + L_{af} i_F)^2 + (L_s i_Q)^2}{2}} \tag{11.38}$$

Similarly, the transformation equations of Appendix C can be used to show that the rms amplitude of the armature current is equal to

$$I_a = \sqrt{\frac{i_D^2 + i_Q^2}{2}} \tag{11.39}$$

From Eq. 11.32 we see that torque is controlled by the product $i_F i_Q$ of the field current and the quadrature-axis component of the armature current. Thus, simply specifying a desired torque is not sufficient to uniquely determine either i_F or i_Q. In fact, under the field-oriented-control viewpoint presented here, there are actually three indpendent variables, i_F, i_Q and i_D, and, in general, three constraints will be required to uniquely determine them. In addition to specifying the desired torque, a typical controller will implement additional constraints on terminal flux-linkages and current using the basic relationships found in Eqs. 11.38 and 11.39.

Figure 11.13a shows a typical field-oriented torque-control system in block-diagram form. The torque-controller block has two inputs, T_{ref}, the reference value or set point for torque and $(i_F)_{ref}$, the reference value or set point for the field current, which is also supplied to the power supply which supplies the current i_F to the motor field winding. $(i_F)_{ref}$ is determined by an auxiliary controller which also determines

[3] Strictly speaking, armature resistance should be included in the voltage expression, in which case the rms amplitude of the armature voltage would be given by the expression

$$V_a = \sqrt{\frac{v_D^2 + v_Q^2}{2}} = \sqrt{\frac{(R_a i_D - \omega_e \lambda_Q)^2 + (R_a i_Q + \omega_e \lambda_D)^2}{2}}$$

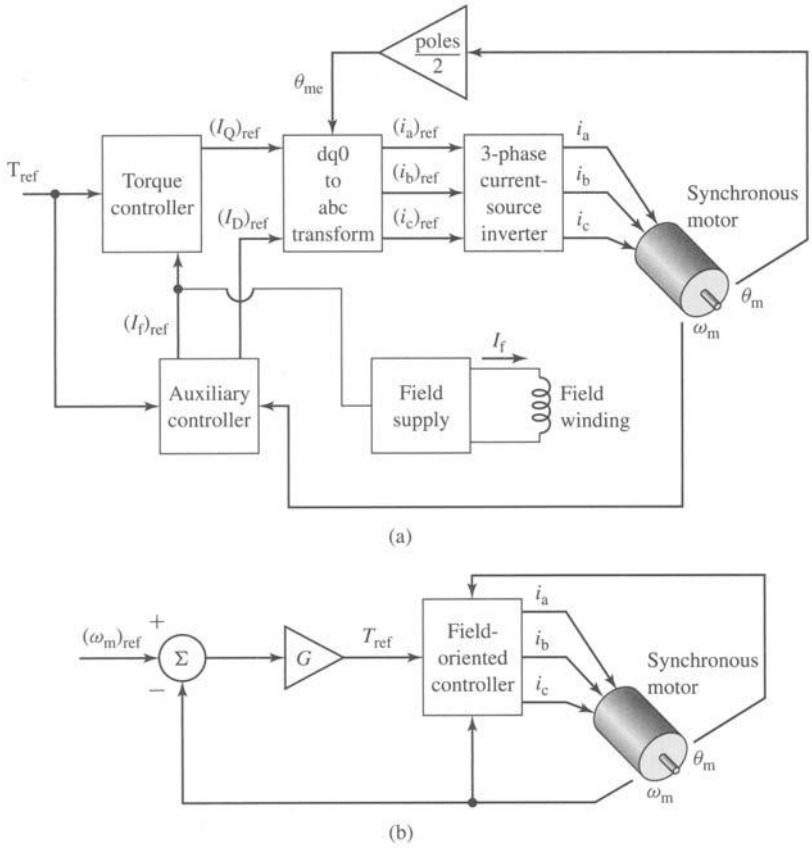

Figure 11.13 (a) Block diagram of a field-oriented torque-control system for a synchronous motor. (b) Block diagram of a synchronous-motor speed-control loop built around a field-oriented torque control system.

the reference value $(i_D)_{ref}$ of the direct-axis current, based upon desired values for the armature current and voltage. The torque controller calculates the desired quadrature-axis current from Eq. 11.32 based upon T_{ref} and $(i_F)_{ref}$

$$(i_Q)_{ref} = \frac{2}{3}\left(\frac{2}{\text{poles}}\right)\frac{T_{ref}}{L_{af}(i_F)_{ref}} \tag{11.40}$$

Note that a position sensor is required to determine the angular position of the rotor in order to implement the dq0 to abc transformation.

In a typical application, the ultimate control objective is not to control motor torque but to control speed or position. Figure 11.13b shows how the torque-control system of Fig. 11.13b can be used as a component of a speed-control loop, with speed feedback forming an outer control loop around the inner torque-control loop.

EXAMPLE 11.8

Consider again the 45-kVA, 220-V, six-pole synchronous motor of Example 11.7 operating at 60 Hz with a field current of 2.84 A. If the motor is loaded to rated torque and operating under a field-oriented control system such that $i_D = 0$, calculate (*a*) the phase currents $i_a(t)$, $i_b(t)$, and $i_c(t)$ as well as the per-unit value of the armature current and (*b*) the motor terminal voltage in per unit. Assume that $\theta_{me} = 0$ at time $t = 0$ (i.e., the rotor direct axis is aligned with phase *a* at $t = 0$).

■ Solution

a. We must first calculate L_{af}. From Example 11.7, we see that the motor produces rated open-circuit voltage (220-V rms, line-to-line) at a field current of 2.84 A. From Eq. 11.34

$$L_{af} = \frac{\sqrt{2}E_{af}}{\omega_e i_F}$$

where E_{af} is the rms, line-to-neutral generated voltage. Thus

$$L_{af} = \frac{\sqrt{2}(220/\sqrt{3})}{120\pi \times 2.84} = 0.168 \text{ H}$$

Rated torque for this six-pole motor is equal to

$$T_{rated} = \frac{P_{rated}}{(\omega_m)_{rated}} = \frac{P_{rated}}{(\omega_e)_{rated}(2/\text{poles})}$$
$$= \frac{45 \times 10^3}{120\pi(2/6)} = 358 \text{ N} \cdot \text{m}$$

Thus, setting $T_{ref} = T_{rated} = 358$ N·m and $(i_F)_{ref} = 2.84$ A, we can find i_Q from Eq. 11.40 as

$$i_Q = \frac{2}{3}\left(\frac{2}{\text{poles}}\right)\frac{T_{ref}}{L_{af}(i_F)_{ref}} = \frac{2}{3}\left(\frac{2}{6}\right)\frac{358}{0.168 \times 2.84} = 167 \text{ A}$$

Using the fact that $\theta_{me} = \omega_e t$ and setting $i_D = 0$, the transformation from dq0 variables to abc variables (Eq. C.2 of Appendix C) gives

$$i_a(t) = i_D \cos(\omega_e t) - i_Q \sin(\omega_e t) = -167 \sin(\omega_e t) = -\sqrt{2}(118)\sin(\omega_e t) \text{ A}$$

where $\omega_e = 120\pi \approx 377$ rad/sec. Similarly

$$i_b(t) = -\sqrt{2}(118)\sin(\omega_e t - 120°) \text{ A}$$

and

$$i_c(t) = -\sqrt{2}(118)\sin(\omega_e t + 120°) \text{ A}$$

The rms armature current is 118 A and the machine base current is equal to

$$I_{base} = \frac{P_{base}}{\sqrt{3}V_{base}} = \frac{45 \times 10^3}{\sqrt{3}\,220} = 118 \text{ A}$$

Thus the per-unit machine terminal current is equal to $I_a = 118/118 = 1.0$ per unit.

b. The motor terminal voltage can most easily be found from the rms phasor relationship

$$\hat{V}_a = jX_s\hat{I}_a + \hat{E}_{af}$$

In part (a) we found that $i_a = -\sqrt{2}(118)\sin(\omega_e t)$ A and thus

$$\hat{I}_a = j118 \text{ A}$$

We can find E_{af} from Eq. 11.34 as

$$E_{af} = \frac{\omega_e L_{af} i_F}{\sqrt{2}} = \frac{120\pi \times 0.168 \times 2.84}{\sqrt{2}} = 127 \text{ V line-to-neutral}$$

and, thus, since $(\hat{E}_{af})_{rms}$ lies along the quadrature axis, as does $\hat{I}_a$,

$$\hat{E}_{af} = j127 \text{ V}$$

The base impedance of the machine is equal to

$$Z_{base} = \frac{V_{base}^2}{P_{base}} = \frac{220^2}{45 \times 10^3} = 1.076\ \Omega$$

and the synchronous reactance of 0.836 pu is equal to $X_s = 0.836 \times 1.076 = 0.899\ \Omega$. Thus the rms line-to-neutral terminal voltage

$$\hat{V}_a = jX_s\hat{I}_a + \hat{E}_{af} = j0.899(j118) + j127$$
$$= -106 + j127 = 165\angle 129.9^\circ \text{ V line-to-neutral}$$

or $V_a = 287$ V rms line-to-line $= 1.30$ per unit.

Note that the terminal voltage for this operating condition is considerably in excess of the rated voltage of this machine, and hence such operation would not be acceptable. As we shall now discuss, a control algorithm which takes advantage of the full capability to vary i_F, i_D, and i_Q can achieve rated torque while not exceeding rated terminal voltage.

Practice Problem 11.8

Calculate the per-unit terminal voltage and current of Example 11.8 if the field-oriented controller maintains $i_D = 0$ while reducing i_F to 2.6 A.

Solution

$V_a = 1.29$ per unit and $I_a = 1.09$ per unit.

As we have discussed, a practical field-oriented control must determine values for all three currents i_F, i_D, and i_Q. In Example 11.8 two of these values were chosen relatively arbitrarily ($i_F = 2.84$ and $i_D = 0$) and the result was a control that achieved the desired torque but with a terminal voltage 30 percent in excess of the motor-rated voltage. In a practical system, additional constraints are required to achieve an acceptable control algorithm.

One such algorithm would be to require that the motor operate at rated flux and at unity terminal power factor. Such an algorithm can be derived with reference to the

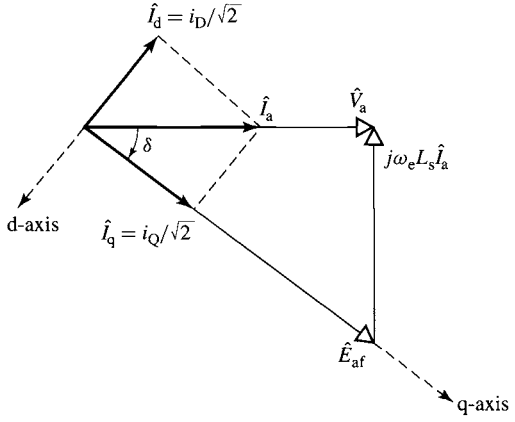

Figure 11.14 Phasor diagram for unity-power-factor field-oriented-control algorithm.

phasor diagram of Fig 11.14 and can be implemented using the following steps:

Step 1. Calculate the line-to-neutral armature voltage corresponding to rated flux as

$$V_a = (V_a)_{rated}\left(\frac{\omega_m}{(\omega_m)_{rated}}\right) \tag{11.41}$$

where $(V_a)_{rated}$ is the rated line-to-neutral armature voltage at rated motor speed, ω_m is the desired motor speed, and $(\omega_m)_{rated}$ is its rated speed.

Step 2. Calculate the rms armature current from the desired torque T_{ref} as

$$I_a = \frac{P_{ref}}{3V_a} = \frac{T_{ref}\,\omega_m}{3V_a} \tag{11.42}$$

where P_{ref} is the mechanical power corresponding to the desired torque.

Step 3. Calculate the angle δ based upon the phasor diagram of Fig 11.14

$$\delta = -\tan^{-1}\left(\frac{\omega_e L_s I_a}{V_a}\right) \tag{11.43}$$

where $\omega_e = \omega_{me} = (\text{poles}/2)\omega_m$ is the electrical frequency corresponding to the desired motor speed.

Step 4. Calculate $(i_Q)_{ref}$ and $(i_D)_{ref}$

$$(i_Q)_{ref} = \sqrt{2} I_a \cos\delta \tag{11.44}$$

$$(i_D)_{ref} = \sqrt{2} I_a \sin\delta \tag{11.45}$$

Step 5. Calculate $(i_F)_{ref}$ from Eq. 11.32

$$(i_F)_{ref} = \frac{2}{3}\left(\frac{2}{\text{poles}}\right)\frac{T_{ref}}{L_{af}(i_Q)_{ref}} \tag{11.46}$$

This algorithm is illustrated in Example 11.9.

EXAMPLE 11.9

The 45-kVA, 220-V synchronous motor of Example 11.8 is to be again operated at rated torque and speed from a field-oriented control system. Calculate the required motor field current and the per-unit terminal voltage and current if the unity-power-factor algorithm described above is implemented.

■ Solution

We will follow the individual steps outlined above.

Step 1. Since the motor is operating at rated speed, the desired terminal voltage will be the rated line-to-neutral voltage of the machine.

$$V_a = \frac{220}{\sqrt{3}} = 127 \text{ V} = 1.0 \text{ per unit}$$

Step 2. Setting $T_{ref} = 358$ N·m and $\omega_m = (2/\text{poles})\omega_e = 40\pi$, the rms armature current can be calculated from Eq. 11.42

$$I_a = \frac{T_{ref}\,\omega_m}{3(V_a)} = \frac{358 \times (40\pi)}{3 \times 127} = 118 \text{ A}$$

As calculated in Example 11.8, $I_{base} = 118$ A and thus $I_a = 1.0$ per unit. This is as expected, since we want the motor to operate at rated torque, speed and terminal voltage, and at unity power factor.

Step 3. Next calculate δ from Eq. 11.43. This calculation requires that we determine the synchronous inductance L_s.

$$L_s = \frac{X_s}{(\omega_e)_{rated}} = \frac{0.899}{120\pi} = 2.38 \text{ mH}$$

Thus

$$\delta = -\tan^{-1}\left(\frac{\omega_e L_s I_a}{V_a}\right)$$

$$= -\tan^{-1}\left(\frac{120\pi 2.38 \times 10^{-3} \times 118}{127}\right) = -0.695 \text{ rad} = -39.8°$$

Step 4. We can now calculate the desired values of i_Q and i_D from Eqs. 11.44 and 11.45.

$$(i_Q)_{ref} = \sqrt{2} I_a \cos\delta = 128 \text{ A}$$

and

$$(i_D)_{ref} = \sqrt{2} I_a \sin\delta = -107 \text{ A}$$

Step 5. $(i_F)_{ref}$ is found from Eq. 11.46

$$(i_F)_{ref} = \frac{2}{3}\left(\frac{2}{\text{poles}}\right)\frac{T_{ref}}{L_{af}(i_Q)_{ref}} = \frac{2}{3}\left(\frac{2}{6}\right)\frac{358}{0.168 \times 128} = 3.70 \text{ A}$$

Practice Problem 11.9

Repeat Example 11.9 for the motor operating at rated torque and half of rated speed. Calculate (*a*) the desired motor field current, (*b*) the line-to-neutral terminal voltage (in volts), and (*c*) the armature current (in amperes).

Solution

a. $(i_F)_{ref} = 3.70$ A
b. $V_a = 63.5$ V line-to-neutral
c. $I_a = 118$ A

The discussion of this section has focused upon synchronous machines with field windings and the corresponding capability to control the field excitation. The basic concept, of course, also applies to synchronous machines with permanent magnets on the rotor. However, in the case of permanent-magnet synchronous machines, the effective field excitation is fixed and, as a result, there is one less degree of freedom for the field-oriented control algorithm.

For a permanent-magnet synchronous machine, since the effective equivalent field current is fixed by the permanent magnet, the quadrature-axis current is determined directly by the desired torque. Consider a three-phase permanent-magnet motor whose rated rms, line-to-neutral open-circuit voltage is $(E_{af})_{rated}$ at electrical frequency $(\omega_e)_{rated}$. From Eq. 11.34 we see that the equivalent $L_{af}I_f$ product for this motor, which we will refer to by the symbol Λ_{PM}, is

$$\Lambda_{PM} = \frac{\sqrt{2}(E_{af})_{rated}}{(\omega_e)_{rated}} \tag{11.47}$$

Thus, the direct-axis flux-current relationship for this motor, corresponding to Eq. 11.24, becomes

$$\lambda_D = L_d i_D + \Lambda_{PM} \tag{11.48}$$

and the torque expression of Eq. 11.32 becomes

$$T_{mech} = \frac{3}{2}\left(\frac{\text{poles}}{2}\right)\Lambda_{PM} i_Q \tag{11.49}$$

From Eq. 11.49 we see that, for a permanent-magnet sychronous machine under field-oriented control, the quadrature-axis current is uniquely determined by the desired torque and Eq. 11.40 becomes

$$(i_Q)_{ref} = \frac{2}{3}\left(\frac{2}{\text{poles}}\right)\frac{T_{ref}}{\Lambda_{PM}} \tag{11.50}$$

Once $(i_Q)_{ref}$ has been specified, the only remaining control choice remains to determine the desired value for the direct-axis current, $(i_D)_{ref}$. One possibility is simply to set $(i_D)_{ref} = 0$. This will clearly result in the lowest possible armature current for a given torque. However, as we have seen in Example 11.8, this is likely to result in terminal voltages in excess of the rated voltage of the machine. As a

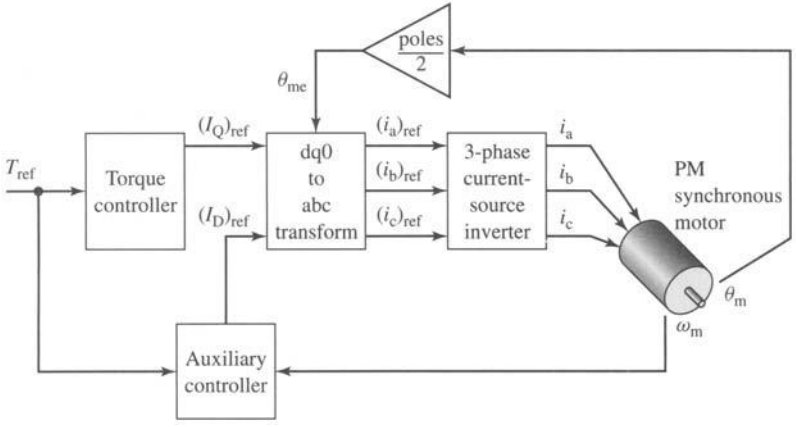

Figure 11.15 Block diagram of a field-oriented torque-control system for a permanent-magnet synchronous motor.

result, it is common to supply direct-axis current so as to reduce the direct-axis flux linkage of Eq. 11.48, which will in turn result in reduced terminal voltage. This technique is commonly referred to as *flux weakening* and comes at the expense of increased armature current.[4] In practice, the chosen operating point is determined by a trade-off between reducing the armature voltage and an increase in armature current. Figure 11.15 shows the block diagram for a field-oriented-control system for use with a permanent-magnet motor.

EXAMPLE 11.10

A 25-kW, 4000-rpm, 220-V, two-pole, three-phase permanent-magnet synchronous motor produces rated open-circuit voltage at a rotational speed of 3200 r/min and has a synchronous inductance of 1.75 mH. Assume the motor is to be operated under field-oriented control at 2800 r/min and 65 percent of rated torque.

a. Calculate the required quadrature-axis current.
b. If the controller is designed to minimize armature current by setting $i_D = 0$, calculate the resultant armature flux linkage in per-unit.
c. If the controller is designed to maintain the armature flux-linkage at its rated value, calculate the corresponding value of i_D and the corresponding rms and per-unit values of the armature current.

■ Solution

a. The rated speed of this machine is

$$(\omega_m)_{rated} = 4000\left(\frac{\pi}{30}\right) = 419 \text{ rad/sec}$$

[4] See T. M. Jahns, "Flux-Weakening Regime Operation of an Interior Permanent Magnet Synchronous Motor Drive," *IEEE Transactions on Industry Applications*, Vol. 23, pp. 681–689.

and the rated torque is

$$T_{\text{rated}} = \frac{P_{\text{rated}}}{(\omega_{\text{m}})_{\text{rated}}} = \frac{25 \times 10^3}{419} = 59.7 \text{ N} \cdot \text{m}$$

This motor achieves its rated-open-circuit voltage of $220/\sqrt{3} = 127$ V rms at a speed of $n = 3200$ r/min. The corresponding electrical frequency is

$$\omega_{\text{e}} = \left(\frac{\text{poles}}{2}\right)\left(\frac{\pi}{30}\right) n = \left(\frac{\pi}{30}\right) 3200 = 335 \text{ rad/sec}$$

From Eq. 11.47,

$$\Lambda_{\text{PM}} = \frac{\sqrt{2}(E_{\text{af}})_{\text{rated}}}{\omega_{\text{e}}} = \frac{\sqrt{2}\,127}{335} = 0.536 \text{ Wb}$$

Thus, setting $T_{\text{ref}} = 0.65 T_{\text{rated}} = 38.8$ N·m, from Eq. 11.50 we find that

$$(i_{\text{Q}})_{\text{ref}} = \frac{2}{3}\left(\frac{2}{\text{poles}}\right)\frac{T_{\text{ref}}}{\Lambda_{\text{PM}}} = \frac{2}{3}\left(\frac{38.8}{0.536}\right) = 48.3 \text{ A}$$

b. With $(i_{\text{D}})_{\text{ref}} = 0$,

$$\lambda_{\text{D}} = \Lambda_{\text{PM}} = 0.536 \text{ Wb}$$

and

$$\lambda_{\text{Q}} = L_{\text{s}} i_{\text{Q}} = (1.75 \times 10^{-3})48.3 = 0.0845 \text{ Wb}$$

Thus, the rms line-to-neutral armature flux is equal to

$$\lambda_{\text{a}} = \sqrt{\frac{\lambda_{\text{D}}^2 + \lambda_{\text{Q}}^2}{2}} = \sqrt{\frac{0.536^2 + 0.0845^2}{2}} = 0.384 \text{ Wb}$$

The base rms line-to-neutral armature flux can be determined from the base line-to-neutral voltage $(V_{\text{a}})_{\text{base}} = 127$ V and the base frequency $(\omega_{\text{e}})_{\text{base}} = 419$ rad/sec as

$$(\lambda_{\text{a}})_{\text{base}} = \frac{(V_{\text{a}})_{\text{base}}}{(\omega_{\text{e}})_{\text{base}}} = 0.303 \text{ Wb}$$

Thus, the per-unit armature flux is equal to $0.384/0.303 = 1.27$ per unit. From this calculation we see that the motor is significantly saturated at this operating condition. In fact, the calculation is probably not accurate because such a degree of saturation will most likely give rise to a reduction in the synchronous inductance as well as the magnetic coupling between the rotor and the stator.

c. In order to maintain rated armature flux linkage, the control will have to produce a direct-axis component of armature current to reduce the direct-axis flux linkage such that the total armature flux linkage is equal to the rated value $(\lambda_{\text{a}})_{\text{base}}$. Specifically, we must have

$$\lambda_{\text{D}} = \sqrt{2(\lambda_{\text{a}})_{\text{base}}^2 - \lambda_{\text{Q}}^2} = \sqrt{2 \times 0.303^2 - 0.0844^2} = 0.420 \text{ Wb}$$

We can now find $(i_D)_{ref}$ from Eq. 11.48 (setting $L_d = L_s$)

$$(i_D)_{ref} = \frac{\lambda_D - \Lambda_{PM}}{L_s} = \frac{0.420 - 0.536}{1.75 \times 10^{-3}} = -66.3 \text{ A}$$

The corresponding rms armature current is

$$I_a = \sqrt{\frac{(i_D)_{ref}^2 + (i_Q)_{ref}^2}{2}} = \sqrt{\frac{66.3^2 + 48.3^2}{2}} = 58.0 \text{ A}$$

The base rms armature current for this machine is equal to

$$I_{base} = \frac{P_{base}}{\sqrt{3} V_{base}} = \frac{25 \times 10^3}{\sqrt{3}\ 220} = 65.6 \text{ A}$$

and hence the per-unit armature current is equal to 58.0/65.6 = 0.88 per unit.

Comparing the results of parts (b) and (c) we see how flux weakening by the introduction of direct-axis current can be used to control the terminal voltage of a permanent-magnet synchronous motor under field-oriented control.

Practice Problem 11.10

Consider again the motor of Example 11.10. Repeat the calculations of parts (b) and (c) of Example 11.10 for the case in which the motor is operating at 80 percent of rated torque at a speed of 2500 r/min.

Solution

For part (b), $\lambda_a = 1.27$ per unit.

For part (c), $I_a = 0.98$ per unit.

11.3 CONTROL OF INDUCTION MOTORS

11.3.1 Speed Control

Induction motors supplied from a constant-frequency source admirably fulfill the requirements of substantially constant-speed drives. Many motor applications, however, require several speeds or even a continuously adjustable range of speeds. From the earliest days of ac power systems, engineers have been interested in the development of adjustable-speed ac motors.

The synchronous speed of an induction motor can be changed by (*a*) changing the number of poles or (*b*) varying the line frequency. The operating slip can be changed by (*c*) varying the line voltage, (*d*) varying the rotor resistance, or (*e*) applying voltages of the appropriate frequency to the rotor circuits. The salient features of speed-control methods based on these five possibilities are discussed in the following five sections.

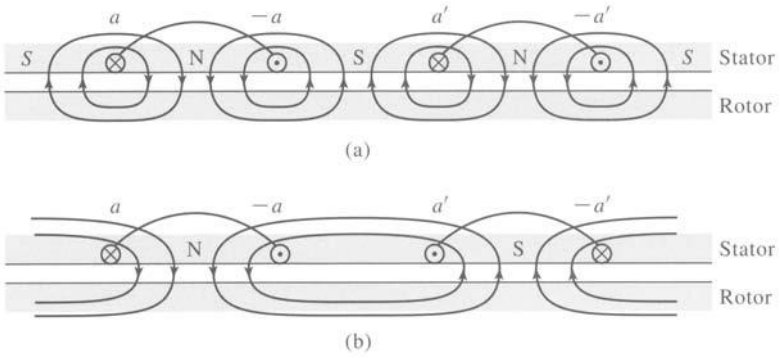

Figure 11.16 Principles of the pole-changing winding.

Pole-Changing Motors In pole-changing motors, the stator winding is designed so that, by simple changes in coil connections, the number of poles can be changed in the ratio 2 to 1. Either of two synchronous speeds can then be selected. The rotor is almost always of the squirrel-cage type, which reacts by producing a rotor field having the same number of poles as the inducing stator field. With two independent sets of stator windings, each arranged for pole changing, as many as four synchronous speeds can be obtained in a squirrel-cage motor, for example, 600, 900, 1200, and 1800 r/min for 60-Hz operation.

The basic principles of the pole-changing winding are shown in Fig. 11.16, in which aa and $a'a'$ are two coils comprising part of the phase-a stator winding. An actual winding would, of course, consist of several coils in each group. The windings for the other stator phases (not shown in the figure) would be similarly arranged. In Fig. 11.16a the coils are connected to produce a four-pole field; in Fig. 11.16b the current in the $a'a'$ coil has been reversed by means of a controller, the result being a two-pole field.

Figure 11.17 shows the four possible arrangements of these two coils: they can be connected in series or in parallel, and with their currents either in the same direction (four-pole operation) or in the opposite direction (two-pole operation). Additionally, the machine phases can be connected either in Y or Δ, resulting in eight possible combinations.

Note that for a given phase voltage, the different connections will result in differing levels of air-gap flux density. For example, a change from a Δ to a Y connection will reduce the coil voltage (and hence the air-gap flux density) for a given coil arrangement by $\sqrt{3}$. Similarly, changing from a connection with two coils in series to two in parallel will double the voltage across each coil and therefore double the magnitude of the air-gap flux density. These changes in flux density can, of course, be compensated for by changes in the applied winding voltage. In any case, they must be considered, along with corresponding changes in motor torque, when the configuration to be used in a specific application is considered.

Armature-Frequency Control The synchronous speed of an induction motor can be controlled by varying the frequency of the applied armature voltage. This method

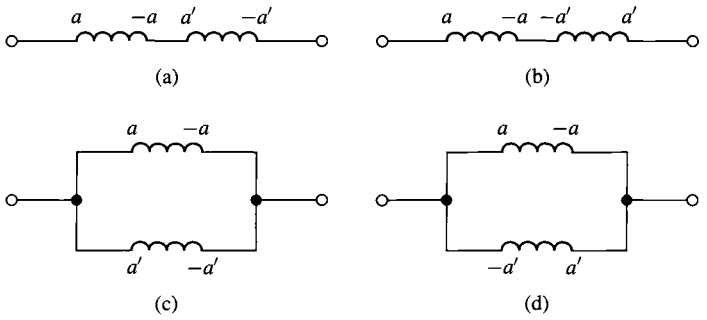

Figure 11.17 Four possible arrangements of phase-a stator coils in a pole-changing induction motor: (a) series-connected, four-pole; (b) series-connected, two-pole; (c) parallel-connected, four-pole; (d) parallel-connected, two-pole.

of speed control is identical to that discussed in Section 11.2.1 for synchronous machines. In fact, the same inverter configurations used for synchronous machines, such as the three-phase voltage-source inverter of Fig. 11.11, can be used to drive induction motors. As is the case with any ac motor, to maintain approximately constant flux density, the armature voltage should also be varied directly with the frequency (constant-volts-per-hertz).

The torque-speed curve of an induction motor for a given frequency can be calculated by using the methods of Chapter 6 within the accuracy of the motor parameters at that frequency. Consider the torque expression of Eq. 6.33 which is repeated here.

$$T_{\text{mech}} = \frac{1}{\omega_s}\left[\frac{n_{\text{ph}} V_{1,\text{eq}}^2 (R_2/s)}{(R_{1,\text{eq}} + (R_2/s))^2 + (X_{1,\text{eq}} + X_2)^2}\right] \tag{11.51}$$

where $\omega_s = (2/\text{poles})\omega_e$ and ω_e is the electrical excitation frequency of the motor in rad/sec,

$$\hat{V}_{1,\text{eq}} = \hat{V}_1\left(\frac{jX_m}{R_1 + j(X_1 + X_m)}\right) \tag{11.52}$$

and

$$R_{1,\text{eq}} + jX_{1,\text{eq}} = \frac{jX_m(R_1 + jX_1)}{R_1 + j(X_1 + X_m)} \tag{11.53}$$

To investigate the effect of changing frequency, we will assume that R_1 is negligible. In this case,

$$\hat{V}_{1,\text{eq}} = \hat{V}_1\left(\frac{X_m}{X_1 + X_m}\right) \tag{11.54}$$

$$R_{1,\text{eq}} = 0 \tag{11.55}$$

and

$$X_{1,eq} = \frac{X_m X_1}{X_1 + X_m} \tag{11.56}$$

Let the subscript 0 represent rated-frequency values of each of the induction-motor parameters. As the electrical-excitation frequency is varied, we can then write

$$(X_{1,eq} + X_2) = \left(\frac{\omega_e}{\omega_{e0}}\right)(X_{1,eq} + X_2)_0 \tag{11.57}$$

Under constant-volts-per-hertz control, we can also write the equivalent source voltage as

$$\hat{V}_1 = \left(\frac{\omega_e}{\omega_{e0}}\right)(\hat{V}_1)_0 \tag{11.58}$$

and hence, since $\hat{V}_{1,eq}$ is equal to $\hat{V}_1$ multiplied by a reactance ratio which stays constant with changing frequency,

$$\hat{V}_{1,eq} = \left(\frac{\omega_e}{\omega_{e0}}\right)(\hat{V}_{1,eq})_0 \tag{11.59}$$

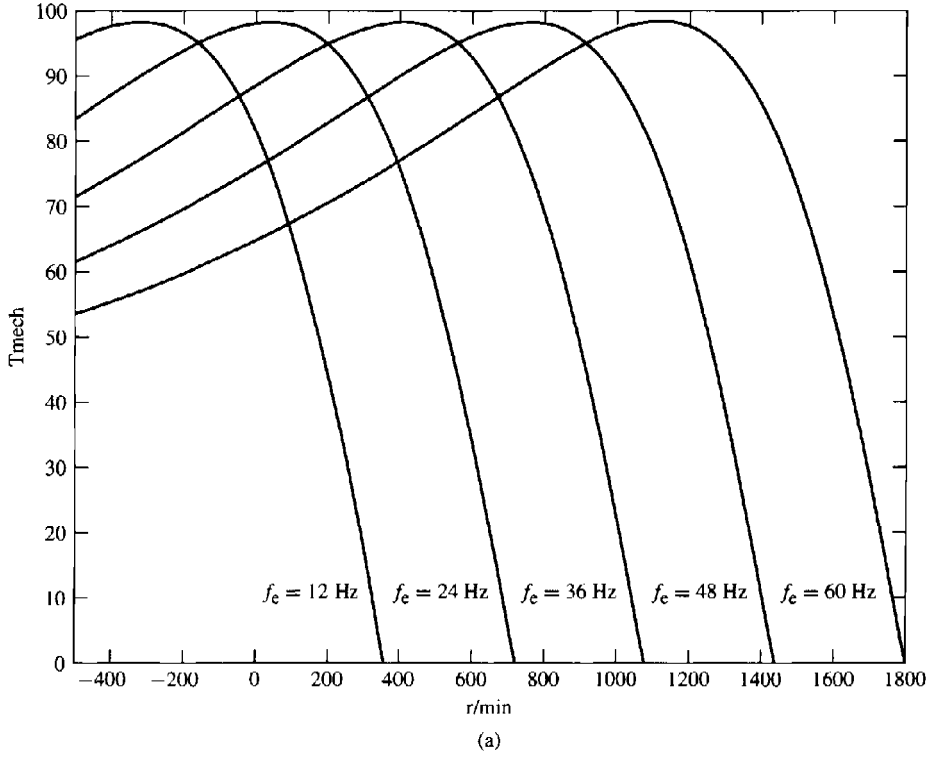

Figure 11.18 A family of typical induction-motor speed-torque curves for a four-pole motor for various values of the electrical supply frequency. (a) R_1 sufficiently small so that its effects are negligible. (b) R_1 not negligible.

Finally, we can write the motor slip as

$$s = \frac{\omega_s - \omega_m}{\omega_s} = \frac{\text{poles}}{2}\left(\frac{\Delta\omega_m}{\omega_e}\right) \tag{11.60}$$

where $\Delta\omega_m = \omega_s - \omega_m$ is the difference between the synchronous and mechanical angular velocities of the motor.

Substitution of Eqs. 11.57 through 11.60 into Eq. 11.51 gives

$$T_{mech} = \frac{n_{ph}[(V_{1,eq})_0]^2(R_2/\Delta\omega)}{\left[\left(\frac{2\omega_{e0}}{\text{poles}}\right)(R_2/\Delta\omega)\right]^2 + [(X_{1,eq} + X_2)_0]^2} \tag{11.61}$$

Equation 11.61 shows the general trend in which we see that the frequency dependence of the torque-speed characteristic of an induction motor appears only in the term $R_2/\Delta\omega$. Thus, under the assumption that R_1 is negligible, as the electrical supply frequency to an induction motor is changed, the shape of the speed-torque curve as a function of $\Delta\omega$ (the difference between the synchronous speed and the motor speed) will remain unchanged. As a result, the torque-speed characteristic will simply shift along the speed axis as $\omega_e(f_e)$ is varied.

A set of such curves is shown in Fig. 11.18a. Note that as the electrical frequency (and hence the synchronous speed) is decreased, a given value of $\Delta\omega$ corresponds to a

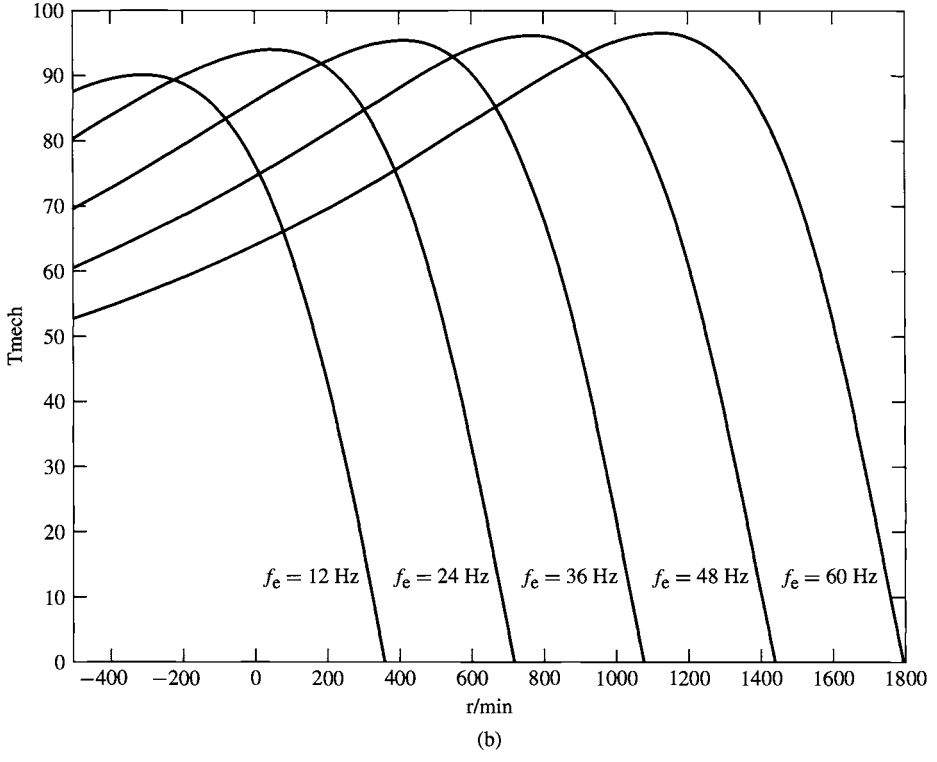

(b)

Figure 11.18 (*Continued*)

larger slip. Thus, for example, if the peak torque of a four-pole motor driven at 60 Hz occurs at 1638 r/min, corresponding to a slip of 9 percent, when driven at 30 Hz, the peak torque will occur at 738 r/min, corresponding to a slip of 18 percent.

In practice, the effects of R_1 may not be fully negligible, especially for large values of slip. If this is the case, the shape of the speed-torque curves will vary somewhat with the applied electrical frequency. Figure 11.18b shows a typical family of curves for this case.

EXAMPLE 11.11

The three-phase, 230-V, 60-Hz, 12-kW, four-pole induction motor of Example 6.4 (with $R_2 = 0.2\ \Omega$) is to be operated from a variable-frequency, constant-volts-per-hertz motor drive whose terminal voltage is 230 V at 60 Hz. The motor is driving a load whose power can be assumed to vary as

$$P_{load} = 10.5\left(\frac{n}{1800}\right)^3 \text{ kW}$$

where n is the load speed in r/min. Motor rotational losses can be assumed to be negligible.

Write a MATLAB script to find the line-to-line terminal voltage, the motor speed in r/min, the slip and the motor load in kW for (*a*) a source frequency of 60 Hz and (*b*) a source frequency of 40 Hz.

■ Solution

As the electrical frequency f_e is varied, the motor reactances given in Example 6.4 must be varied as

$$X = X_0\left(\frac{f_e}{60}\right)$$

where X_0 is the reactance value at 60 Hz. Similarly, the line-to-neutral armature voltage must be varied as

$$V_1 = \frac{220}{\sqrt{3}}\left(\frac{f_e}{60}\right) = 127\left(\frac{f_e}{60}\right) \text{ V}$$

From Eq. 4.40, the synchronous angular velocity of the motor is equal to

$$\omega_s = \left(\frac{4\pi}{\text{poles}}\right) f_e = \pi f_e \text{ rad/sec}$$

and, at any given motor speed ω_m, the corresponding slip is given by

$$s = \frac{\omega_s - \omega_m}{\omega_s}$$

Using Eqs. 11.51 through 11.53, the motor speed can be found by searching over ω_m for that speed at which $P_{load} = \omega_m T_{mech}$. If this is done, the result is:

a. For $f_e = 60$ Hz:

Terminal voltage = 230 V line-to-line

Speed = 1720 r/min

Slip = 4.4%

$P_{load} = 9.17$ kW

b. For $f_e = 40$ Hz:

Terminal voltage = 153 V line-to-line

Speed = 1166 r/min

Slip = 2.8%

$P_{load} = 2.86$ kW

Here is the MATLAB script:

```
clc
clear
%Here are the 60-Hz motor parameters
V10 = 230/sqrt(3);
Nph = 3;
poles = 4;
fe0 = 60;
R1 = 0.095;
R2 = 0.2;
X10 = 0.680;
X20 = 0.672;
Xm0 = 18.7;
% Two frequency values
fe1 = 60;
fe2 = 40;
for m = 1:2,
   if m == 1
        fe = fe1;
   else
        fe = fe2;
   end
% Calculate the reactances and the voltage
   X1 = X10*(fe/fe0);
   X2 = X20*(fe/fe0);
   Xm = Xm0*(fe/fe0);
   V1 = V10*(fe/fe0);
%Calculate the synchronous speed
   omegas = 4*pi*fe/poles;
   ns = 120*fe/poles;
%Calculate stator Thevenin equivalent
   V1eq = abs(V1*j*Xm/(R1 + j*(X1+Xm)));
```

```
   Z1eq = j*Xm*(R1+j*X1)/(R1 + j*(X1+Xm));
   R1eq = real(Z1eq);
   X1eq = imag(Z1eq);
%Search over the slip until the Pload = Pmech
   slip = 0.;
   error = 1;
   while error >= 0;
      slip = slip + 0.00001;
      rpm = ns*(1-slip);
      omegam = omegas*(1-slip);
      Tmech = (1/omegas)*Nph*V1eq^2*(R2/slip);
      Tmech = Tmech/((R1+R2/slip)^2 + (X1+X2)^2);
      Pmech = Tmech*omegam;
      Pload = 10.5e3*(rpm/1800)^3;
      error = Pload - Pmech;
   end  %End of while loop
   fprintf('\nFor fe = %g [Hz]:',fe)
   fprintf('\n   Terminal voltage = %g [V l-l]',V1*sqrt(3))
   fprintf('\n   rpm = %g',rpm)
   fprintf('\n   slip = %g [percent] ',100*slip)
   fprintf('\n   Pload = %g [kW]',Pload/1000)
   fprintf('\n\n')
end
```

Practice Problem 11.11

Repeat Example 11.11 for a source frequency of 50 Hz.

Solution

Terminal voltage = 192 V line-to-line

Speed = 1447 r/min

Slip = 3.6%

P_{load} = 5.45 kW

Line-Voltage Control The internal torque developed by an induction motor is proportional to the square of the voltage applied to its primary terminals, as shown by the two torque-speed characteristics in Fig. 11.19. If the load has the torque-speed characteristic shown by the dashed line, the speed will be reduced from n_1 to n_2. This method of speed control is commonly used with small squirrel-cage motors driving fans, where cost is an issue and the inefficiency of high-slip operation can be tolerated. It is characterized by a rather limited range of speed control.

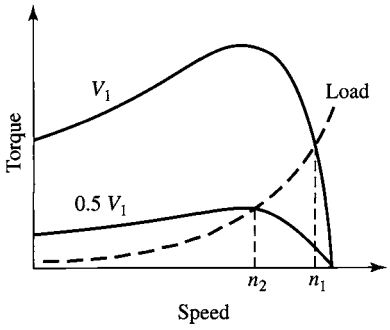

Figure 11.19 Speed control by means of line voltage.

Rotor-Resistance Control The possibility of speed control of a wound-rotor motor by changing its rotor-circuit resistance has already been pointed out in Section 6.7.1. The torque-speed characteristics for three different values of rotor resistance are shown in Fig. 11.20. If the load has the torque-speed characteristic shown by the dashed line, the speeds corresponding to each of the values of rotor resistance are n_1, n_2, and n_3. This method of speed control has characteristics similar to those of dc shunt-motor speed control by means of resistance in series with the armature.

The principal disadvantages of both line-voltage and rotor-resistance control are low efficiency at reduced speeds and poor speed regulation with respect to change in load. In addition, the cost and maintenance requirements of wound-rotor induction motors are sufficiently high that squirrel-cage motors combined with solid-state drives have become the preferred option in most applications.

11.3.2 Torque Control

In Section 11.2.2 we developed the concept of field-oriented-control for synchronous machines. Under this viewpoint, the armature flux and current are resolved into two components which rotate synchronously with the rotor and with the air-gap flux wave.

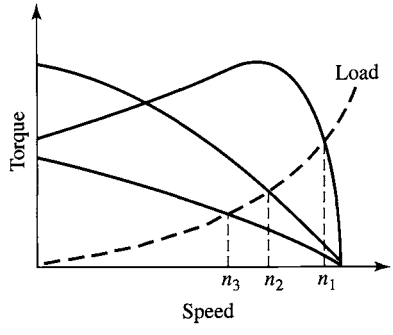

Figure 11.20 Speed control by means of rotor resistance.

The components of armature current and flux which are aligned with the field-winding are referred to as *direct-axis components* while those which are perpendicular to this axis are referred to as *quadrature-axis components.*

It turns out that the same viewpoint which we applied to synchronous machines can be applied to induction machines. As is discussed in Section 6.1, in the steady-state the mmf and flux waves produced by both the rotor and stator windings of an induction motor rotate at synchronous speed and in synchronism with each other. Thus, the torque-producing mechanism in an induction machine is equivalent to that of a synchronous machine. The difference between the two is that, in an induction machine, the rotor currents are not directly supplied but rather are induced as the induction-motor rotor slips with respect to the rotating flux wave produced by the stator currents.

To examine the application of field-oriented control to induction machines, we begin with the dq0 transformation of Section C.3 of Appendix C. This transformation transforms both the stator and rotor quantities into a synchronously rotating reference frame. Under balanced-three-phase, steady-state conditions, zero-sequence quantities will be zero and the remaining direct- and quadrature-axis quantites will be constant. Hence the flux-linkage current relationships of Eqs. C.52 through C.58 become

$$\lambda_D = L_S i_D + L_m i_{DR} \tag{11.62}$$

$$\lambda_Q = L_S i_Q + L_m i_{QR} \tag{11.63}$$

$$\lambda_{DR} = L_m i_D + L_R i_{DR} \tag{11.64}$$

$$\lambda_{QR} = L_m i_Q + L_R i_{QR} \tag{11.65}$$

In these equations, the subscripts D, Q, DR, and QR represent the constant values of the direct- and quadrature-axis components of the stator and rotor quantities respectively. It is a straight-forward matter to show that the inductance parameters can be determined from the equivalent-circuit parameters as

$$L_m = \frac{X_{m0}}{\omega_{e0}} \tag{11.66}$$

$$L_S = L_m + \frac{X_{10}}{\omega_{e0}} \tag{11.67}$$

$$L_R = L_m + \frac{X_{20}}{\omega_{e0}} \tag{11.68}$$

where the subscript 0 indicates the rated-frequency value.

The transformed voltage equations Eqs. C.63 through C.68 become

$$v_D = R_a i_D - \omega_e \lambda_Q \tag{11.69}$$

$$v_Q = R_a i_Q + \omega_e \lambda_D \tag{11.70}$$

$$0 = R_{aR} i_{DR} - (\omega_e - \omega_{me}) \lambda_{QR} \tag{11.71}$$

$$0 = R_{aR} i_{QR} + (\omega_e - \omega_{me}) \lambda_{DR} \tag{11.72}$$

where one can show that the resistances are related to those of the equivalent circuit as

$$R_a = R_1 \tag{11.73}$$

and

$$R_{aR} = R_2 \tag{11.74}$$

For the purposes of developing a field-oriented-control scheme, we will begin with the torque expression of Eq. C.70

$$T_{mech} = \frac{3}{2}\left(\frac{\text{poles}}{2}\right)\left(\frac{L_m}{L_R}\right)(\lambda_{DR} i_q - \lambda_{QR} i_d) \tag{11.75}$$

For the derivation of the dq0 transformation in Section C.3, the angular velocity of the reference frame was chosen to the synchronous speed as determined by the stator electrical frequency ω_e. It was not necessary for the purposes of the derivation to specify the absolute angular location of the reference frame. It is convenient at this point to choose the direct axis of the reference frame aligned with the rotor flux.

If this is done

$$\lambda_{QR} = 0 \tag{11.76}$$

and the torque expression of Eq. 11.75 becomes

$$T_{mech} = \frac{3}{2}\left(\frac{\text{poles}}{2}\right)\left(\frac{L_m}{L_R}\right)\lambda_{DR} i_Q \tag{11.77}$$

From Eq. 11.71 we see that

$$i_{DR} = 0 \tag{11.78}$$

and thus

$$\lambda_{DR} = L_m i_D \tag{11.79}$$

and

$$\lambda_D = L_S i_D \tag{11.80}$$

From Eqs. 11.79 and 11.80 we see that by choosing set $\lambda_{QR} = 0$ and thus aligning the synchronously rotating reference frame with the axis of the rotor flux, the direct-axis rotor flux (which is, indeed, the total rotor flux) as well as the direct-axis flux are determined by the direct-axis component of the armature current. Notice the direct analogy with a dc motor. In a dc motor, the field- and direct-axis armature fluxes are determined by the field current and in this field-oriented control scheme, the rotor and direct-axis armature fluxes are determined by the direct-axis armature current. In other words, in this field-oriented control scheme, the direct-axis component of armature current serves the same function as the field current in a dc machine.

The torque equation, Eq. 11.77, completes the analogy with the dc motor. We see that once the rotor direct-axis flux λ_{DR} is set by the direct-axis armature current, the

torque is then determined by the quadrature-axis armature current just as the torque is determined by the armature current in a dc motor.

In a practical implementation of the technique which we have derived, the direct- and quadrature-axis currents i_D and i_Q must be transformed into the three motor phase currents $i_a(t)$, $i_b(t)$, and $i_c(t)$. This can be done using the inverse dq0 transformation of Eq. C.48 which requires knowledge of θ_S, the electrical angle between the axis of phase a, and the direct-axis of the synchronously rotating reference frame.

Since it is not possible to measure the axis of the rotor flux directly, it is necessary to calculate θ_S, where $\theta_S = \omega_e t + \theta_0$ as given by Eq. C.46. Solving Eq. 11.72 for ω_e gives

$$\omega_e = \omega_{me} - R_{aR}\left(\frac{i_{QR}}{\lambda_{DR}}\right) \tag{11.81}$$

From Eq. 11.65 with $\lambda_{QR} = 0$ we see that

$$i_{QR} = -\left(\frac{L_m}{L_R}\right) i_Q \tag{11.82}$$

Eq. 11.82 in combination with Eq. 11.79 then gives

$$\omega_e = \omega_{me} + \frac{R_{aR}}{L_R}\left(\frac{i_Q}{i_D}\right) = \omega_{me} + \frac{1}{\tau_R}\left(\frac{i_Q}{i_D}\right) \tag{11.83}$$

where $\tau_R = L_R/R_{aR}$ is the rotor time constant.

We can now integrate Eq. 11.83 to find

$$\hat{\theta}_S = \left[\omega_{me} + \frac{1}{\tau_R}\left(\frac{i_Q}{i_D}\right)\right] t + \theta_0 \tag{11.84}$$

where $\hat{\theta}_S$ indicates the calculated value of θ_S (often referred to as the *estimated value* of θ_S). In the more general dynamic sense

$$\hat{\theta}_S = \int_0^t \left[\omega_{me} + \frac{1}{\tau_R}\left(\frac{i_Q}{i_D}\right)\right] dt' + \theta_0 \tag{11.85}$$

Note that both Eqs. 11.84 and 11.85 require knowledge of θ_0, the value of θ_S at $t = 0$. Although we will not prove it here, it turns out that in a practical implementation, the effects of an error in this initial angle decay to zero with time, and hence it can be set to zero without any loss of generality.

Figure 11.21a shows a block diagram of a field-oriented torque-control system for an induction machine. The block labeled "Estimator" represents the calculation of Eq. 11.85 which calculates the estimate of θ_S required by the transformation from dq0 to abc variables.

Note that a speed sensor is required to provide the rotor speed measurement required by the estimator. Also notice that the estimator requires knowledge of the rotor time constant $\tau_R = L_R/R_{aR}$. In general, this will not be known exactly, both due to uncertainty in the machine parameters as well as due to the fact that the rotor

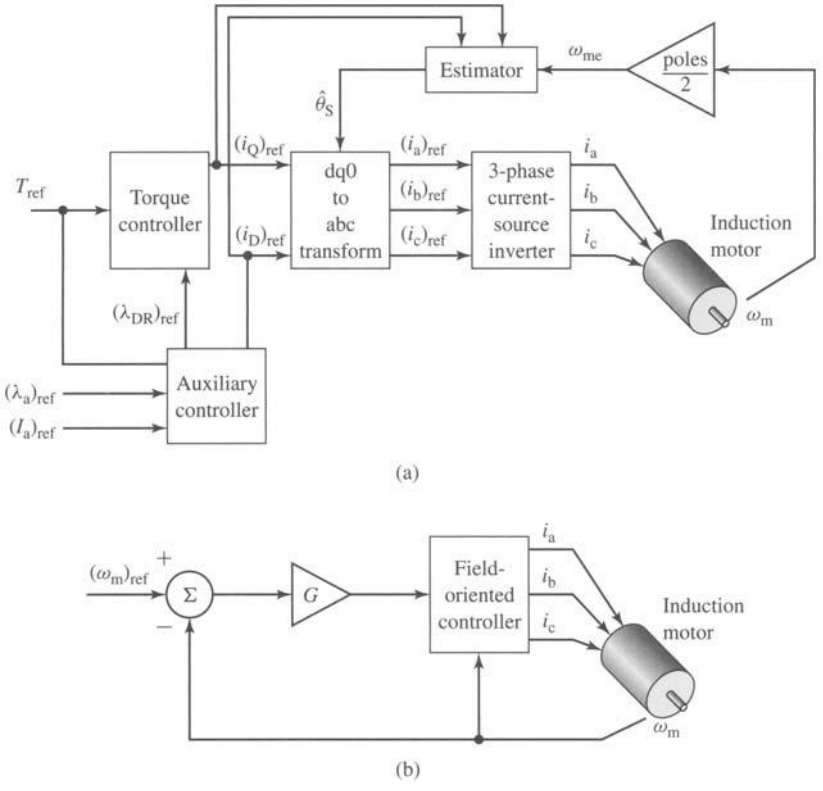

Figure 11.21 (a) Block diagram of a field-oriented torque-control system for an induction motor. (b) Block diagram of an induction-motor speed-control loop built around a field-oriented torque control system.

resistance R_{aR} will undoubtedly change with temperature as the motor is operated. It can be shown that errors in τ_R result in an offset in the estimate of θ_S, which in turn will result in an error in the estimate for the position of the rotor flux with the result that the applied armature currents will not be exactly aligned with the direct- and quadrature-axes. The torque controller will still work basically as expected, although there will be corresponding errors in the torque and rotor flux.

As with the synchronous motor, the rms armature flux-linkages can be found from Eq. 11.38 as

$$(\lambda_a)_{rms} = \sqrt{\frac{\lambda_D^2 + \lambda_Q^2}{2}} \tag{11.86}$$

Combining Eqs. 11.63 and 11.82 gives

$$\lambda_Q = L_S i_Q + L_m i_{QR} = \left(L_S - \frac{L_m^2}{L_R}\right) i_Q \tag{11.87}$$

Substituting Eqs. 11.80 and 11.87 into Eq. 11.86 gives

$$(\lambda_a)_{rms} = \sqrt{\frac{L_S^2 i_D^2 + \left(L_S - \frac{L_m^2}{L_R}\right)^2 i_Q^2}{2}} \tag{11.88}$$

Finally, as discussed in the footnote to Eq. 11.37, the rms line-to-neutral armature voltage can be found as

$$V_a = \sqrt{\frac{v_D^2 + v_Q^2}{2}} = \sqrt{\frac{(R_a i_D - \omega_e \lambda_Q)^2 + (R_a i_Q + \omega_e \lambda_D)^2}{2}}$$

$$= \sqrt{\frac{\left(R_a i_D - \omega_e \left(L_S - \frac{L_m^2}{L_R}\right) i_Q\right)^2 + (R_a i_Q + \omega_e L_S i_D)^2}{2}} \tag{11.89}$$

These equations show that the armature flux linkages and terminal voltage are determined by both the direct- and quadrature-axis components of the armature current. Thus, the block marked "Auxiliary Controller" in Fig. 11.21a, which calculates the reference values for the direct- and quadrature-axis currents, must calculate the reference currents $(i_D)_{ref}$ and $(i_Q)_{ref}$ which achieve the desired torque subject to constraints on armature flux linkages (to avoid saturation in the motor), armature current, $(I_a)_{rms} = \sqrt{(i_D^2 + i_Q^2)/2}$ (to avoid excessive armature heating) and armature voltage (to avoid potential insulation damage).

Note that, as we discussed with regard to synchronous machines in Section 11.2.2, the torque-control system of Fig. 11.21a is typically imbedded within a larger control loop. One such example is the speed-control loop of Fig. 11.21b.

EXAMPLE 11.12

The three-phase, 230-V, 60-Hz, 12-kW, four-pole induction motor of Example 6.7 and Example 11.11 is to be driven by a field-oriented speed-control system (similar to that of Fig. 11.21b) at a speed of 1740 r/min. Assuming the controller is programmed to set the rotor flux linkages λ_{DR} to the machine rated peak value, find the rms amplitude of the armature current, the electrical frequency, and the rms terminal voltage, if the electromagnetic power is 9.7 kW and the motor is operating at a speed of 1680 r/min.

■ Solution

We must first determine the parameters for this machine. From Eqs. 11.66 through Eq. 11.74

$$L_m = \frac{X_{m0}}{\omega_{e0}} = \frac{18.7}{120\pi} = 49.6 \text{ mH}$$

$$L_S = L_m + \frac{X_{10}}{\omega_{e0}} = 49.6 \text{ mH} + \frac{0.680}{120\pi} = 51.41 \text{ mH}$$

$$L_R = L_m + \frac{X_{20}}{\omega_{e0}} = 49.6 \text{ mH} + \frac{0.672}{120\pi} = 51.39 \text{ mH}$$

$$R_a = R_1 = 0.095\ \Omega$$

$$R_{aR} = R_2 = 0.2\ \Omega$$

The rated rms line-to-neutral terminal voltage for this machine is $230/\sqrt{3} = 132.8$ V and thus the peak rated flux for this machine is

$$(\lambda_{\text{rated}})_{\text{peak}} = \frac{\sqrt{2}(V_a)_{\text{rated}}}{\omega_e} = \frac{\sqrt{2} \times 132.8}{120\pi} = 0.498 \text{ Wb}$$

For the specified operating condition

$$\omega_m = n\left(\frac{\pi}{30}\right) = 1680\left(\frac{\pi}{30}\right) = 176 \text{ rad/sec}$$

and the mechanical torque is

$$T_{\text{mech}} = \frac{P_{\text{mech}}}{\omega_m} = \frac{9.7 \times 10^3}{176} = 55.1 \text{ N} \cdot \text{m}$$

From Eq. 11.77, with $\lambda_{DR} = \lambda_{\text{rated}} = 0.498$ Wb

$$i_Q = \frac{2}{3}\left(\frac{2}{\text{poles}}\right)\left(\frac{L_R}{L_m}\right)\left(\frac{T_{\text{mech}}}{\lambda_{DR}}\right)$$

$$= \frac{2}{3}\left(\frac{2}{4}\right)\left(\frac{51.39 \times 10^{-3}}{49.6 \times 10^{-3}}\right)\left(\frac{55.1}{0.498}\right) = 38.2 \text{ A}$$

From Eq. 11.79,

$$i_D = \frac{\lambda_{DR}}{L_m} = \frac{0.498}{49.6 \times 10^{-3}} = 10.0 \text{ A}$$

The rms armature current is thus

$$I_a = \sqrt{\frac{i_D^2 + i_Q^2}{2}} = \sqrt{\frac{10.0^2 + 38.2^2}{2}} = 27.9 \text{ A}$$

The electrical frequency can be found from Eq. 11.81

$$\omega_e = \omega_{me} + \frac{R_{aR}}{L_R}\left(\frac{i_Q}{i_D}\right)$$

With $\omega_{me} = (\text{poles}/2)\omega_m = 2 \times 176 = 352$ rad/sec

$$\omega_e = 352 + \left(\frac{0.2}{51.39 \times 10^{-3}}\right)\left(\frac{38.2}{10.0}\right) = 367 \text{ rad/sec}$$

and $f_e = \omega_e/(2\pi) = 58.4$ Hz.

Finally, from Eq. 11.89, the rms line-to-neutral terminal voltage

$$V_a = \sqrt{\frac{\left(R_a i_D - \omega_e\left(L_S - \frac{L_m^2}{L_R}\right)i_Q\right)^2 + (R_a i_Q + \omega_e L_S i_D)^2}{2}}$$

$$= 140.6 \text{ V line-to-neutral} = 243.6 \text{ V line-to-line}$$

Practice Problem 11.12

Consider again the induction motor and field-oriented-control system of Example 11.12. Assume that the speed is readjusted to 1700 r/min and that the electromagnetic power is known to increase to 10.0 kW. Find the rms amplitude of the armature current, the electrical frequency, and the rms terminal voltage for this new operating condition.

Solution

Armature current = 28.4 A

$f_e = 59.1$ Hz

Terminal voltage = 142.5 V line-to-neutral = 246.9 V line-to-line

---

The ability to independently control the rotor flux and the torque has important control implications. Consider, for example, the response of the direct-axis rotor flux to a change in direct-axis current. Equation C.66, with $\lambda_{qR} = 0$, becomes

$$0 = R_{aR} i_{dR} + \frac{d\lambda_{dR}}{dt} \tag{11.90}$$

Substituting for i_{dR} in terms of λ_{dR}

$$i_{dR} = \frac{\lambda_{dR} - L_m i_d}{L_R} \tag{11.91}$$

gives a differential equation for the rotor flux linkages λ_{DR}

$$\frac{d\lambda_{dR}}{dt} + \left(\frac{R_{aR}}{L_R}\right)\lambda_{dR} = \left(\frac{L_m}{L_R}\right) i_d \tag{11.92}$$

From Eq. 11.92 we see that the response of the rotor flux to a step change in direct-axis current i_d is relatively slow; λ_{dR} will change exponentially with the rotor time constant of $\tau_R = L_R/R_{aR}$. Since the torque is proportional to the product $\lambda_{dR} i_q$ we see that fast torque response will be obtained from changes in i_q. Thus, for example, to implement a step change in torque, a practical control algorithm might start with a step change in $(i_Q)_{ref}$ to achieve the desired torque change, followed by an adjustment in $(i_D)_{ref}$ (and hence λ_{dR}) to readjust the armature current or terminal voltage as desired. This adjustment in $(i_D)_{ref}$ would be coupled with a compensating adjustment in $(i_Q)_{ref}$ to maintain the torque at its desired value.

EXAMPLE 11.13

Consider again the induction motor of Example 11.12. Assuming the motor speed and electromagnetic power remain constant (at 1680 r/min and 9.7 kW), use MATLAB to plot the per-unit armature current I_a and terminal voltage V_a as a function of i_D as $(\lambda_{DR})_{ref}$ is varied between 0.8 and 1.2 per unit, where 1.0 per unit corresponds to the rated peak value.

■ Solution

The desired plot is given in Fig. 11.22. Note that the armature current decreases and the terminal voltage increases as λ_{DR} is increased. This clearly shows how i_D, which controls λ_{DR}, can be

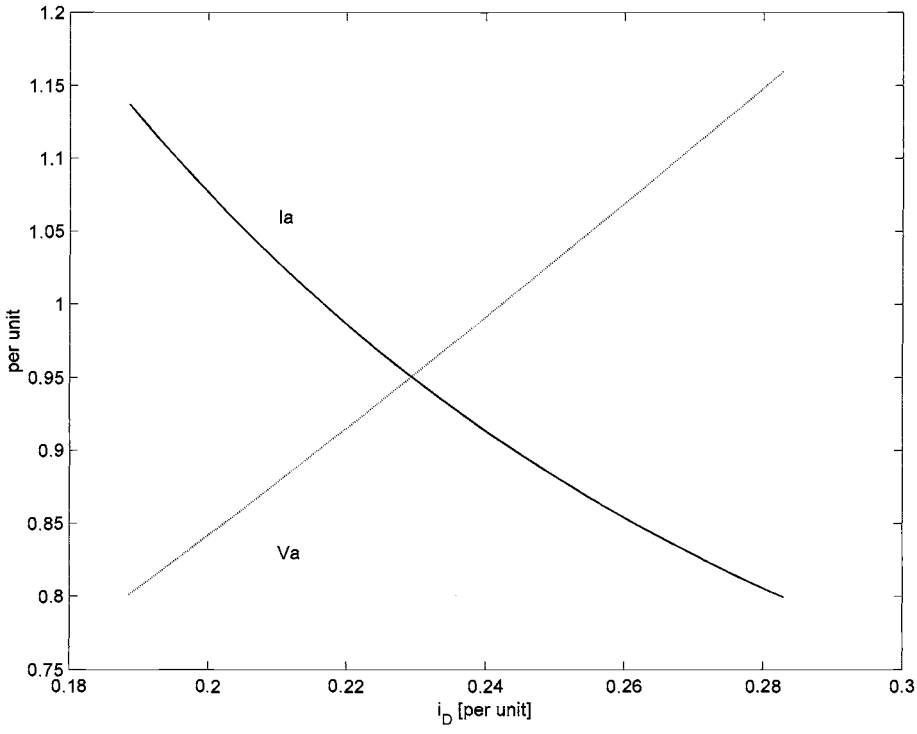

Figure 11.22 MATLAB plot for Example 11.13 showing the effect of the direct-axis current i_D on the armature voltage and current for an induction motor at constant speed and load.

chosen to optimize the tradeoff between such quantities as armature current, armature flux linkages, and terminal voltage.

Here is the MATLAB script:

```
clc
clear
%Motor rating and characteristics
Prated = 12e3;
Vrated = 230;
Varated = 230/sqrt(3);
ferated = 60;
omegaerated = 2*pi*ferated;
Lambdarated = sqrt(2)*Varated/omegaerated;
Irated = Prated/(sqrt(3)*Vrated);
Ipeakbase = sqrt(2)*Irated;
poles = 4;
%Here are the 60-Hz motor parameters
```

```
V10 = Vrated/sqrt(3);
X10 = 0.680;
X20 = 0.672;
Xm0 = 18.7;
R1 = 0.095;
R2 = 0.2;
%Calculate required dq0 parameters
Lm = Xm0/omegaerated;
LS = Lm + X10/omegaerated;
LR = Lm + X20/omegaerated;
Ra = R1;
RaR = R2;
% Operating point
n = 1680;
omegam = n*pi/30;
omegame = (poles/2)*omegam;
Pmech = 9.7e3;
Tmech = Pmech/omegam;
% Loop to plot over lambdaDR
for n = 1:41
   lambdaDR = (0.8 + (n-1)*0.4/40)*Lambdarated;
   lambdaDRpu(n) = lambdaDR/Lambdarated;
   iQ = (2/3)*(2/poles)*(LR/Lm)*(Tmech/lambdaDR);
   iD = (lambdaDR/Lm);
   iDpu(n) = iD/Ipeakbase;
   iQR = - (Lm/LR)*iQ;
   Ia = sqrt((iD^2 + iQ^2)/2);
   Iapu(n) = Ia/Irated;
   omegae = omegame - (RaR/LR)*(iQ/iD);
   fe(n) = omegae/(2*pi);
   Varms = sqrt(((Ra*iD-omegae*(LS-Lm^2/LR)*iQ)^2 + ...
         (Ra*iQ+ omegae*LS*iD)^2)/2);
   Vapu(n) = Varms/Varated;
end
%Now plot
plot(iDpu,Iapu)
hold
plot(iDpu,Vapu,':')
hold
xlabel('i_D [per unit]')
ylabel('per unit')
text(.21,1.06,'Ia')
text(.21,.83,'Va')
```

11.4 CONTROL OF VARIABLE-RELUCTANCE MOTORS

Unlike dc and ac (synchronous or induction) machines, VRMs cannot be simply "plugged in" to a dc or ac source and then be expected to run. As is dicussed in Chapter 8, the phases must be excited with (typically unipolar) currents, and the timing of these currents must be carefully correlated with the position of the rotor poles in order to produce a useful, time-averaged torque. The result is that although the VRM itself is perhaps the simplest of rotating machines, a practical VRM drive system is relatively complex.

VRM drive systems are competitive only because this complexity can be realized easily and inexpensively through power and microelectronic circuitry. These drive systems require a fairly sophisticated level of controllability for even the simplest modes of VRM operation. Once the capability to implement this control is available, fairly sophisticated control features can be added (typically in the form of additional software) at little additional cost, further increasing the competitive position of VRM drives.

In addition to the VRM itself, the basic VRM drive system consists of the following components: a rotor-position sensor, a controller, and an inverter. The function of the rotor-position sensor is to provide an indication of shaft position which can be used to control the timing and waveform of the phase excitation. This is directly analogous to the timing signal used to control the firing of the cylinders in an automobile engine.

The controller is typically implemented in software in microelectronic (microprocessor) circuitry. Its function is to determine the sequence and waveforms of the phase excitation required to achieve the desired motor speed-torque characteristics. In addition to set points of desired speed and/or torque and shaft position (from the shaft-position sensor), sophisticated controllers often employ additional inputs including shaft-speed and phase-current magnitude. Along with the basic control function of determining the desired torque for a given speed, the more sophisticated controllers attempt to provide excitations which are in some sense optimized (for maximum efficiency, stable transient behavior, etc.).

The control circuitry consists typically of low-level electronics which cannot be used to directly supply the currents required to excite the motor phases. Rather its output consists of signals which control an inverter which in turn supplies the phase currents. Control of the VRM is achieved by the application of an appropriate set of currents to the VRM phase windings.

Figures 11.23a to c show three common configurations found in inverter systems for driving VRMs. Note that these are simply H-bridge inverters of the type discussed in Section 10.3. Each inverter is shown in a two-phase configuration. As is clear from the figures, extension of each configuration to drive additional phases can be readily accomplished.

The configuration of Fig. 11.23a is perhaps the simplest. Closing switches S_{1a} and S_{1b} connects the phase-1 winding across the supply ($v_1 = V_0$) and causes the winding current to increase. Opening just one of the switches forces a short across

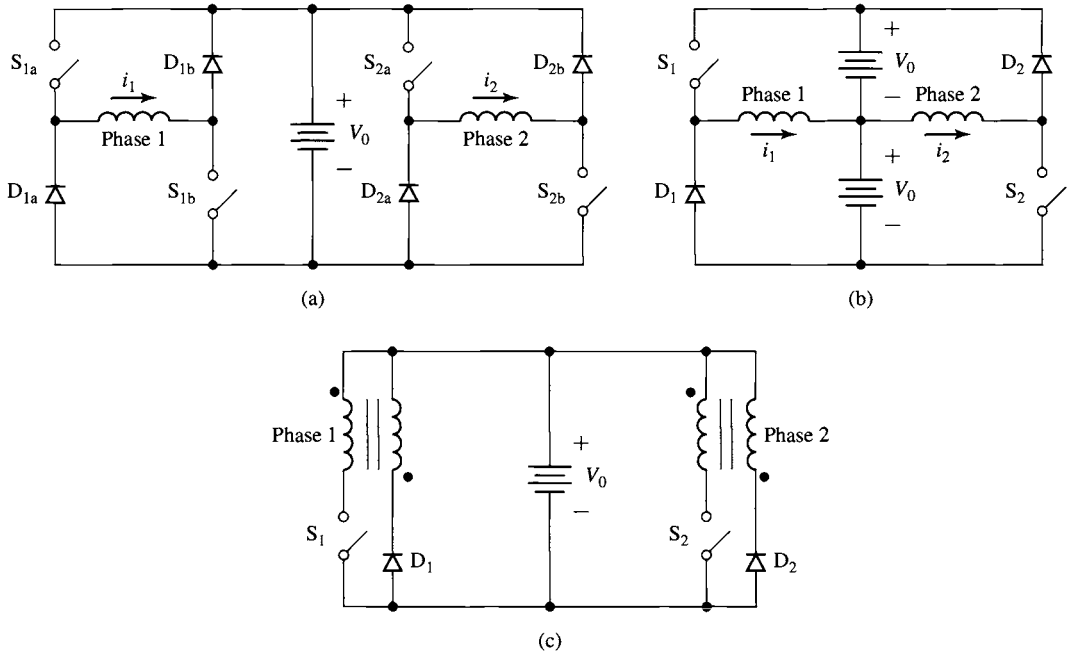

Figure 11.23 Inverter configurations. (a) Two-phase inverter which uses two switches per phase. (b) Two-phase inverter which uses a split supply and one switch per phase. (c) Two-phase inverter with bifilar phase windings and one switch per phase.

the winding and the current will decay, while opening both switches connects the winding across the supply with negative polarity through the diodes ($v_1 = -V_0$) and the winding current will decay more rapidly. Note that this configuration is capable of regeneration (returning energy to the supply), but not of supplying negative current to the phase winding. However, since the torque in a VRM is proportional to the square of the phase current, there is no need for negative winding current.

As discussed in Section 10.3.2, the process of pulse-width modulation, under which a series of switch configurations alternately charge and discharge a phase winding, can be used to control the average winding current. Using this technique, an inverter such as that of Fig. 11.23a can readily be made to supply the range of waveforms required to drive a VRM.

The inverter configuration of Fig. 11.23a is perhaps the simplest of H-bridge configurations which provide regeneration capability. Its main disadvantage is that it requires two switches per phase. In many applications, the cost of the switches (and their associated drive circuitry) dominates the cost of the inverter, and the result is that this configuration is less attractive in terms of cost when compared to other configurations which require one switch per phase.

Figure 11.23b shows one such configuration. This configuration requires a split supply (i.e., two supplies of voltage V_0) but only a single switch and diode per phase.

Closing switch S1 connects the phase-1 winding to the upper dc source. Opening the switch causes the phase current to transfer to diode D1, connecting the winding to the bottom dc source. Phase 1 is thus supplied by the upper dc source and regenerates through the bottom source. Note that to maintain symmetry and to balance the energy supplied from each source equally, phase 2 is connected oppositely so that it is supplied from the bottom source and regenerates into the top source.

The major disadvantages of the configuration of Fig. 11.23b are that it requires a split supply and that when the switch is opened, the switch must withstand a voltage of $2V_0$. This can be readily seen by recognizing that when diode D1 is forward-biased, the switch is connected across the two supplies. Such switches are likely to be more expensive than the switches required by the configuration of Fig. 11.23a. Both of these issues will tend to offset some of the economic advantage which can be gained by the elimination of one switch and one diode as compared with the inverter circuit of Fig. 11.23a.

A third inverter configuration is shown in Fig. 11.23c. This configuration requires only a single dc source and uses only a single switch and diode per phase. This configuration achieves regeneration through the use of *bifilar* phase windings. In a bifilar winding, each phase is wound with two separate windings which are closely coupled magnetically (this can be achieved by winding the two windings at the same time) and can be thought of as the primary and secondary windings of a transformer.

When switch S1 is closed, the primary winding of phase 1 is energized, exciting the phase winding. Opening the switch induces a voltage in the secondary winding (note the polarity indicated by the dots in Fig. 11.23c) in such a direction as to forward-bias D1. The result is that current is transferred from the primary to the secondary winding with a polarity such that the current in the phase decays to zero and energy is returned to the source.

Although this configuration requires only a single dc source, it requires a switch which must withstand a voltage in excess of $2V_0$ (the degree of excess being determined by the voltage developed across the primary leakage reactance as current is switched from the primary to the secondary windings) and requires the more complex bifilar winding in the machine. In addition, the switches in this configuration must include snubbing circuitry (typically consisting of a resistor-capacitor combination) to protect them from transient overvoltages. These overvoltages result from the fact that although the two windings of the bifilar winding are wound such that they are as closely coupled as possible, perfect coupling cannot be achieved. As a result, there will be energy stored in the leakage fields of the primary winding which must be dissipated when the switch is opened.

As is discussed in Section 10.3, VRM operation requires control of the current applied to each phase. For example, one control strategy for constant torque production is to apply constant current to each phase during the time that $dL/d\theta_m$ for that phase is constant. This results in constant torque proportional to the square of the phase-current magnitude. The magnitude of the torque can be controlled by changing the magnitude of the phase current.

The control required to drive the phase windings of a VRM is made more complex because the phase-winding inductances change both with rotor position and

with current levels due to saturation effects in the magnetic material. As a result, it is not possible in general to implement an open-loop PWM scheme based on a precalculated algorithm. Rather, pulse-width-modulation is typically accomplished through the use of current feedback. The instantaneous phase current can be measured and a switching scheme can be devised such that the switch can be turned off when the current has been found to reach a desired maximum value and turned on when the current decays to a desired minimum value. In this manner the average phase current is controlled to a predetermined function of the rotor position and desired torque.

This section has provided a brief introduction to the topic of drive systems for variable-reluctance machines. In most cases, many additional issues must be considered before a practical drive system can be implemented. For example, accurate rotor-position sensing is required for proper control of the phase excitation, and the control loop must be properly compensated to ensure its stability. In addition, the finite rise and fall times of current buildup in the motor phase windings will ultimately limit the maximum achievable rotor torque and speed.

The performance of a complete VRM drive system is intricately tied to the performance of all its components, including the VRM, its controller, and its inverter. In this sense, the VRM is quite different from the induction, synchronous, and dc machines discussed earlier in this chapter. As a result, it is useful to design the complete drive system as an integrated package and not to design the individual components (VRM, inverter, controller, etc.) separately. The inverter configurations of Fig. 11.23 are representative of a number of possible inverter configurations which can be used in VRM drive systems. The choice of an inverter for a specific application must be made based on engineering and economic considerations as part of an integrated VRM drive system design.

11.5 SUMMARY

This chapter introduces various techniques for the control of electric machines. The broad topic of electric machine control requires a much more extensive discussion than is possible here so our objectives have been somewhat limited. Most noticeably, the discussion of this chapter focuses almost exclusively on steady-state behavior, and the issues of transient and dynamic behavior are not considered.

Much of the control flexibility that is now commonly associated with electric machinery comes from the capability of the power electronics that is used to drive these machines. This chapter builds therefore on the discussion of power electronics in Chapter 10.

The starting point is a discussion of dc motors for which it is convenient to subdivide the control techniques into two categories: speed and torque control. The algorithm for speed control in a dc motor is relatively straight forward. With the exception of a correction for voltage drop across the armature resistance, the steady-state speed is determined by the condition that the generated voltage must be equal to the applied armature voltage. Since the generated voltage is proportional to the field

flux and motor speed, we see that the steady-state motor speed is proportional to the armature voltage and inversely proportional to the field flux.

An alternative viewpoint is that of torque control. Because the commutator/brush system maintains a constant angular relationship between the field and armature flux, the torque in a dc motor is simply proportional to the product of the armature current and the field flux. As a result, dc motor torque can be controlled directly by controlling the armature current as well as the field flux.

Because synchronous motors develop torque only at synchronous speed, the speed of a synchronous motor is simply determined by the electrical frequency of the applied armature excitation. Thus, steady-state speed control is simply a matter of armature frequency control. Torque control is also possible. By transforming the stator quantities into a reference frame rotating synchronously with the rotor (using the dq0 transformation of Appendix C), we found that torque is proportional to the field flux and the component of armature current in space quadrature with the field flux. This is directly analogous to the torque production in a dc motor. Control schemes which adopt this viewpoint are referred to as *vector* or *field-oriented* control.

Induction machines operate asynchronously; rotor currents are induced by the relative motion of the rotor with respect to the synchronously rotating stator-produced flux wave. When supplied by a constant-frequency source applied to the armature winding, the motor will operate at a speed somewhat lower than synchronous speed, with the motor speed decreasing as the load torque is increased. As a result, precise speed regulation is not a simple matter, although in most cases the speed will not vary from synchronous speed by an excessive amount.

Analogous to the situation in a synchronous motor, in spite of the fact that the rotor of an induction motor rotates at less than synchronous speed, the interaction between the rotor and stator flux waves is indeed synchronous. As a result, a transformation into a synchronously rotating reference frame results in rotor and stator flux waves which are constant. The torque can then be expressed in terms of the product of the rotor flux linkages and the component of armature current in quadrature with the rotor flux linkages (referred to as the *quadrature-axis component* of the armature current) in a fashion directly analogous to the field-oriented viewpoint of a synchronous motor. Furthermore, it can be shown that the rotor flux linkages are proportional to the direct-axis component of the armature current, and thus the direct-axis component of armature current behaves much like the field current in a synchronous motor. This field-oriented viewpoint of induction machine control, in combination with the power-electronic and control systems required to implement it, has led to the widespread applicability of induction machines to a wide range of variable-speed applications.

Finally, this chapter ends with a brief discussion of the control of variable-reluctance machines. To produce useful torque, these machines typically require relatively complex, nonsinusoidal current waveforms whose shape must be controlled as a function of rotor position. Typically, these waveforms are produced by pulse-width modulation combined with current feedback using an H-bridge inverter of the type

discussed in Chapter 10. The details of these waveforms depend heavily upon the geometry and magnetic properties of the VRM and can vary significantly from motor to motor.

11.6 BIBLIOGRAPHY

Many excellent books are available which provide a much more thorough discussion of electric-machinery control than is possible in the introductory discussion presented here. This bibliography lists a few of the many textbooks available for readers who wish to study this topic in more depth.

Boldea, I., *Reluctance Synchronous Machines and Drives.* New York: Clarendon Press·Oxford, 1996.

Kenjo, T., *Stepping Motors and Their Microprocessor Controls.* New York: Clarendon Press·Oxford, 1984.

Leonhard, W., *Control of Electric Drives.* Berlin: Springer, 1996.

Miller, T. J. E., *Brushless Permanent-Magnet and Reluctance Motor Drives.* New York: Clarendon Press·Oxford, 1989.

Miller, T. J. E., *Switched Reluctance Motors and Their Controls.* New York: Magna Press Publishing and Clarendon Press·Oxford, 1993.

Mohan, N., *Advanced Electric Drives: Analysis, Control and Modeling Using Simulink.* Minneapolis: MNPERE (http://www.MNPERE.com), 2001.

Mohan, N., *Electric Drives: An Integrative Approach.* Minneapolis: MNPERE (http://www.MNPERE.com), 2001.

Murphy, J. M. D., and F. G. Turnbull, *Power Electronic Control of AC Motors.* New York: Pergamon Press, 1988.

Novotny, D. W., and T. A. Lipo, *Vector Control and Dynamics of AC Drives.* New York: Clarendon Press·Oxford, 1996.

Subrahmanyam, V., *Electric Drives: Concepts and Applications.* New York: McGraw-Hill, 1996.

Trzynadlowski, A. M., *Control of Induction Motors.* San Diego, California: Academic Press, 2001.

Vas, P., *Sensorless Vector and Direct Torque Control.* Oxford: Oxford University Press, 1998.

11.7 PROBLEMS

11.1 When operating at rated voltage, a 3-kW, 120-V, 1725 r/min separately excited dc motor achieves a no-load speed of 1718 r/min at a field current of 0.70 A. The motor has an armature resistance of 145 mA and a shunt-field resistance of 104 Ω. For the purposes of this problem you may assume the rotational losses to be negligible.

This motor will control the speed of a load whose torque is constant at 15.2 N·m over the speed range of 1500–1800 r/min. The motor will be operated at a constant armature voltage of 120 V. The field-winding will be supplied from the 120-V dc armature supply via a pulse-width modulation

system, and the motor speed will be varied by varying the duty cycle of the pulse-width modulation.

a. Calculate the field current required to achieve operation at 15.2 N·m torque and 1800 r/min. Calculate the corresponding PWM duty cycle D.

b. Calculate the field current required to achieve operation at 15.2 N·m torque and 1500 r/min. Calculate the corresponding PWM duty cycle.

c. Plot the required PWM duty cycle as a function of speed over the desired speed range of 1500 to 1800 r/min.

11.2 Repeat Problem 11.1 for a load whose torque is 15.2 N·m at 1600 r/min and which varies as the speed to the 1.8 power.

11.3 The dc motor of Problem 11.1 has a field-winding inductance $L_f = 3.7$ H and a moment of inertia $J = 0.081$ kg·m^2. The motor is operating at rated terminal voltage and an initial speed of 1300 r/min.

a. Calculate the initial field current I_f and duty cycle D.

At time $t = 0$, the PWM duty cycle is suddenly switched from the value found in part (a) to $D = 0.60$.

b. Calculate the final values of the field current and motor speed after the transient has died out.

c. Write an expression for the field-current transient as a function of time.

d. Write a differential equation for the motor speed as a function of time during this transient.

11.4 A shunt-connected 240-V, 15-kW, 3000 r/min dc motor has the following parameters

Field resistance:	$R_f = 132\ \Omega$
Armature resistance:	$R_a = 0.168\ \Omega$
Geometric constant:	$K_f = 0.422$ V/(A·rad/sec)

When operating at rated voltage, no-load, the motor current is 1.56 A.

a. Calculate the no-load speed and rotational loss.

b. Assuming the rotational loss to be constant, use MATLAB to plot the motor output power as a function of speed. Limit your plot to a maximum power output of 15 kW.

c. Armature-voltage control is to be used to maintain constant motor speed as the motor is loaded. For this operating condition, the shunt field voltage will be held constant at 240-V. Plot the armature voltage as a function of power output required to maintain the motor at a constant speed of 2950 r/min.

d. Consider that the situation for armature-voltage control is applied to this motor while the field winding remains connected in shunt across the armature terminals. Repeat part (c) for this operating condition. Is such operation feasible? Why is the motor behavior significantly different from that in part (c)?

11.5 The data sheet for a small permanent-magnet dc motor provides the following parameters:

Rated voltage:	$V_{rated} = 3$ V
Rated output power:	$P_{rated} = 0.28$ W
No-load speed:	$n_{nl} = 12{,}400$ r/min
Torque constant:	$K_m = 0.218$ mV/(r/min)
Stall torque:	$T_{stall} = 0.094$ oz·in

a. Calculate the motor armature resistance.

b. Calculate the no-load rotational loss.

c. Assume the motor to be connected to a load such that the total shaft power (actual load plus rotational loss) is equal 0.25 W at a speed of 12,000 r/min. Assuming this load to vary as the square of the motor speed, write a MATLAB script to plot the motor speed as a function of terminal voltage for $1.0 \text{ V} \leq V_a \leq 3.0$ V.

11.6 The data sheet for a 350-W permanent-magnet dc motor provides the following parameters:

Rated voltage:	$V_{rated} = 24$ V
Armature resistance:	$R_a = 97$ mΩ
No-load speed:	$n_{nl} = 3580$ r/min
No-load current:	$I_{a,nl} = 0.47$ A

a. Calculate the motor torque-constant K_m in V/(rad/sec).

b. Calculate the no-load rotational loss.

c. The motor is supplied from a 30-V dc supply through a PWM inverter. Table 11.1 gives the measured motor current as a function of the PWM duty cycle D.

Complete the table by calculating the motor speed and the load power for each value of D. Assume that the rotational losses vary as the square of the motor speed.

Table 11.1 Motor-performance data for Problem 11.6.

D	I_a (A)	r/min	P_{load} (W)
0.80	13.35		
0.75	12.70		
0.70	12.05		
0.65	11.40		
0.60	10.70		
0.55	10.05		
0.50	9.30		

11.7 The motor of Problem 11.5 has a moment of inertia of 6.4×10^{-7} oz·in·sec^2. Assuming it is unloaded and neglecting any effects of rotational loss, calculate the time required to achieve a speed of 12,000 r/min if the motor is supplied by a constant armature current of 100 mA.

11.8 An 1100-W, 150-V, 3000-r/min permanent-magnet dc motor is to be operated from a current-source inverter so as to provide direct control of the motor torque. The motor torque constant is $K_m = 0.465$ V/(rad/sec); its armature resistance is 1.37 Ω. The motor rotational loss at a speed of 3000 r/min is 87 W. Assume that the rotational loss can be represented by a constant loss torque as the motor speed varies.

a. Calculate the rated armature current of this motor. What is the corresponding mechanical torque in N·m?

b. The current source supplies a current of 6.2 A to the motor armature, and the motor speed is measured to be 2670 r/min. Calculate the load torque and power.

c. Assume the load torque of part (b) to vary linearly with speed and the motor and load to have a combined inertia of 2.28×10^{-3} kg·m^2. Calculate the motor speed as a function of time if the armature current is suddenly increased to 7.0 A.

11.9 The permanent-magnet dc motor of Problem 11.8 is operating at its rated speed of 3000 r/min and no load. If rated current is suddenly applied to the motor armature in such a direction as to slow the motor down, how long will it take the motor to reach zero speed? The inertia of the motor alone is 1.86×10^{-3} kg·m^2. Ignore the effects of rotational loss.

11.10 A 1100-kVA, 4600-V, 60-Hz, three-phase, four-pole synchronous motor is to be driven from a variable-frequency, three-phase, constant V/Hz inverter rated at 1250-kVA. The synchronous motor has a synchronous reactance of 1.18 per unit and achieves rated open-circuit voltage at a field current of 85 A.

a. Calculate the rated speed of the motor in r/min.

b. Calculate the rated current of the motor.

c. With the motor operating at rated voltage and speed and an input power of 1000-kW, calculate the field current required to achieve unity-power-factor operation.

The load power of part (c) varies as the speed to the 2.5 power. With the motor field-current held fixed, the inverter frequency is reduced such that the motor is operating at a speed of 1300 r/min.

d. Calculate the inverter frequency and the motor input power and power factor.

e. Calculate the field current required to return the motor to unity power factor.

11.11 Consider a three-phase synchronous motor for which you are given the following data:

Rated line-to-line voltage (V)
Rated volt-amperes (VA)
Rated frequency (Hz) and speed (r/min)
Synchronous reactance in per unit
Field current at rated open-circuit voltage (AFNL) (A)

The motor is to be operated from a variable-frequency, constant V/Hz inverter at speeds of up to 120 percent of the motor-rated speed.

a. Under the assumption that the motor terminal voltage and current cannot exceed their rated values, write a MATLAB script which calculates, for a given operating speed, the motor terminal voltage, the maximum possible motor input power, and the corresponding field current required to achieve this operating condition. You may consider the effects of saturation and armature resistance to be negligible.

b. Exercise your program on the synchronous motor of Problem 11.10 for motor speeds of 1500 and 2000 r/min.

11.12 For the purposes of performing field-oriented control calculations on non-salient synchronous motors, write a MATLAB script that will calculate the synchronous inductance L_s and armature-to-field mutual inductance L_{af}, both in henries, and the rated torque in N·m, given the following data:

Rated line-to-line voltage (V)
Rated (VA)
Rated frequency (Hz)
Number of poles
Synchronous reactance in per unit
Field current at rated open-circuit voltage (AFNL) (A)

11.13 A 100-kW, 460-V, 60-Hz, four-pole, three-phase synchronous machine is to be operated as a synchronous motor under field-oriented torque control using a system such as that shown in Fig. 11.13a. The machine has a synchronous reactance of 0.932 per unit and AFNL = 15.8 A. The motor is operating at rated speed, loaded to 50 percent of its rated torque at a field current of 14.0 A with the field-oriented controller set to maintain $i_D = 0$.

a. Calculate the synchronous inductance L_s and armature-to-field mutual inductance L_{af}, both in henries.

b. Find the quadrature-axis current i_Q and the corresponding rms magnitude of the armature current i_a.

c. Find the motor line-to-line terminal voltage.

11.14 The synchronous motor of Problem 11.13 is operating under field-oriented torque control such that $i_D = 0$. With the field current set equal to 14.5 A and

with the torque reference set equal to 0.75 of the motor rated torque, the motor speed is observed to be 1475 r/min.

a. Calculate the motor output power.

b. Find the quadrature-axis current i_Q and the corresponding rms magnitude of the armature current i_a.

c. Calculate the stator electrical frequency

d. Find the motor line-to-line terminal voltage.

11.15 Consider the case in which the load on the synchronous motor in the field-oriented torque-control system of Problem 11.13 is increased, and the motor begins to slow down. Based upon some knowledge of the load characteristic, it is determined that it will be necessary to raise the torque set point T_{ref} from 50 percent to 80 percent of the motor-rated torque to return the motor to its rated speed.

a. If the field current were left unchanged at 14.0 A, calculate the values of quadrature-axis current, rms armature current, and motor line-to-line terminal voltage (in V and in per unit) which would result in response to this change in reference torque.

b. To achieve this operating condition with reasonable armature terminal voltage, the field-oriented control algorithm is changed to the unity-power-factor algorithm described in the text prior to Example 11.9. Based upon that algorithm, calculate

(i) the motor terminal line-to-line terminal voltage (in V and in per unit).

(ii) the rms armature current.

(iii) the direct- and quadrature-axis currents, i_D and i_Q.

(iv) the motor field current.

11.16 Consider a 500-kW, 2300-V, 50-Hz, eight-pole synchronous motor with a synchronous reactance of 1.18 per unit and AFNL = 94 A. It is to be operated under field-oriented torque control using the unity-power-factor algorithm described in the text following Example 11.8. It will be used to drive a load whose torque varies quadratically with speed and whose torque at a speed of 750 r/min is 5900 N·m. The complete drive system will include a speed-control loop such as that shown in Fig. 11.13b.

Write a MATLAB script whose input is the desired motor speed (up to 750 r/min) and whose output is the motor torque, the field current, the direct- and quadrature-axis currents, the armature current, and the line-to-line terminal voltage. Exercise your script for a motor speed of 650 r/min.

11.17 A 2-kVA, 230-V, two-pole, three-phase permanent magnet synchronous motor achieves rated open-circuit voltage at a speed of 3500 r/min. Its synchronous inductance is 17.2 mH.

a. Calculate Λ_{PM} for this motor.

b. If the motor is operating at rated voltage and rated current at a speed of 3600 r/min, calculate the motor power in kW and the peak direct- and

quadrature-axis components of the armature current, i_D and i_Q respectively.

11.18 Field-oriented torque control is to be applied to the permanent-magnet synchronous motor of Problem 11.18. If the motor is to be operated at 4000 r/min at rated terminal voltage, calculate the maximum torque and power which the motor can supply and the corresponding values of i_D and i_Q.

11.19 A 15-kVA, 230-V, two-pole, three-phase permanent-magnet synchronous motor has a maximum speed of 10,000 r/min and produces rated open-circuit voltage at a speed of 7620 r/min. It has a synchronous inductance of 1.92 mH. The motor is to be operated under field-oriented torque control.

a. Calculate the maximum torque the motor can produce without exceeding rated armature current.

b. Assuming the motor to be operated with the torque controller adjusted to produce maximum torque (as found in part (a)) and $i_D = 0$, calculate the maximum speed at which it can be operated without exceeding rated armature voltage.

c. To operate at speeds in excess of that found in part (b), flux weakening will be employed to maintain the armature voltage at its rated value. Assuming the motor to be operating at 10,000 r/min with rated armature voltage and current, calculate
   (i) the direct-axis current i_D.
   (ii) the quadrature-axis current i_Q.
   (iii) the motor torque.
   (iv) the motor power and power factor.

11.20 The permanent magnet motor of Problem 11.17 is to be operated under vector control using the following algorithm.

Terminal voltage not to exceed rated value

Terminal current not to exceed rated value

$i_D = 0$ unless flux weakening is required to avoid excessive armature voltage

Write a MATLAB script to produce plots of the maximum power and torque which this system can produce as a function of motor speed for speeds up to 10,000 r/min.

11.21 Consider a 460-V, 25-kW, four-pole, 60-Hz induction motor which has the following equivalent-circuit parameters in ohms per phase referred to the stator:

$$R_1 = 0.103 \quad R_2 = 0.225 \quad X_1 = 1.10 \quad X_2 = 1.13 \quad X_m = 59.4$$

The motor is to be operated from a variable frequency, constant-V/Hz drive whose output is 460-V at 60-Hz. Neglect any effects of rotational loss. The motor drive is initially adjusted to a frequency of 60 Hz.

a. Calculate the peak torque and the corresponding slip and motor speed in r/min.

b. Calculate the motor torque at a slip of 2.9 percent and the corresponding output power.

c. The drive frequency is now reduced to 35 Hz. If the load torque remains constant, estimate the resultant motor speed in r/min. Find the resultant motor slip, speed in r/min, and output power.

11.22 Consider the 460-V, 250-kW, four-pole induction motor and drive system of Problem 11.21.

a. Write a MATLAB script to plot the speed-torque characteristic of the motor at drive frequencies of 20, 40, and 60 Hz for speeds ranging from −200 r/min to the synchronous speed at each frequency.

b. Determine the drive frequency required to maximize the starting torque and calculate the corresponding torque in N·m.

11.23 A 550-kW, 2400-V, six-pole, 60-Hz three-phase induction motor has the following equivalent-circuit parameters in ohms-per-phase-Y referred to the stator:

$$R_1 = 0.108 \quad R_2 = 0.296 \quad X_1 = 1.18 \quad X_2 = 1.32 \quad X_m = 48.4$$

The motor will be driven by a constant-V/Hz drive whose voltage is 2400 V at a frequency of 60 Hz.

The motor is used to drive a load whose power is 525 kW at a speed of 1138 r/min and which varies as the cube of speed. Using MATLAB, plot the motor speed as a function of frequency as the drive frequency is varied between 20 and 60 Hz.

11.24 A 150-kW, 60-Hz, six-pole, 460-V three-phase wound-rotor induction motor develops full-load torque at a speed of 1157 r/min with the rotor short-circuited. An external noninductive resistance of 870 mΩ is placed in series with each phase of the rotor, and the motor is observed to develop its rated torque at a speed of 1072 r/min. Calculate the resistance per phase of the original motor.

11.25 The wound rotor of Problem 11.24 will be used to drive a constant-torque load equal to the rated full-load torque of the motor. Using the results of Problem 11.24, calculate the external rotor resistance required to adjust the motor speed to 850 r/min.

11.26 A 75-kW, 460-V, three-phase, four-pole, 60-Hz, wound-rotor induction motor develops a maximum internal torque of 212 percent at a slip of 16.5 percent when operated at rated voltage and frequency with its rotor short-circuited directly at the slip rings. Stator resistance and rotational losses may be neglected, and the rotor resistance may be assumed to be constant, independent of rotor frequency. Determine

a. the slip at full load in percent.

b. the rotor I^2R loss at full load in watts.

c. the starting torque at rated voltage and frequency N·m.

If the rotor resistance is now doubled (by inserting external series resistance at the slip rings), determine

d. the torque in N·m when the stator current is at its full-load value.

e. the corresponding slip.

11.27 A 35-kW, three-phase, 440-V, six-pole wound-rotor induction motor develops its rated full-load output at a speed of 1169 r/min when operated at rated voltage and frequency with its slip rings short-circuited. The maximum torque it can develop at rated voltage and frequency is 245 percent of full-load torque. The resistance of the rotor winding is 0.23 Ω/phase Y. Neglect rotational and stray-load losses and stator resistance.

a. Compute the rotor I^2R loss at full load.

b. Compute the speed at maximum torque.

c. How much resistance must be inserted in series with the rotor to produce maximum starting torque?

The motor is now run from a 50-Hz supply with the applied voltage adjusted so that, for any given torque, the air-gap flux wave has the same amplitude as it does when operated 60 Hz at the same torque level.

d. Compute the 50-Hz applied voltage.

e. Compute the speed at which the motor will develop a torque equal to its rated value at 60-Hz with its slip rings short-circuited.

11.28 The three-phase, 2400-V, 550-kW, six-pole induction motor of Problem 11.23 is to be driven from a field-oriented speed-control system whose controller is programmed to set the rotor flux linkages λ_{DR} equal to the machine rated peak value. The machine is operating at 1148 r/min driving a load which is known to be 400 kW at this speed. Find:

a. the value of the peak direct- and quadrature-axis components of the armature currents i_D and i_Q.

b. the rms armature current under this operating condition.

c. the electrical frequency of the drive in Hz.

d. the rms line-to-line armature voltage.

11.29 A field-oriented drive system will be applied to a 230-V, 20-kW, four-pole, 60-Hz induction motor which has the following equivalent-circuit parameters in ohms per phase referred to the stator:

$$R_1 = 0.0322 \quad R_2 = 0.0703 \quad X_1 = 0.344 \quad X_2 = 0.353 \quad X_m = 18.6$$

The motor is connected to a load whose torque can be assumed proportional to speed as $T_{load} = 85(n/1800)$ N·m, where n is the motor speed in r/min.

The field-oriented controller is adjusted such that the rotor flux linkages λ_{DR} are equal to the machine's rated peak flux linkages, and the motor speed is 1300 r/min. Find

a. the electrical frequency in Hz.

b. the rms armature current and line-to-line voltage.

c. the motor input kVA.

If the field-oriented controller is set to maintain the motor speed at 1300 r/min, write a MATLAB script to plot the rms armature V/Hz as a percentage of the rated V/Hz as a function of λ_{DR} as λ_{DR} is varied between 80 and 120 percent of the machine's rated peak flux linkages.

11.30 The 20-kW induction motor-drive and load of Problem 11.29 is operating at a speed of 1450 r/min with the field-oriented controller adjusted to maintain the rotor flux linkages λ_{DR} equal to the machine's rated peak value.

a. Calculate the corresponding values of the direct- and quadrature-axis components of the armature current, i_D and i_Q, and the rms armature current.

b. Calculate the corresponding line-to-line terminal voltage drive electrical frequency.

The quadrature-axis current i_Q is now increased by 10 percent while the direct-axis current is held constant.

c. Calculate the resultant motor speed and power output.

d. Calculate the terminal voltage and drive frequency.

e. Calculate the total kVA input into the motor.

f. With the controller set to maintain constant speed, determine the set point for λ_{DR}, as a percentage of rated peak flux linkages, that sets the terminal V/Hz equal to the rated machine rated V/Hz. (Hint: This solution is most easily found using a MATLAB script to search for the desired result.)

11.31 A three-phase, eight-pole, 60-Hz, 4160-V, 1250-kW squirrel-cage induction motor has the following equivalent-circuit parameters in ohms-per-phase-Y referred to the stator:

$$R_1 = 0.212 \quad R_2 = 0.348 \quad X_1 = 1.87 \quad X_2 = 2.27 \quad X_m = 44.6$$

It is operating from a field-oriented drive system at a speed of 805 r/min and a power output of 1050 kW. The field-oriented controller is set to maintain the rotor flux linkages λ_{DR} equal to the machine's rated peak flux linkages.

a. Calculate the motor rms line-to-line terminal voltage, rms armature current, and electrical frequency.

b. Show that steady-state induction-motor equivalent circuit and corresponding calculations of Chapter 6 give the same output power and terminal current when the induction motor speed is 828 r/min and the terminal voltage and frequency are equal to those found in part (a).

APPENDIX A

Three-Phase Circuits

Generation, transmission, and heavy-power utilization of ac electric energy almost invariably involve a type of system or circuit called a *polyphase system* or *polyphase circuit*. In such a system, each voltage source consists of a group of voltages having related magnitudes and phase angles. Thus, an n-phase system employs voltage sources which typically consist of n voltages substantially equal in magnitude and successively displaced by a phase angle of $360°/n$. A *three-phase system* employs voltage sources which typically consist of three voltages substantially equal in magnitude and displaced by phase angles of 120°. Because it possesses definite economic and operating advantages, the three-phase system is by far the most common, and consequently emphasis is placed on three-phase circuits in this appendix.

The three individual voltages of a three-phase source may each be connected to its own independent circuit. We would then have three separate *single-phase systems*. Alternatively, as will be shown in Section A.1, symmetrical electric connections can be made between the three voltages and the associated circuitry to form a three-phase system. It is the latter alternative that we are concerned with in this appendix. Note that the word *phase* now has two distinct meanings. It may refer to a portion of a polyphase system or circuit, or, as in the familiar steady-state circuit theory, it may be used in reference to the angular displacement between voltage or current phasors. There is very little possibility of confusing the two.

A.1 GENERATION OF THREE-PHASE VOLTAGES

Consider the elementary two-pole, three-phase generator of Fig. A.1. On the armature are three coils aa', bb', and cc' whose axes are displaced 120° in space from each other. This winding can be represented schematically as shown in Fig. A.2. When the field is excited and rotated, voltages will be generated in the three phases in accordance with Faraday's law. If the field structure is designed so that the flux is

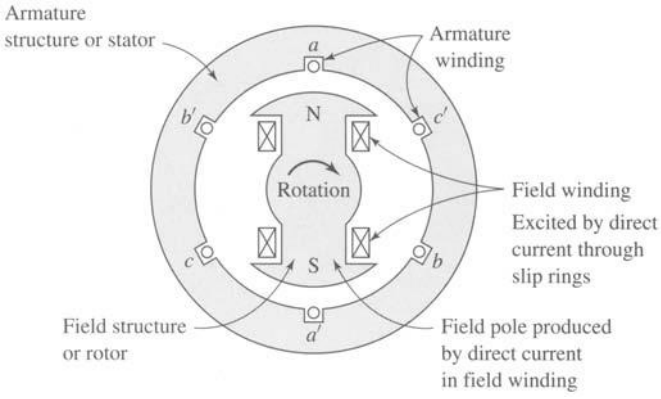

Figure A.1 Elementary two-pole, three-phase generator.

distributed sinusoidally over the poles, the flux linking any phase will vary sinusoidally with time, and sinusoidal voltages will be induced in the three phases. As shown in Fig. A.3, these three voltages will be displaced 120° electrical degrees in time as a result of the phases being displaced 120° in space. The corresponding phasor diagram is shown in Fig. A.4. In general, the time origin and the reference axis in diagrams such as Figs. A.3 and A.4 are chosen on the basis of analytical convenience.

There are two possibilities for the utilization of voltages generated in this manner. The six terminals a, a', b, b', c, and c' of the three-phase winding may be connected to three independent single-phase systems, or the three phases of the winding may be interconnected and used to supply a three-phase system. The latter procedure is adopted almost universally. The three phases of the winding may be interconnected in two possible ways, as shown in Fig. A.5. Terminals a', b', and c' may be joined to form the neutral o, yielding a Y *connection,* or terminals a and b', b and c', and c and a' may be joined individually, yielding a Δ *connection*. In the Y connection, a neutral conductor, shown dashed in Fig. A.5a, may or may not be brought out. If a neutral conductor exists, the system is a four-wire, three-phase system; if not, it is a three-wire, three-phase system. In the Δ connection (Fig. A.5b), no neutral exists and only a three-wire, three-phase system can be formed.

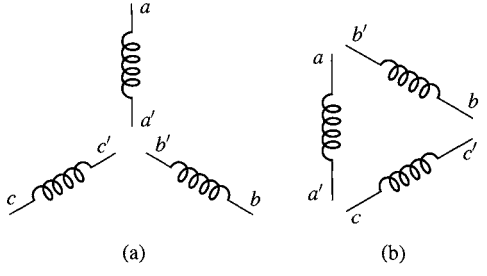

Figure A.2 Schematic representation of the windings of Fig. A.1.

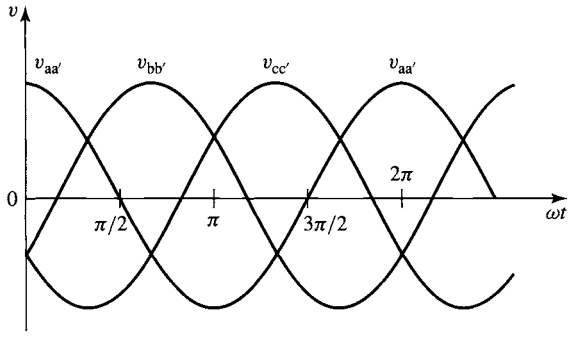

Figure A.3 Voltages generated in the windings of Figs. A.1 and A.2.

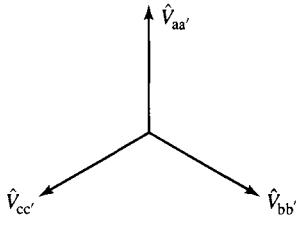

Figure A.4 Phasor diagram of generated voltages.

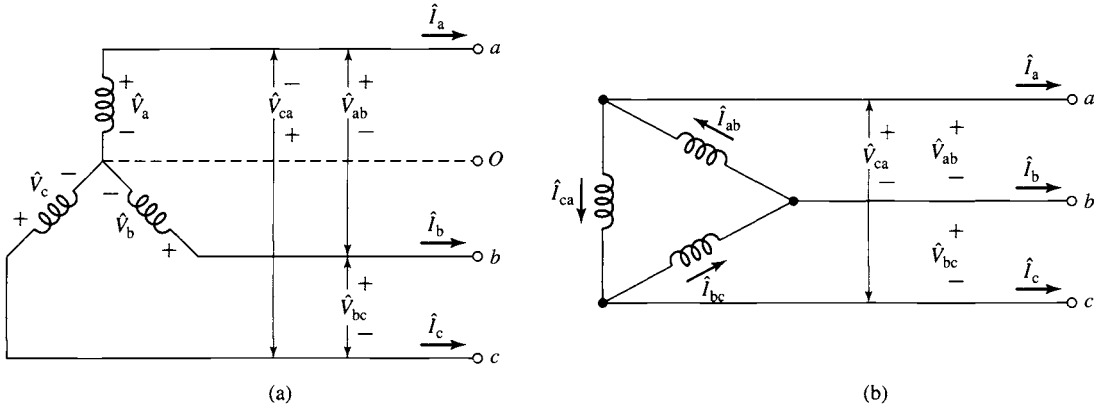

Figure A.5 Three-phase connections: (a) Y connection and (b) Δ connection.

The three phase voltages of Figs. A.3 and A.4, are equal and displaced in phase by 120 degrees, a general characteristic of a *balanced three-phase system*. Furthermore, in a balanced three-phase system the impedance in any one phase is equal to that in either of the other two phases, so that the resulting phase currents are also equal and displaced in phase from each other by 120 degrees. Likewise, equal power and equal

reactive power flow in each phase. An *unbalanced three-phase system,* however, may be unbalanced in one or more of many ways; the source voltages may be unbalanced, either in magnitude or in phase, or the phase impedances may not be equal. Note that *only balanced systems are treated in this appendix, and none of the methods developed or conclusions reached apply to unbalanced systems.* Most practical analyses are conducted under the assumption of a balanced system. Many industrial loads are three-phase loads and therefore inherently balanced, and in supplying single-phase loads from a three-phase source definite efforts are made to keep the three-phase system balanced by assigning approximately equal single-phase loads to each of the three phases.

A.2 THREE-PHASE VOLTAGES, CURRENTS, AND POWER

When the three phases of the winding in Fig. A.1 are Y-connected, as in Fig. A.5a, the phasor diagram of voltages is that of Fig. A.6. The *phase order* or *phase sequence* in Fig. A.6 is *abc*; that is, the voltage of phase *a* reaches its maximum 120° before that of phase *b*.

The three-phase voltages $\hat{V}_a$, $\hat{V}_b$, and $\hat{V}_c$ are called *line-to-neutral voltages.* The three voltages $\hat{V}_{ab}$, $\hat{V}_{bc}$, and $\hat{V}_{ca}$ are called *line-to-line voltages.* The use of

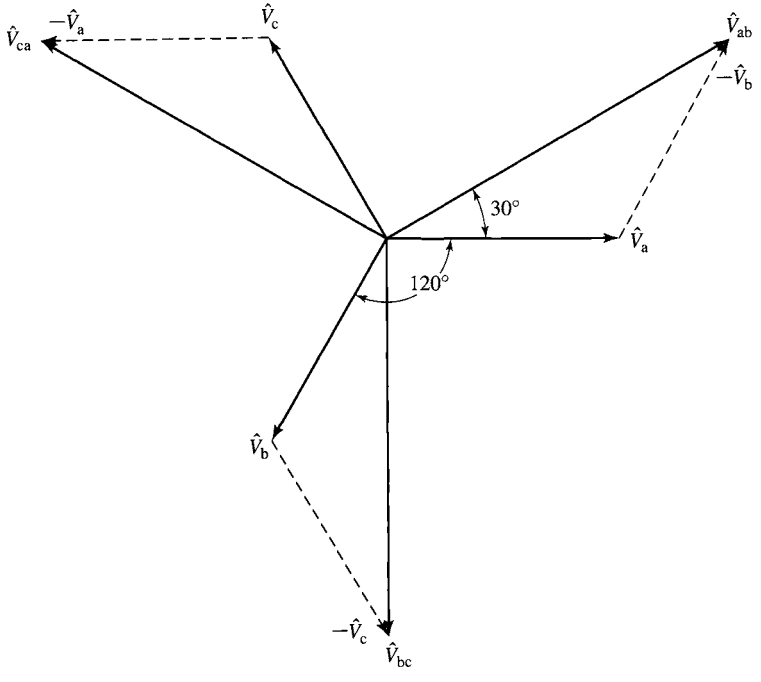

Figure A.6 Voltage phasor diagram for a Y-connected system.

double-subscript notation in Fig. A.6 greatly simplifies the task of drawing the complete diagram. The subscripts indicate the points between which the voltage is determined; for example, the voltage $\hat{V}_{ab}$ is calculated as $\hat{V}_{ab} = \hat{V}_a - \hat{V}_b$.

By Kirchhoff's voltage law, the line-to-line voltage $\hat{V}_{ab}$ is

$$\hat{V}_{ab} = \hat{V}_a - \hat{V}_b = \sqrt{3}\,\hat{V}_a \angle 30^\circ \tag{A.1}$$

as shown in Fig. A.6. Similarly,

$$\hat{V}_{bc} = \sqrt{3}\,\hat{V}_b \angle 30^\circ \tag{A.2}$$

and

$$\hat{V}_{ca} = \sqrt{3}\,\hat{V}_c \angle 30^\circ \tag{A.3}$$

These equations show that *the magnitude of the line-to-line voltage is $\sqrt{3}$ times the line-to-neutral voltage.*

When the three phases are Δ-connected, the corresponding phasor diagram of currents is given in Fig. A.7. The Δ currents are $\hat{I}_{ab}$, $\hat{I}_{bc}$, and $\hat{I}_{ca}$. By Kirchhoff's current law, the line current $\hat{I}_a$ is

$$\hat{I}_a = \hat{I}_{ab} - \hat{I}_{ca} = \sqrt{3}\,\hat{I}_{ab} \angle -30^\circ \tag{A.4}$$

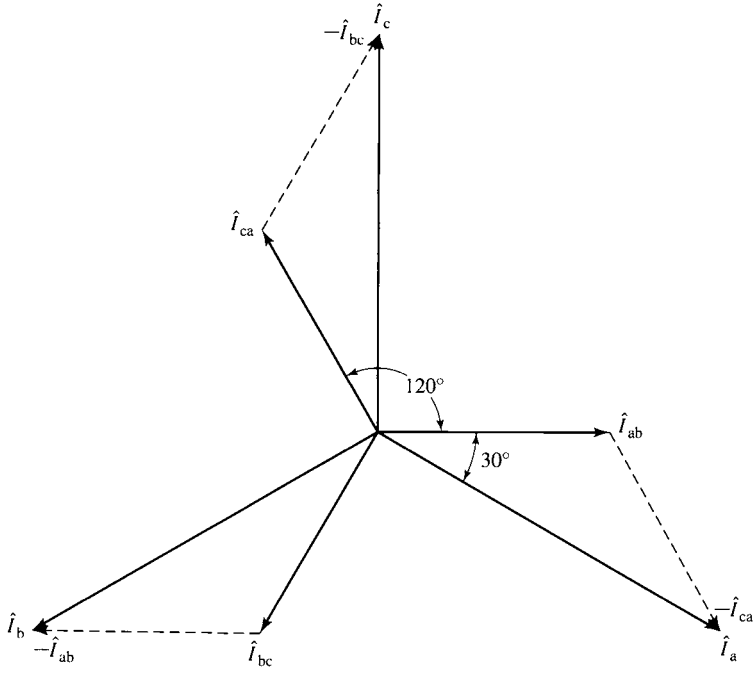

Figure A.7 Current phasor diagram for Δ connection.

as can be seen from the phasor diagram of Fig. A.7. Similarly,

$$\hat{I}_b = \sqrt{3}\,\hat{I}_{bc}\angle -30^\circ \tag{A.5}$$

and

$$\hat{I}_c = \sqrt{3}\,\hat{I}_{ca}\angle -30^\circ \tag{A.6}$$

Stated in words, Eqs. A.4 to A.6 show that for a Δ connection, *the magnitude of the line current is* $\sqrt{3}$ *times that of the* Δ *current.* Evidently, the relations between Δ currents and line currents of a Δ connection are similar to those between the line-to-neutral and line-to-line voltages of a Y connection.

With the time origin taken at the maximum positive point of the phase-*a* voltage wave, the instantaneous voltages of the three phases are

$$v_a(t) = \sqrt{2}\,V_{rms}\cos\omega t \tag{A.7}$$

$$v_b(t) = \sqrt{2}\,V_{rms}\cos(\omega t - 120^\circ) \tag{A.8}$$

$$v_c(t) = \sqrt{2}\,V_{rms}\cos(\omega t + 120^\circ) \tag{A.9}$$

where V_{rms} is the rms value of the phase-to-neutral voltage. When the phase currents are displaced from the corresponding phase voltages by the angle θ, the instantaneous phase currents are

$$i_a(t) = \sqrt{2}\,I_{rms}\cos(\omega t + \theta) \tag{A.10}$$

$$i_b(t) = \sqrt{2}\,I_{rms}\cos(\omega t + \theta - 120^\circ) \tag{A.11}$$

$$i_c(t) = \sqrt{2}\,I_{rms}\cos(\omega t + \theta + 120^\circ) \tag{A.12}$$

where I_{rms} is the rms value of the phase current.

The instantaneous power in each phase then becomes

$$p_a(t) = v_a(t)i_a(t) = V_{rms}I_{rms}[\cos(2\omega t + \theta) + \cos\theta] \tag{A.13}$$

$$p_b(t) = v_b(t)i_b(t) = V_{rms}I_{rms}[\cos(2\omega t + \theta - 240^\circ) + \cos\theta] \tag{A.14}$$

$$p_c(t) = v_c(t)i_c(t) = V_{rms}I_{rms}[\cos(2\omega t + \theta + 240^\circ) + \cos\theta] \tag{A.15}$$

Note that the average power of each phase is equal

$$<p_a(t)> = <p_b(t)> = <p_c(t)> = V_{rms}I_{rms}\cos\theta \tag{A.16}$$

The phase angle θ between the voltage and current is referred to as the *power-factor angle* and $\cos\theta$ is referred to as the *power factor.* If θ is negative, then the power factor is said to be *lagging;* if θ is power, then the power factor is said to be *leading.*

The total instantaneous power for all three phases is

$$p(t) = p_a(t) + p_b(t) + p_c(t) = 3V_{rms}I_{rms}\cos\theta \tag{A.17}$$

Notice that the sum of the cosine terms which involve time in Eqs. A.13 to A.15 (the first terms in the brackets) is zero. We have shown that *the total of the instantaneous power for the three phases of a balanced three-phase circuit is constant and*

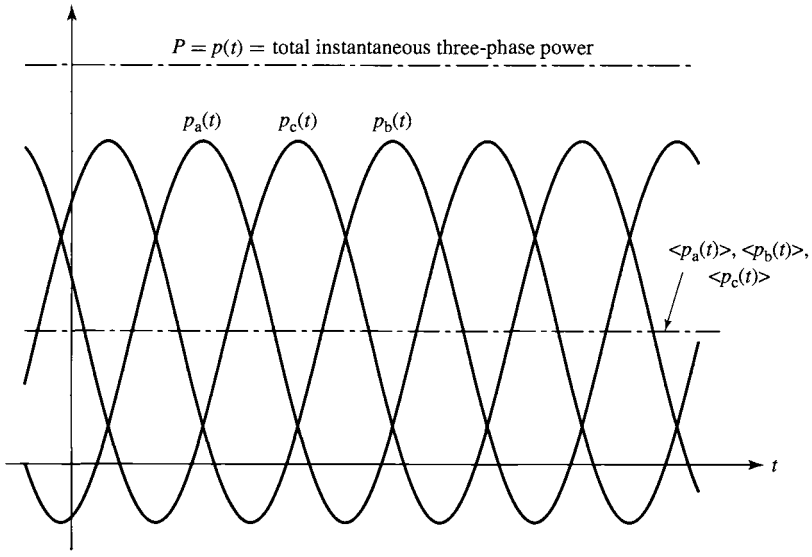

Figure A.8 Instantaneous power in a three-phase system.

does not vary with time. This situation is depicted graphically in Fig. A.8. Instantaneous powers for the three phases are plotted, together with the total instantaneous power, which is the sum of the three individual waves. *The total instantaneous power for a balanced three-phase system is equal to 3 times the average power per phase.* This is one of the outstanding advantages of polyphase systems. It is of particular advantage in the operation of polyphase motors since it means that the shaft-power output is constant and that torque pulsations, with the consequent tendency toward vibration, do not result.

On the basis of single-phase considerations, the average power per phase P_p for either a Y- or Δ-connected system connected to a balanced three-phase load of impedance $Z_p = R_p + jX_p\ \Omega$/phase is

$$P_p = V_{rms} I_{rms} \cos\theta = I_p^2 R_p \tag{A.18}$$

Here R_p is the resistance per phase. The total three-phase power P is

$$P = 3P_p \tag{A.19}$$

Similarly, for reactive power per phase Q_p and total three-phase reactive power Q,

$$Q_p = V_{rms} I_{rms} \sin\theta = I_p^2 X_p \tag{A.20}$$

and

$$Q = 3Q_p \tag{A.21}$$

where X_p is the reactance per phase.

The voltamperes per phase $(VA)_p$ and total three-phase voltamperes VA are

$$(VA)_p = V_{rms} I_{rms} = I_{rms}^2 Z_p \tag{A.22}$$

$$VA = 3(VA)_p \tag{A.23}$$

In Eqs. A.18 and A.20, θ is the angle between phase voltage and phase current. As in the single-phase case, it is given by

$$\theta = \tan^{-1} \frac{X_p}{R_p} = \cos^{-1} \frac{R_p}{Z_p} = \sin^{-1} \frac{X_p}{Z_p} \tag{A.24}$$

The power factor of a balanced three-phase system is therefore equal to that of any one phase.

A.3 Y- AND Δ-CONNECTED CIRCUITS

Three specific examples are given to illustrate the computational details of Y- and Δ-connected circuits. Explanatory remarks which are generally applicable are incorporated into the solutions.

EXAMPLE A.1

In Fig. A.9 is shown a 60-Hz transmission system consisting of a line having the impedance $Z_l = 0.05 + j0.20\ \Omega$, at the receiving end of which is a load of equivalent impedance $Z_L = 10.0 + j3.00\ \Omega$. The impedance of the return conductor should be considered zero.

a. Compute the line current I; the load voltage V_L; the power, reactive power, and voltamperes taken by the load; and the power and reactive-power loss in the line.

   Suppose now that three such identical systems are to be constructed to supply three such identical loads. Instead of drawing the diagrams one below the other, let them be drawn in the fashion shown in Fig. A.10, which is, of course, the same electrically.

b. For Fig. A.10 give the current in each line; the voltage at each load; the power, reactive power, and voltamperes supplied to each load; the power and reactive-power loss in each of the three transmission systems; the total power, reactive power, and voltamperes supplied to the loads; and the total power and reactive-power loss in the three transmission systems.

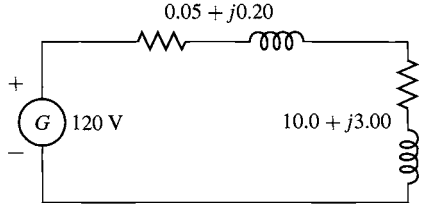

Figure A.9 Circuit for Example A.1, part (a).

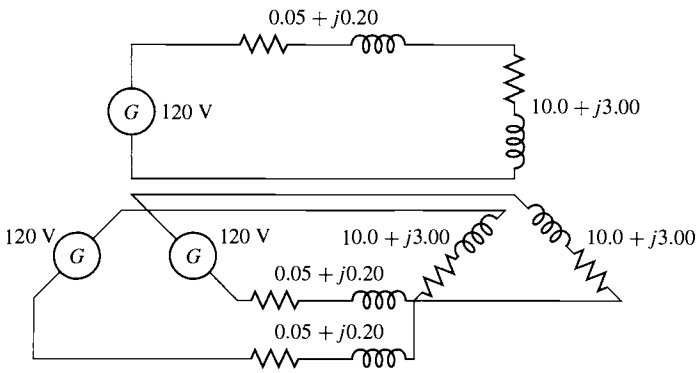

Figure A.10 Circuit for Example A.1, part (b).

Next consider that the three return conductors are combined into one and that the phase relationship of the voltage sources is such that a balanced four-wire, three-phase system results, as in Fig. A.11.

c. For Fig. A.11 give the line current; the load voltage, both line-to-line and line-to-neutral; the power, reactive power, and voltamperes taken by each phase of the load; the power and reactive-power loss in each line; the total three-phase power, reactive power, and voltamperes taken by the load; and the total power and reactive-power loss in the lines.
d. In Fig. A.11 what is the current in the combined return or neutral conductor?
e. Can this conductor be dispensed with in Fig. A.11 if desired?

Assume now that this neutral conductor is omitted. This results in the three-wire, three-phase system of Fig. A.12.

f. Repeat part (c) for Fig. A.12.
g. On the basis of the results of this example, outline briefly the method of reducing a balanced three-phase Y-connected circuit problem to its equivalent single-phase problem. Be careful to distinguish between the use of line-to-line and line-to-neutral voltages.

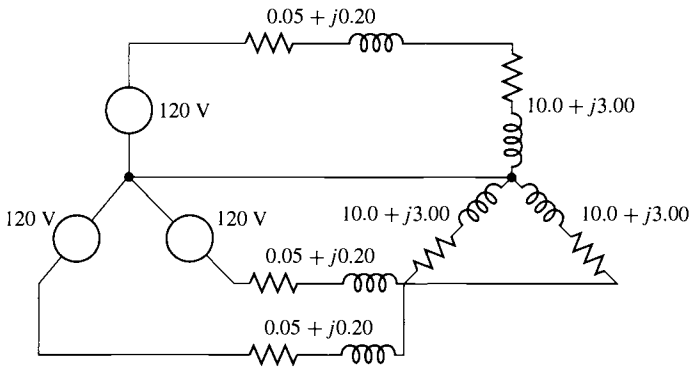

Figure A.11 Circuit for Example A.1, parts (c) to (e).

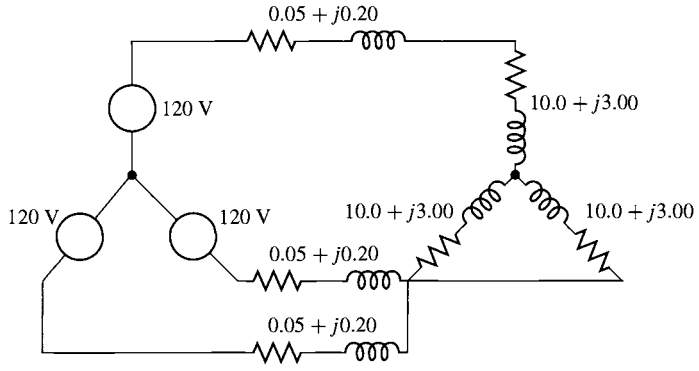

Figure A.12 Circuit for Example A.1 part (f).

■ Solution

a.

$$I = \frac{120}{\sqrt{(0.05 + 10.0)^2 + (0.20 + 3.00)^2}} = 11.4 \text{ A}$$

$$V_L = I|Z_L| = 11.4\sqrt{(10.0)^2 + (3.00)^2} = 119 \text{ V}$$

$$P_L = I^2 R_L = (11.4)^2(3.00) = 1200 \text{ W}$$

$$Q_L = I^2 X_L = (11.4)^2(3.00) = 390 \text{ VA reactive}$$

$$(\text{VA})_L = I^2|Z_L| = (11.4)^2\sqrt{(10.0)^2 + (3.00)^2} = 1360 \text{ VA}$$

$$P_l = I^2 R_l = (11.4)^2(0.05) = 6.5 \text{ W}$$

$$Q_l = I^2 X_l = (11.4)^2(0.20) = 26 \text{ VA reactive}$$

b. The first four obviously have the same values as in part (a).

Total power $= 3P_L = 3(1300) = 3900$ W

Total reactive power $= 3Q_L = 3(390) = 1170$ VA reactive

Total VA $= 3(\text{VA})_L = 3(1360) = 4080$ VA

Total power loss $= 3P_l = 3(6.5) = 19.5$ W

Total reactive-power loss $= 3Q_l = 3(26) = 78$ VA reactive

c. The results obtained in part (b) are unaffected by this change. The voltage in parts (a) and (b) is now the line-to-neutral voltage. The line-to-line voltage is

$$\sqrt{3}(119) = 206 \text{ V}$$

d. By Kirchhoff's current law, the neutral current is the phasor sum of the three line currents. These line currents are equal and displaced in phase by 120°. Since the phasor sum of three equal phasors 120° apart is zero, the neutral current is zero.

e. The neutral current being zero, the neutral conductor can be dispensed with if desired.

f. Since the presence or absence of the neutral conductor does not affect conditions, the values are the same as in part (c).

g. A neutral conductor can be assumed, regardless of whether one is physically present. Since the neutral conductor in a balanced three-phase circuit carries no current and hence has no voltage drop across it, the neutral conductor should be considered to have zero impedance. Then one phase of the Y, together with the neutral conductor, can be removed for study. Since this phase is uprooted at the neutral, *line-to-neutral voltages must be used.* This procedure yields the single-phase equivalent circuit, in which all quantities correspond to those in one phase of the three-phase circuit. Conditions in the other two phases being the same (except for the 120° phase displacements in the currents and voltages), there is no need for investigating them individually. Line currents in the three-phase system are the same as in the single-phase circuit, and total three-phase power, reactive power, and voltamperes are three times the corresponding quantities in the single-phase circuit. If line-to-line voltages are desired, they must be obtained by multiplying voltages in the single-phase circuit by $\sqrt{3}$.

EXAMPLE A.2

Three impedances of value $Z_Y = 4.00 + j3.00 = 5.00\angle 36.9°\ \Omega$ are connected in Y, as shown in Fig. A.13. For balanced line-to-line voltages of 208 V, find the line current, the power factor, and the total power, reactive power, and voltamperes.

■ Solution

The rms line-to-neutral voltage V on any one phase, such as phase a, is

$$V = \frac{208}{\sqrt{3}} = 120\ \text{V}$$

Hence, the line current

$$\hat{I} = \frac{V}{Z_Y} = \frac{120}{5.00\angle 36.9°} = 24.0\ \angle -36.9°\ \text{A}$$

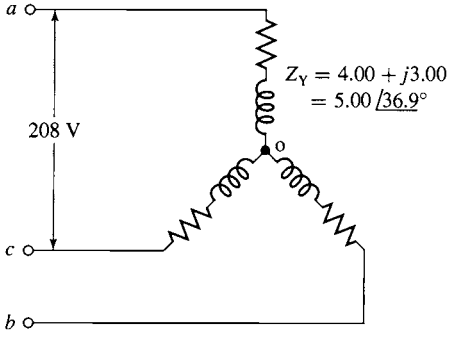

Figure A.13 Circuit for Example A.2.

and the power factor is equal to

$$\text{Power factor} = \cos\theta = \cos(-36.9°) = 0.80 \text{ lagging}$$

Thus

$$P = 3I^2R_Y = 3(24.0)^2(4.00) = 6910 \text{ W}$$

$$Q = 3I^2X_Y = 3(24.0)^2(3.00) = 5180 \text{ VA reactive}$$

$$\text{VA} = 3VI = 3(120)(24.0) = 8640 \text{ VA}$$

Note that phases *a* and *c* (Fig. A.13) do not form a simple series circuit. Consequently, the current cannot be found by dividing 208 V by the sum of the phase-*a* and -*c* impedances. To be sure, an equation can be written for voltage between points *a* and *c* by Kirchhoff's voltage law, but this must be a phasor equation taking account of the 120° phase displacement between the phase-*a* and phase-*c* currents. As a result, the method of thought outlined in Example A.1 leads to the simplest solution.

EXAMPLE A.3

Three impedances of value $Z_\Delta = 12.00 + j9.00 = 15.00\angle 36.9° \ \Omega$ are connected in Δ, as shown in Fig. A.14. For balanced line-to-line voltages of 208 V, find the line current, the power factor, and the total power, reactive power, and voltamperes.

■ Solution

The voltage across any one leg of the Δ, V_Δ is equal to the line-to-line voltage V_{l-l}, which is equal to $\sqrt{3}$ times the line-to-neutral voltage V. Consequently,

$$V = \frac{V_{l-l}}{\sqrt{3}} = \frac{208}{\sqrt{3}} = 120 \text{ V}$$

and the current in the Δ is given by the line-to-line voltage divided by the Δ impedance

$$\hat{I}_\Delta = \frac{V_{l-l}}{Z_\Delta} = \frac{208}{15.00\angle 36.9°} = 13.87\angle -36.9° \text{ A}$$

$$\text{Power factor} = \cos\theta = \cos(-36.9°) = 0.80 \text{ lagging}$$

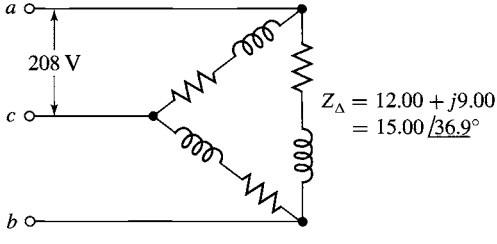

Figure A.14 Circuit for Example A.3.

From Eq. A.4 the phase current is equal to

$$I = \sqrt{3}I_\Delta = \sqrt{3}(13.87) = 24.0 \text{ A}$$

Also

$$P = 3P_\Delta = 3I_\Delta^2 R_\Delta = 3(13.87)^2(12.00) = 6910 \text{ W}$$

$$Q = 3Q_\Delta = 3I_\Delta^2 X_\Delta = 3(13.87)^2(9.00) = 5180 \text{ VA reactive}$$

and

$$\text{VA} = 3(\text{VA})_\Delta = 3V_{l-l}I_\Delta = 3(208)(13.87) = 8640 \text{ VA}$$

Note that phases *ab* and *bc* do not form a simple series circuit, nor does the path *cba* form a simple parallel combination with the direct path through the phase *ca*. Consequently, the line current cannot be found by dividing 208 V by the equivalent impedance of Z_{ca} in parallel with $Z_{ab} + Z_{bc}$. Kirchhoff's-law equations involving quantities in more than one phase can be written, but they must be phasor quantities taking account of the 120° phase displacement between phase currents and phase voltages. As a result, the method outlined above leads to the simplest solution.

Comparison of the results of Examples A.2 and A.3 leads to a valuable and interesting conclusion. Note that the line-to-line voltage, line current, power factor, total power, reactive power, and voltamperes are precisely equal in the two cases; in other words, conditions viewed from the terminals *A*, *B*, and *C* are identical, and one cannot distinguish between the two circuits from their terminal quantities. It will also be seen that the impedance, resistance, and reactance per phase of the Y connection (Fig. A.13) are exactly one-third of the corresponding values per phase of the Δ connection (Fig. A.14). Consequently, a balanced Δ connection can be replaced by a balanced Y connection providing that the circuit constants per phase obey the relation

$$Z_Y = \frac{1}{3}Z_\Delta \tag{A.25}$$

Conversely, a Y connection can be replaced by a Δ connection provided Eq. A.25 is satisfied. The concept of this Y-Δ equivalence stems from the general Y-Δ transformation and is not the accidental result of a specific numerical case.

Two important corollaries follow from this equivalence: (1) A general computational scheme for balanced circuits can be based entirely on Y-connected circuits or entirely on Δ-connected circuits, whichever one prefers. Since it is frequently more convenient to handle a Y connection, the former scheme is usually adopted. (2) In the frequently occurring problems in which the connection is not specified and is not pertinent to the solution, either a Y or a Δ connection may be assumed. Again the Y connection is more commonly selected. In analyzing three-phase motor performance, for example, the actual winding connections need not be known unless the investigation is to include detailed conditions within the windings themselves. The entire analysis can then be based on an assumed Y connection.

A.4 ANALYSIS OF BALANCED THREE-PHASE CIRCUITS; SINGLE-LINE DIAGRAMS

By combining the principle of Δ-Y equivalence with the technique revealed by Example A.1, a simple method of reducing a balanced three-phase-circuit problem to its corresponding single-phase problem can be developed. All the methods of single-phase-circuit analysis thus become available for its solution. The end results of the single-phase analysis are then translated back into three-phase terms to give the final results.

In carrying out this procedure, phasor diagrams need be drawn for only one phase of the Y connection, the diagrams for the other two phases being unnecessary repetition. Furthermore, circuit diagrams can be simplified by drawing only one phase. Examples of such *single-line diagrams* are given in Fig. A.15, showing two three-phase generators with their associated lines or cables supplying a common substation load. Specific connections of apparatus can be indicated if desired. Thus, Fig. A.15b shows that G_1 is Y-connected and G_2 is Δ-connected. Impedances are given in ohms per phase.

When one is dealing with power, reactive power, and voltamperes, it is sometimes more convenient to deal with the entire three-phase circuit at once instead of concentrating on one phase. This possibility arises because simple expressions for three-phase power, reactive power, and voltamperes can be written in terms of line-to-line voltage and line current regardless of whether the circuit is Y- or Δ-connected. Thus, from Eqs. A.18 and A.19, three-phase power is

$$P = 3P_p = 3V_pI_p\cos\theta \tag{A.26}$$

Since $V_{l-l} = \sqrt{3}V_p$, Eq. A.26 becomes

$$P = \sqrt{3}V_{l-l}I_p\cos\theta \tag{A.27}$$

Similarly,

$$Q = \sqrt{3}V_{l-l}I_p\sin\theta \tag{A.28}$$

and

$$\text{VA} = \sqrt{3}V_{l-l}I_p \tag{A.29}$$

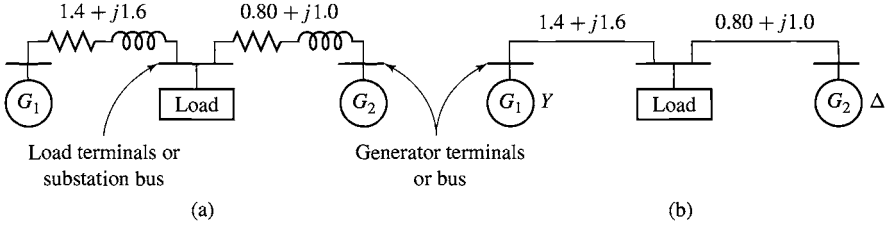

Figure A.15 Examples of single-line diagrams.

It should be borne in mind, however, that the power-factor angle θ, given by Eq. A.24, is the angle between $\hat{V}_p$ and $\hat{I}_p$ and not that between $\hat{V}_{l-l}$ and $\hat{I}_p$.

EXAMPLE A.4

Figure A.15 is the equivalent circuit of a load supplied from two three-phase generating stations over lines having the impedances per phase given on the diagram. The load requires 30 kW at 0.80 power factor lagging. Generator G_1 operates at a terminal voltage of 797 V line-to-line and supplies 15 kW at 0.80 power factor lagging. Find the load voltage and the terminal voltage and power and reactive-power output of G_2.

■ Solution

Let I, P, and Q, respectively, denote line current and three-phase active and reactive power. The subscripts 1 and 2 denote the respective branches of the system; the subscript r denotes a quantity measured at the receiving end of the line. We then have

$$I_1 = \frac{P_1}{\sqrt{3}E_1 \cos\theta_1} = \frac{15{,}000}{\sqrt{3}(797)(0.80)} = 13.6 \text{ A}$$

$$P_{r1} = P_1 - 3I_1^2 R_1 = 15{,}000 - 3(13.6)^2(1.4) = 14{,}220 \text{ W}$$

$$Q_{r1} = Q_1 - 3I_1^2 X_1 = 15{,}000 \tan(\cos^{-1} 0.80) - 3(13.6)^2(1.6) = 10{,}350 \text{ VA reactive}$$

The factor 3 appears before $I_1^2 R_1$ and $I_1^2 X_1$ in the last two equations because the current I_1 is the phase current. The load voltage is

$$V_L = \frac{\text{VA}}{\sqrt{3}(\text{current})} = \frac{\sqrt{(14{,}220)^2 + (10{,}350)^2}}{\sqrt{3}(13.6)}$$

$$= 748 \text{ V line-to-line}$$

Since the load requires 30,000 W of real power and 30,000 tan $(\cos^{-1} 0.80) = 22{,}500$ VA of reactive power,

$$P_{r2} = 30{,}000 - 14{,}220 = 15{,}780 \text{ W}$$

and

$$Q_{r2} = 22{,}500 - 10{,}350 = 12{,}150 \text{ VA reactive}$$

$$I_2 = \frac{\text{VA}}{\sqrt{3}V_{l-l}} = \frac{\sqrt{(15{,}780)^2 + (12{,}150)^2}}{\sqrt{3}(748)} = 15.4 \text{ A}$$

$$P_2 = P_{r2} + 3I_2^2 R_2 = 15{,}780 + 3(15.4)^2(0.80) = 16{,}350 \text{ W}$$

$$Q_2 = Q_{r2} + 3I_2^2 X_2 = 12{,}150 + 3(15.4)^2(1.0) = 12{,}870 \text{ VA reactive}$$

$$V_2 = \frac{\text{VA}}{\sqrt{3}I_2} = \frac{\sqrt{(16{,}350)^2 + (12{,}870)^2}}{\sqrt{3}(15.4)}$$

$$= 780 \text{ V (l-l)}$$

A.5 OTHER POLYPHASE SYSTEMS

Although three-phase systems are by far the most common of all polyphase systems, other numbers of phases are used for specialized purposes. The five-wire, four-phase system (Fig. A.16) is sometimes used for low-voltage distribution. It has the advantage that for a phase voltage of 115 V, single-phase voltages of 115 (between a, b, c, or d and o, Fig. A.16) and 230 V (between a and c or b and d) are available as well as a system of polyphase voltages. Essentially the same advantages are possessed by four-wire, three-phase systems having a line-to-neutral voltage of 120 V and a line-to-line voltage of 208 V, however.

Four-phase systems are obtained from three-phase systems by means of special transformer connections. Half of the four-phase system—the part *aob* (Fig. A.16), for example—constitutes a two-phase system. In some rectifier circuits, 6-, 12-, 18-, and 36-phase connections are used for the conversion of alternating to direct current. These systems are also obtained by transformation from three-phase systems.

When the loads and voltages are balanced, the methods of analysis for three-phase systems can be adapted to any of the other polyphase systems by considering one phase of that polyphase system. Of course, the basic voltage, current, and power relations must be modified to suit the particular polyphase system.

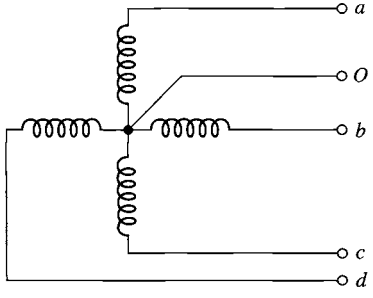

Figure A.16 A five-wire, four-phase system.

B APPENDIX

Voltages, Magnetic Fields, and Inductances of Distributed AC Windings

Both amplitude and waveform of the generated voltage and armature mmf's in machines are determined by the winding arrangements and general machine geometry. These configurations in turn are dictated by economic use of space and materials in the machine and by suitability for the intended service. In this appendix we supplement the introductory discussion of these considerations in Chapter 4 by analytical treatment of ac voltages and mmf's in the balanced steady state. Attention is confined to the time-fundamental component of voltages and the space-fundamental component of mmf's.

B.1 GENERATED VOLTAGES

In accordance with Eq. 4.50, the rms generated voltage per phase for a concentrated winding having N_{ph} turns per phase is

$$E = \sqrt{2}\,\pi f N_{ph} \Phi \tag{B.1}$$

where f is the frequency and Φ the fundamental flux per pole.

A more complex and practical winding will have coil sides for each phase distributed in several slots per pole. Equation B.1 can then be used to compute the voltage distribution of individual coils. To determine the voltage of an entire phase group, the voltages of the component coils must be added as phasors. Such addition of fundamental-frequency voltages is the subject of this article.

B.1.1 Distributed Fractional-Pitch Windings

A simple example of a distributed winding is illustrated in Fig. B.1 for a three-phase, two-pole machine. This case retains all the features of a more general one with any integral number of phases, poles, and slots per pole per phase. At the same time, a *double-layer winding* is shown. Double-layer windings usually lead to simpler end connections and to a machine which is more economical to manufacture and are found in all machines except some small motors below 10 kW. Generally, one side of a coil, such as a_1, is placed in the bottom of a slot, and the other side, $-a_1$, is placed in the top of another slot. Coil sides such as a_1 and a_3 or a_2 and a_4 which are in adjacent slots and associated with the same phase constitute a phase belt. All phase belts are alike when an integral number of slots per pole per phase are used, and for the normal machine the peripheral angle subtended by a phase belt is 60 electrical degrees for a three-phase machine and 90 electrical degrees for a two-phase machine.

Individual coils in Fig. B.1 all span a full pole pitch, or 180 electrical degrees; accordingly, the winding is a full-pitch winding. Suppose now that all coil sides in the tops of the slots are shifted one slot counterclockwise, as in Fig. B.2. Any coil, such as a_1, $-a_1$, then spans only five-sixths of a pole pitch or $\frac{5}{6}(180) = 150$ electrical degrees, and the winding is a fractional-pitch, or chorded, winding. Similar shifting by two slots yields a $\frac{2}{3}$-pitch winding, and so forth. Phase groupings are now intermingled, for some slots contain coil sides in phases a and b, a and c, and b and c. Individual phase

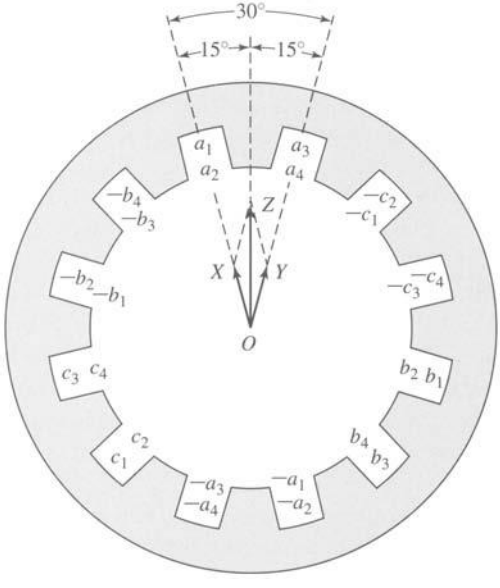

Figure B.1 Distributed two-pole, three-phase full-pitch armature winding with voltage phasor diagram.

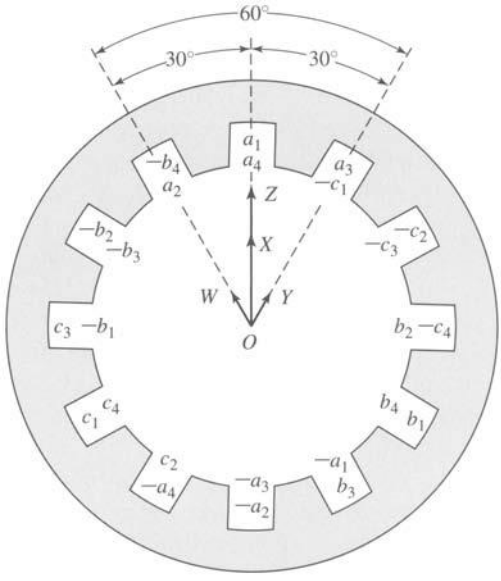

Figure B.2 Distributed two-pole, three-phase fractional-pitch armature winding with voltage phasor diagram.

groups, such as that formed by a_1, a_2, a_3, a_4 on one side and $-a_1, -a_2, -a_3, -a_4$ on the other, are still displaced by 120 electrical degrees from the groups in other phases so that three-phase voltages are produced. Besides the minor feature of shortening the end connections, fractional-pitch windings can be shown to decrease the harmonic content of both voltage and mmf waves.

The end connections between the coil sides are normally in a region of negligible flux density, and hence altering them does not significantly affect the mutual flux linkages of the winding. Allocation of coil sides in slots is then the factor determining the generated voltages, and only that allocation need be specified in Figs. B.1 and B.2. The only requisite is that all coil sides in a phase be included in the interconnection in such a manner that individual voltages make a positive contribution to the total. The practical consequence is that end connections can be made according to the dictates of manufacturing simplicity; the theoretical consequence is that when computational advantages result, the coil sides in a phase can be combined in an arbitrary fashion to form equivalent coils.

One sacrifice is made in using the distributed and fractional-pitch windings of Figs. B.1 and B.2 compared with a concentrated full-pitch winding: for the same number of turns per phase, the fundamental-frequency generated voltage is lower. The harmonics are, in general, lowered by an appreciably greater factor, however, and the total number of turns which can be accommodated on a fixed iron geometry is increased. The effect of distributing the winding in Fig. B.1 is that the voltages of coils a_1 and a_2 are not in phase with those of coils a_3 and a_4. Thus, the voltage of

coils a_1 and a_2 can be represented by phasor OX in Fig. B.1, and that of coils a_3 and a_4 by the phasor OY. The time-phase displacement between these two voltages is the same as the electrical angle between adjacent slots, so that OX and OY coincide with the centerlines of adjacent slots. The resultant phasor OZ for phase a is obviously smaller than the arithmetic sum of OX and OY.

In addition, the effect of fractional pitch in Fig. B.2 is that a coil links a smaller portion of the total pole flux than if it were a full-pitch coil. The effect can be superimposed on that of distributing the winding by regarding coil sides a_2 and $-a_1$ as an equivalent coil with the phasor voltage OW (Fig. B.2), coil sides a_1, a_4, $-a_2$, and $-a_3$ as two equivalent coils with the phasor voltage OX (twice the length of OW), and coil sides a_3 and $-a_4$ as an equivalent coil with phasor voltage OY. The resultant phasor OZ for phase a is obviously smaller than the arithmetic sum of OW, OX, and OY and is also smaller than OZ in Fig. B.1.

The combination of these two effects can be included in a *winding factor* k_w to be used as a reduction factor in Eq. B.1. Thus, the generated voltage per phase is

$$E = \sqrt{2}\pi k_w f N_{ph} \Phi \tag{B.2}$$

where N_{ph} is the total turns in series per phase and k_w accounts for the departure from the concentrated full-pitch case. For a three-phase machine, Eq. B.2 yields the line-to-line voltage for a Δ-connected winding and the line-to-neutral voltage for a Y-connected winding. As in any balanced Y connection, the line-to-line voltage of the latter winding is $\sqrt{3}$ times the line-to-neutral voltage.

B.1.2 Breadth and Pitch Factors

By separately considering the effects of distributing and of chording the winding, reduction factors can be obtained in generalized form convenient for quantitative analysis. The effect of distributing the winding in n slots per phase belt is to yield n voltage phasors displaced in phase by the electrical angle γ between slots, γ being equal to 180 electrical degrees divided by the number of slots per pole. Such a group of phasors is shown in Fig. B.3a and, in a more convenient form for addition, again in Fig. B.3b. Each phasor AB, BC, and CD is the chord of a circle with center at O and subtends the angle γ at the center. The phasor sum AD subtends the angle $n\gamma$, which, as noted previously, is 60 electrical degrees for the normal, uniformly distributed three-phase machine and 90 electrical degrees for the corresponding two-phase machine. From triangles OAa and OAd, respectively,

$$OA = \frac{Aa}{\sin(\gamma/2)} = \frac{AB}{2\sin(\gamma/2)} \tag{B.3}$$

$$OA = \frac{Ad}{\sin(n\gamma/2)} = \frac{AD}{2\sin(n\gamma/2)} \tag{B.4}$$

Equating these two values of OA yields

$$AD = AB\,\frac{\sin(n\gamma/2)}{\sin(\gamma/2)} \tag{B.5}$$

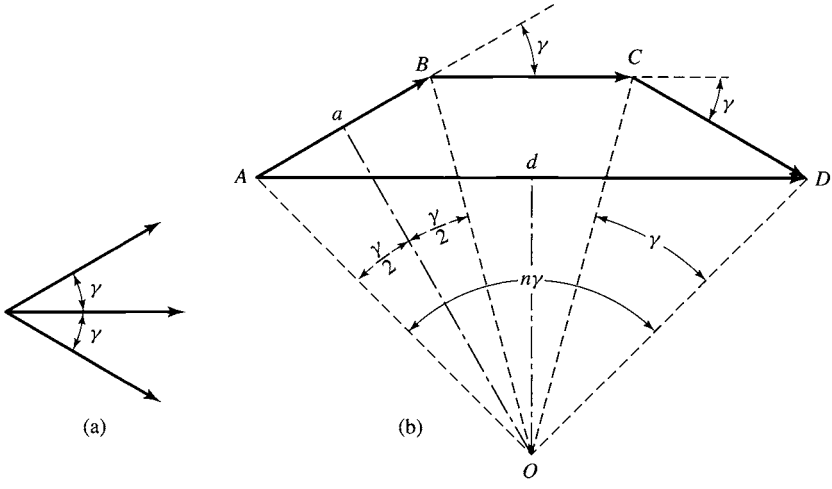

Figure B.3 (a) Coil voltage phasors and (b) phasor sum.

But the arithmetic sum of the phasors is $n(AB)$. Consequently, the reduction factor arising from distributing the winding is

$$k_b = \frac{AD}{nAB} = \frac{\sin(n\gamma/2)}{n\sin(\gamma/2)} \tag{B.6}$$

The factor k_b is called the *breadth factor* of the winding.

The effect of chording on the coil voltage can be obtained by first determining the flux linkages with the fractional-pitch coil. Since there are n coils per phase and N_{ph} total series turns per phase, each coil will have $N = N_{ph}/n$ turns per coil. From Fig. B.4 coil side $-a$ is only ρ electrical degrees from side a instead of the full 180°. The flux linkages with the N-turn coil are

$$\lambda = NB_{peak}lr\left(\frac{2}{\text{poles}}\right)\int_{\rho+\alpha}^{\alpha}\sin\theta\, d\theta \tag{B.7}$$

$$\lambda = NB_{peak}lr\left(\frac{2}{\text{poles}}\right)[\cos(\alpha+\rho)-\cos\alpha] \tag{B.8}$$

where

l = axial length of coil side
r = coil radius
poles = number of poles

With α replaced by ωt to indicate rotation at ω electrical radians per second, Eq. B.8 becomes

$$\lambda = NB_{peak}lr\left(\frac{2}{\text{poles}}\right)[\cos(\omega t+\rho)-\cos\omega t] \tag{B.9}$$

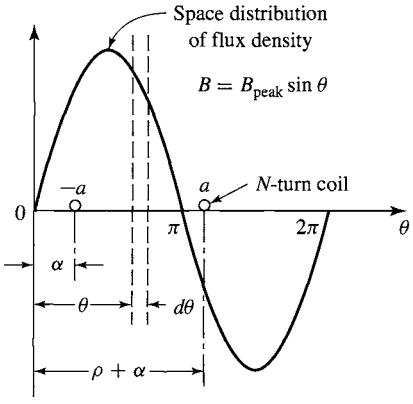

Figure B.4 Fractional-pitch coil in sinusoidal field.

The addition of cosine terms required in the brackets of Eq. B.9 may be performed by a phasor diagram as indicated in Fig. B.5, from which it follows that

$$\cos(\omega t + \rho) - \cos \omega t = -2 \cos\left(\frac{\pi - \rho}{2}\right) \cos\left(\omega t - \left(\frac{\pi - \rho}{2}\right)\right) \tag{B.10}$$

a result which can also be obtained directly from the terms in Eq. B.9 by the appropriate trigonometric transformations.

The flux linkages are then

$$\lambda = -N B_{peak} l r \left(\frac{4}{\text{poles}}\right) \cos\left(\frac{\pi - \rho}{2}\right) \cos\left(\omega t - \left(\frac{\pi - \rho}{2}\right)\right) \tag{B.11}$$

and the instantaneous voltage is

$$e = \frac{d\lambda}{dt} = \omega N B_{peak} l r \left(\frac{4}{\text{poles}}\right) \cos\left(\frac{\pi - \rho}{2}\right) \sin\left(\omega t - \left(\frac{\pi - \rho}{2}\right)\right) \tag{B.12}$$

The phase angle $(\pi - \rho)/2$ in Eq. B.12 merely indicates that the instantaneous voltage is no longer zero when α in Fig. B.4 is zero. The factor $\cos[(\pi - \rho)/2]$ is an

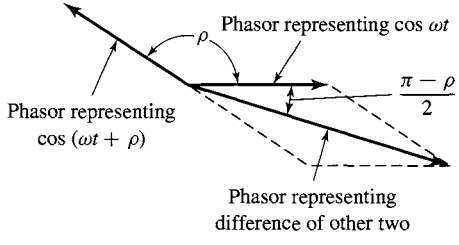

Figure B.5 Phasor addition for fractional-pitch coil.

amplitude-reduction factor, however, so that the rms voltage of Eq. B.1 is modified to

$$E = \sqrt{2}\pi k_p f N_{ph} \Phi \tag{B.13}$$

where the pitch factor k_p is

$$k_p = \cos\left(\frac{\pi - \rho}{2}\right) = \sin\left(\frac{\rho}{2}\right) \tag{B.14}$$

When both the breadth and pitch factors apply, the rms voltage is

$$E = \sqrt{2}\pi k_b k_p f N_{ph} \Phi = \sqrt{2}\,\pi k_w f N_{ph} \Phi \tag{B.15}$$

which is an alternate form of Eq. B.2; the winding factor k_w is seen to be the product of the pitch and breadth factors.

$$k_w = k_b k_p \tag{B.16}$$

EXAMPLE B.1

Calculate the breadth, pitch, and winding factors for the distributed fractional-pitch winding of Fig. B.2.

■ Solution

The winding of Fig. B.2 has two coils per phase belt, separated by an electrical angle of 30°. From Eq. B.6 the breadth factor is

$$k_b = \frac{\sin(n\gamma/2)}{n \sin(\gamma/2)} = \frac{\sin[2(30°)/2]}{2 \sin(30°/2)} = 0.966$$

The fractional-pitch coils span $150° = 5\pi/6$ rad, and from Eq. B.14 pitch factor is

$$k_p = \sin\left(\frac{\rho}{2}\right) = \sin\left(\frac{5\pi}{12}\right) = 0.966$$

The winding factor is

$$k_w = k_b k_p = 0.933$$

B.2 ARMATURE MMF WAVES

Distribution of a winding in several slots per pole per phase and the use of fractional-pitch coils influence not only the emf generated in the winding but also the magnetic field produced by it. Space-fundamental components of the mmf distributions are examined in this article.

B.2.1 Concentrated Full-Pitch Windings

We have seen in Section 4.3 that a concentrated polyphase winding of N_{ph} turns in a multipole machine produces a rectangular mmf wave around the air-gap circumference. With excitation by a sinusoidal current of amplitude I, the time-maximum amplitude of the space-fundamental component of the wave is, in accordance

with Eq. 4.6,

$$(F_{ag1})_{peak} = \frac{4}{\pi}\frac{N_{ph}}{\text{poles}}(\sqrt{2}I)\ \text{A}\cdot\text{turns/pole} \tag{B.17}$$

where the winding factor k_w of Eq. 4.6 has been set equal to unity since in this case we are discussing the mmf wave of a concentrated winding.

Each phase of a polyphase concentrated winding creates such a time-varying standing mmf wave in space. This situation forms the basis of the analysis leading to Eq. 4.39. For concentrated windings, Eq. 4.39 can be rewritten as

$$\mathcal{F}(\theta_{ae}, t) = \frac{3}{2}\frac{4}{\pi}\left(\frac{N_{ph}}{\text{poles}}\right)(\sqrt{2}I)\cos(\theta_{ae} - \omega t) = \frac{6}{\pi}\left(\frac{N_{ph}}{\text{poles}}\right)(\sqrt{2}I)\cos(\theta_{ae} - \omega t) \tag{B.18}$$

The amplitude of the resultant mmf wave in a three-phase machine in ampere-turns per pole is then

$$F_A = \frac{6}{\pi}\left(\frac{N_{ph}}{\text{poles}}\right)(\sqrt{2}I)\ \text{A}\cdot\text{turns/pole} \tag{B.19}$$

Similarly, for a n_{ph}-phase machine, the amplitude is

$$F_A = \frac{2n_{ph}}{\pi}\left(\frac{N_{ph}}{\text{poles}}\right)(\sqrt{2}I)\ \text{A}\cdot\text{turns/pole} \tag{B.20}$$

In Eqs. B.19 and B.20, I is the rms current per phase. The equations include only the fundamental component of the actual distribution and apply to concentrated full-pitch windings with balanced excitation.

B.2.2 Distributed Fractional-Pitch Winding

When the coils in each phase of a winding are distributed among several slots per pole, the resultant space-fundamental mmf can be obtained by superposition from the preceding simpler considerations for a concentrated winding. The effect of distribution can be seen from Fig. B.6, which is a reproduction of the two-pole, three-phase, full-pitch winding with two slots per pole per phase given in Fig. B.1. Coils a_1 and a_2, b_1 and b_2, and c_1 and c_2 by themselves constitute the equivalent of a three-phase, two-pole concentrated winding because they form three sets of coils excited by polyphase currents and mechanically displaced 120° from each other. They therefore produce a rotating space-fundamental mmf; the amplitude of this contribution is given by Eq. B.19 when N_{ph} is taken as the sum of the series turns in coils a_1 and a_2 only. Similarly, coils a_3 and a_4, b_3 and b_4, and c_3 and c_4 produce another identical mmf wave, but one which is phase-displaced in space by the slot angle γ from the former wave. The resultant space-fundamental mmf wave for the winding can be obtained by adding these two sinusoidal contributions.

The mmf contribution from the $a_1a_2b_1b_2c_1c_2$ coils can be represented by the phasor OX in Fig. B.6. Such phasor representation is appropriate because the waveforms concerned are sinusoidal, and phasor diagrams are simply convenient means for

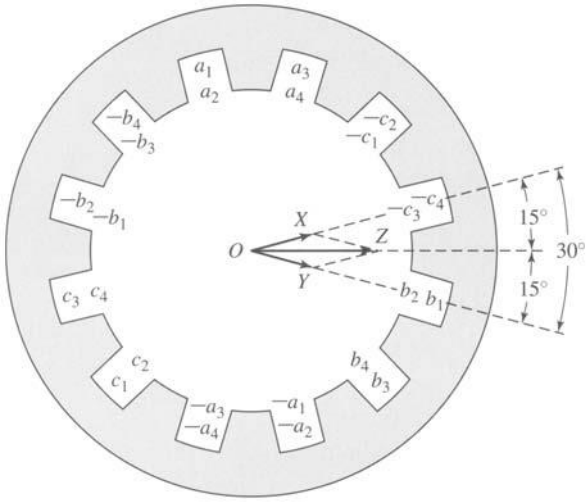

Figure B.6 Distributed two-pole, three-phase, full-pitch armature winding with mmf phasor diagram.

adding sine waves. These are space sinusoids, however, not time sinusoids. Phasor OX is drawn in the space position of the mmf peak for an instant of time when the current in phase a is a maximum. The length of OX is proportional to the number of turns in the associated coils. Similarly, the mmf contribution from the $a_3a_4b_3b_4c_3c_4$ coils may be represented by the phasor OY. Accordingly, the phasor OZ represents the resultant mmf wave. Just as in the corresponding voltage diagram, the resultant mmf is seen to be smaller than if the same number of turns per phase were concentrated in one slot per pole.

In like manner, mmf phasors can be drawn for fractional-pitch windings as illustrated in Fig. B.7, which is a reproduction of the two-pole, three-phase, fractional-pitch winding with two slots per pole per phase given in Fig. B.2. Phasor OW represents the contribution for the equivalent coils formed by conductors a_2 and $-a_1$, b_2 and $-b_1$, and c_2 and $-c_1$; OX for a_1a_4 and $-a_3\ -a_2$, b_1b_4 and $-b_3\ -b_2$, and c_1c_4 and $-c_3\ -c_2$; and OY for a_3 and $-a_4$, b_3 and $-b_4$, and c_3 and $-c_4$. The resultant phasor OZ is, of course, smaller than the algebraic sum of the individual contributions and is also smaller than OZ in Fig. B.6.

By comparison with Figs. B.1 and B.2, these phasor diagrams can be seen to be identical with those for generated voltages. It therefore follows that pitch and breadth factors previously developed can be applied directly to the determination of resultant mmf. Thus, for a distributed, fractional-pitch, polyphase winding, the amplitude of the space-fundamental component of mmf can be obtained by using $k_b k_p N_{ph} = k_w N_{ph}$ instead of simply N_{ph} in Eqs. B.19 and B.20. These equations then become

$$F_A = \frac{6}{\pi}\left(\frac{k_b k_p N_{ph}}{\text{poles}}\right)(\sqrt{2}I) = \frac{6}{\pi}\left(\frac{k_w N_{ph}}{\text{poles}}\right)(\sqrt{2}I) \qquad \text{(B.21)}$$

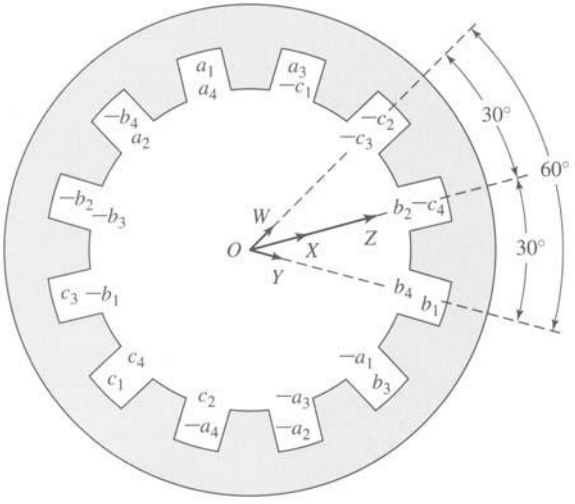

Figure B.7 Distributed two-pole, three-phase, fractional-pitch armature winding with mmf phasor diagram.

for a three-phase machine and

$$F_A = \frac{2n_{ph}}{\pi}\left(\frac{k_b k_p N_{ph}}{\text{poles}}\right)(\sqrt{2}I) = \frac{2n_{ph}}{\pi}\left(\frac{k_w N_{ph}}{\text{poles}}\right)(\sqrt{2}I) \tag{B.22}$$

for a n_{ph}-phase machine, where F_A is in ampere-turns per pole.

B.3 AIR-GAP INDUCTANCES OF DISTRIBUTED WINDINGS

Figure B.8a shows an N-turn, full-pitch, concentrated armature winding in a two-pole magnetic structure with a concentric cylindrical rotor. The mmf of this configuration is shown in Fig. B.8b. Since the air-gap length g is much smaller than the average air-gap radius r, the air-gap radial magnetic field can be considered uniform and equal to the mmf divided by g. From Eq. 4.3 the space-fundamental mmf is given by

$$\mathcal{F}_{ag1} = \frac{4}{\pi}\frac{Ni}{2}\cos\theta_a \tag{B.23}$$

and the corresponding air-gap flux density is

$$\mathcal{B}_{ag1} = \mu_0\frac{\mathcal{F}_{ag1}}{g} = \frac{2\mu_0 Ni}{\pi g}\cos\theta_a \tag{B.24}$$

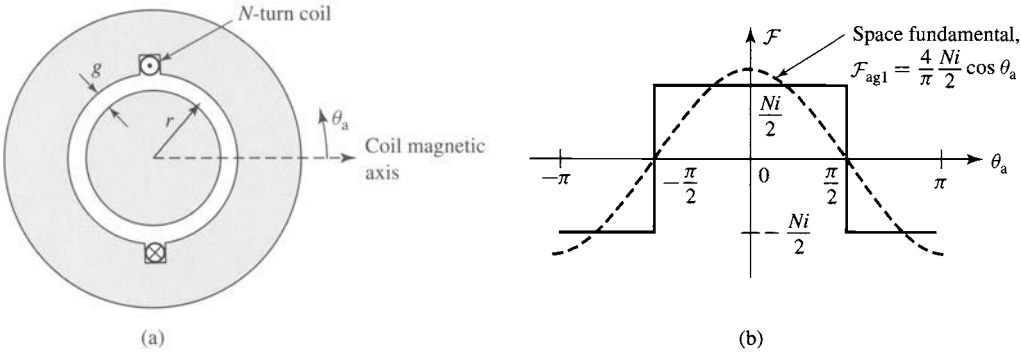

Figure B.8 (a) *N*-turn concentrated coil and (b) resultant mmf.

Equation B.24 can be integrated to find the fundamental air-gap flux per pole (Eq. 4.44)

$$\Phi = l\int_{-\pi/2}^{\pi/2} \mathcal{B}_{ag1} r\, d\theta = \frac{4\mu_0 N l r}{\pi g} i \tag{B.25}$$

where l is the axial length of the air gap. The air-gap inductance of the coil can be found from Eq. 1.29

$$L = \frac{\lambda}{i} = \frac{N\Phi}{i} = \frac{4\mu_0 N^2 l r}{\pi g} \tag{B.26}$$

For a distributed multipole winding with N_{ph} series turns and a winding factor $k_w = k_b k_p$, the air-gap inductance can be found from Eq. B.26 by substituting for N the effective turns per pole pair ($2k_w N_{ph}$/poles)

$$L = \frac{4\mu_0 l r}{\pi g}\left(\frac{2k_w N_{ph}}{\text{poles}}\right)^2 = \frac{16\mu_0 l r}{\pi g}\left(\frac{k_w N_{ph}}{\text{poles}}\right)^2 \tag{B.27}$$

Finally, Fig. B.9 shows schematically two coils (labeled 1 and 2) with winding factors k_{w1} and k_{w2} and with $2N_1$/poles and $2N_2$/poles turns per pole pair, respectively; their magnetic axes are separated by an electrical angle α (equal to poles/2 times their spatial angular displacement). The mutual inductance between these two windings is given by

$$\begin{aligned} L_{12} &= \frac{4\mu_0}{\pi}\left(\frac{2k_{w1}N_1}{\text{poles}}\right)\left(\frac{2k_{w2}N_2}{\text{poles}}\right)\frac{lr}{g}\cos\alpha \\ &= \frac{16\mu_0(k_{w1}N_1)(k_{w2}N_2)lr}{\pi g(\text{poles})^2}\cos\alpha \end{aligned} \tag{B.28}$$

Although the figure shows one winding on the rotor and the second on the stator, Eq. B.28 is equally valid for the case where both windings are on the same member.

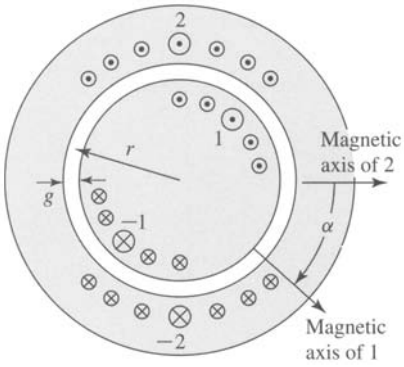

Figure B.9 Two distributed windings separated by electrical angle α.

EXAMPLE B.2

The two-pole stator-winding distribution of Fig. B.2 is found on an induction motor with an air-gap length of 0.381 mm, an average rotor radius of 6.35 cm, and an axial length of 20.3 cm. Each stator coil has 15 turns, and the coil phase connections are as shown in Fig. B.10. Calculate the phase-a air-gap inductance L_{aa0} and the phase-a to phase-b mutual inductance L_{ab}.

■ Solution

Note that the placement of the coils around the stator is such that the flux linkages of each of the two parallel paths are equal. In addition, the air-gap flux distribution is unchanged if, rather than dividing equally between the two legs, as actually occurs, one path were disconnected and all the current were to flow in the remaining path. Thus, the phase inductances can be found by calculating the inductances associated with only one of the parallel paths.

This result may appear to be somewhat puzzling because the two paths are connected in parallel, and thus it would appear that the parallel inductance should be one-half that of the single-path inductance. However, the inductances share a common magnetic circuit, and their

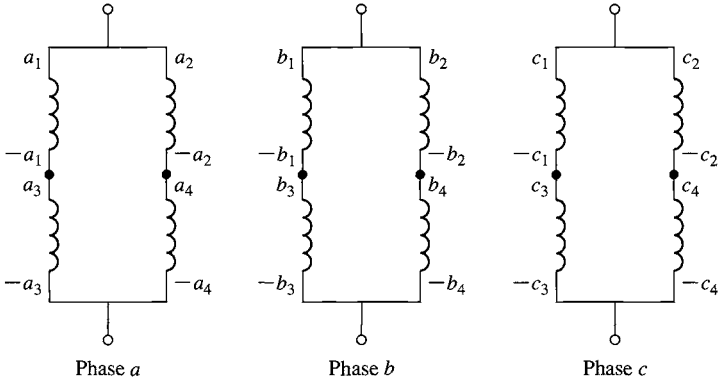

Figure B.10 Coil phase connections of Fig. B.2 for Example B.2.

combined inductance must reflect this fact. It should be pointed out, however, that the phase resistance is one-half that of each of the paths.

The winding factor has been calculated in Example B.1. Thus, from Eq. B.27,

$$\begin{aligned} L_{aa0} &= \frac{16\mu_0 lr}{\pi g}\left(\frac{k_w N_{ph}}{\text{poles}}\right)^2 \\ &= \frac{16(4\pi \times 10^{-7}) \times 0.203 \times 0.0635}{\pi(3.81 \times 10^{-4})}\left(\frac{0.933 \times 30}{2}\right)^2 \\ &= 42.4 \text{ mH} \end{aligned}$$

The winding axes are separated by $\alpha = 120°$, and thus from Eq. B.28

$$L_{ab} = \frac{16\mu_0 (k_w N_{ph})^2 lr}{\pi g (\text{poles})^2}\cos\alpha = -21.2 \text{ mH}$$

APPENDIX C

The dq0 Transformation

In this appendix, the direct- and quadrature-axis (dq0) theory introduced in Section 5.6 is formalized. The formal mathematical transformation from three-phase stator quantities to their direct- and quadrature-axis components is presented. These transformations are then used to express the governing equations for a synchronous machine in terms of the dq0 quantities.

C.1 TRANSFORMATION TO DIRECT- AND QUADRATURE-AXIS VARIABLES

In Section 5.6 the concept of resolving synchronous-machine armature quantities into two rotating components, one aligned with the field-winding axis, the direct-axis component, and one in quadrature with the field-winding axis, the quadrature-axis component, was introduced as a means of facilitating analysis of salient-pole machines. The usefulness of this concept stems from the fact that although each of the stator phases sees a time-varying inductance due to the saliency of the rotor, the transformed quantities rotate with the rotor and hence see constant magnetic paths. Although not discussed here, additional saliency effects are present under transient conditions, due to the different conducting paths in the rotor, rendering the concept of this transformation all the more useful.

Similarly, this transformation is useful from the point of view of analyzing the interaction of the rotor and stator flux- and mmf-waves, independent of whether or not saliency effects are present. By transforming the stator quantities into equivalent quantities which rotate in synchronism with the rotor, under steady-state conditions these interactions become those of constant mmf- and flux-waves separated by a constant spatial angle. This indeed is the point of view which corresponds to that of an observer in the rotor reference frame.

The idea behind the transformation is an old one, stemming from the work of Andre Blondel in France, and the technique is sometimes referred to as the *Blondel two-reaction method*. Much of the development in the form used here was carried out

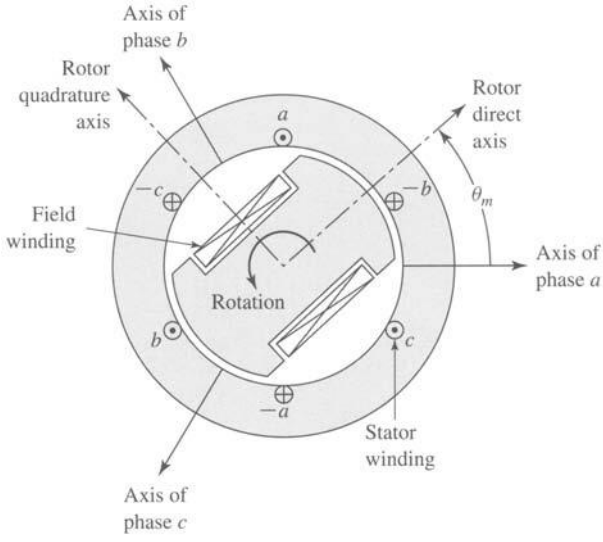

Figure C.1 Idealized synchronous machine

by R. E. Doherty, C. A. Nickle, R. H. Park, and their associates in the United States. The transformation itself, known as the *dq0 transformation,* can be represented in a straightforward fashion in terms of the electrical angle θ_{me} (equal to poles/2 times the spatial angle θ_m) between the rotor direct axis and the stator phase-a axis, as defined by Eq. 4.1 and shown in Fig. C.1.

Letting S represent a stator quantity to be transformed (current, voltage, or flux), we can write the transformation in matrix form as

$$\begin{bmatrix} S_d \\ S_q \\ S_0 \end{bmatrix} = \frac{2}{3} \begin{bmatrix} \cos(\theta_{me}) & \cos(\theta_{me} - 120°) & \cos(\theta_{me} + 120°) \\ -\sin(\theta_{me}) & -\sin(\theta_{me} - 120°) & -\sin(\theta_{me} + 120°) \\ \frac{1}{2} & \frac{1}{2} & \frac{1}{2} \end{bmatrix} \begin{bmatrix} S_a \\ S_b \\ S_c \end{bmatrix} \quad \text{(C.1)}$$

and the inverse transformation as

$$\begin{bmatrix} S_a \\ S_b \\ S_c \end{bmatrix} = \begin{bmatrix} \cos(\theta_{me}) & -\sin(\theta_{me}) & 1 \\ \cos(\theta_{me} - 120°) & -\sin(\theta_{me} - 120°) & 1 \\ \cos(\theta_{me} + 120°) & -\sin(\theta_{me} + 120°) & 1 \end{bmatrix} \begin{bmatrix} S_d \\ S_q \\ S_0 \end{bmatrix} \quad \text{(C.2)}$$

Here the letter S refers to the quantity to be transformed and the subscripts d and q represent the direct and quadrature axes, respectively. A third component, the *zero-sequence component,* indicated by the subscript 0, is also included. This component is required to yield a unique transformation of the three stator-phase quantities; it corresponds to components of armature current which produce no net air-gap flux and hence no net flux linking the rotor circuits. As can be seen from Eq. C.1, under balanced-three-phase conditions, there are no zero-sequence components. Only balanced-three-phase conditions are considered in this book, and hence zero-sequence components are not discussed in any detail.

Note that the dq0 transformation applies to the instantaneous values of the quantities to be transformed, not rms values. Thus when applying the formal instantaneous transformations as presented here, one must be careful to avoid the use of rms values, as are frequently used in phasor analyses such as are found in Chapter 5.

EXAMPLE C.1

A two-pole synchronous machine is carrying balanced three-phase armature currents

$$i_a = \sqrt{2}I_a \cos \omega t \qquad i_b = \sqrt{2}I_a \cos(\omega t - 120°) \qquad i_c = \sqrt{2}I_a \cos(\omega t + 120°)$$

The rotor is rotating at synchronous speed ω, and the rotor direct axis is aligned with the stator phase-a axis at time $t = 0$. Find the direct- and quadrature-axis current components.

■ Solution

The angle between the rotor direct axis and the stator phase-a axis can be expressed as

$$\theta_{me} = \omega t$$

From Eq. C.1

$$\begin{aligned} i_d &= \frac{2}{3}[i_a \cos \omega t + i_b \cos(\omega t - 120°) + i_c \cos(\omega t + 120°)] \\ &= \frac{2}{3}\sqrt{2}I_a[\cos^2 \omega t + \cos^2(\omega t - 120°) + \cos^2(\omega t + 120°)] \end{aligned}$$

Using the trigonometric identity $\cos^2 \alpha = \frac{1}{2}(1 + \cos 2\alpha)$ gives

$$i_d = \sqrt{2}I_a$$

Similarly,

$$\begin{aligned} i_q &= -\frac{2}{3}[i_a \sin \omega t + i_b \sin(\omega t - 120°) + i_c \sin(\omega t + 120°)] \\ &= -\frac{2}{3}\sqrt{2}I_a[\cos \omega t \sin \omega t + \cos(\omega t - 120°) \sin(\omega t - 120°) \\ &\quad + \cos(\omega t + 120°) \sin(\omega t + 120°)] \end{aligned}$$

and using the trigonometric identity $\cos \alpha \sin \alpha = \frac{1}{2} \sin 2\alpha$ gives

$$i_q = 0$$

This result corresponds directly to our physical picture of the dq0 transformation. From the discussion of Section 4.5 we recognize that the balanced three-phase currents applied to this machine produce a synchronously rotating mmf wave which produces flux along the stator phase-a axis at time $t = 0$. This flux wave is thus aligned with the rotor direct axis at $t = 0$ and remains so since the rotor is rotating at the same speed. Hence the stator current produces only direct-axis flux and thus consists only of a direct-axis component.

C.2 BASIC SYNCHRONOUS-MACHINE RELATIONS IN dq0 VARIABLES

Equations 5.2 to 5.5 give the flux-linkage current relationships for a synchronous machine consisting of a field winding and a three-phase stator winding. This simple machine is sufficient to demonstrate the basic features of the machine representation in dq0 variables; the effects of additional rotor circuits such as damper windings can be introduced in a straightforward fashion.

The flux-linkage current relationships in terms of phase variables (Eqs. 5.2 to 5.5) are repeated here for convenience

$$\begin{bmatrix} \lambda_a \\ \lambda_b \\ \lambda_c \\ \lambda_f \end{bmatrix} = \begin{bmatrix} \mathcal{L}_{aa} & \mathcal{L}_{ab} & \mathcal{L}_{ac} & \mathcal{L}_{af} \\ \mathcal{L}_{ba} & \mathcal{L}_{bb} & \mathcal{L}_{bc} & \mathcal{L}_{bf} \\ \mathcal{L}_{ca} & \mathcal{L}_{cb} & \mathcal{L}_{cc} & \mathcal{L}_{cf} \\ \mathcal{L}_{fa} & \mathcal{L}_{fb} & \mathcal{L}_{fc} & \mathcal{L}_{ff} \end{bmatrix} \begin{bmatrix} i_a \\ i_b \\ i_c \\ i_f \end{bmatrix} \tag{C.3}$$

Unlike the analysis of Section 5.2, this analysis will include the effects of saliency, which causes the stator self and mutual inductances to vary with rotor position.

For the purposes of this analysis the idealized synchronous machine of Fig. C.1 is assumed to satisfy two conditions: (1) the air-gap permeance has a constant component as well as a smaller component which varies cosinusoidally with rotor angle as measured from the direct axis, and (2) the effects of space harmonics in the air-gap flux can be ignored. Although these approximations may appear somewhat restrictive, they form the basis of classical dq0 machine analysis and give excellent results in a wide variety of applications. Essentially they involve neglecting effects which result in time-harmonic stator voltages and currents and are thus consistent with our previous assumptions neglecting harmonics produced by discrete windings.

The various machine inductances can then be written in terms of the electrical rotor angle θ_{me} (between the rotor direct axis and the stator phase-a axis), using the notation of Section 5.2, as follows. For the stator self-inductances

$$\mathcal{L}_{aa} = L_{aa0} + L_{al} + L_{g2} \cos 2\theta_{me} \tag{C.4}$$

$$\mathcal{L}_{bb} = L_{aa0} + L_{al} + L_{g2} \cos (2\theta_{me} + 120°) \tag{C.5}$$

$$\mathcal{L}_{cc} = L_{aa0} + L_{al} + L_{g2} \cos (2\theta_{me} - 120°) \tag{C.6}$$

For the stator-to-stator mutual inductances

$$\mathcal{L}_{ab} = \mathcal{L}_{ba} = -\frac{1}{2} L_{aa0} + L_{g2} \cos (2\theta_{me} - 120°) \tag{C.7}$$

$$\mathcal{L}_{bc} = \mathcal{L}_{cb} = -\frac{1}{2} L_{aa0} + L_{g2} \cos 2\theta_{me} \tag{C.8}$$

$$\mathcal{L}_{ac} = \mathcal{L}_{ca} = -\frac{1}{2} L_{aa0} + L_{g2} \cos (2\theta_{me} + 120°) \tag{C.9}$$

For the field-winding self-inductance

$$\mathcal{L}_{ff} = L_{ff} \tag{C.10}$$

and for the stator-to-rotor mutual inductances

$$\mathcal{L}_{af} = \mathcal{L}_{fa} = L_{af} \cos \theta_{me} \tag{C.11}$$

$$\mathcal{L}_{bf} = \mathcal{L}_{fb} = L_{af} \cos (\theta_{me} - 120°) \tag{C.12}$$

$$\mathcal{L}_{cf} = \mathcal{L}_{fc} = L_{af} \cos (\theta_{me} + 120°) \tag{C.13}$$

Comparison with Section 5.2 shows that the effects of saliency appear only in the stator self- and mutual-inductance terms as an inductance term which varies with $2\theta_{me}$. This twice-angle variation can be understood with reference to Fig. C.1, where it can be seen that rotation of the rotor through 180° reproduces the original geometry of the magnetic circuit. Notice that the self-inductance of each stator phase is a maximum when the rotor direct axis is aligned with the axis of that phase and that the phase-phase mutual inductance is maximum when the rotor direct axis is aligned midway between the two phases. This is the expected result since the rotor direct axis is the path of lowest reluctance (maximum permeance) for air-gap flux.

The flux-linkage expressions of Eq. C.3 become much simpler when they are expressed in terms of dq0 variables. This can be done by application of the transformation of Eq. C.1 to both the flux linkages and the currents of Eq. C.3. The manipulations are somewhat laborious and are omitted here because they are simply algebraic. The results are

$$\lambda_d = L_d i_d + L_{af} i_f \tag{C.14}$$

$$\lambda_q = L_q i_q \tag{C.15}$$

$$\lambda_f = \frac{3}{2} L_{af} i_d + L_{ff} i_f \tag{C.16}$$

$$\lambda_0 = L_0 i_0 \tag{C.17}$$

In these equations, new inductance terms appear:

$$L_d = L_{al} + \frac{3}{2}(L_{aa0} + L_{g2}) \tag{C.18}$$

$$L_q = L_{al} + \frac{3}{2}(L_{aa0} - L_{g2}) \tag{C.19}$$

$$L_0 = L_{al} \tag{C.20}$$

The quantities L_d and L_q are the *direct-axis* and *quadrature-axis synchronous inductances,* respectively, corresponding directly to the direct- and quadrature-axis synchronous reactances discussed in Section 5.6 (i.e., $X_d = \omega_e L_d$ and $X_q = \omega_e L_q$). The inductance L_0 is the *zero-sequence inductance.* Notice that the transformed flux-linkage current relationships expressed in Eqs. C.14 to C.17 no longer contain inductances which are functions of rotor position. This feature is responsible for the usefulness of the dq0 transformation.

Transformation of the voltage equations

$$v_a = R_a i_a + \frac{d\lambda_a}{dt} \tag{C.21}$$

$$v_b = R_a i_b + \frac{d\lambda_b}{dt} \tag{C.22}$$

$$v_c = R_a i_c + \frac{d\lambda_c}{dt} \tag{C.23}$$

$$v_f = R_f i_f + \frac{d\lambda_f}{dt} \tag{C.24}$$

results in

$$v_d = R_a i_d + \frac{d\lambda_d}{dt} - \omega_{me}\lambda_q \tag{C.25}$$

$$v_q = R_a i_q + \frac{d\lambda_q}{dt} + \omega_{me}\lambda_d \tag{C.26}$$

$$v_f = R_f i_f + \frac{d\lambda_f}{dt} \tag{C.27}$$

$$v_0 = R_a i_0 + \frac{d\lambda_0}{dt} \tag{C.28}$$

(algebraic details are again omitted), where $\omega_{me} = d\theta_{me}/dt$ is the rotor electrical angular velocity.

In Eqs. C.25 and C.26 the terms $\omega_{me}\lambda_q$ and $\omega_{me}\lambda_d$ are speed-voltage terms which come as a result of the fact that we have chosen to define our variables in a reference frame rotating at the electrical angular velocity ω_{me}. These speed voltage terms are directly analogous to the speed-voltage terms found in the dc machine analysis of Chapter 9. In a dc machine, the commutator/brush system performs the transformation which transforms armature (rotor) voltages to the field-winding (stator) reference frame.

We now have the basic relations for analysis of our simple synchronous machine. They consist of the flux-linkage current equations C.14 to C.17, the voltage equations C.25 to C.28, and the transformation equations C.1 and C.2. When the rotor electrical angular velocity ω_{me} is constant, the differential equations are linear with constant coefficients. In addition, the transformer terms $d\lambda_d/dt$ and $d\lambda_q/dt$ in Eqs. C.25 and C.26 are often negligible with respect to the speed-voltage terms $\omega_{me}\lambda_q$ and $\omega_{me}\lambda_d$, providing further simplification. Omission of these terms corresponds to neglecting the harmonics and dc component in the transient solution for stator voltages and currents. In any case, the transformed equations are generally much easier to solve, both analytically and by computer simulation, than the equations expressed directly in terms of the phase variables.

In using these equations and the corresponding equations in the machinery literature, careful note should be made of the sign convention and units employed. Here

we have chosen the motor-reference convention for armature currents, with positive armature current flowing into the machine terminals. Also, SI units (volts, amperes, ohms, henrys, etc.) are used here; often in the literature one of several per-unit systems is used to provide numerical simplifications.[1]

To complete the useful set of equations, expressions for power and torque are needed. The instantaneous power into the three-phase stator is

$$p_s = v_a i_a + v_b i_b + v_c i_c \tag{C.29}$$

Phase quantities can be eliminated from Eq. C.29 by using Eq. C.2 written for voltages and currents. The result is

$$p_s = \frac{3}{2}(v_d i_d + v_q i_q + 2v_0 i_0) \tag{C.30}$$

The electromagnetic torque, T_{mech}, is readily obtained by using the techniques of Chapter 3 as the power output corresponding to the speed voltages divided by the shaft speed (in mechanical radians per second). From Eq. C.30 with the speed-voltage terms from Eqs. C.25 and C.26, and by recognizing ω_{me} as the rotor speed in electrical radians per second, we get

$$T_{mech} = \frac{3}{2}\left(\frac{\text{poles}}{2}\right)(\lambda_d i_q - \lambda_q i_d) \tag{C.31}$$

A word about sign conventions. When, as is the case in the derivation of this appendix, the motor-reference convention for currents is chosen (i.e., the positive reference direction for currents is into the machine), the torque of Eq. C.31 is the torque acting to accelerate the rotor. Alternatively, if the generator-reference convention is chosen, the torque of Eq. C.31 is the torque acting to decelerate the rotor. This result is, in general, conformity with torque production from interacting magnetic fields as expressed in Eq. 4.81. In Eq. C.31 we see the superposition of the interaction of components: the direct-axis magnetic flux produces torque via its interaction with the quadrature-axis mmf and the quadrature-axis magnetic flux produces torque via its interaction with the direct-axis mmf. Note that, for both of these interactions, the flux and interacting mmf's are 90 electrical degrees apart; hence the sine of the interacting angle (see Eq. 4.81) is unity which in turns leads to the simple form of Eq. C.31.

As a final cautionary note, the reader is again reminded that the currents, fluxes, and voltages in Eqs. C.29 through Eq. C.31 are instantaneous values. Thus, the reader is urged to avoid the use of rms values in these and the other transformation equations found in this appendix.

---

[1] See A. W. Rankin, "Per-Unit Impedances of Synchronous Machines," *Trans. AIEE* 64:569–573, 839–841 (1945).

C.3 BASIC INDUCTION-MACHINE RELATIONS IN dq0 VARIABLES

In this derivation we will assume that the induction machine includes three-phase windings on both the rotor and the stator and that there are no saliency effects. In this case, the flux-linkage current relationships can be written as

$$\begin{bmatrix} \lambda_a \\ \lambda_b \\ \lambda_c \\ \lambda_{aR} \\ \lambda_{bR} \\ \lambda_{cR} \end{bmatrix} = \begin{bmatrix} \mathcal{L}_{aa} & \mathcal{L}_{ab} & \mathcal{L}_{ac} & \mathcal{L}_{aaR} & \mathcal{L}_{abR} & \mathcal{L}_{acR} \\ \mathcal{L}_{ba} & \mathcal{L}_{bb} & \mathcal{L}_{bc} & \mathcal{L}_{baR} & \mathcal{L}_{bbR} & \mathcal{L}_{bcR} \\ \mathcal{L}_{ca} & \mathcal{L}_{cb} & \mathcal{L}_{cc} & \mathcal{L}_{caR} & \mathcal{L}_{cbR} & \mathcal{L}_{ccR} \\ \mathcal{L}_{Aa} & \mathcal{L}_{aRb} & \mathcal{L}_{aRc} & \mathcal{L}_{aRaR} & \mathcal{L}_{aRbR} & \mathcal{L}_{aRC} \\ \mathcal{L}_{bRa} & \mathcal{L}_{bRb} & \mathcal{L}_{bRc} & \mathcal{L}_{bRaR} & \mathcal{L}_{bRbR} & \mathcal{L}_{bRcR} \\ \mathcal{L}_{cRa} & \mathcal{L}_{cRb} & \mathcal{L}_{cRc} & \mathcal{L}_{cRaR} & \mathcal{L}_{cRbR} & \mathcal{L}_{cRcR} \end{bmatrix} \begin{bmatrix} i_a \\ i_b \\ i_c \\ i_{aR} \\ i_{bR} \\ i_{cR} \end{bmatrix} \tag{C.32}$$

where the subscripts (a, b, c) refer to stator quantities while the subscripts (aR, bR, cR) refer to rotor quantities.

The various machine inductances can then be written in terms of the electrical rotor angle θ_{me} (defined in this case as between the rotor phase-aR and the stator phase-a axes), as follows. For the stator self-inductances

$$\mathcal{L}_{aa} = \mathcal{L}_{bb} = \mathcal{L}_{cc} = L_{aa0} + L_{al} \tag{C.33}$$

where L_{aa0} is the air-gap component of the stator self-inductance and L_{al} is the leakage component.

For the rotor self-inductances

$$\mathcal{L}_{aRaR} = \mathcal{L}_{bRbR} = \mathcal{L}_{cRcR} = L_{aRaR0} + L_{aRl} \tag{C.34}$$

where L_{aRaR0} is the air-gap component of the rotor self-inductance and L_{aRl} is the leakage component.

For the stator-to-stator mutual inductances

$$\mathcal{L}_{ab} = \mathcal{L}_{ba} = \mathcal{L}_{ac} = \mathcal{L}_{ca} = \mathcal{L}_{bc} = \mathcal{L}_{cb} = -\frac{1}{2}L_{aa0} \tag{C.35}$$

For the rotor-to-rotor mutual inductances

$$\mathcal{L}_{aRbR} = \mathcal{L}_{bRaR} = \mathcal{L}_{aRcR} = \mathcal{L}_{cRaR} = \mathcal{L}_{bRcR} = \mathcal{L}_{cRbR} = -\frac{1}{2}L_{aRaR0} \tag{C.36}$$

and for the stator-to-rotor mutual inductances

$$\mathcal{L}_{aaR} = \mathcal{L}_{aRa} = \mathcal{L}_{bbR} = \mathcal{L}_{bRb} = \mathcal{L}_{ccR} = \mathcal{L}_{cRc} = L_{aaR}\cos\theta_{me} \tag{C.37}$$

$$\mathcal{L}_{baR} = \mathcal{L}_{aRb} = \mathcal{L}_{cbR} = \mathcal{L}_{bRc} = \mathcal{L}_{acR} = \mathcal{L}_{cRa} = L_{aaR}\cos(\theta_{me} - 120^\circ) \tag{C.38}$$

$$\mathcal{L}_{caR} = \mathcal{L}_{aRc} = \mathcal{L}_{abR} = \mathcal{L}_{bRa} = \mathcal{L}_{bcR} = \mathcal{L}_{cRb} = L_{aaR}\cos(\theta_{me} + 120^\circ) \tag{C.39}$$

The corresponding voltage equations become

$$v_a = R_a i_a + \frac{d\lambda_a}{dt} \tag{C.40}$$

$$v_b = R_a i_b + \frac{d\lambda_b}{dt} \tag{C.41}$$

$$v_c = R_a i_c + \frac{d\lambda_c}{dt} \tag{C.42}$$

$$v_{aR} = 0 = R_{aR} i_{aR} + \frac{d\lambda_{aR}}{dt} \tag{C.43}$$

$$v_{bR} = 0 = R_{aR} i_{bR} + \frac{d\lambda_{bR}}{dt} \tag{C.44}$$

$$v_{cR} = 0 = R_{aR} i_{cR} + \frac{d\lambda_{cR}}{dt} \tag{C.45}$$

where the voltages v_{aR}, v_{bR}, and v_{cR} are set equal to zero because the rotor windings are shorted at their terminals.

In the case of a synchronous machine in which the stator flux wave and rotor rotate in synchronism (at least in the steady state), the choice of reference frame for the dq0 transformation is relatively obvious. Specifically, the most useful transformation is to a reference frame fixed to the rotor.

The choice is not so obvious in the case of an induction machine. For example, one might choose a reference frame fixed to the rotor and apply the transformation of Eqs. C.1 and C.2 directly. If this is done, because the rotor of an induction motor does not rotate at synchronous speed, the flux linkages seen in the rotor reference frame will not be constant, and hence the time derivatives in the transformed voltage equations will not be equal to zero. Correspondingly, the direct- and quadrature-axis flux linkages, currents, and voltages will be found to be time-varying, with the result that the transformation turns out to be of little practical value.

An alternative choice is to choose a reference frame rotating at the synchronous angular velocity. In this case, both the stator and rotor quantities will have to be transformed. In the case of the stator quantities, the rotor angle θ_{me} in Eqs. C.1 and C.2 would be replaced by θ_S where

$$\theta_S = \omega_e t + \theta_0 \tag{C.46}$$

is the angle between the axis of phase a and that of the synchronously-rotating dq0 reference frame and θ_0.

The transformation equations for the stator quantities then become

$$\begin{bmatrix} S_d \\ S_q \\ S_0 \end{bmatrix} = \frac{2}{3} \begin{bmatrix} \cos(\theta_S) & \cos(\theta_S - 120°) & \cos(\theta_S + 120°) \\ -\sin(\theta_S) & -\sin(\theta_S - 120°) & -\sin(\theta_S + 120°) \\ \frac{1}{2} & \frac{1}{2} & \frac{1}{2} \end{bmatrix} \begin{bmatrix} S_a \\ S_b \\ S_c \end{bmatrix} \tag{C.47}$$

and the inverse transformation

$$\begin{bmatrix} S_a \\ S_b \\ S_c \end{bmatrix} = \begin{bmatrix} \cos(\theta_S) & -\sin(\theta_S) & 1 \\ \cos(\theta_S - 120°) & -\sin(\theta_S - 120°) & 1 \\ \cos(\theta_S + 120°) & -\sin(\theta_S + 120°) & 1 \end{bmatrix} \begin{bmatrix} S_d \\ S_q \\ S_0 \end{bmatrix} \tag{C.48}$$

Similarly, in the case of the rotor, θ_S would be replaced by θ_R where

$$\theta_R = (\omega_e - \omega_{me})t + \theta_0 \tag{C.49}$$

is the angle between the axis of rotor phase aR and that of the synchronously-rotating dq0 reference frame and $(\omega_e - \omega_{me})$ is the electrical angular velocity of the synchronously rotating reference frame as seen from the rotor frame.

The transformation equations for the rotor quantities then become

$$\begin{bmatrix} S_{dR} \\ S_{qR} \\ S_{0R} \end{bmatrix} = \frac{2}{3} \begin{bmatrix} \cos(\theta_R) & \cos(\theta_R - 120°) & \cos(\theta_R + 120°) \\ -\sin(\theta_R) & -\sin(\theta_R - 120°) & -\sin(\theta_R + 120°) \\ \frac{1}{2} & \frac{1}{2} & \frac{1}{2} \end{bmatrix} \begin{bmatrix} S_{aR} \\ S_{bR} \\ S_{cR} \end{bmatrix} \tag{C.50}$$

and the inverse transformation

$$\begin{bmatrix} S_{aR} \\ S_{bR} \\ S_{cR} \end{bmatrix} = \begin{bmatrix} \cos(\theta_R) & -\sin(\theta_R) & 1 \\ \cos(\theta_R - 120°) & -\sin(\theta_R - 120°) & 1 \\ \cos(\theta_R + 120°) & -\sin(\theta_R + 120°) & 1 \end{bmatrix} \begin{bmatrix} S_{dR} \\ S_{qR} \\ S_{0R} \end{bmatrix} \tag{C.51}$$

Using this set of transformations for the rotor and stator quantities, the transformed flux-linkage current relationships become

$$\lambda_d = L_S i_d + L_m i_{dR} \tag{C.52}$$

$$\lambda_q = L_S i_q + L_m i_{qR} \tag{C.53}$$

$$\lambda_0 = L_0 i_0 \tag{C.54}$$

for the stator and

$$\lambda_{dR} = L_m i_d + L_R i_{dR} \tag{C.55}$$

$$\lambda_{qR} = L_m i_q + L_R i_{qR} \tag{C.56}$$

$$\lambda_{0R} = L_{0R} i_{0R} \tag{C.57}$$

for the rotor

Here we have defined a set of new inductances

$$L_S = \frac{3}{2} L_{aa0} + L_{al} \tag{C.58}$$

$$L_m = \frac{3}{2} L_{aaR0} \tag{C.59}$$

$$L_0 = L_{al} \tag{C.60}$$

$$L_R = \frac{3}{2} L_{aRaR0} + L_{aRl} \tag{C.61}$$

$$L_{0R} = L_{aRl} \tag{C.62}$$

The transformed stator-voltage equations are

$$v_d = R_a i_d + \frac{d\lambda_d}{dt} - \omega_e \lambda_q \tag{C.63}$$

$$v_q = R_a i_q + \frac{d\lambda_q}{dt} + \omega_e \lambda_d \tag{C.64}$$

$$v_0 = R_a i_0 + \frac{d\lambda_0}{dt} \tag{C.65}$$

and those for the rotor are

$$0 = R_{aR} i_{dR} + \frac{\lambda_{dR}}{dt} - (\omega_e - \omega_{me})\lambda_{qR} \tag{C.66}$$

$$0 = R_{aR} i_{qR} + \frac{d\lambda_{qR}}{dt} + (\omega_e - \omega_{me})\lambda_{dR} \tag{C.67}$$

$$0 = R_{aR} i_{0R} + \frac{d\lambda_{0R}}{dt} \tag{C.68}$$

Finally, using the techniques of Chapter 3, the torque can be expressed in a number of equivalent ways including

$$T_{mech} = \frac{3}{2}\left(\frac{\text{poles}}{2}\right)(\lambda_d i_q - \lambda_q i_d) \tag{C.69}$$

and

$$T_{mech} = \frac{3}{2}\left(\frac{\text{poles}}{2}\right)\left(\frac{L_m}{L_R}\right)(\lambda_{dR} i_q - \lambda_{qR} i_d) \tag{C.70}$$

D APPENDIX

Engineering Aspects of Practical Electric Machine Performance and Operation

In this book the basic essential features of electric machinery have been discussed; this material forms the basis for understanding the behavior of electric machinery of all types. In this appendix our objective is to introduce practical issues associated with the engineering implementation of the machinery concepts which have been developed. Issues common to all electric machine types such as losses, cooling, and rating are discussed.

D.1 LOSSES

Consideration of machine losses is important for three reasons: (1) Losses determine the efficiency of the machine and appreciably influence its operating cost; (2) losses determine the heating of the machine and hence the rating or power output that can be obtained without undue deterioration of the insulation; and (3) the voltage drops or current components associated with supplying the losses must be properly accounted for in a machine representation. Machine efficiency, like that of transformers or any energy-transforming device, is given by

$$\text{Efficiency} = \frac{\text{output}}{\text{input}} \tag{D.1}$$

which can also be expressed as

$$\text{Efficiency} = \frac{\text{input} - \text{losses}}{\text{input}} = 1 - \frac{\text{losses}}{\text{input}} \tag{D.2}$$

$$\text{Efficiency} = \frac{\text{output}}{\text{output} + \text{losses}} \tag{D.3}$$

Rotating machines in general operate efficiently except at light loads. For example, the full-load efficiency of average motors ranges from 80 to 90 percent for motors on the order of 1 to 10 kW, 90 to 95 percent for motors up to a few hundred kW, and up to a few percent higher for larger motors.

The forms given by Eqs. D.2 and D.3 are often used for electric machines, since their efficiency is most commonly determined by measurement of losses instead of by directly measuring the input and output under load. Efficiencies determined from loss measurements can be used in comparing competing machines if exactly the same methods of measurement and computation are used in each case. For this reason, the various losses and the conditions for their measurement are precisely defined by the American National Standards Institute (ANSI), the Institute of Electrical and Electronics Engineers (IEEE), and the National Electrical Manufacturers Association (NEMA). The following discussion summarizes some of the various commonly considered loss mechanisms.

Ohmic Losses *Ohmic,* or I^2R *losses,* are found in all windings of a machine. By convention, these losses are computed on the basis of the dc resistances of the winding at 75°C. Actually the I^2R loss depends on the effective resistance of the winding under the operating frequency and flux conditions. The increment in loss represented by the difference between dc and effective resistances is included with stray load losses, discussed below. In the field windings of synchronous and dc machines, only the losses in the field winding are charged against the machine; the losses in external sources supplying the excitation are charged against the plant of which the machine is a part. Closely associated with I^2R loss is the *brush-contact loss* at slip rings and commutators. By convention, this loss is normally neglected for induction and synchronous machines. For industrial-type dc machines the voltage drop at the brushes is regarded as constant at 2 V total when carbon and graphite brushes with shunts (pigtails) are used.

Mechanical Losses *Mechanical losses* consist of brush and bearing friction, windage, and the power required to circulate air through the machine and ventilating system, if one is provided, whether by self-contained or external fans (except for the power required to force air through long or restricted ducts external to the machine). Friction and windage losses can be measured by determining the input to the machine running at the proper speed but unloaded and unexcited. Frequently they are lumped with core loss and determined at the same time.

Open-Circuit, or No-Load, Core Loss *Open-circuit core loss* consists of the hysteresis and eddy-current losses arising from changing flux densities in the iron of the machine with only the main exciting winding energized. In dc and synchronous machines, these losses are confined largely to the armature iron, although the flux variations arising from slot openings will cause losses in the field iron as well, particularly in the pole shoes or surfaces of the field iron. In induction machines the losses are confined largely to the stator iron. Open-circuit core loss can be found by measuring the input to the machine when it is operating unloaded at rated speed or frequency and under the appropriate flux or voltage conditions, and then deducting

the friction and windage loss and, if the machine is self-driven during the test, the no-load armature I^2R loss (no-load stator I^2R loss for an induction motor). Usually, data are taken for a curve of core loss as a function of armature voltage in the neighborhood of rated voltage. The core loss under load is then considered to be the value at a voltage equal to rated voltage corrected for the armature resistance drop under load (a phasor correction for an ac machine). For induction motors, however, this correction is dispensed with, and the core loss at rated voltage is used. For efficiency determination alone, there is no need to segregate open-circuit core loss and friction and windage loss; the sum of these two losses is termed the *no-load rotational loss.*

Eddy-current loss varies with the square of the flux density, the frequency, and the thickness of laminations. Under normal machine conditions it can be expressed to a sufficiently close approximation as

$$P_e = K_e(B_{max} f \delta)^2 \tag{D.4}$$

where

δ = lamination thickness
B_{max} = maximum flux density
f = frequency
K_e = proportionality constant

The value of K_e depends on the units used, volume of iron, and resistivity of the iron.

Variation of *hysteresis loss* can be expressed in equation form only on an empirical basis. The most commonly used relation is

$$P_h = K_h f B_{max}^n \tag{D.5}$$

where K_h is a proportionality constant dependent on the characteristics and volume of iron and the units used and the exponent n ranges from 1.5 to 2.5, a value of 2.0 often being used for estimating purposes in machines. In both Eqs. D.4 and D.5, frequency can be replaced by speed and flux density by the appropriate voltage, with the proportionality constants changed accordingly.

When the machine is loaded, the space distribution of flux density is significantly changed by the mmf of the load currents. The actual core losses may increase noticeably. For example, mmf harmonics cause appreciable losses in the iron near the air-gap surfaces. The total increment in core loss is classified as part of the stray load loss.

Stray Load Loss *Stray load loss* consists of the losses arising from nonuniform current distribution in the copper and the additional core losses produced in the iron by distortion of the magnetic flux by the load current. It is a difficult loss to determine accurately. By convention it is taken as 1.0 percent of the output for dc machines. For synchronous and induction machines it can be found by test.

D.2 RATING AND HEATING

The rating of electrical devices such as machines and transformers is often determined by mechanical and thermal considerations. For example, the maximum winding current is typically determined by the maximum operating temperature which

the insulation can withstand without damage or excessive loss of life. Similarly the maximum speed of a motor or generator is typically determined by mechanical considerations related to the structural integrity of the rotor or the performance of the bearings. The temperature rise resulting from the losses considered in Section D.1 is therefore a major factor in the rating of a machine.

The operating temperature of a machine is closely associated with its life expectancy because deterioration of the insulation is a function of both time and temperature. Such deterioration is a chemical phenomenon involving slow oxidation and brittle hardening and leading to loss of mechanical durability and dielectric strength. In many cases the deterioration rate is such that the life of the insulation can be represented as an exponential

$$\text{Life} = \text{A}e^{\text{B}/T} \tag{D.6}$$

where A and B are constants and T is the absolute temperature. Thus, according to Eq. D.6, when life is plotted to a logarithmic scale against the reciprocal of absolute temperature on a uniform scale, a straight line should result. Such plots form valuable guides in the thermal evaluation of insulating materials and systems. A very rough idea of the life-temperature relation can be obtained from the old and more or less obsolete rule of thumb that the time to failure of organic insulation is halved for each 8 to 10°C rise.

The evaluation of insulating materials and insulation systems (which may include widely different materials and techniques in combination) is to a large extent a functional one based on accelerated life tests. Both normal life expectancy and service conditions will vary widely for different classes of electric equipment. Life expectancy, for example, may be a matter of minutes in some military and missile applications, may be 500 to 1000 h in certain aircraft and electronic equipment, and may range from 10 to 30 years or more in large industrial equipment. The test procedures will accordingly vary with the type of equipment. Accelerated life tests on models, called *motorettes,* are commonly used in insulation evaluation. Such tests, however, cannot be easily applied to all equipment, especially the insulation systems of large machines.

Insulation life tests generally attempt to simulate service conditions. They usually include the following elements:

- Thermal shock resulting from heating to the test temperature.
- Sustained heating at that temperature.
- Thermal shock resulting from cooling to room temperature or below.
- Vibration and mechanical stress such as may be encountered in actual service.
- Exposure to moisture.
- Dielectric testing to determine the condition of the insulation.

Enough samples must be tested to permit statistical methods to be applied in analyzing the results. The life-temperature relations obtained from these tests lead to the classification of the insulation or insulating system in the appropriate temperature class.

For the allowable temperature limits of insulating systems used commercially, the latest standards of ANSI, IEEE, and NEMA should be consulted. The three NEMA

insulation-system classes of chief interest for industrial machines are class B, class F, and class H. Class B insulation includes mica, glass fiber, asbestos, and similar materials with suitable bonding substances. Class F insulation also includes mica, glass fiber, and synthetic substances similar to those in class B, but the system must be capable of withstanding higher temperatures. Class H insulation, intended for still higher temperatures, may consist of materials such as silicone elastomer and combinations including mica, glass fiber, asbestos, and so on, with bonding substances such as appropriate silicone resins. Experience and tests showing the material or system to be capable of operation at the recommended temperature form the important classifying criteria.

When the temperature class of the insulation is established, the permissible observable temperature rises for the various parts of industrial-type machines can be found by consulting the appropriate standards. Reasonably detailed distinctions are made with respect to type of machine, method of temperature measurement, machine part involved, whether the machine is enclosed, and the type of cooling (air-cooled, fan-cooled, hydrogen-cooled, etc.). Distinctions are also made between general-purpose machines and definite- or special-purpose machines. The term *general-purpose motor* refers to one of standard rating "up to 200 hp with standard operating characteristics and mechanical construction for use under usual service conditions without restriction to a particular application or type of application." In contrast a *special-purpose motor* is "designed with either operating characteristics or mechanical construction, or both, for a particular application." For the same class of insulation, the permissible rise of temperature is lower for a general-purpose motor than for a special-purpose motor, largely to allow a greater factor of safety where service conditions are unknown. Partially compensating the lower rise, however, is the fact that general-purpose motors are allowed a *service factor* of 1.15 when operated at rated voltage; the service factor is a multiplier which, applied to the rated output, indicates a permissible loading which may be carried continuously under the conditions specified for that service factor.

Examples of allowable temperature rises can be seen from Table D.1. The table applies to integral-horsepower induction motors, is based on 40°C ambient temperature, and assumes measurement of temperature rise by determining the increase of winding resistances.

The most common machine rating is the *continuous rating* defining the output (in kilowatts for dc generators, kilovoltamperes at a specified power factor for ac generators, and horsepower or kilowatts for motors) which can be carried indefinitely

Table D.1 Allowable temperature rise, °C[†].

Motor type	Class B	Class F	Class H
1.15 service factor	90	115	
1.00 service factor, encapsulated windings	85	110	
Totally enclosed, fan-cooled	80	105	125
Totally enclosed, nonventilated	85	110	135

[†]Excerpted from NEMA standards.

without exceeding established limitations. For intermittent, periodic, or varying duty, a machine may be given a short-time rating defining the load which can be carried for a specific time. Standard periods for short-time ratings are 5, 15, 30, and 60 minutes. Speeds, voltages, and frequencies are also specified in machine ratings, and provision is made for possible variations in voltage and frequency. Motors, for example, must operate successfully at voltages 10 percent above and below rated voltage and, for ac motors, at frequencies 5 percent above and below rated frequency; the combined variation of voltage and frequency may not exceed 10 percent. Other performance conditions are so established that reasonable short-time overloads can be carried. Thus, the user of a motor can expect to be able to apply for a short time an overload of, say, 25 percent at 90 percent of normal voltage with an ample margin of safety.

The converse problem to the rating of machinery, that of choosing the size of machine for a particular application, is a relatively simple one when the load requirements remain substantially constant. For many motor applications, however, the load requirements vary more or less cyclically and over a wide range. The duty cycle of a typical crane or hoist motor offers a good example. From the thermal viewpoint, the average heating of the motor must be found by detailed study of the motor losses during the various parts of the cycle. Account must be taken of changes in ventilation with motor speed for open and semiclosed motors. Judicious selection is based on a large amount of experimental data and considerable experience with the motors involved. For estimating the required size of motors operating at substantially constant speeds, it is sometimes assumed that the heating of the insulation varies as the square of the load, an assumption which obviously overemphasizes the role of armature I^2R loss at the expense of the core loss. The rms ordinate of the power-time curve representing the duty cycle is obtained by the same technique used to find the rms value of periodically varying currents, and a motor rating is chosen on the basis of the result; i.e.,

$$\text{rms kW} = \sqrt{\frac{\Sigma(\text{kW})^2 \times \text{time}}{\text{running time} + (\text{standstill time}/k)}} \tag{D.7}$$

where the constant k accounts for the poorer ventilation at standstill and equals approximately 4 for an open motor. The time for a complete cycle must be short compared with the time for the motor to reach a steady temperature.

Although crude, the rms-kW method is used fairly often. The necessity for rounding the result to a commercially available motor size[1] obviates the need for precise computations. Special consideration must be given to motors that are frequently started or reversed, for such operations are thermally equivalent to heavy overloads. Consideration must also be given to duty cycles having such high torque

[1] Commercially available motors are generally found in standard sizes as defined by NEMA. NEMA Standards on Motors and Generators specify motor rating as well as the type and dimensions of the motor frame.

peaks that motors with continuous ratings chosen on purely thermal bases would be unable to furnish the torques required. It is to such duty cycles that special-purpose motors with short-time ratings are often applied. Short-time-rated motors in general have better torque-producing capability than motors rated to produce the same power output continuously, although, of course, they have a lower thermal capacity. Both these properties follow from the fact that a short-time-rated motor is designed for high flux densities in the iron and high current densities in the copper. In general, the ratio of torque capacity to thermal capacity increases as the period of the short-time rating decreases. Higher temperature rises are allowed in short-time-rated motors than for general-purpose motors. A motor with a 150-kW, 1-hr, 50°C rating, for example, may have the torque ability of a 200-kW continuously rated motor; it will be able to carry only about 0.8 times its rated output, or 120 kW continuously, however. In many cases it will be the economical solution for a drive requiring a continuous thermal capacity of 120 kW but having torque peaks which require the capability of a 200-kW continuously rated motor.

D.3 COOLING MEANS FOR ELECTRIC MACHINES

The cooling problem in electric apparatus in general increases in difficulty with increasing size. The surface area from which the heat must be carried away increases roughly as the square of the dimensions, whereas the heat developed by the losses is roughly proportional to the volume and therefore increases approximately as the cube of the dimensions. This problem is a particularly serious one in large turbine generators, where economy, mechanical requirements, shipping, and erection all demand compactness, especially for the rotor forging. Even in moderate size machines, for example, above a few thousand kVA for generators, a closed ventilating system is commonly used. Rather elaborate systems of cooling ducts must be provided to ensure that the cooling medium will effectively remove the heat arising from the losses.

For turbine generators, hydrogen is commonly used as the cooling medium in the totally enclosed ventilating system. Hydrogen has the following properties which make it well suited to the purpose:

- Its density is only about 0.07 times that of air at the same temperature and pressure, and therefore windage and ventilating losses are much less.
- Its specific heat on an equal-weight basis is about 14.5 times that of air. This means that, for the same temperature and pressure, hydrogen and air are about equally effective in their heat-storing capacity per unit volume, but the heat transfer by forced convection between the hot parts of the machine and the cooling gas is considerably greater with hydrogen than with air.
- The life of the insulation is increased and maintenance expenses decreased because of the absence of dirt, moisture, and oxygen.

- The fire hazard is minimized. A hydrogen-air mixture will not explode if the hydrogen content is above about 70 percent.

The result of the first two properties is that for the same operating conditions the heat which must be dissipated is reduced and at the same time the ease with which it can be carried off is increased.

The machine and its water-cooled heat exchanger for cooling the hydrogen must be sealed in a gas-tight envelope. The crux of the problem is in sealing the bearings. The system is maintained at a slight pressure (at least 0.5 psi) above atmospheric so that gas leakage is outward and an explosive mixture cannot accumulate in the machine. At this pressure, the rating of the machine can be increased by about 30 percent above its aircooled rating, and the full-load efficiency increased by about 0.5 percent. The trend is toward the use of higher pressures (15 to 60 psi). Increasing the hydrogen pressure from 0.5 to 15 psi increases the output for the same temperature rise by about 15 percent; a further increase to 30 psi provides about an additional 10 percent.

An important step which has made it possible almost to double the output of a hydrogen-cooled turbine-generator of given physical size is the development of *conductor cooling*, also called *inner cooling*. Here the coolant (liquid or gas) is forced through hollow ducts inside the conductor or conductor strands. Examples of such conductors can be seen in Fig. D.1. Thus, the thermal barrier presented by the electric insulation is largely circumvented, and the conductor losses can be absorbed directly by the coolant. Hydrogen is usually the cooling medium for the rotor conductors. Either gas or liquid cooling may be used for the stator conductors. Hydrogen is the coolant in the former case, and transit oil or water is commonly used in the latter. A sectional view of a conductor-cooled turbine generator is given in Fig. D.2. A large hydroelectric generator in which both stator and rotor are water-cooled is shown in Figs. 4.1 and 4.9.

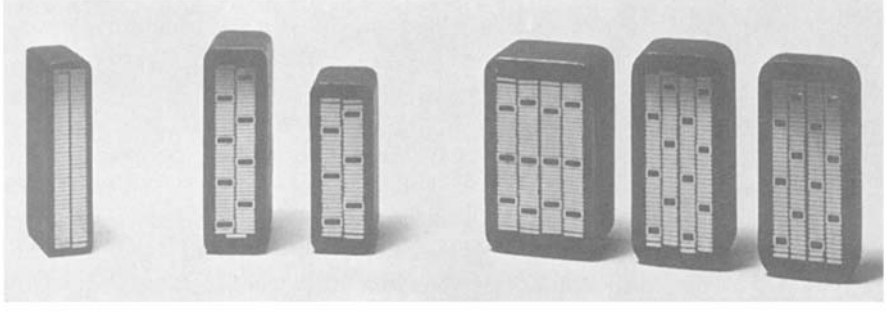

Figure D.1 Cross sections of bars for two-layer stator windings of turbine-generators. Insulation system consists of synthetic resin with vacuum impregnation. (a) Indirectly cooled bar with tubular strands; (b) water-cooled bars, two-wire-wide mixed strands, (c) water-cooled bars, four-wire-wide mixed strands. (*Brown Boveri Corporation.*)

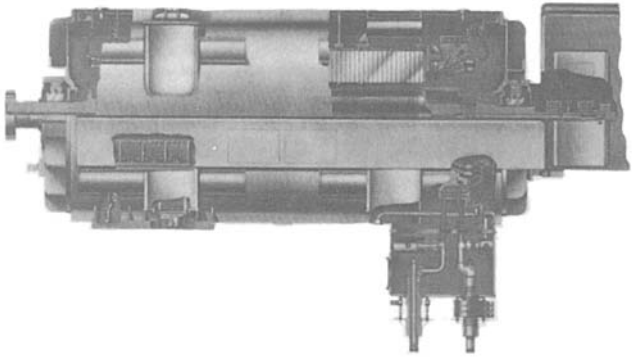

Figure D.2 Cutaway view of a two-pole 3600 r/min turbine rated at 500 MVA, 0.90 power factor, 22 kV, 60 Hz, 45 psig H_2 pressure. Stator winding is water-cooled; rotor winding is hydrogen-cooled. (*General Electric Company.*)

D.4 EXCITATION

The resultant flux in the magnetic circuit of a machine is established by the combined mmf of all the windings on the machine. For the conventional dc machine, the bulk of the effective mmf is furnished by the field windings. For the transformer, the net excitation may be furnished by either the primary or the secondary winding, or a portion may be furnished by each. A similar situation exists in ac machines. Furnishing excitation to ac machines has two different operational aspects which are of economic importance in the application of the machines.

D.4.1 Power Factor in AC Machines

The power factor at which ac machines operate is an economically important feature because of the cost of reactive kilovoltamperes. Low power factor adversely affects system operation in three principal ways. (1) Generators, transformers, and transmission equipment are rated in terms of kVA rather than kW because their losses and heating are very nearly determined by voltage and current regardless of power factor. The physical size and cost of ac apparatus are roughly proportional to kVA rating. The investment in generators, transformers, and transmission equipment for supplying a given useful amount of active power therefore is roughly inversely proportional to the power factor. (2) Low power factor means more current and greater I^2R losses in the generating and transmitting equipment. (3) A further disadvantage is poor voltage regulation.

Factors influencing reactive-kVA requirements in motors can be visualized readily in terms of the relationship of these requirements to the establishment of magnetic flux. As in any electromagnetic device, the resultant flux necessary for motor operation must be established by a magnetizing component of current. It makes no difference either in the magnetic circuit or in the fundamental energy conversion process whether

this magnetizing current be carried by the rotor or stator winding, just as it makes no basic difference in a transformer which winding carries the exciting current. In some cases, part of it is supplied from each winding. If all or part of the magnetizing current is supplied by an ac winding, the input to that winding must include lagging reactive kVA, because magnetizing current lags voltage drop by 90°. In effect, the lagging reactive kVA set up flux in the motor.

The only possible source of excitation in an induction motor is the stator input. The induction motor therefore must operate at a lagging power factor. This power factor is very low at no load and increases to about 85 to 90 percent at full load, the improvement being caused by the increased real-power requirements with increasing load.

With a synchronous motor, there are two possible sources of excitation: alternating current in the armature or direct current in the field winding. If the field current is just sufficient to supply the necessary mmf, no magnetizing-current component or reactive kVA are needed in the armature and the motor operates at unity power factor. If the field current is less, i.e., the motor is *underexcited,* the deficit in mmf must be made up by the armature and the motor operates at a lagging power factor. If the field current is greater, i.e., the motor is *overexcited,* the excess mmf must be counterbalanced in the armature and a leading component of current is present; the motor then operates at a leading power factor.

Because magnetizing current must be supplied to inductive loads such as transformers and induction motors, the ability of overexcited synchronous motors to supply lagging current is a highly desirable feature which may have considerable economic importance. In effect, overexcited synchronous motors act as generators of lagging reactive kilovoltamperes and thereby relieve the power source of the necessity for supplying this component. They thus may perform the same function as a local capacitor installation. Sometimes unloaded synchronous machines are installed in power systems solely for power-factor correction or for control of reactive-kVA flow. Such machines, called *synchronous condensers,* may be more economical in the larger sizes than static capacitors.

Both synchronous and induction machines may become self-excited when a sufficiently heavy capacitive load is present in their stator circuits. The capacitive current then furnishes the excitation and may cause serious overvoltage or excessive transient torques. Because of the inherent capacitance of transmission lines, the problem may arise when synchronous generators are energizing long unloaded or lightly loaded lines. The use of shunt reactors at the sending end of the line to compensate the capacitive current is sometimes necessary. For induction motors, it is normal practice to avoid self-excitation by limiting the size of any parallel capacitor when the motor and capacitor are switched as a unit.

D.4.2 Turbine-Generator Excitation Systems

As the available ratings of turbine-generators have increased, the problems of supplying the dc field excitation (amounting to 4000 A or more in the larger units) have grown progressively more difficult. A common excitation source is a shaft-driven dc generator whose output is supplied to the alternator field through brushes and

slip rings. Alternatively, excitation may be supplied from a shaft-driven alternator of conventional design as the main exciter. This alternator has a stationary armature and a rotating-field winding. Its frequency may be 180 or 240 Hz. Its output is fed to a stationary solid-state rectifier, which in turn supplies the turbine-generator field through slip rings.

Cooling and maintenance problems are inevitably associated with slip rings, commutators, and brushes. Many modern excitation systems have minimized these problems by minimizing the use of sliding contacts and brushes. As a result, some excitation systems employ shaft-driven ac alternators whose field windings are stationary and whose ac windings rotate. By the use of rotating rectifiers, dc excitation can be applied directly to the generator field winding without the use of slip rings.

Excitation systems of the latest design are being built without any sort of rotating exciter-alternator. In these systems, the excitation power is obtained from a special auxiliary transformer fed from the local power system. Alternatively it may be obtained directly from the main generator terminals; in one system a special armature winding is included in the main generator to supply the excitation power. In each of these systems the power is rectified using phase-controlled silicon controlled rectifiers (SCRs). These types of excitation system, which have been made possible by the development of reliable, high-power SCRs, are relatively simple in design and provide the fast response characteristics required in many modern applications.

D.5 ENERGY EFFICIENCY OF ELECTRIC MACHINERY

With increasing concern for both the supply and cost of energy comes a corresponding concern for efficiency in its use. Although electric energy can be converted to mechanical energy with great efficiency, achieving maximum efficiency requires both careful design of the electric machinery and proper matching of machine and intended application.

Clearly, one means to maximize the efficiency of an electric machine is to minimize its internal losses, such as those described in Section D.1. For example, the winding I^2R losses can be reduced by increasing the slot area so that more copper can be used, thus increasing the cross-sectional area of the windings and reducing the resistance.

Core loss can be reduced by decreasing the magnetic flux density in the iron of the machine. This can be done by increasing the volume of iron, but although the loss goes down in terms of watts per pound, the total volume of material (and hence the mass) is increased; depending on how the machine design is changed, there may be a point beyond which the losses actually begin to increase. Similarly, for a given flux density, eddy-current losses can be reduced by using thinner iron laminations.

One can see that there are trade-offs involved here; machines of more efficient design generally require more material and thus are bigger and more costly. Users will generally choose the "lowest-cost" solution to a particular requirement; if the increased capital cost of a high-efficiency motor can be expected to be offset by

energy savings over the expected lifetime of the machine, they will probably select the high-efficiency machine. If not, users are very unlikely to select this option in spite of the increased efficiency.

Similarly, some types of electric machines are inherently more efficient than others. For example, single-phase capacitor-start induction motors (Section 9.2) are relatively inexpensive and highly reliable, finding use in all sorts of small appliances, e.g., refrigerators, air conditioners, and fans. Yet they are inherently less efficient than their three-phase counterparts. Modifications such as a capacitor-run feature can lead to greater efficiency in the single-phase induction motor, but they are expensive and often not economically justifiable.

To optimize the efficiency of use of electric machinery the machine must be properly matched to the application, both in terms of size and performance. Since typical induction motors tend to draw nearly constant reactive power, independent of load, and since this causes resistive losses in the supply lines, it is wise to pick the smallest-rating induction motor which can properly satisfy the requirements of a specific application. Alternatively, capacitative power-factor correction may be used. Proper application of modern solid-state control technology can also play an important role in optimizing both performance and efficiency.

There are, of course, practical limitations which affect the selection of the motor for any particular application. Chief among them is that motors are generally available only in certain standard sizes. For example, a typical manufacturer might make fractional-horsepower ac motors rated at $\frac{1}{8}$, $\frac{1}{6}$, $\frac{1}{4}$, $\frac{1}{3}$, $\frac{1}{2}$, $\frac{3}{4}$, and 1 hp (NEMA standard ratings). This discrete selection thus limits the ability to fine-tune a particular application; if the need is 0.8 hp, the user will undoubtedly end up buying a 1-hp device and settling for a somewhat lower than optimum efficiency. A custom-designed and manufactured 0.8-hp motor can be economically justified only if it is needed in large quantities.

It should be pointed out that an extremely common source of inefficiency in electric motor applications is the mismatch of the motor to its application. Even the most efficient 50-kW motors will be somewhat inefficient when driving a 20-kW load. Yet mismatches of this type often occur in practice, due in great extent to the difficulty in characterizing operating loads and a tendency on the part of application engineers to be conservative to make sure that the system in question is guaranteed to operate in the face of design uncertainties. More careful attention to this issue can go a long way toward increasing the efficiency of energy use in electric machine applications.

E APPENDIX

Table of Constants and Conversion Factors for SI Units

Constants

Permeability of free space	$\mu_0 = 4\pi \times 10^{-7}$ H/m
Permittivity of free space	$\epsilon_0 = 8.854 \times 10^{-12}$ F/m

Conversion Factors

Length	1 m = 3.281 ft = 39.37 in
Mass	1 kg = 0.0685 slug = 2.205 lb (mass) = 35.27 oz
Force	1 N = 0.225 lbf = 7.23 poundals
Torque	1 N·m = 0.738 lbf·ft = 141.6 oz·in
Pressure	1 Pa (N/m^2) = 1.45×10^{-4} lbf/in^2 = 9.86×10^{-6} atm
Energy	1 J (W·sec) = 9.48×10^{-4} BTU = 0.239 calories
Power	1 W = 1.341×10^{-3} hp = 3.412 BTU/hr
Moment of intertia	1 kg·m^2 = 0.738 slug·ft^2 = 23.7 lb·ft^2 = 141.6 oz·in·sec^2
Magnetic flux	1 Wb = 10^8 lines (maxwells)
Magnetic flux density	1 T (Wb/m^2) = 10,000 gauss = 64.5 kilolines/in^2
Magnetizing force	1 A·turn/m = 0.0254 A·turn/in = 0.0126 oersted

U

V

W

Y

Z